

DEVELOPMENT AND EVALUATION OF A CANADIAN PRAIRIE
NUTRIENT TRANSPORT MODEL

A Thesis Submitted to the
College of Graduate Studies and Research
in Partial Fulfillment of the Requirements
for the degree of Master of Science
in the Department of Geography
University of Saskatchewan
Saskatoon

By
Jennifer Roste

©Jennifer Roste, July 2015. All rights reserved.

PERMISSION TO USE

In presenting this thesis in partial fulfilment of the requirements for a Postgraduate degree from the University of Saskatchewan, I agree that the Libraries of this University may make it freely available for inspection. I further agree that permission for copying of this thesis in any manner, in whole or in part, for scholarly purposes may be granted by the professor or professors who supervised my thesis work or, in their absence, by the Head of the Department or the Dean of the College in which my thesis work was done. It is understood that any copying or publication or use of this thesis or parts thereof for financial gain shall not be allowed without my written permission. It is also understood that due recognition shall be given to me and to the University of Saskatchewan in any scholarly use which may be made of any material in my thesis.

Requests for permission to copy or to make other use of material in this thesis in whole or part should be addressed to:

Head of the Department of Geography

Kirk Hall, 117 Science Place, Saskatoon, Saskatchewan S7N 5C8

ABSTRACT

Agriculture is one of the main sources of phosphorous and nitrogen (P and N) contributing to cultural eutrophication of freshwater lakes and estuaries. In cold regions, the effects of agricultural management practices used to mitigate the runoff loss of these nutrients remain uncertain. In particular, the use of forage crops and minimum tillage, have not reduced some forms of P and N in runoff to streams, in part, as a result of freeze-thaw induced losses of mobile P and N from forages and crop residues. The purpose of this research is to improve the current understanding of the controls on P and N loss from Canadian Prairie fields to ultimately aid in the development and evaluation of beneficial agricultural management practices that perform predictably in cold regions. This study aims to provide new insights into the effects of cold regions hydrological processes on runoff quality through the development and application of a novel inductive - deductive modelling approach. Runoff flowpaths resulting from the three infiltration regimes identified for frozen soils ([Granger et al., 1984](#)) are hypothesized to impact the chemistry of field scale meltwater runoff by varying meltwater interaction with agricultural soils and vegetation. Hydrochemistry data from six intensively monitored minimum tillage and forage cropped fields in South Tobacco Creek, Manitoba were used to develop a nutrient model to integrate with a physics-based hydrological modelling platform that can represent the frozen soil infiltration regimes, in addition to other important cold region hydrological processes. The inductive development of a nutrient model, integrated with a deductive physics-based hydrological platform, enabled the modelling of meltwater flowpaths and freeze-thaw induced losses from vegetation. Further testing of the developed model and field experimentation are required to test the hypothesis that runoff generated over a basal ice layer eliminates the transfer of soil nutrients to runoff. Comparison of predicted and observed field scale runoff concentrations and masses suggest that this method of inductive-deductive model development has potential to predict the performance of agricultural management practices in cold regions.

ACKNOWLEDGEMENTS

I would like to thank my supervisors, Drs. John Pomeroy and Howard Wheeler, committee member, Dr. Helen Baulch, and team member, Dr. Jane Elliot, all of whom asked the right questions to guide my research. Thank you also to my external examiner, Dr. Charles Maulé, for his academic critique of my research.

There are several other folks that I would like to thank. Dr. Taufique Mahmood set up the CRHM model for this project and aided in the presentation of site maps for this thesis. Kevin Shook, at the Centre for Hydrology, helped with technical support for the R statistical package and served as a sounding board for ideas throughout my research. Tom Brown provided help with CRHM and its various modules and structure. Several of my fellow students at the Centre for Hydrology helped with reasoning and working through the research process.

Funding for this research was provided by the Canadian Water Network as part of a larger project in the Tobacco Creek Model Watershed, Manitoba. Thank you to Dr. Jane Elliott with Environment Canada and the team at Agriculture and Agri-Food Canada for the provision of both data and data support. Additionally, thank you to Don Cruikshank and Les McEwan with Deerwood Soil and Water Management Association for teaching me about the watershed.

CONTENTS

Title	1
Permission to Use	i
Abstract	ii
Acknowledgements	iii
Contents	iv
List of Tables	vii
List of Figures	viii
List of Abbreviations	x
1 Introduction	1
1.1 Objectives	4
2 Literature Review	6
2.1 Hydrological Processes for Runoff P and N	6
2.1.1 Rain, Snow, and Rain-on-Snow Precipitation	6
2.1.2 Wind Redistribution of Snow	8
2.1.3 Soil Water Movement	8
2.1.4 Runoff	9
2.2 P and N Cycling	11
2.2.1 Phosphorous	12
2.2.2 Nitrogen	13
2.3 Predicting Runoff Transport of P and N	16
2.3.1 Annual P and N Soil Budgets	16
2.3.2 Nutrient Legacies	18
2.3.3 Field Sources of P and N	19
2.3.4 Transport of Field P and N	22
2.4 Modelling P and N Transport	24
2.4.1 An Inductive Canadian Prairie Nutrient Model	28
3 Field Sites and Data	30

3.1	Site Description	31
3.2	Sampling Design	32
3.2.1	Agricultural Record	33
3.2.2	Hydrochemistry Sampling	34
	Runoff flow sampling	34
	Runoff chemistry sampling	38
3.2.3	Soil Sampling	42
	Soil chemistry surveys	42
	Soil moisture surveys	45
3.2.4	Snow Sampling	46
	Snow depth and density surveys	46
	Snow chemistry surveys	46
4	Data Analyses and Key Messages	49
4.1	The agricultural field scale nutrient budget	49
4.2	Field scale flows and P and N exports	55
4.3	Snowmelt and rainfall runoff nutrient exports	56
4.4	Nutrient sources during snowmelt runoff	59
4.4.1	Tillage Induced Mineralization	63
4.4.2	Forage Vegetation as a Leachate Source	66
5	Model Development	69
5.1	Prairie Nutrient Snowmelt Conceptual Model	69
5.2	Hydrological Model Platform	73
5.3	Prairie Nutrient Snowmelt Model	79
5.3.1	Model Assumptions	80
5.3.2	Model Equations	84
	csnow	84
	csoil	85
	cveg	90
5.3.3	Model Inputs and Operation	92
6	Model Performance	94
6.1	Agricultural and Hydrological Context	94
6.2	Model Results	96
6.2.1	Hydrology	96
6.2.2	Nutrient Model	98
6.3	Model Sensitivity	107
7	Summary Discussion and Conclusions	110
7.1	Summary Discussion	110
7.1.1	Inductive Model Development	110
7.1.2	A Cold Regions Nutrient Hydrology Model	112
7.2	Conclusion	116
	References	118

A Literature Review Supporting Data	139
A.1 Phosphorous Mass Balance Scratch Sheet	139
A.2 Nitrogen Mass Balance Scratch Sheet	139
A.3 CREAMS Formulae	141
B Field Scale Data Analyses Plots	142
C Model Development Plots and Model Code	157
C.1 Model Plots	157
C.2 Model Code	159
C.2.1 main.R	159
C.2.2 CVd.R	164
C.2.3 musigma.R	164
C.2.4 EsseryPomeroy2004.R	165
C.2.5 strptimeDate.R	165
C.2.6 runoff_PN.R	165
C.2.7 Amarawansha2013.R	172
C.2.8 new_concentration.R	173
C.2.9 grassland_disturbance.R	173
C.2.10 freeze_thaw_cycles.R	174
C.2.11 Bechmann2005_TDPcurve.R	177
C.2.12 NP_stoichiometry.R	178
C.2.13 calculate_csoilNO3.R	179
C.2.14 soil_temperature.R	179
C.2.15 calculate_max_subnivean_nitrification_days.R	180
C.2.16 Stein_etal_1986.R	181
C.2.17 rainfall_chem.R	183
D Model Performance	184
D.1 Model Statistics	184
D.2 Performance Plots	185

LIST OF TABLES

3.1	Sub-basin2 Fields 3 and 4 Agricultural Record	35
3.2	Sub-basin2 Fields 7 and 9 Agricultural Record	36
3.3	Twin Watershed Agricultural Record	37
5.1	Bechmann Curve	91
5.2	Elliott (2013) Table 4	92
5.3	Elliott (2013) Table 4	93
5.4	Model Equations and Inputs	93
6.1	Model Performance Statistics	103
B.1	Mean snowcover and EOF solute concentrations	142
D.1	Simulated and Observed EOF Nutrient Mass Exports	186

LIST OF FIGURES

1.1	Simplified runoff flowpaths for P and N	5
2.1	Annual field scale P and N inputs and outputs	17
2.2	Prairie snowmelt hydrochemistry	20
3.1	South Tobacco Creek Watershed Map	32
3.2	Sub-basin2 and Twin Fields	33
3.3	Circular Flume	38
3.4	V-notched weir	38
3.5	Dry circular flume with intake	38
3.6	V-notched weir with intake	38
3.7	Typical runoff and chemical sampling resolution	39
3.8	Sigma Data logger GUI	39
3.9	Auto-sampler	39
3.10	Total Phosphorous and Total Nitrogen Annual Mass Flux	42
3.11	Soil P Sample Results	43
3.12	Soil N Sample Results	44
3.13	Fields 10 and 11 Fall Soil Moisture Contents	45
3.14	Snow depth vs density plot	47
4.1	Phosphorous and Nitrogen Field Scale Net Mass Balance	50
4.2	P and N Agricultural field mass balance	54
4.3	Concentration vs EOF discharge plots	56
4.4	Concentration vs EOF discharge plots for ROS, snowmelt and rainfall events.	57
4.5	Snowmelt Contribution to Nutrient Exports	58
4.6	Phosphorous and Nitrogen Exports, dissolved vs total fractions.	59
4.7	Edge-of-field CF_f and LF_f	61
4.8	Snowcover and EOF Meltwater Solute Probability Density Functions	62
4.9	NO_3 EOF Time Series	64
4.10	Tillage Disturbance effects on Soil and Meltwater NO_3	65
4.11	Annual Freeze-Thaw Cycle Count	66
4.12	EOF Concentrations vs FTCs	67
5.1	Conceptual Model: Sources of P and N in Field Scale Snowmelt Runoff	71
5.2	Prairie Nutrient Snowmelt Model Paradigm	72
5.3	Hydrological Model Flowchart	77
5.4	Conceptualized Basin setup for CRHM	78

5.5	Prairie Nutrient Model Structure	79
5.6	Field Snow Surveys	87
6.1	Sub-basin2 Fields 7 and 9 Observed Nutrient Exports	95
6.2	Simulated and Observed Runoff	99
6.3	F7 Hourly Simulated and Observed Runoff	100
6.4	Simulated and Observed EOF Nutrient Mass Exports	101
6.5	Simulated and Observed EOF Concentration Time Series	104
6.6	Simulated vs Observed EOF Concentration Plots	105
6.7	Simulated EOF CF_f and LF_f	106
6.8	Sensitivity Plots	108
B.1	Annual Observed Rainfall	143
B.2	Observed 15 minute Edge-of-Field Runoff	144
B.3	Observed Cumulative Edge-of-Field Runoff	145
B.4	Observed Dissolved Phosphorous Concentration at the Edge-of-Field	146
B.5	Observed Nitrate Concentration at the Edge-of-Field	147
B.6	Observed Ammonia Concentration at the Edge-of-Field	148
B.7	Observed 15 minute Edge-of-Field Runoff During ROS Events	149
B.8	Annual Observed Snowcover Nutrient Concentrations	150
B.9	Annual Observed March Snowcover SWE	151
B.10	EOF Concentration vs Discharge	152
B.11	Phosphorous and Nitrogen Exports, dissolved vs total fractions (all data).	153
B.12	Annual TDP Density Distribution Plots	154
B.13	Annual NO_3 Density Distribution Plots	155
B.14	Annual NH_3 Density Distribution Plots	156
C.1	EOF Solute Concentrations and Freeze Thaw Cycle Counts	158
D.1	Simulated and Observed Daily Runoff	185
D.2	Simulated vs Observed Mean Daily EOF Concentration Plots	187
D.3	TDP Snow Sensitivity Plot	188

LIST OF ABBREVIATIONS

AAFC	Agriculture and Agri - Food Canada
AHC	Antecedent Hydrological Conditions
AT	Annually tilled cereal grains and oilseeds
bioP	Bio-available Phosphorous
C	Carbon
c	Concentration
CF_f	Field scale Concentration Factor
CF_{Stein}	Stein et al. (1986) Concentration Factor
CRHM	Cold Regions Hydrological Modelling platform
CV	Coefficient of Variation
DAP	Diammonium Phosphate
DP	Dissolved Phosphorus
EOF	Edge-of-field
FTC	Freeze-thaw cycle
FWMC	Flow weighted mean concentration
HRU	Hydrological Response Unit
LAI	Leaf Area Index
LF_f	Field scale Load Factor
MT	Cereal grains and oilseeds crops with no tillage disturbance
N	Nitrogen
NH ₃	Total ammonia, unionized and ionized
NO ₃	Nitrate - Nitrite
P	Phosphorus
ROS	Rain on Snow
SWE	Snow Water Equivalent
TDN	Total Dissolved Nitrogen
TDP	Total Dissolved Phosphorous
TIN	Total Inorganic Nitrogen
TN	Total Nitrogen
TP	Total Dissolved Phosphorous
q	Flow
w.c.	Water Content (as in soil water content)
WEP	Water Extractable Phosphorous
WEBs	Watershed Evaluation of Beneficial Management Practices
x.s.	Cross sectional area

CHAPTER 1

INTRODUCTION

Phosphorus (P) and nitrogen (N) are essential nutrients in terrestrial and aquatic ecosystems. P is required for DNA, RNA and energy transfer and N for protein synthesis (Conley et al., 2009). P and N are often key limiting nutrients to animal and plant growth (Conley et al., 2009) and yet their surplus in aquatic ecosystems due, in part, to anthropogenic inputs of P and N, has impaired many surface water bodies worldwide (Carpenter et al., 1998). *Cultural eutrophication*, the ecological transformation of water bodies induced by nutrient pollution (Kleinman et al., 2011b), from sources such as agricultural fertilization, wastewater discharges and atmospheric deposition of volatilized N leads to increased biomass of phytoplankton; increased biomass of benthic and epiphytic algae; changes in the macrophyte species composition and biomass; decreased water transparency; oxygen depletion; taste, odour and water treatment problems; increased incidence of fish kills; and/or decreased perceived aesthetic value of the water body (Carpenter et al., 1998). P and N accumulation in freshwaters, estuaries, and marine waters worldwide has been recognized as an aesthetic, aquatic, and public health problem requiring global action (European Union, 2000; Ospar Commission, 1998; USEPA, 2000). In Canada, point source and diffuse phosphorus and nitrogen loads have caused the current impaired state of lakes such as Lake Simcoe, Ontario; the Qu'Appelle Lakes, Saskatchewan; Lake Winnipeg, Manitoba; and Lac La Biche, Alberta (Chambers et al., 2001; Environment Canada, 2011a; Schindler et al., 2008).

P and N in mineral and manure fertilizers applied to crop land, livestock urine and dung, and atmospheric deposition of volatilized N from agricultural activities (Carpenter et al., 1998; Conley et al., 2009; Elser et al., 2009; Kleinman et al., 2011b; Schindler, 2012) are major sources of P and N pollution that contribute to cultural eutrophication. P and N loads from agriculture are diffuse, and this coupled with their temporal and spatial variability, make them a challenge to regulate or control. Agricultural land sourced fluxes of P and N

primarily follow hydrologic pathways such as groundwater leaching (mostly N; P in organic soils ([Macrae et al., 2005](#))), runoff and erosive transport (P and N), and atmospheric deposition during rainfall and snowfall of volatilized agricultural N ([Carpenter et al., 1998](#)). Surface runoff of P and N is the most significant pathway for P and N flux on the Canadian Prairies and understanding the surface hydrologic pathways is very important in understanding these nutrient fluxes. Wind redistribution of snow, seasonally frozen soils, snowmelt, evaporation from cold soils and soil moisture in agricultural soils are important hydrologic processes on the Canadian Prairie ([Pomeroy et al., 1998a](#)) that will influence P and N runoff transport.

It is a controversial issue and the subject of much research as to which nutrient, P or N, to focus reduction efforts on. Controlling cultural eutrophication of surface waters has been espoused to be a problem of too much P ([Schindler, 1977](#)) which has led to regulations controlling the point source release of P. Control of P inputs, notably by way of P regulation in detergents to reduce wastewater effluent P sources (i.e. [Government of Canada \(1999\)](#)) combined with USA efforts regarding the Great Lakes ([Litke, 1999](#)), led to the recovery of Lake Erie, Lake Ontario, Kootenay Lake, Meretta Lake, and Gravenhurst Bay in addition to others globally ([Schindler, 2012](#)). Recently, the need for N control has become a topic of considerable debate. For example, [Conley et al. \(2009\)](#) conceded that the water quality in some lakes may have improved as a result of P control but that broader ecosystem goals encompassing downstream health of estuaries and coastal marine systems were not achieved. Increased anthropogenic inputs of N have been shown to shift the natural N:P stoichiometric relationships in surface waters and change the limiting nutrient ([Elser et al., 2009](#)), and may be associated with increased toxicity of harmful algae ([Granieli and Flynn, 2006](#)). Canada's recent Wastewater System Effluent Regulations limit un-ionized ammonia to 1.25 mg/l ([Government of Canada, 2012](#)), recognizing the role of N in the impairment of surface waters, and the potential for direct toxic effects of ammonia.

Efforts to restore Lake Winnipeg, a Canadian Prairie lake, to pre-1970 nutrient levels have involved the reduction in both P and N loads to the lake with a focus on P reduction ([Lake Winnipeg Stewardship Board, 2009](#)). Just over half of the nutrient load comes from the Red River Basin ([Lake Winnipeg Stewardship Board, 2009](#)), a watershed located in both Canada and the USA, that, similar to the Lake Winnipeg Basin as a whole, is home

to many grain and intensive livestock farming operations. One of the primary efforts in nutrient reduction for Lake Winnipeg includes the reduction of diffuse nutrient inputs from agriculture such as those contributed by fertilizers, and animal urine and dung, that are typically mobilized with snowmelt runoff ([Corriveau et al., 2011](#); [Lake Winnipeg Stewardship Board, 2009](#)). Runoff losses of P and N associated with fertilization are influenced by a variety of factors such as fertilizer application rates, timing of application, chemical form, method of application, amount and timing of precipitation and runoff after application, and vegetative cover ([Carpenter et al., 1998](#)) in addition to catchment hydrology, biogeochemistry and soil physics; an indication of the complexity involved in the understanding, prediction, and regulation of agricultural P and N. This complexity is an indication, too, as to the investment in research and time required to sustainably restore the water quality in Lake Winnipeg.

Agricultural practices such as such as minimum tillage, riparian buffer strips, holding ponds, small reservoirs, and conversion to forage crops, have been adopted in Canada as Beneficial Management Practices (BMPs) to reduce nutrient fluxes from agricultural land. These five BMPs are the subject of research in the Red River Basin in the South Tobacco Creek watershed ([AAFC, 2010](#); [Agriculture and Agri-Food Canada, 2010a](#); [Lake Winnipeg Stewardship Board, 2009](#)). Generally, the impact of BMPs on the field scale mobilization of P and N is not fully understood on the cold, flat, and snowmelt runoff dominated prairie ([Corriveau et al., 2011](#); [Li et al., 2011](#)) as, historically, BMPs have been developed in regions that are relatively wet, sloped, rainfall-runoff dominated, and subject to significant erosion mobilized particulate P and N ([Cade-Menun et al., 2013](#); [Li et al., 2011](#)). Field scale research in the South Tobacco Creek watershed has shown that the implementation of some BMPs such as minimum tillage and conversion to forage cropping, in cold regions such as the Canadian Prairie, where the role of erosion in runoff is diminished and dissolved nutrient fluxes dominate, has not produced the desired beneficial outcome of reducing nutrient fluxes ([Corriveau et al., 2011](#); [Liu et al., 2014a](#); [Tiessen et al., 2010](#)). Further research and monitoring is required before BMPs can be developed to effectively reduce nutrient export ([Wheater et al., 2013](#)) in the relatively dry, flat, and snowmelt dominated regions of the world. [Wheater et al. \(2013\)](#) called for improved computer modelling of watersheds as a decision support tool to

aid in the selection and assessment of the performance of current BMPs - hence forward referred to as agricultural management practices until their performance in cold regions is assessed.

1.1 Objectives

On the Canadian Prairie, agricultural management practices such as forage crops and minimum tillage have not reduced some forms of P and N in runoff to streams (Liu et al., 2014a; Tiessen et al., 2010, South Tobacco Creek, Manitoba). While there is a diminished role of erosion in P and N exports, in this region where there is a more than 80% annual contribution of snowmelt runoff to streamflow, there is a dominant role for the transport of dissolved nutrients (Gray and Landine, 1988; Li et al., 2011). The continual presence of vegetation related to minimum tillage and forage crops has also proven important on the Canadian Prairie. Freeze-thaw cycling damages cell tissues in this vegetation releasing P and N that are dissolved and mobilized during runoff (Elliott, 2013; Liu et al., 2014a).

Runoff from the flat, cultivated Canadian Prairie can be related to four flowpaths as shown in Figure 1.1. Snow meltwater infiltration into frozen soils is described by Granger et al. (1984) and rainfall runoff falls into the categories of infiltration and saturation excess. In meltwater runoff from frozen soil, Lilbaek (2007) referred to the formation of a basal ice layer as a switch, changing flowpath and meltwater runoff chemistry at the same time. In Section 2.3.3, the three primary sources of P and N on a cultivated ungrazed field will be presented as snow (atmospheric deposition to snow), soil, and vegetation. The four flowpaths described in Figure 1.1 based on Granger et al. (1984) and Lilbaek (2007) will vary the interaction with these three sources and are hypothesized to determine the contribution of these sources to concentrations of P and N in field scale runoff. Succinctly, runoff during restricted infiltration will eliminate interaction with soils.

It is the purpose of this research to identify the hydrological and biogeochemical controls on the field scale export of P and N solute, and to develop an appropriate simulation model to represent these. This will facilitate the future modelling and development of agricultural management practices with predictable performance in cold regions. The influence of flow-path is one of the potentially important controls on the field scale transport of P and N to





Runoff during snowmelt, ROS, and rainfall events	Basal ice / concrete frost during snowmelt or ROS runoff	Snowmelt, ROS or rain event on saturated soils	Snowmelt, ROS or rain event on unsaturated soils	Snowmelt, ROS or rain event on unsaturated soils
event precipitation crop vegetation agricultural soil				
Runoff Volume	100% of precipitation and/or SWE	100% of precipitation and/or SWE	>0% and <100% of precipitation and/or SWE	0% of precipitation and/or SWE
Soil contact	assumed no contact but it can occur (Lilbaek, 2007)	contact	contact	contact
Vegetation Contact	contact	contact	contact	contact
Infiltration regime	restricted	limited	limited	unlimited
P and N solute exported	100% of precipitation and/or SWE solute mass	>100% of precipitation and/or SWE solute mass	>0% of precipitation and/or SWE solute mass	none

Figure 1.1: Simplified runoff flowpaths for P and N. This schematic illustrates the runoff flowpaths during snowmelt, rain, and rain-on-snow (ROS) events as they relate to the phosphorous (P) and nitrogen (N) loads exported. Format taken from (Lilbaek, 2007).

streams. The purpose of this research will be met by accomplishing the following objectives, to:

1. investigate the influence of frozen soil infiltration, specifically restricted infiltrability, on runoff interactions with field nutrient sources and the transport of phosphorous and nitrogen from agricultural fields under forage conversion and minimum tillage agricultural management practices
2. verify if the surface runoff export of total ammonia (NH_3), nitrate-nitrite (NO_3), and total dissolved phosphorous (TDP) can be simulated with a nutrient hydrology model developed using both field hydrochemistry data and principles established in the scientific literature

CHAPTER 2

LITERATURE REVIEW

2.1 Hydrological Processes for Runoff P and N

The hydrological processes of importance in the runoff export of P and N include precipitation in the form of snowfall, rainfall, and rain-on-snow; wind redistribution of snow; soil water movement; depressional storage and runoff. Rainfall runoff production is determined by rainfall rates, soil water movement, and infiltration into unfrozen soils whereas snowmelt runoff production further involves the redistribution of snow, melt energetics (that determine melt rate), and infiltration into frozen soils.

2.1.1 Rain, Snow, and Rain-on-Snow Precipitation

Rainfall and snowfall events transport P and N aerosols and condensed N atmospheric vapour to receiving soils, snowcovers, and water surfaces in concentrations that vary spatially and temporally with the form of the precipitation; proximity to sources such as urban centres, industrial and agricultural emitters, and the sea; and the properties of the solute (Cadle, 1991; Chambers et al., 2001; Köchy and Wilson, 2001). Deposition rates tend to be higher in the summer than the winter (Cadle, 1991; Holtan and Stuanes, 1988) and for N, higher in eastern than western Canada (Chambers et al., 2001) and up to 10 fold higher to wet than to dry snowcovers (Dasch and Cadle, 1986). Deposition of solutes with precipitation events, termed *wet deposition*, and the continuous transfer of gases and particles (Cadle, 1991) onto the soil and snowcover surface, termed *dry deposition*, occur at variable rates across Canada with bulk (wet + dry) deposition rates reported in Canada from $0.68 - 2.21 \text{ g} \cdot \text{m}^{-2} \cdot \text{yr}^{-1}$ for N and $0.001 - 0.074 \text{ g} \cdot \text{m}^{-2} \cdot \text{yr}^{-1}$ for P (Cadle, 1991; Chambers et al., 2001; Köchy and Wilson, 2001).

Rain-on-snow (ROS) events have a particular significance as one ROS event can constitute

most of the dissolved phosphorous (DP) annually exported from an agricultural catchment (Coelho et al., 2012; Miles et al., 2013). ROS can mobilize snowcover P and N (Tranter, 1991) in addition to transmitting some or all of the P and N in the rain, and frozen soil conditions during these events can lead to large runoff and nutrient export events (Coelho et al., 2012).

Snowcovers can be sinks for nutrients over the winter period. Snowcovers overlying agricultural land will acquire nutrients from a variety of sources including urine and dung deposition from grazing animals (Smith et al., 2011), winter spread manure (Coelho et al., 2012), atmospheric deposition of P and N on snow surface (Cadle, 1991), leaching from over-winter crop vegetation and residues (Elliott, 2013), eroded dirt from nearby wind scoured fields or roads, and redistributed snow (Pomeroy et al., 1991).

As the snow season progresses, a snowcover undergoes densification or metamorphosis (Colbeck, 1987, 1981) and snowcover ions are redistributed with a concentration of ions building up on a liquid film on the edge of the snow crystals as a result of exclusion during refreezing (Davis, 1991; Pomeroy and Jones, 2005). At the time of melt these excluded ions are quickly mobilized and eluted from the pack preferentially (Brimblecombe et al., 1987; Tranter et al., 1986), leading to the early melt ionic pulse (Davis, 1991; Lilbaek and Pomeroy, 2008, for example) which can involve the release of up to 50 - 80% of ions during the first 1/3 of the melt (Maule and Stein, 1990). This process is referred to as solute fractionation from the ice lattice in meltwater from snowcovers (Johannessen and Henricksen, 1978). Laboratory and field investigations have quantified fractionation based on a concentration factor, CF, or the ratio of the eluted meltwater concentration to the bulk snowcover concentration of a solute (Johannessen and Henricksen, 1978; Stein et al., 1986) and found that CFs ranged 2 to 39 fold (Hodson 2006, Table 4; Tranter 1991, Tables 1 & 2) with the typical CFs on the range of 2 to 6 fold (Tranter, 1991) and the higher range 23 to 39 fold related to meltwater runoff over a basal ice layer (Hodson, 2006). In a laboratory investigation, Lilbaek and Pomeroy (2008) reported elevated meltwater CFs in the presence of a basal ice layer due to the process of ion exclusion during the freezing of the basal ice layer. Ion exclusion from the ice lattice occurs (Kahan et al., 2014; Lilbaek, 2007) where salts remain in the liquid water content of frozen soils as a result of salt induced freezing point depression which is a function of

salt concentration and soil texture and moisture as they affect tension forces in the matrix (capillary and absorptive forces, [Ireson et al. 2013](#); [Gray and Granger 1986](#); [Lilbaek 2007](#)). [Kahan et al. \(2014\)](#) found that observations of the excluded nitrate ions at the ice surface were similar to bulk solution concentrations, and therefore lower than expected or predicted by thermodynamic principles perhaps due to the nitrate remaining in pockets within the bulk ice or other unexplained mechanism. The solute composition of snowcovers and snow meltwaters coupled with the timing and spatial distribution of the melt have implications for the chemistry of the runoff at the field and watershed scale ([Davis, 1991](#)).

2.1.2 Wind Redistribution of Snow

Blowing snow is common on cultivated prairie fields and it can redistribute a substantial amount of the snowcover from open, exposed areas to sheltered, vegetated areas and cause spatial variability in the snowcover ([Pomeroy et al., 1991](#)). This can affect the hydrology and chemistry of snowmelt in addition to subsurface biogeochemical processes that may or may not occur over winter. The chemistry of the snowcover will change due to winter transport and transformation processes ([Pomeroy and Jones, 1996](#)). The transfer of ions bonded to snow particles, aerosols and vapour is not a conservative process and the snowcover chemistry will change when ions are scavenged or released by blowing snow particles and sublimated water vapour ([Pomeroy et al., 1991](#)). In open fallow areas of the prairie, wind can transport as much as 75% of the snowcover and 15 - 40% of the Canadian prairie snowcover may be lost to sublimation ([Pomeroy and Gray, 1995](#)). This snowcover accumulation and ablation can have significant impact the water balance of prairie ecosystems ([van der Kamp et al., 2003](#)).

2.1.3 Soil Water Movement

Soil water moves both water and solute slowly through the glacial tills of the prairie unsaturated zone ([Nachshon et al., 2013](#)). Soil water recharge of groundwater aquifers is a decadal process ([Joshi and Maule, 2000](#); [Si and de Jong, 2007](#)) on most of the Canadian prairie due to the confinement of deep aquifers with overlying glacial tills ([Nachshon et al., 2013](#)). Groundwater recharge rates on the Prairies have been found to be $\approx 2 \text{ mm} \cdot \text{yr}^{-1}$ at field sites

in Saskatchewan (Hayashi et al., 1998; Si and de Jong, 2007). On the Canadian Prairie, soil water flows upward due to soil water evaporation (Hillel, 1980; Stumpp and Hendry, 2012) and redistribution in frozen unsaturated soils (Gray and Granger, 1986; Harlan, 1973; Ireson et al., 2013); laterally at various times due to competing osmotic, gravitational, capillary and adsorptive gradients (Hayashi et al., 1998; Nachshon et al., 2013; Parsons et al., 2004); and downward to recharge aquifers. Air voids (Hillel, 1980), soil heterogeneity (Stumpp and Hendry, 2012), macropores (Cey et al., 2009), and ice (Groenevelt and Kay, 1974; Jame and Norum, 1980) cause great spatial and temporal variability in soil water movement and P and N fluxes on the Canadian Prairie. Preferential flowpaths can move soil water rapidly through the unsaturated zone, altering historic surface water patterns (Bodhinayake and Si, 2004; van der Kamp et al., 2003), influencing exported nutrient speciation (Eastman et al., 2010) and potentially causing unexpected and toxic pollution of shallow aquifers (Cey et al., 2009). In areas with shallow unconfined aquifers the spring flux of nitrate into the wells can be dramatic (Burns, 2013, pers. comm.). Subsurface transport offers little opportunity for reduction in NO_3^- loads by uptake by either of vegetation, denitrification or dilution (Federal-Provincial-Territorial Committee on Drinking Water, 2013); therefore NO_3^- moves unobstructed to receiving aquifers. In areas of intense agricultural activity this can be a considerable problem (Haslauer et al., 2004). Background levels of nitrate in groundwater range from 0.90 to 2.0 $\text{mg} \cdot \text{l}^{-1}$ NO_3^- -N and in surface water 0.2 to 5.0 $\text{mg} \cdot \text{l}^{-1}$ NO_3^- -N (Federal-Provincial-Territorial Committee on Drinking Water, 2013). All else being equal, deeper, confined wells have lower nitrate levels than shallow, unconfined wells and are less likely to have NO_3^- levels above the Canadian Drinking Water Quality Guideline of 10 $\text{mg} \cdot \text{l}^{-1}$ NO_3^- -N.

2.1.4 Runoff

On the Canadian Prairie, snowmelt runoff accounts for > 80% of the annual runoff volume (Gray and Landine, 1988) and contributes a majority of the annual P and N exported annually as well (Corriveau et al., 2013, Red River watershed, Manitoba). In light of climate non-stationarity (Milly et al., 2008), Dumanski et al. (2015, in review) found the contribution of rainfall to annual streamflow volumes is increasing in a Canadian Prairie catchment due

in part to climate change and wetland drainage in the catchment. A reduction in snowmelt runoff contributions to runoff volumes and land use change involving the drainage of wetlands would be expected to impact P and N runoff exports. P and N exports to streams and freshwaters on the Canadian Prairie are often affected by the hydrologic connectivity of the catchment (Bracken and Croke, 2007; Shook and Pomeroy, 2011b). Wetlands and micro-depressions (Appels et al., 2011) on fields can be isolated sinks for both P and N during runoff (Brunet and Westbrook, 2012) until these sinks fill up with water and spill over (van der Kamp and Hayashi, 2009) moving both water and solutes from sink to receiving streams and lakes.

Surface runoff results when the intensity of a rainfall event exceeds the infiltration capacity of the soil (infiltration excess or Hortonian flow), rain falls on a saturated soil (saturation excess flow), or snow melts producing meltwater in excess of soil infiltration capacity. Research has also shown infiltration excess and saturation excess runoff differ in the amount of P relocated (McDowell, 2012). Laboratory research by Lilbaek (2007) has shown that meltwater flowpaths also have the potential to impact runoff chemistry composition. P and N transport with meltwater may migrate into the soil substrate, runoff overland, or follow some combination of both, depending on the *infiltrability* (Granger et al., 1984) of the soil based on the presence of basal ice (Lilbaek and Pomeroy, 2008), concrete frost (Jones and Pomeroy, 2001), and macropores (Zhao and Gray, 1999) in addition to the soil physical characteristics and soil water content. The existence of a concrete frost or basal ice layer increases the runoff efficiency and limits access to the soil matrix ions, but does not completely restrict access (Lilbaek, 2007). Fine grained wet soils will form an impenetrable concrete frost on freezing and also restrict the meltwater contact with soil matrix (Pierson and Taylor, 1985). The Granger et al. (1984) infiltration regimes of *restricted*, *limited*, and *unlimited*, apportion meltwater accordingly, generating 100% runoff, partially infiltrating the substrate, or 100% infiltrating the substrate respectively. Snowcover nutrients will dominate the exported nutrient loads during restricted infiltration events, whereas neither water nor nutrients will be exported overland during unlimited infiltration events. Meltwater contact with the soil may occur under all three infiltration regimes but it is significantly reduced under restricted infiltration (Pierson and Taylor, 1985).

In an analytical review, [Hayashi \(2013\)](#) discussed the reduced hydraulic conductivity of frozen soils due to ice formation in the larger pores which essentially forces soil water into the smaller, less conductive pores ([Watanabe and Flury, 2008](#)). This reduced hydraulic conductivity coupled with the relatively flat topography typical of the Canadian Prairie lends to the dominance of overland flow during prairie snowmelt events. Research by [Laudon et al. \(2004\)](#) in Northern Sweden, [Shanley and Chalmers \(1999\)](#) in Vermont, [Pierson and Taylor \(1985\)](#) near Peterborough, Ontario, [Banaszuk et al. \(2011\)](#) in Northeastern Poland, and [Steppuhn et al. \(1975\)](#) in Saskatchewan provides evidence that on the frozen soils in the upper reaches of a prairie or agricultural catchment, water observed at the edge-of-field is primarily event water (water from the precipitation [rainfall, snowmelt, or rain-on-snow] event as opposed to pre-event water, water already residing in the catchment [soils] ([Laudon et al., 2004](#))) as a result of overland flow. An estimated 85-100% of the overland flow was attributed to the event water by [Steppuhn et al. \(1975\)](#) and [Laudon et al. \(2004\)](#). At the field scale, the implication of the runoff being dominated by overland flow is that the solute in the snowcover and its elution into meltwater are important, because it is that same solute and solvent (event water) that reach the edge-of-field.

2.2 P and N Cycling

Runoff export of phosphorous and nitrogen is influenced by the various hydrological processes in addition to numerous biogeochemical processes. In cold regions, subzero temperatures, snow, freeze-thaw cycling, and frozen soils impact biogeochemical processes and ultimately the runoff export of P and N. On nutrient rich agricultural fields, the role of isolated snow biogeochemical processes such as immobilization, assimilation and mineralization by soil microbes is diminished (and therefore, not discussed in this thesis), but can be significant for nutrient pools in regions that are not fertilized and in regions where the snowcover is deeper, home to more photosynthetic organisms, or receives more organic litter and debris such as in the boreal forest ([Jones, 1999](#); [Pomeroy et al., 1999](#)) or the Antarctic ([Hodson, 2006](#)).

2.2.1 Phosphorous

Phosphorus is one of the three macronutrients required for plant growth (nitrogen and potassium being the other two) and is found naturally in soils from the weathering of the Apatite minerals in the earth's crust. Inorganic phosphates from weathering are released into the biosphere via uptake by plants; re-precipitation with calcium (Ca), aluminium (Al), or iron (Fe); or carried via hydrologic pathways out to sea ([Holtan and Stuanes, 1988](#)). P in the environment occurs almost exclusively in its +5 oxidative state as orthophosphate (Ortho-P) or simply phosphate (PO_4^{-3}) and phosphate complexes ([Holtan and Stuanes, 1988](#); [Stevenson and Cole, 1999](#)). The distribution of these species is highly dependent on pH but the only bio-available P forms that exist in significant concentrations in soil water are H_2PO_4^- and $\text{H}_2\text{PO}_4^{-2}$ ([Stevenson and Cole, 1999](#)). Most of the P in soils is fixed or insoluble and exists as phosphate minerals, humus P, insoluble Ca, Al and Fe phosphates, and phosphates fixed by silicate minerals and colloidal oxides that require desorptive, dissolution or enzymatic processes prior to uptake into the biosphere (or bio-available) ([Holtan and Stuanes, 1988](#)).

Inorganic P is taken up by plants (*assimilation*) and returned to the soil in dissolved organic forms during decomposition and decay (*immobilization*) and the excretion of faeces/urine from plant eating animals which contains 50% - 80% of the P in the original plants ([Chambers et al., 2001](#)). P in the atmosphere is in the form of aerosols — 82% from wind erosion of mineral P, 12% organic P material, and 5% P from the combustion of fossil fuels ([Mahowald et al., 2008](#)) which may enter soil P pool during wet or dry deposition. Mineral and manure phosphate fertilizers, in addition to natural P inputs to soils, accumulate and enrich natural soil pools especially when applied to the land in excess of crop growth demands ([van Bochove et al., 2012](#)). According to the [Canada Fertilizer Institute \(2013\)](#), the prevalent forms of mineral P added to agricultural land in Canada are monoammonium phosphate (MAP, $(\text{NH}_4)\text{H}_2\text{PO}_4$) and diammonium phosphate (DAP, $(\text{NH}_4)_2\text{HPO}_4$). P cycles from soils to plants, to animals and back to soils (through the excretion of urine/dung) in a growing season whereas the passage of P from land to ocean sediments may take millions of years.

Soil Test P (STP) Phosphorous can be extracted from soil by a variety of methods. There is a positive correlation between the acidity of the extractant and the quantity of P measured by the method (Ketterings and Barney, 2010). The optimal P soil test for a particular soil is affected by the many factors determining soil P sorption/desorption such as fertilizer application; crop and tillage management practices; organic matter content; exchangeable Al, Fe, and Ca; pH; clay content and mineralogy; and initial soil P and soil P sorption capacity (van Bochove et al., 2012). Generally, western Canada uses the Kelowna and central Canada the OlsenP on calcareous soils, and both regions use the Mehlich III on neutral to acidic soils (van Bochove et al., 2012).

The rate at which P cycles through the soil is affected by soil pH, moisture content, temperature, and the availability of organic carbon (C) and other nutrients. A typical C:N:P ratio in soil humus is 140:10:1.3 and has been found to be consistent globally (Stevenson and Cole, 1999). The levels of bio-available P, therefore, in receiving waters are significant at much smaller concentrations than N and low levels of total dissolved phosphorous (TDP) are disturbing natural surface water ecosystems (Canadian Council of Ministers of the Environment, 2004).

2.2.2 Nitrogen

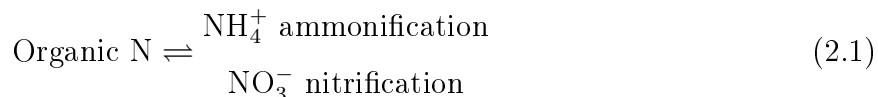
Nitrogen naturally constitutes about 80% of the earth's atmosphere (Galloway et al., 2004; Stevenson and Cole, 1999), is necessary for life, and is therefore found in both plant and animal tissues (Killham, 1994). The cycling of N from atmosphere to cellular tissues involves a series of oxidation - reduction (redox) reactions where protons are donated or accepted by various N species. N is transformed from organic species to inorganic species mediated by microbial bacteria. The processes that transform N into and from nitrate (NO_3^-) and ammonium (NH_4^+) in the soil, forms that are accessible for uptake by plants or transport by water, are the most relevant to agricultural N.

Leguminosae bacteria associated with certain plants *fix* nitrogen naturally and *assimilate* it as organic N for plant growth (Stumm and Morgan, 1996). N is also fixed during combustion of gasoline and fossil fuels, a significant contributor to atmospheric N and a source

of deposition of N to soils and lakes. Mineral fertilizers contribute an annual 25 – 34% (Galloway et al., 2004) of the N inputs to the global N cycle, of which 86% is used in the production of food (1995 Figure from Galloway et al. (2004)). According to the Canada Fertilizer Institute (2013), commonly used mineral N fertilizers are ammonia, Urea ($\text{CO}(\text{NH}_2)_2$), Ammonium Nitrate (NH_4NO_3), and Ammonium Sulphate ($(\text{NH}_4)_2\text{SO}_4$).

Soil N is assimilated by plants through *immobilization* of the mineral forms NH_4^+ and NO_3^- . N is returned to the atmosphere primarily through the *volatilization* of ammonia (NH_3) and *denitrification* of NO_3^- to N_2 . The presence of C is important in the N cycle. Many of the microbes that mediate N reactions are heterotrophs and require complex carbon compounds for energy. The ratio of C:N requirements for any given step of the N cycle varies with the soil organism and substrate type (Killham, 1994), with a global tendency to maintain a C:N balance between 50:1 and 200:1 (Schindler and Bayley, 1993).

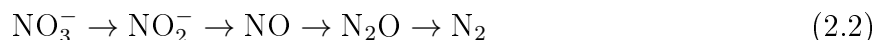
Mineralization and Immobilization *Mineralization* is the “soil process by which organic N is converted to mineral N” (Killham, 1994) and *immobilization* the reverse, or conversion of mineral N to organic forms (Equation 2.1).



Organic sources of N in the mineralization process include plant tissue, microbes and animals (notably urea from animal urine) (Killham, 1994). Plant residues left on a field provide both C for heterotrophic microbes and N for mineralization and uptake again by plants. Mineralization is a two step process comprised of the microbial mediated processes of *ammonification* and *nitrification*. Ammonification produces NH_4^+ which is immediately processed by one of volatilization, nitrification, vegetative uptake, microbial immobilization, ion exchange and clay fixation, or complexation with organic matter (Killham, 1994); therefore, NH_4^+ does not generally pool in the soil water but rather persists in the soil matrix much longer than NO_3^- . Mineralized NO_3^- is soluble and does not complex and form mineral precipitates nor does it adsorb on exchange sites in soils (Appelo and Postma, 2005) but rather pools in soil water and is readily hydrologically transported. Nitrification is sensitive to soil temperature, aeration (oxidizing conditions), soil moisture, pH, and the availability of NH_4^+ (Russel,

1988). Surplus NH_4^+ may occur in soils as a result of reducing conditions (poor aeration, i.e. basal ice), wet conditions that cause drainage of completed NO_3^- from the rooting zone, cold temperatures, and / or acidic conditions (Russel, 1988).

Volatilization and Denitrification Volatilization which is simply the “gaseous loss of ammonia from soil” (Killham, 1994) primarily involves the loss of NH_3 during fertilization with either ammonia or manure, and from animal urine patches. These losses can be more than 50% of deposited N (Killham, 1994; Stevenson and Cole, 1999). Dry, neutral to alkaline soils and windy atmospheric conditions favour volatilization (Killham, 1994) and are not uncommon on the prairies. Denitrification (Equation 2.2) is the “process by which nitrate replaces oxygen as the electron receptor in soil microbial respiration” (Killham, 1994) and ultimately returns N_2 to the atmosphere.



Conditions that reduce the ability of oxygen to be used during respiration, such as high moisture or saturated conditions with adequate NO_3^- supplies to substitute for oxygen, are necessary for denitrification. Deposits of C rich plant residues on anoxic wet soils will stimulate heterotrophic microbial activity and allow for denitrification. The process of reducing NO_3^- to N_2 is not always completed. The intermediary products of nitrite (NO_2^-), nitric oxide (NO) and nitrous oxide (N_2O) are unstable and less prevalent in the natural environment. Nitrite is highly carcinogenic to humans, the fate of nitric oxide is nitric acid (HNO_3) a major component of acid rain (Chambers et al., 2001) and nitrous oxide is a known greenhouse gas. Whether nitrous oxide is the end product or N_2 depends on pH, moisture content, pe, temperature and the availability of NO_3^- (Stevenson and Cole, 1999). Chambers et al. (2001) and Environment Canada (2008) report that 90% of NH_3 and 70% of N_2O Canadian emissions are from agricultural and related activities and Cameron et al. (2013) report that 62% of the total global nitrous oxide is contributed from agricultural land.

The primary sources of mobile N in soils are: mineralized manure and plant residues, biologically fixed N, atmospheric deposition of natural and industrial emissions of N, and, in agricultural soils, mineral fertilizers. An estimated 58% (Schindler et al., 2006) - 89%

([Chambers et al., 2001](#)) of the N added to agricultural land in Canada for food growth is harvested with the crops creating an annual excess of 11% - 42% that contributes to the accumulation of N in the global system. This excess N perturbs natural N cycles and nutrient balances in terrestrial and aquatic ecosystems.

2.3 Predicting Runoff Transport of P and N

Predicting the runoff transport of P and N can be separated into two steps — Step 1. quantify the field sources of P and N from the atmosphere, soils, and vegetation; and, Step 2. quantify the P and N that is eluted, dissolved, or diffused into and transported by the surface runoff. As discussed, in cold regions, it is the transport of P and N with meltwater that is the most significant event in nutrient runoff to receiving waters. The P and N on the field at the time of the melt must be quantified before the quantity of P and N that is transported can be predicted.

Prediction often involves modelling. Aptly described by [Arheimer and Olsson \(2003\)](#) with respect to water quality models:

A model is a numerical method to estimate water quality and [/ or] transport of substances which is based on various theoretical assumptions and generalizations.

A process-based model tries to “imitate nature by describing the physical and biogeochemical processes governing water quality” ([Arheimer and Olsson, 2003](#)).

2.3.1 Annual P and N Soil Budgets

Agricultural soils and their associated vegetation are nutrient rich sources that contribute to P and N in runoff as shown by the green and brown arrows in Figure [2.1](#). The blue arrow is related to P and N atmospheric deposition content in the rainfall, rain-on-snow (ROS), or snowmelt runoff. The annual period used here extends post harvest to post harvest (November 1 to October 31, generally). The input and output fluxes shown in Figure [2.1](#) represent the important input and outputs of P and N for an ungrazed Canadian Prairie agricultural field growing winter wheat. These fluxes are taken from the ranges provided in the literature and calculated explicitly in Sections [A.1](#) and [A.2](#) in Appendix [A](#).

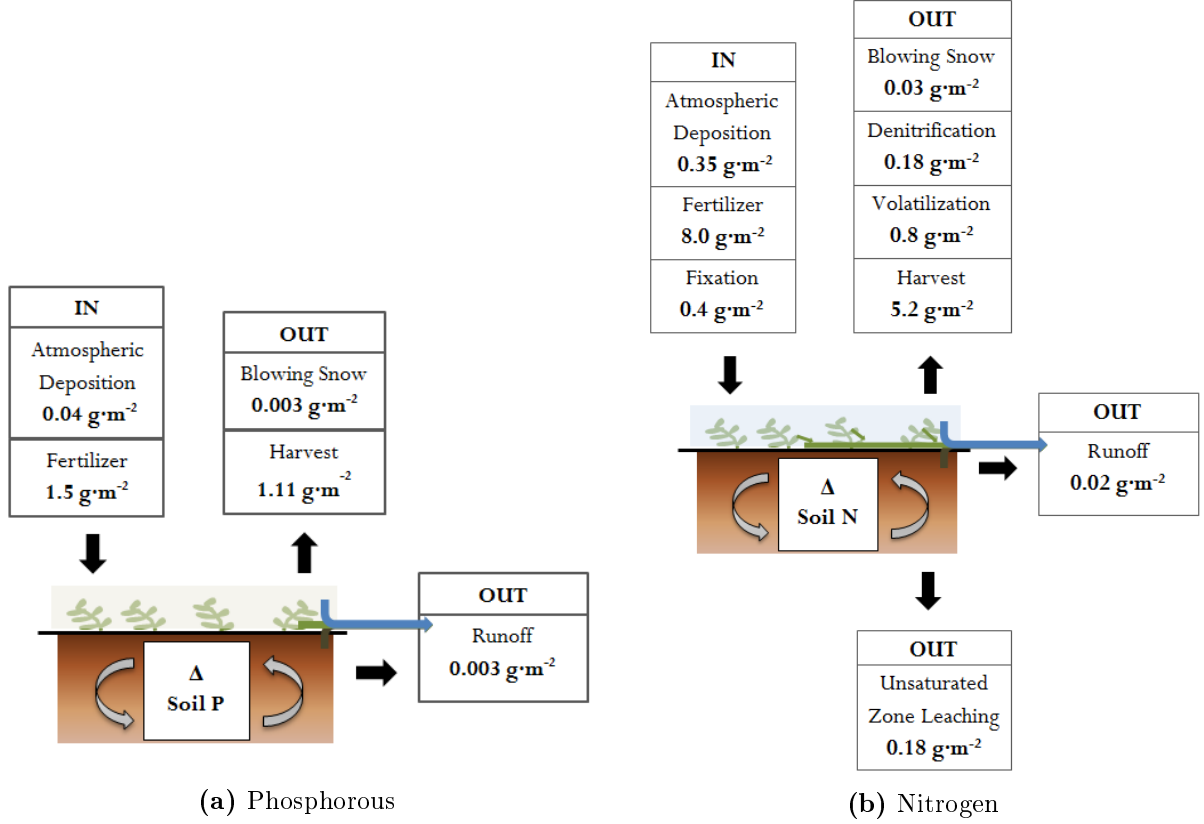


Figure 2.1: Annual field scale P and N inputs and outputs. The annual change in soil P (ΔSoilP) and N (ΔSoilN) on an annually tilled winter wheat crop grown on the Canadian Prairies can be determined based on the inputs and outputs in Equations 2.3 and 2.4. The input and output fluxes provided in this figure are taken from ranges provided in the literature as discussed in the text and calculated explicitly in Sections A.1 and A.2. The brown, green and blue arrows illustrate the fact that vegetation, soils, and precipitation sources all contribute to the P and N lost in the runoff.

This annual nutrient balance for P and N is represented with Equations 2.3 and 2.4, respectively:

$$\Delta\text{SoilP} = P_{atm} + P_{fert} - (P_{crop} + P_{blow} + P_{runoff}) \quad (2.3)$$

$$\Delta\text{SoilN} = N_{atm} + N_{fert} + N_{fix} - (N_{crop} + N_{blow} + N_{gas} + N_{leach}^{unsat} + N_{runoff}) \quad (2.4)$$

where P_{atm} and N_{atm} are atmospheric deposition, P_{fert} and N_{fert} fertilizer, P_{crop} and N_{crop} , harvest removals, P_{blow} and N_{blow} redistribution by blowing snow, and P_{runoff} and N_{runoff} , the snow meltwater, rainfall, or ROS runoff losses of P and N, respectively. In addition, N_{fix} crop fixation, N_{leach}^{unsat} , unsaturated zone leaching from the rooting zone, and N_{gas} losses due to nitrification and volatilization of N are included. For the Canadian Prairie, the practices

of forage cropping, minimum till, and winter wheat cropping have reduced the blowing snow losses significantly. Leaching losses of N down through the unsaturated zone do occur, mostly in wet years, but are typically not significant losses to the N in the rooting zone. On the Prairie, continuously cropped fields have shown little evidence of N leaching (Campbell et al., 2006) but rather enhanced uptake of N with optimized fertilization rates (Campbell et al., 1993).

As illustrated by the magnitude of the fluxes in Figure 2.1, the loss of P and N in runoff is small relative to the annual P and N budgets. As discussed, the forms of P and N of concern to agriculture and aquatic ecosystems are the inorganic mobile forms total dissolved phosphorous (TDP), nitrate-nitrite (NO_3), and total ammonia (NH_3). In a predictive context, quantification of these forms within soils can be achieved by modelling the cycles of P and N in the soil with a series of pools representing organic, inorganic, and mobile forms of P and N (Arnold and Fohrer, 2005; Arnold et al., 1998; Lindström et al., 2010; Wellen et al., 2015). This process of quantifying P and N in soils is subject to multiple sources of error from estimating the inputs and outputs to the soils to determining the rates at which the soil cycling proceeds in a particular setting.

Using Equation 2.3, the annual balance of P on this field would be estimated at $+0.42 \text{ g} \cdot \text{m}^{-2}$ slightly less than the range of $0.8 \text{ g} \cdot \text{m}^2 \cdot \text{y}^{-1}$ to $6.9 \text{ g} \cdot \text{m}^2 \cdot \text{y}^{-1}$ for the Canadian Prairie as reported by van Bochove et al. (2012). According to Equation 2.4, the annual balance for N on this field would be $+2.3 \text{ g} \cdot \text{m}^{-2}$, a residual that is typical of the national rates as calculated by Yang et al. (2007a).

2.3.2 Nutrient Legacies

The surplus application of P and N, as presented in Section 2.3.1, has been ongoing on agricultural land for years, the result of which has led to a build up or legacy of nutrients in soils that act as a buffer to short term changes in the P and N inputs to agricultural soils (Kleinman et al., 2011a,b). This leads to the theory of invariant chemical supply (Basu et al., 2010, 2011; Godsey et al., 2009; Thompson et al., 2011) where hydrology not chemistry is the main limiter in the transport of P and N. According to Basu et al. (2011) such behaviour, “leads to a strong positive linear correlation between annual exported load and

stream discharge” and therefore simplifies the prediction of annual chemical exports from a hydrological and chemical solution to a hydrological solution only. This strong linear correlation between exported load and discharge simplifies prediction of annual loads; but, it must be established how many years of surplus fertilization are required before a nutrient legacy emerges and when this legacy would be depleted (Basu et al., 2010). This is a major challenge to predicting runoff P and N based solely on hydrology.

The existence of an invariant chemical supply is assessed empirically based on the absence of a relationship between observed concentrations, c , and stream discharge, q . The absence of a $c - q$ relationship is one of several, progressively more restrictive, metrics used to identify heavily managed (fertilized) catchments with an invariant chemical supply or constant concentration exports through a full range of flows (Basu et al., 2010, 2011; Godsey et al., 2009; Thompson et al., 2011).

2.3.3 Field Sources of P and N

The sources of P and N on a Canadian Prairie field during a melt as illustrated in Figures 2.1 and 2.2 are atmospheric (in the snow), soil, and vegetation P and N. The inorganic mobile P and N solutes are referred to, as in Section 1.1, as TDP (total dissolved phosphorous), NO_3 (nitrate-nitrite), and NH_3 (total ammonia).

Snow

The content of P and N in a Canadian Prairie snowcover on an ungrazed field is primarily sourced from the atmosphere. Nutrient contents of snowcovers can, therefore, be estimated from bulk rates of atmospheric deposition which for N are found readily in the literature based on both observations and model predictions. As presented in Section 2.1.1, the literature also provides P deposition data, but it is less commonly measured.

Soil

Soil nutrients require the prediction of transformations between the various pools of nutrients as impacted by nature and agriculture. The five most commonly used models in agricultural applications in North America and Europe all use pools with parameters that control the rate

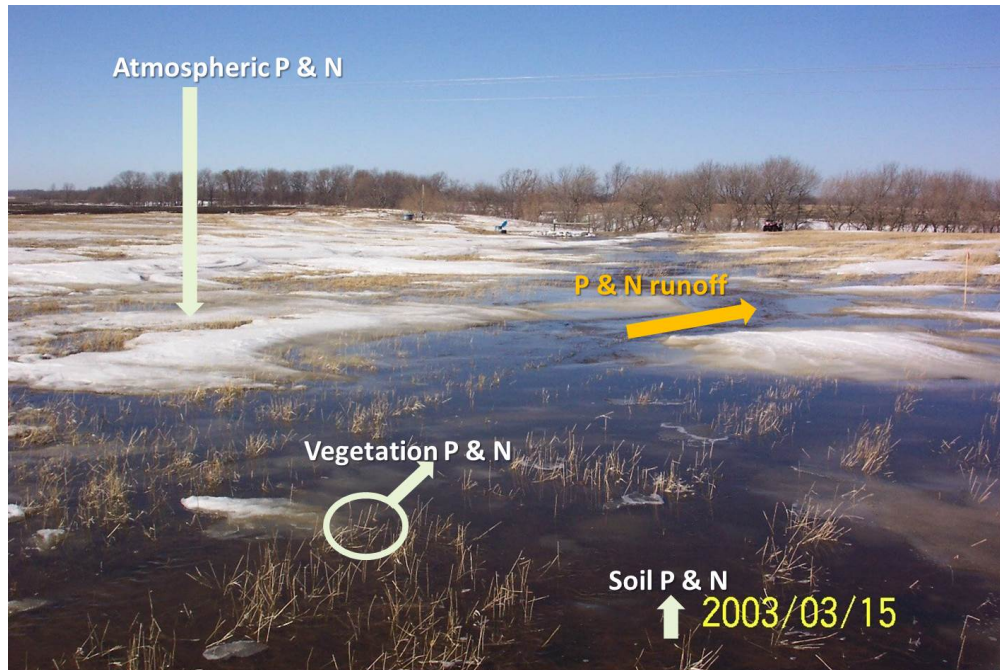


Figure 2.2: Prairie snowmelt hydrochemistry. This photo illustrates how the soil, snow (with its atmospheric P and N inputs), and vegetation sources of P and N interact during a snowmelt runoff event.

at which various transformations between these organic and inorganic pools of P and N occur (Wellen et al., 2015). Over the winter, inorganic N can build up in snow-covered agricultural soils due to the mineralization of organic matter (Austnes et al., 2008; Campbell et al., 2005; Groffman et al., 2001), reduced root uptake (Matzner and Borken, 2008), and gaseous N trapped under basal ice or the pore spaces in frozen soils (Risk et al., 2013; van Bochove et al., 1996, 2001). At spring, meltwater will transport mobile N off the field to streams and release gaseous N to the atmosphere. As discussed, NO_3 is in the soil solution and readily mobilized during melt whereas sources of NH_3 in the runoff are likely from the more mobile fertilizer amendments, vegetation, snow, and mineralized organic matter not typically quantified in soil N (Flaten, 2014, pers. comm.). Agricultural management practices such as fall tillage can also impact the rates of N cycling:

- The act of tilling the soil releases NO_3 via mineralization and nitrification of soil organic material (Campbell et al., 2008; Tiessen et al., 2011). The tillage of perennial crops has also been known to release a large flux of NO_3 (evident in the NO_3 front slowly leaching down through the prairie unsaturated zone following the initial tillage of the prairie

soil in the 1920s (Campbell et al., 1975; Si and de Jong, 2007)). Tillage of fields near Central Butte, SK, after 10 consecutive years of minimal tillage, led to increased NO_3 concentrations in the near-surface layers (0 – 5 cm) of soils (Baan et al., 2009). Tiessen et al. (2010) found a significantly elevated soil NO_3 content in the 0 – 15 cm layer of an annually tilled field when compared with a reduced tilled field. This increase was attributed to mineralization in the tilled soils. Baan et al. (2009) looked at impacts to soil NO_3 levels after tillage of a long term perennial forage crop whereas Tiessen et al. (2010) looked at annual differences in soil NO_3 between minimal and annual tillage; both important in demonstrating the relationship between tillage and mineralization.

For P, potential contributors to the pool of mobile TDP in cold regions include freeze thaw cycles in soils that perturb soil aggregates (Blackwell et al., 2009; Fitzhugh et al., 2001; Özgül et al., 2012) and microorganisms (Roberts et al., 2012); the reduced soil moisture contents of frozen soils (Özgül et al., 2012); and the reduced plant root uptake in cold temperatures (Fitzhugh et al., 2001). Adjusting transformation rates (set by parameters in predictive nutrient models) in the P and N cycles will facilitate the prediction of soil TDP, NH_3 , and NO_3 in soils at the time of runoff.

Vegetation

Vegetation serves as a source, in addition to the soil and atmospheric deposition, of mobile P and N. Winter wheat, forage, and reduced tillage practices have increased the amount of stubble and growing vegetation resident on fields during fall, winter, and spring melt. Freeze-thaw cycling, fresh forages, and actively growing vegetation (forages and winter wheat) have been shown to further enhance the amount of P and N that leaches from this vegetation (Bechmann et al., 2005; Elliott and Henry, 2009; Elliott, 2013; Joseph and Henry, 2008; Liu et al., 2013a; Miller et al., 1994; White, 1973). Freeze-thaw cycles (FTC) cause cells of soil bacteria, roots, and vegetation to lyse and leach TDP, NH_3 , and NO_3 (Bechmann et al., 2005; Elliott and Henry, 2009; Elliott, 2013; Joseph and Henry, 2008; Liu et al., 2013a; Miller et al., 1994; White, 1973). Diurnal FTC amplitudes of $> 10^\circ\text{C}$ have been associated with enhanced nutrient release from successive FTCs up to the point (6-8 FTCs) where, as a result of the repeated damage to cellular tissues, all the biomass P becomes water extractable

(Bechmann et al., 2005). Milder FTCs do not show enhanced leaching of P and N, but rather a consistent leaching trend in up to 11 successive FTC/leaching experiments (Joseph and Henry, 2008). Additionally, the P leached in the more extreme FTCs performed on rye grass crops established in Pennsylvania soils (Bechmann et al., 2005) were noted to be extreme values as leaching experiments on more cold hardy plants leach less with the same FTC amplitude and durations (Miller et al., 1994) and due to the optimal growth conditions of the study offer potential leaching rather than field leaching rates (Bechmann et al., 2005). Elliott (2013) used a laboratory bucket study to investigate the interaction of the residue and active soil layers during a three cycle FTC laboratory experiment performed on winter wheat and wheat stubble using extreme FTCs similar to Bechmann et al. (2005). Elliott (2013) showed that the soil will moderate TDP and NH_3 leaching whereas it will greatly enrich NO_3 losses. Predicting the runoff losses of P and N contributed by the pool of vegetation leached nutrients on fields, therefore, requires interpretation of these laboratory studies for use in the Canadian Prairie.

2.3.4 Transport of Field P and N

It has been established in the literature (Buda et al., 2009; McDowell, 2012; Sánchez and Boll, 2005; Wellen et al., 2015) and applied in some predictive nutrient models (Lindström et al., 2010; Viney and Sivapalan, 2000) that the rainfall runoff pathways, either saturation excess or infiltration excess runoff, mobilize nutrients (especially P) from soils differently. The simulation of saturation excess flow involves the interaction of landscape topography and soils (Gérard-Marchant et al., 2006; Hively et al., 2006) to identify critical source areas in the landscape that can contribute a large proportion of the nutrients during runoff (Buda et al., 2009). In addition, the increased interaction between soil and runoff associated with saturation excess flow is thought to facilitate the release of P from the soil matrix. Linear relationships related to the measured soil phosphorous content and contact time have both been reported in the literature (Amarawansa, 2013; Sharpley, 1995, 1985).

The near surface soil, 0 – 5 cm, P content has been found to be linearly related to the amount of TDP in rainfall runoff (Sharpley, 1995, 1985). This relationship is often site specific as land management, slope, and soil type (physics and chemistry) influence the TDP

in the runoff (Sharpley, 1995). Linear regressions for OlsenP [mg/kg] and dissolved reactive phosphorous (DRP) for Arkansas Ultisols took on the shape of $y = mx - b$ where x is the OlsenP [mg/kg], y the DRP [mg/l], and m the slope and b the y-intercept coefficients of the regression, specific to the site and soil (Pote et al., 1999). The ability of x to explain y was quantified with an r^2 between 0.86 and 0.94.

P has also been shown to release with increased contact or ponding time (Amarawansha, 2013), a condition that can produce saturated and anaerobic soils. Contingent on the antecedent hydrological conditions and size of the event, both snowmelt and heavy rainfall on the prairies can lead to ponding or flooding (Water Management and Hydrology Section, 2012). In a laboratory study, Amarawansha (2013) found that ponding time induced anaerobic conditions that enhanced the release of DRP from most Manitoba soils (except clayey ones). In this study, DRP content in the ponded waters was observed to comprise 75% and 83% of TDP for unamended and fertilized soils, respectively (Amarawansha, 2013, Table 2.2). Using a partial least squares linear regression analysis, Amarawansha (2013, Table 3.9) found a relationship (Equation 5.9) with limited predictive certainty ($r^2 = 0.42$) for the duration of ponding time and the release of DRP from soils during summer precipitation events. This relationship is specific to the calcareous soils of Manitoba and would be affected by site hydrology, land management, and ponded water temperature (this linear regression was based on summer water temperatures which tend to be more reactive than colder spring temperatures (Sánchez and Boll, 2005)).

As with P, the interaction of runoff with NO_3 in soils is often limited to a very thin surface layer. Knisel (1980a,b) and others (Arnold and Williams, 1987; Young et al., 1987) assume this surface layer to be 10 mm and unlike with P, assume any infiltration that occurs prior to the generation of surface runoff will also flush this surface layer via convective transport of the solute with the infiltrate:

$$\frac{dc}{dt} = k_1 f(t)(c_r - c) \quad (2.5)$$

where c and t represent concentration and time, k_1 rate constant for downward NO_3 movement, c_r the concentration of NO_3 in the rainfall, and $f(t)$ is the infiltration rate. To determine the concentration in the soil, c_1 , after infiltration this expression can be integrated

and evaluated with total infiltration, $F = f(t)t$. This yields Equation 2.6:

$$\int_{c_o}^{c_1} \frac{dc}{(c_r - c)} = \int_0^t k_1 f(t) dt$$

$$c_1 = (c_o - c_r)e^{-k_1 F} + c_r \quad (2.6)$$

where c_o is the concentration of NO_3 in the soil. For the step-by-step evaluation of Equation 2.6 see Section A.3. To determine what concentration of NO_3 is transferred to surface runoff, a partitioning coefficient is calculated, a common practice in the simplification and conceptual rendering of complex physical processes.

Lindström et al. (2010) and Viney and Sivapalan (2000) distinguish saturation excess and infiltration excess runoff concentrations for both P and N with saturation excess flows taking on the concentration of the solute in the soil water and infiltration excess flows maintaining the concentration of solute in the precipitation. NO_3 , as discussed, is readily mobilized whereas ionized NH_3 is relatively immobile from soils and can be modelled as immobile with respect to leaching and runoff from soils (Johnsson et al., 1987) and TDP is somewhere between.

Unlike saturation excess and infiltration excess flowpaths during rainfall runoff, frozen soil infiltration flowpaths during snowmelt runoff on the Canadian Prairie as described by Granger et al. (1984), to this author’s knowledge, have not been used in the prediction of P and N concentrations during runoff.

2.4 Modelling P and N Transport

Computer models can be useful tools to assist in the prediction of agricultural management practice performance when implemented in different agricultural fields, sub-watersheds, or watersheds. This only works if the hydrological and nutrient processes in the computer model represent reality. The outcome of using a model not based on reality may result in the models that produce simulations that are in direct contradiction to observations (Liu et al., 2014a; Yang et al., 2014). It has been established that most of the existing nutrient models lack representation of important cold regions processes (Deelstra et al., 2009; Han et al., 2010; Radcliffe et al., 2009; Wellen et al., 2015) such as frozen soils runoff, freeze-thaw cycling,

and snowcover redistribution. [Lindenschmidt and Ollesch \(2004\)](#) found that improvements in the hydrological platform improve the ability to predict solute transport.

A computer model can help to identify the significant control(s) on the runoff export of P and N from a Canadian Prairie field. As discussed in Section 2.1, some of the important hydrological processes related to the transport of P and N at the field scale on the Canadian Prairie are rainfall, rain-on-snow, and snowfall; wind redistribution of snowcovers; soil water movement; and frozen soil runoff. In addition, hydrological phenomena on the Prairies such as variable contributing areas, frozen soils, and basal ice are important. Hydrological conditions are dynamic and current hydrological states are related to past (antecedent) hydrological states, therefore continuous (rather than event based) simulation of hydrology is needed. Failing to consider antecedent hydrological conditions would render impossible the ability to distinguish saturation and infiltration excess runoff ([Buda et al., 2009](#)), in addition to the prediction of large scale hydrological events, such as the Prairie floods of 2011 ([Water Management and Hydrology Section, 2012](#)). To represent the Canadian Prairie at the field scale, the landscape elements in the hydrological model need to provide routing or connectivity by aerodynamic and overland flowpaths, as snowcover redistribution by wind and runoff drainage in the absence of a stream network are both significant flowpaths. In a meta-data analysis of peer reviewed nutrient water quality modelling studies, [Wellen et al. \(2015\)](#), reported that of the 257 studies published between 1992 – 2012 very few looked at individual flowpaths to the stream and only 4% simulated overland flow. Many models lacked the time scale resolution to do so, as snowmelt, the ionic pulse, and flowpaths change on a hourly time step rather than the daily or monthly time step that 92% of catchment scale models tend to use ([Wellen et al., 2015](#)).

There are many catchment scale hydrological models in use today. Three semi-distributed catchment scale process based models considered for the purposes of this research are SWAT ([Arnold and Fohrer, 2005](#); [Arnold et al., 1998](#)), HYPE ([Lindström et al., 2010](#)) and CRHM ([Pomeroy et al., 2007b](#)). SWAT and HYPE are both daily time step models — SWAT was considered for its frequency of use in agricultural catchments worldwide and HYPE for its open source code and focus on cold regions processes. CRHM ([Pomeroy et al., 2007b](#)) was considered for the flexibility of its spatial and temporal resolution and its focus on cold regions

processes, in addition to the access to key model development personnel at the University of Saskatchewan.

Soil Water Assessment Tool As a research tool, the USDA Agricultural Research Service Soil and Water Assessment Tool (SWAT, [Arnold and Fohrer \(2005\)](#); [Arnold et al. \(1998\)](#)) has been applied on the Canadian Prairie ([Yang et al., 2008](#)), specifically the South Tobacco Creek watershed ([Watershed Evaluation Group Department of Geography University of Guelph, 2013](#); [Yang et al., 2007b](#)). It is the most commonly used model in North American and European agricultural catchments ([Wellen et al., 2015](#)). Recent developments to SWAT, as yet unpublished, to include cold regions processes such as snow redistribution by wind and frozen soil to create canSWAT have improved the performance of SWAT on the Canadian landscape specifically in South Tobacco Creek ([Watershed Evaluation Group Department of Geography University of Guelph, 2013](#)). SWAT handles runoff with the empirical SCS Curve Number (CN), a method lacking physical basis, and developed for climate conditions in the United States. It also employs the empirical degree day method for estimating melt. In modelling DP transport in a German river basin, [Lindenschmidt and Ollesch \(2004\)](#) found, in agreement with a review of models by [Radcliffe et al. \(2009\)](#), that physics - based hydrological models are required to determine how different runoff components and their spatial and temporal variations within a basin because mechanisms such as infiltration and saturation excess overland flow affect DP transport. The use of the CN does not allow any such determination. A recent iteration of SWAT made some modification to simulate saturation excess flow using the CN and soil topographic index ([Woodbury et al., 2014](#)).

Hydrological Predictions for the Environment The Hydrological Predictions for the Environment model (HYPE, [Lindström et al. \(2010\)](#)) is an open source integrated hydrological and nutrient model. HYPE was developed by the Swedish Meteorological and Hydrological Institute with a spatial resolution of $\geq 10 \text{ km}^2$ and a focus on nutrient processes, predictions in ungauged basins, and efficient computational structure ([Lindström et al., 2010](#)). It was developed based on the experience of the developers with nutrient models such as HBV-NP ([Lindström et al., 2005](#)), SOILN ([Johnsson et al., 2002](#)), ICECREAM ([Tattari et al., 2001](#)) and ANIMO ([Groenendijk and Kroes, 1999](#)) with the intent of striking

a balance with parsimony and necessary complexity. The Arctic-HYPE project simulates climate impact on the 23 million km^2 Arctic Ocean watershed which includes a vast chunk of Canada some of which is prairie landscape (SMHI, 2015). HYPE captures key cold regions processes such as snow accumulation and melt, frozen soils, overland flow, soil water flow, macropore flow, and glacier melt. Blowing snow and the related aerodynamic connectivity between landscape elements is not provided whereas stream, groundwater and overland flows are. Snowmelt is accomplished using the degree day method, a method without physical basis, that fails to incorporate the dynamics of the melt as affected by factors such as slope, latitude, atmospheric variables, and albedo (Gray and Landine, 1988).

Cold Regions Hydrological Model Platform The Cold Regions Hydrological Model (CRHM) platform developed at the University of Saskatchewan is one hydrological model that both captures the major cold regions prairie hydrological processes (Pomeroy et al., 2007b) and has been applied successfully with minimal or no calibration (Fang and Pomeroy, 2008, 2009; Fang et al., 2010; Mahmood et al., 2015) to catchments on the Canadian Prairie. The CRHM platform contains models of the above mentioned prairie hydrological processes and other cold regions processes based on decades of field research. Experience has shown that a model such as the CRHM suite where the physics of processes are well represented can be applied in many different basins with meaningful outcomes in spite of different and changing climatic conditions (i.e. Canadian Prairie (Pomeroy et al., 2011); Canadian mountain basins (Pomeroy et al., 2011); and cold regions worldwide (Krogh et al., 2015)). Fang et al. (2010) performed a simulation on an agricultural prairie catchment in Smith Creek, SK and proved that wind distribution of snow, snow melt, changing frozen soil moisture content and the resultant stream flow could be captured with CRHM without calibration on the basin.

CRHM is a modular platform that allows the modeller to implement various processes with the appropriate equations (or models) recognizing that one model construct is not suitable in all environments, i.e. mountains and prairie environments. A process(es) may be added or subtracted in model *falsification* to determine its impact on the simulation. This flexibility and transparency in model construction allows the modeller to develop a good understanding of the processes, the various algorithms that represent them and the impacts

of both on catchment hydrology.

Field scale snowmelt runoff simulation is the focus of this research. HYPE and SWAT both utilize empirical formulae to estimate the melt (degree day method (HYPE, SWAT)), runoff generation (CN (SWAT)), and lack accounting for blowing snow (HYPE, SWAT) and frozen soils (SWAT) whereas CHRM has a physics-based representation of the melt energetics, blowing snow, frozen soils and runoff generation, a robust approach for simulating field scale snowmelt runoff. CHRM lacks any nutrient functionality and HYPE, having been designed specifically for application in cold regions of the world, shows promise as a nutrient model. The necessary nutrient functionality can be added to CHRM in this research through a combination of inductive approach (Dornes, 2013; Klemes, 1983; Pomeroy et al., 2013) based on the data and (ultimately) nesting within a fully functional nutrient model such as HYPE. Therefore, the resident technical expertise, at the University of Saskatchewan, with the CHRM software package and its merit as a cold regions hydrological model render it a tool suitable for the purposes of identifying the significant control(s) on the runoff export of P and N from a Canadian Prairie field.

2.4.1 An Inductive Canadian Prairie Nutrient Model

Predicting P and N transport in snowmelt runoff from Canadian Prairie agricultural fields involves the incorporation of vegetation as a source of nutrients in runoff (Section 2.3.3), in addition to the identification of how the different meltwater runoff pathways impact the transport of solutes in meltwater runoff (Section 2.3.4), neither approach yet incorporated as standard practice in nutrient models. There is an approach to predictive modelling, driven by analyses of field data, termed inductive modelling where field data based on research in a catchment typical of the cultivated Canadian Prairie could help develop a predictive response to vegetation and meltwater flowpaths on TDP, NH_3 , and NO_3 concentrations in surface runoff. This inductive approach to modelling avoids theoretical assumptions as much as possible in the initial stages of analysis and infers a model structure from observational data (Dornes, 2013; Klemes, 1983). Integrating this inductive model with CHRM, a deductive model “describing a hydrological system by deterministic mathematical equations founded on

well-known scientific laws” ([Dornes, 2013](#)) reduces the predictive uncertainty of the overall model and is sensitive to the limitations of the data ([Dornes, 2013](#); [Pomeroy et al., 2013](#)).

CHAPTER 3

FIELD SITES AND DATA

The South Tobacco Creek watershed on the Canadian Prairie is a research basin with a multi-year record of edge-of-field (EOF) hydrochemistry data, recorded meteorological history, and a corresponding record of agricultural activities that includes five BMPs, namely retention ponds, small reservoirs, minimum tillage, conversion to forage cropping, and riparian buffer strips. Extending back to 1992 and up to present day much has been researched and published on the land use — water quality relationships gleaned from the intensive event-based water quality monitoring and detailed field-by-field documentation of the agricultural activities performed by the farmers in the watershed (Glozier et al., 2006). Glozier et al. (2006) reported the EOF hydrochemistry observations to be higher in dissolved nutrients (especially at snowmelt) than the downstream 2nd and 3rd order stream sites, and that the downstream 2nd order site exhibits increased dissolved nutrient concentrations over time, a concern for downstream Lake Winnipeg. Agricultural land under forage cropping doubled from 6% to 12% over this period and land under minimal tillage practices remained steady at 15% (Glozier et al., 2006). Forage cropping (Liu et al., 2014a) and minimum tillage (Tiessen et al., 2010) specific research, have both identified vegetation as a potential source of the observed elevated dissolved nutrients during runoff events, particularly at snowmelt, the dominant runoff event of the year.

This field scale and event based data set is an appropriate starting point for the development of a nutrient hydrology model for the cultivated Canadian Prairie. The availability of an extensive agricultural record of land use activities, meteorological record, and EOF hydrochemical observation record facilitate the development of a model capable of predicting the effects of changes in agricultural management practice and changes in climate on EOF hydrochemistry. Additional research in South Tobacco Creek regarding the use of the 5 BMPs together (Li et al., 2011), small reservoirs (Tiessen et al., 2011), and tillage practices

(Liu et al., 2014b) has been published and shows promise for the future expansion of the model beyond the BMPs of forage cropping and minimum tillage.

Data were compiled in collaboration with Dr. Jane Elliott, Water Quality Specialist with Environment Canada, from the forage and minimum tillage projects in the 73 km^2 South Tobacco Creek watershed (49°20'N, 98°22'W) in southeastern Manitoba, 150 km southwest of Winnipeg, MB; specifically from two subwatersheds within South Tobacco Creek namely Sub-basin2 (2.01 km^2) (Mahmood et al., 2015) and Twin (0.11 km^2) (Figure 3.1).

Runoff monitoring and water sampling sites have been maintained in Sub-basin2 since the 1990s, with a total of 19 flow and 17 water quality sites monitored today, most of which were established in 2004 with the Agriculture and Agri-Food Canada (AAFC) Watershed Evaluation of Beneficial Management Practices (WEBs) program (Agriculture and Agri-Food Canada, 2010b). In addition to EOF hydrochemistry event sampling, soil and snow sampling programs were carried out once a year. The Twin watershed, adjacent to Sub-basin2 and comprised of fields 10 (0.04 km^2) and 11 (0.06 km^2), was monitored intensively from 1993-2007 to compare reduced and conventional tillage impacts on water quality (Tiessen et al., 2010). Sub-basin2 is a producer owned and operated farm comprised of cattle and cereals and oilseed operations with a consistent historical record of agricultural activities for fields 3 (0.08 km^2), 4 (0.02 km^2), 7 (0.13 km^2) and 9 (0.10 km^2) and the subject of research related to conversion to perennial forages (Liu et al., 2014a).

3.1 Site Description

The climate in South Tobacco Creek (Figure 3.1) is classified as humid continental receiving an average 550 mm of precipitation annually of which an average 25%-30% is snowfall. Annual average temperature is 3°C with highs of 40°C in the summer and lows of -40°C in the winter season (Environment Canada, 2015a). The soils are mostly Dark Gray Chernozemic clay - loams formed on moderately to strongly calcareous glacial till which overlays shale bedrock (Li et al., 2011; Soil Classification Working Group, 1998). South Tobacco Creek watershed is located in the Pembina Hills on the edge of the Manitoba escarpment and its creek drains into Morris Creek, the Red River and eventually Lake Winnipeg. South Tobacco Creek is ephemeral with flows occurring at spring melt but typically not persisting

throughout the summer. Small dams in the area supply water needs to farmers in addition to attenuating peak flows in the creek. Groundwater aquifers are deep, saline and overlain by a clay layer (Gottfried et al., 2004).

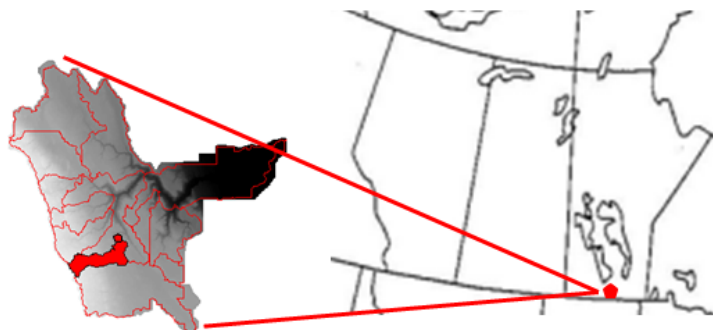


Figure 3.1: South Tobacco Creek Watershed Map. Location of South Tobacco Creek watershed and the Twin and Sub-basin2 watersheds within.

3.2 Sampling Design

A field scale data set with a comprehensive record of event flows and concentrations would help inform the development of a model to predict edge-of-field (EOF) runoff TDP, NH_3 , and NO_3 from fields using forage and minimum tillage practices. Sub-basin2 fields 3, 4, 7 and 9 and Twin fields 10 and 11 (Figure 3.2) were chosen for this task as minimum tillage and forage cropping were employed on these fields at the same time as the record of EOF flows, EOF concentrations, and agricultural record were maintained. All six fields have an extensive hydrochemistry record for both snowmelt and rainfall runoff events. The records for 2009-2012 for F3 and F4, 2005-2012 for F7 and F9, and 2004-2012 for F10 and F11 were used for this research. Annual soil samples (2005-2012) and snow samples (2006-2012) taken on the Twin and Sub-basin fields 3 and 4, enhance the data set and remove several unknowns from the modelling process, allowing for further simplification of the initial modelling development process as neither snowcover chemistry nor soil chemistry would have to be predicted.

The methods used to gather and analyse these hydrochemistry, soils, and snow chemistry data are discussed in the sections below.

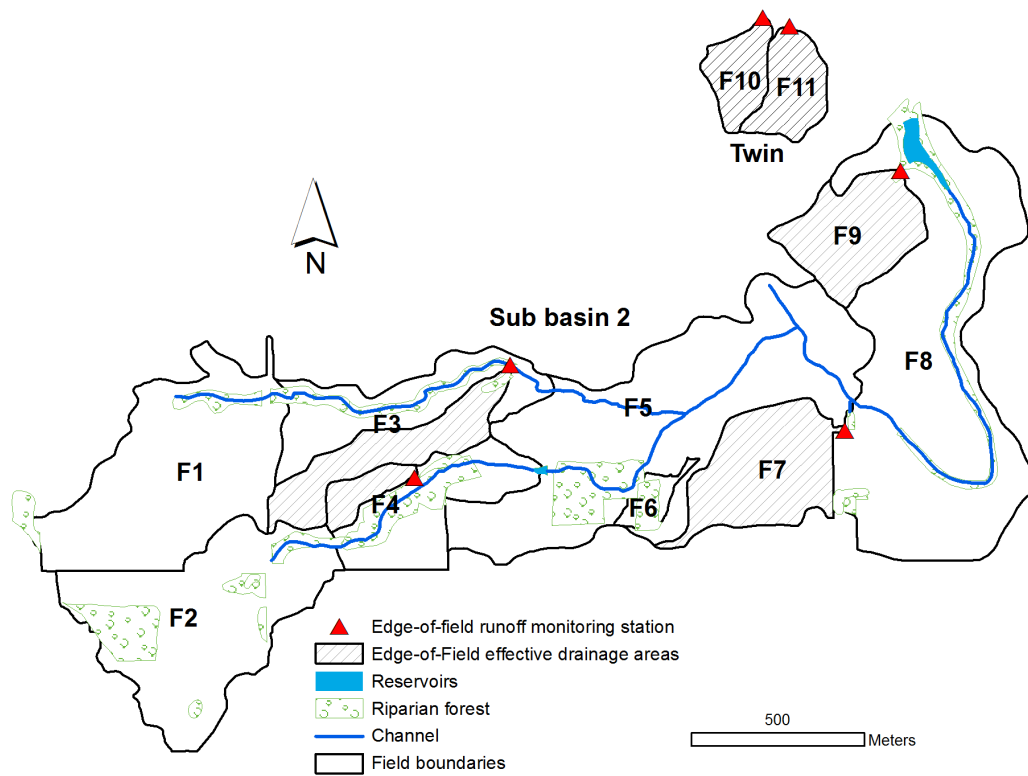


Figure 3.2: Sub-basin2 and Twin Fields. Sub-basin2 and Twin watershed field numbers and monitoring stations.

3.2.1 Agricultural Record

The agricultural record for Sub-basin2 fields 3, 4, 7, and 9 (Tables 3.1 and 3.2) and Twin fields 10 and 11 (Table 3.3) used in this research includes tillage type and dates; fertilization type, rate and date; seeded crop and seeding date; and harvest date and yield. Using this record, the cropping practices were binned into three general categories for this research: perennial forage (forage), minimum tillage cereal grains and oilseeds (MT), and annually tilled cereal grains and oilseeds (AT). Forage crops are perennial alfalfa - timothy mix or green feed oats grown for multiple years in sequence. The forage crops were baled at harvest and not subject to tillage or fertilization once established. Minimum tillage refers to crops

that receive minimum tillage other than during the seeding operation. Annually tilled crops are subject to some degree of tillage disturbance either in the fall and/or spring in preparation for seeding. In the agricultural record, tillage disturbance was classified based on the amount of crop residue that a particular implement left on the field. Crop residue values assigned on these fields were 0.60, 0.70, 0.8, and 1.0 representing disturbance of a heavy duty cultivator, a light duty cultivator, a harrow or anhydrous rig, and no tillage pass respectively. In this research, the crop residue values assigned to each of the two fall tillage passes were further multiplied to create an overall assessment of fall tillage disturbance, termed *tillage*. The *tillage* values range between 0 and 1: $tillage < 0.6$ indicates conventionally disruptive tillage, and $0.6 \leq tillage < 1.0$ refers to reduced tillage. Minimum tillage fields and forage crops both have $tillage = 1.0$ for the fall *tillage* assessment.

The activities on the field (i.e. tillage and fertilization) following harvest and prior to snowfall are related to the farming activities in the subsequent year. For that reason, a farming year, as referred to in this thesis, extends post harvest to post harvest (generally November 1 to October 31) and is referred to by the year in which seeding and harvest take place.

3.2.2 Hydrochemistry Sampling

Runoff flow sampling

Edge-of-field flows were measured in basins constrained by constructed soil berms using circular flumes (fields F3, F7, and F9; Figure 3.3) or compound angle v-notched weirs (fields F4, F10, F11; Figure 3.4). The water level above the notch (weir) or above the base of the culvert (flume) was measured at 5 - 15 minute intervals with an ultrasonic sensor (Figure 3.4) and a data logger (Tiessen et al., 2010). Flow rates were later calculated based on the air temperature corrected measured heads using traditional hydraulic calculation methods (Smith, 1985). Manual water levels were taken to verify the sensor data.

Precipitation events were measured with tipping bucket rain gauge located on the Twin watershed (Tiessen et al., 2010).

Observed EOF runoff for the Sub-basin2 and Twin fields is shown as 15 minute flows in Appendix B Figure B.2 and cumulative runoff in Figure B.3. The Twin fields have flows

Table 3.1: Sub-basin2 Fields 3 and 4 Agricultural Record. Abbreviations: Heavy Duty Cultivator (HDC), Light Duty Cultivator (LDC), Diammonium Phosphate (DAP), and date formats (week(wk) / month / year).

Field	Year	Fall Tillage (crop residue fraction)	Spring Tillage	Crop Seeded Date	Yield Harvest Date kg/ha	Fall N Date kg/ha	Spring N Date kg/ha	Spring P Date kg/ha	Fertilizer Type Fall/Spring
3	2003	HDC (0.6) + Anhydrous Rig (0.8)	LDC (0.7) + Harrow (0.8)	Canola 2wk/5/2003	2218 4wk/8/2003	78.5 1wk/10/2002	78.5 2wk/5/2003	12.2 2wk/5/2003	Urea/DAP
3	2004	HDC (0.6)	LDC (0.7)	Oats 2wk/5/2004	7392 4wk/9/2004	0.0	56.0 2wk/5/2004	14.7 2wk/5/2004	-/DAP
3	2005	HDC (0.6)	LDC (0.7)	Flax/Linola 4wk/5/2005	1344 4wk/9/2005	0.0	53.8 3wk/5/2005	0.0	-/Urea
3	2006	Harrow (0.8) + HDC (0.6)	LDC (0.7)	Wheat 2wk/5/2006	2352 3wk/8/2006	0.0	72.9 with seed + 1wk/5	4.9 with seed	-/DAP + Urea
3	2007	HDC (0.6)	LDC (0.7)	Canola 2wk/5/2007	2352 1wk/9/2007	100.9 3wk/10/2006	22.4 with seed	9.8 with seed	Urea/DAP
3	2008	HDC (0.6)	LDC (0.7)	Wheat 1wk/5/2008	3494 4wk/8/2008	84.1 4wk/10/2007	11.2 with seed	4.9 with seed	Urea/DAP
3	2009	HDC (0.6)	LDC (0.7) + Harrow (0.8)	Green Feed Oats 2wk/6/2009	9416 4wk/7/2009	0.0	56.0 1wk/6/2009	0.0	-/Urea
3	2010	No tillage (1.0)	No tillage (1.0)	Alfalfa/Timothy post harvest 2009	10976 ?wk/?/2009	0.0	0	0	-/-
3	2011	No tillage (1.0)	No tillage (1.0)	Alfalfa/Timothy post harvest 2009	10089 2wk/7/2011	0.0	0	0	-/-
3	2012	HDC (0.6)	No tillage (1.0)	Alfalfa/Timothy post harvest 2009	6726 ?wk/?/2012	0.0	0	0	-/-
4	2003	HDC (0.6) + Anhydrous Rig (0.8)	LDC (0.7) + Harrow (0.8)	Canola 2wk/5/2003	2218 4wk/8/2003	78.5 1wk/10/2002	78.5 2wk/5/2003	12.2 2wk/5/2003	Urea/DAP
4	2004	HDC (0.6)	LDC (0.7)	Oats 2wk/5/2004	7392 4wk/9/2004	0.0	56.0 2wk/5/2004	14.7 2wk/5/2004	-/DAP
4	2005	HDC (0.6)	LDC (0.7)	Alfalfa/Timothy 3wk/6/2005	4036 4wk/7/2005	0.0	53.8 4wk/5/2005	0.0	-/Urea
4	2006	No tillage (1.0)	No tillage (1.0)	Alfalfa/Timothy 3wk/6/2005	6726 ?wk/?/2006	0.0	0.0	0.0	-/-
4	2007	No tillage (1.0)	No tillage (1.0)	Alfalfa/Timothy 3wk/6/2005	7847 4wk/7/2007	0.0	0.0	0.0	-/-
4	2008	No tillage (1.0)	No tillage (1.0)	Alfalfa/Timothy 3wk/6/2005	6726 ?wk/?/2008	0.0	0.0	0.0	-/-
4	2009	No tillage (1.0)	No tillage (1.0)	Alfalfa/Timothy 3wk/6/2005	4484 2wk/7/2009	0.0	0.0	0.0	-/-
4	2010	HDC (0.6) + LDC (0.7)	LDC (0.7)	Canola 3wk/5/2010	4032 1wk/8/2010	0.0	112.1 with seed + 4wk/4	9.8 with seed	-/DAP + Urea
4	2011	HDC (0.6) + Harrow (0.8)	Anhydrous Rig (0.8)	Wheat 1wk/5/2011	3696 4wk/8/2011	0.0	95.2 with seed + 1wk/5	16.8 with seed	-/DAP + Urea
4	2012	No tillage (1.0)	LDC (0.7) + LDC (0.7)	Canola 1wk/5/2012	2822.4 3wk/8/2012	0.0	115.36 with seed + 4wk/4	16.8 with seed	-/DAP + Urea

Table 3.2: Sub-basin2 Fields 7 and 9 Agricultural Record. Abbreviations: Heavy Duty Cultivator (HDC), Light Duty Cultivator (LDC), Diammonium Phosphate (DAP), and date formats (week(wk) / month / year).

Field	Year	Fall Tillage (crop residue fraction)	Spring Tillage	Crop Seeded Date	Yield Harvest Date	Fall N Date	Spring N Date	Spring P Date	Fertilizer Type Fall/Spring
7	2004	HDC (0.6)	LDC (0.7)	Barley 1wk/5/2004	5040 1wk/10/2004	0.0	78.45970545 1wk/5/2004	17.10421579 1wk/5/2004	-/DAP
7	2005	HDC (0.6)	LDC (0.7)	Alfalfa/Timothy 3wk/6/2005	4036 4wk/7/2005	0.0	53.8 4wk/5/2005	0.0	-/Urea
7	2006	No tillage (1.0)	No tillage (1.0)	Alfalfa/Timothy 3wk/6/2005	6726 2wk/7/2006	0.0	0.0	0.0	-/-
7	2007	No tillage (1.0)	No tillage (1.0)	Alfalfa/Timothy 3wk/6/2005	7847 4wk/7/2007	0.0	0	0	-/-
7	2008	No tillage (1.0)	No tillage (1.0)	Alfalfa/Timothy 3wk/6/2005	6278 2wk/7/2008	0.0	0	0	-/-
7	2009	No tillage (1.0)	No tillage (1.0)	Alfalfa/Timothy 3wk/6/2005	4484 2wk/7/2009	0.0	0	0	-/-
7	2010	HDC (0.6) + LDC (0.7)	LDC (0.7)	Wheat 4wk/4/2010	3024 3wk/8/2010	0.0	95.3 with seed + 3wk/4	4.9 with seed	-/DAP + Urea
7	2011	HDC (0.6) + Harrow (0.8)	Anhydrous Rig (0.8)	Canola 1wk/6/2011	2016 2wk/9/2011	0.0	117.6 with seed + 1wk/6	16.8	-/DAP + Urea
7	2012	Harrow (0.8) + HDC (0.6)	LDC (0.7)	Wheat 4wk/4/2012	4032 2wk/8/2012	0.0	101.9 with seed + 2wk/4	11.2	-/DAP + Urea
9	2004	HDC (0.6)	LDC (0.7)	Canola 2wk/6/2004	2822.4 2wk/10/2004	0.0	95.3 4wk/5/2004 + 2wk/6	17.1 2wk/6/2004	-/DAP + Urea
9	2005	HDC (0.6)	LDC (0.7)	Oats 4wk/5/2005	4032 4wk/8/2005	0.0	56.0 1wk/5/2005	0.0	-/Urea
9	2006	HDC (0.6)	LDC (0.7)	Flax/Linola 2wk/5/2006	1680 4wk/8/2006	0.0	56.0 1wk/5/2006	0.0	-/Urea
9	2007	HDC (0.6)	LDC (0.7)	Barley 4wk/4/2007	5376 3wk/8/2007	78.5 2wk/10/2006	11.2 with seed	4.9 with seed	Urea/DAP
9	2008	Harrow (0.8) + HDC (0.6)	LDC (0.7)	Canola 1wk/5/2008	3024 2wk/9/2008	95.3 4wk/10/2007	13.5 with seed	4.9 with seed	Urea/DAP
9	2009	HDC (0.6)	LDC (0.7) + Harrow (0.8)	Green Feed Oats 2wk/6/2009	9416 4wk/7/2009	0.0	56.0 1wk/6/2009	0.0	-/Urea
9	2010	No tillage (1.0)	No tillage (1.0)	Alfalfa/Timothy post harvest 2009	10976 2wk/7/2010	0.0	0	0	-/-
9	2011	No tillage (1.0)	No tillage (1.0)	Alfalfa/Timothy post harvest 2009	10089 2wk/7/2011	0.0	0	0	-/-
9	2012	No tillage (1.0)	No tillage (1.0)	Alfalfa/Timothy post harvest 2009	- 2wk/7/2012	0.0	0.0	0.0	-/-

Table 3.3: Twin Watershed Agricultural Record. Abbreviations: Heavy Duty Cultivator (HDC), Light Duty Cultivator (LDC), Diammonium Phosphate (DAP), and date formats (week(wk) / month / year).

Field	Year	Fall Tillage (crop residue fraction)	Spring Tillage	Crop Seeded Date	Yield Harvest Date	Fall N Date	Spring N Date	Spring P Date	Fertilizer Type Fall/Spring
10	2003	Harrow (0.8) + HDC (0.6)	LDC (0.7)	Wheat 2wk/5/2003	3360 3wk/8/2003	0.0	72.9 2wk/5/2003	12.2 2wk/5/2003	-/DAP
10	2004	HDC (0.6)	LDC (0.7)	Canola 1wk/6/2004	2016 1wk/10/2004	0.0	89.7 3wk/5/2004	17.1 3wk/5/2004	-/DAP
10	2005	HDC (0.6)	LDC (0.7) + Anhydrous Rig (0.8)	Barley 1wk/5/2005	3360 4wk/8/2005	0.0	67.2511761 1wk/5/2005	0	-/Urea
10	2006	HDC (0.6)	LDC (0.7) + Anhydrous Rig (0.8)	Canola 3wk/5/2006	1344 3wk/8/2006	0.0	78.5 with seed + 1wk/5	4.9 with seed	-/DAP + Urea
10	2007	HDC (0.6)	LDC (0.7)	Wheat 4wk/4/2007	3025 3wk/8/2007	0.0	89.7 with seed + 4wk/4	4.9 with seed	-/DAP + Urea
10	2008	HDC (0.6)	LDC (0.7)	Canola 1wk/5/2008	3024 2wk/9/2008	95.3 3wk/10/2007	13.5 with seed	4.9 with seed	Urea/DAP
10	2009	HDC (0.6)	LDC (0.7) + HDC (0.6)	Wheat 2wk/5/2009	3360 1wk/9/2009	0.0	89.7 with seed + 1wk/5	4.9 with seed	-/DAP + Urea
10	2010	HDC (0.6)	LDC (0.7)	Canola 3wk/5/2010	4032 2wk/9/2010	0.0	112.1 with seed + 4wk/4	9.8 with seed	-/DAP + Urea
10	2011	HDC (0.6)	Anhydrous Rig (0.8)	Wheat 1wk/5/2011	3360 4wk/8/2011	0.0	100.8 with seed + 1wk/5	16.8 with seed	-/DAP + Urea
10	2012	No tillage (1.0)	LDC (0.7)	Canola 2wk/5/2012	2688 3wk/8/2012	0.0	115.4 with seed + 4wk/4	16.8 with seed	-/DAP + Urea
11	2003	Harrow (0.8)	No tillage (1.0)	Wheat 2wk/5/2003	3024 3wk/8/2003	0.0	72.9 2wk/5/2003	12.2 2wk/5/2003	-/DAP
11	2004	No tillage (1.0)	No tillage (1.0)	Canola 1wk/6/2004	2016 1wk/10/2004	0.0	89.7 3wk/5/2004	17.1 3wk/5/2004	-/DAP
11	2005	No tillage (1.0)	Anhydrous Rig (0.8)	Barley 1wk/5/2005	3360 3wk/8/2005	0.0	67.3 1wk/5/2005	0.0	-/Urea
11	2006	Harrow (0.8)	No tillage (1.0)	Canola 3wk/5/2006	1344 3wk/8/2006	0.0	78.5 with seed + 1wk/5	4.9 with seed	-/DAP + Urea
11	2007	No tillage (1.0)	No tillage (1.0)	Wheat 4wk/4/2007	3024 3wk/8/2007	0.0	89.7 with seed + 3wk/4	4.9 with seed	-/DAP + Urea
11	2008	HDC (0.6)	No tillage (1.0)	Canola 1wk/5/2008	3024 2wk/9/2008	95.3 3wk/10/2007	13.5 with seed	4.9 with seed	Urea/DAP
11	2009	No tillage (1.0)	Harrow (0.8)	Wheat 2wk/5/2009	3360 2wk/9/2009	0.0	100.9 with seed + 1wk/5	4.9 with seed	-/DAP + Urea
11	2010	HDC (0.6)	No tillage (1.0)	Canola 3wk/5/2010	4032 2wk/9/2010	0.0	112.1 with seed + 4wk/4	9.8 with seed	-/DAP + Urea
11	2011	HDC (0.6)	No tillage (1.0)	Wheat 1wk/5/2011	3360 4wk/8/2011	0.0	100.8 with seed + 1wk/5	16.8 with seed	-/DAP + Urea
11	2012	No tillage (1.0)	LDC (0.7) + LDC (0.7)	Canola 2wk/5/2012	2688 3wk/8/2012	0.0	115.4 with seed + 4wk/4	16.8 with seed	-/DAP + Urea



Figure 3.3: Circular Flume.



Figure 3.4: V-notched weir with pressure head sensor.

recorded for 2004-2012 inclusive, Sub-basin2 Fields 7 and 9 for 2009-2012 and Fields 3 and 4 2010-2012. The 15 minute flows ranged 0 to $\approx 0.150 \text{ m}^3 \cdot \text{s}^{-1}$ and in the larger flow years, cumulative runoff at the EOF approached 150 *mm*.



Figure 3.5: Dry circular flume with intake. The yellow open container provides a cleanable location to sit the chemical sampler intake.



Figure 3.6: V-notched weir with intake. The black hose contains the sampler intake tubing. This sits at the apex of the notch.

Runoff chemistry sampling

Chemistry samples were drawn from the base of the circular flume (Figure 3.5) or the apex of the v-notched weir (Figure 3.6) when triggered by step changes in flow during events. The number of samples per event ranged from three to more than 20. Samples were drawn with enough frequency to cover the rising limb, peak, and falling limb of each runoff event (Tiessen et al., 2010). A typical example is shown in Figure 3.7. Samples were stored in the auto-sampler (Figure 3.8 and 3.9) and emptied daily. During low flow events grab samples were taken to supplement the automatic samples (Tiessen et al., 2010). Samples from the Twin fields were sent to the Environment Canada National Canadian Association

for Laboratory Accreditation certified lab in Saskatoon, SK and Sub-basin2 samples were sent to the Fisheries and Oceans Canada's Freshwater Institute Laboratory in Winnipeg, MB (FWI) for processing. All samples were retrieved from the field daily, preserved (in the case of NH_3) and packed on ice for transport.

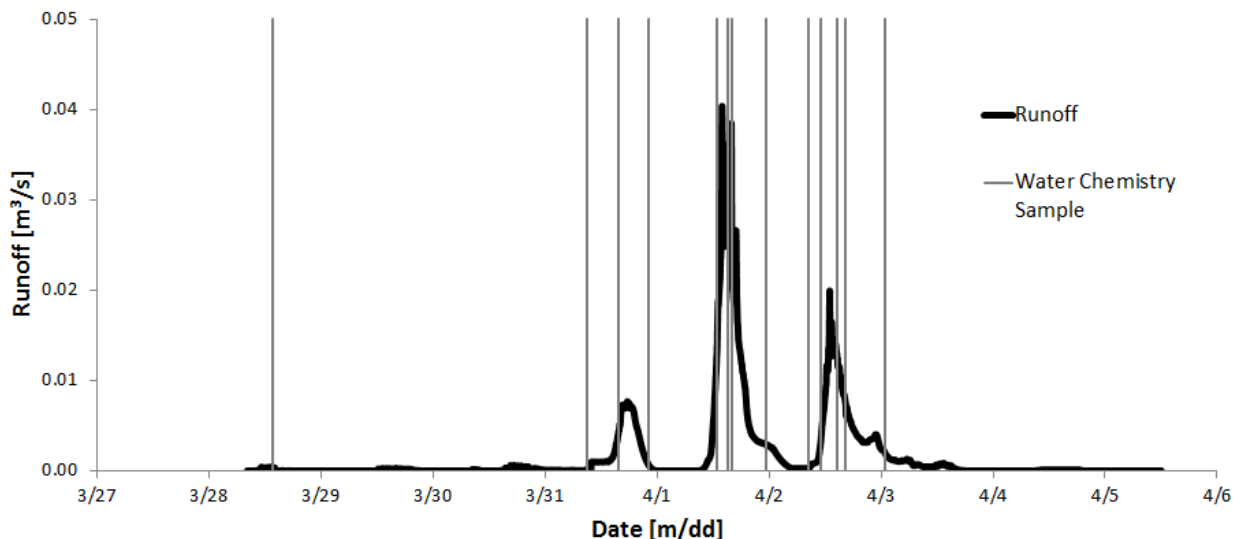


Figure 3.7: Typical runoff and chemical sampling resolution. This plot illustrates the frequency of chemical samples taken during runoff events. The event shown is a 2011 runoff event on Twin field 11, an event representing a typical sampling regime.



Figure 3.8: Sigma Data logger GUI. Sigma SD900 data logger and SL800 auto-sampler control



Figure 3.9: Auto-sampler. This auto-sampler (typical) was emptied daily during flow events.

Dissolved nutrient determination was performed on $0.45\ \mu\text{m}$ filtered aliquots. Analytical methods for the Sub-basin2 fields are covered in the discussion of the snow sampling methods in Section 3.2.4. Analytical methods for nitrogen and phosphorous on the Twin fields are summarized below:

- **Nitrogen** These methods are summarized from the methods described in [Tiessen et al. \(2010\)](#) and [Elliott \(2013\)](#). Total nitrogen, TN, and total ammonia, NH_3 , (this includes both unionized and ionized forms of ammonia) analyses were performed on the unfiltered aliquot. Total dissolved nitrogen, TDN, and nitrate+nitrite, NO_3 , were filtered through a Whatman glass $0.45\mu\text{m}$ cellulose acetate filter after being baked at 525°C for 4 h. Total NH_3 analyses used sulphuric acid to stabilize the aliquot prior to determination by reaction with hypochlorite and alkaline phenol ([Skougstad et al., 1979](#)). Nitrate+nitrite was determined with the cadmium reduction method ([Eaton et al., 2005](#)). For TN and TDN, organic N was oxidized to nitrate by digestion with alkaline potassium persulphate. The determined concentrations were reported as mg N l^{-1} .
- **Phosphorous** Both TDP and TP were determined as orthophosphate by reduction using stannous chloride as described in [Environment Canada \(1979a\)](#). The aliquots were first treated with a sulphuric acid - persulphate mixture to release organically bound phosphates and hydrolyzed polyphosphates to soluble reactive P prior to reduction ([Environment Canada, 1979b](#)). This is as noted in [Tiessen et al. \(2010\)](#) and [Elliott \(2013\)](#).

In the hydrochemistry data provided, the determined chemistry concentrations (Appendix B Figures B.4 - B.6) and flows were used to calculate the mass of each solute exported at the EOF. The method for this is discussed in [Tiessen et al. \(2010\)](#). To summarize, measured concentrations were plotted along the EOF runoff hydrograph corresponding to the sample time. Concentrations were interpolated or extrapolated to correspond to each flow measurement on the hydrograph to make a best estimation of the concentrations at the measured flows. The calculation for the mass flux $[\text{g} \cdot \text{m}^{-2}]$ for a field is shown in Equation 3.1:

$$\text{mass flux} = \frac{\sum_{i=1}^n q_i \cdot t_i \cdot c_i}{A_{\text{eff}}} \quad (3.1)$$

where n is the number of samples taken for an event; q_i the EOF discharge in m^3/s , t_i the time over which the discharge applies in s , and c_i , the concentration observed at that time for the i^{th} sample in $\text{g} \cdot \text{m}^3$; and A_{eff} the effective drainage area, m^2 , of the field on which the

hydrochemistry samples were taken.

The error associated with the calculation of mass fluxes was not provided with the original data. Error for the provided flows can be estimated at $\pm 3\%$ based on Zoski (2015, pers. comm.) and Hager (1988). Additional sources of error in the measurement of flows that cannot be quantified include that from the downstream tailwater and in water depth measurements (Zoski, 2015, pers. comm.). The concentrations have error associated with the sample location (difficult to quantify how representative of the field the sampling location might be), in addition to the error associated with the analytical methods used to quantify the concentrations. Methods for TDP and NH_3 are accurate to $\pm 0.005 \text{ mg} \cdot \text{l}^{-1}$ and for TDN and NO_3 to $\pm 0.01 \text{ mg} \cdot \text{l}^{-1}$ (Elliott, 2015, pers. comm.). The robustness of the calculation method for load determination was tested by Dr. Jane Elliott by removing concentration samples from the set and recalculating loads. As an example, removing every second sample from a 14 sample event changed the calculated load by 1.3% for NH_3 , 8.8% for NO_3 , 6.6% for TDP, 2.4% for TP, and 5.5% for TN (Elliott, 2015, pers. comm.). Mass fluxes were previously calculated; therefore, for this research, error in the calculation was estimated based on the number of chemical samples and associated analytical error plus a prorated portion of the error estimated in the robustness calculation based on the number of chemical samples (Figure 3.10). Mass calculations involving large numbers of samples potentially have proportionally more analytical error and less error attributable to the method of calculation (less interpolation or extrapolation required for an event).

Rain-on-snow (ROS) events were not identified in this original data set — events were labelled as either a snowmelt or rainfall runoff event. In this research, potential ROS events were identified using CRHM modelled SWE to determine the presence of the spring snowcover in 2004-2011. Rainfall events that exceeded a $5 \text{ mm} \cdot \text{d}^{-1}$ accumulation during an EOF flow event when $\text{SWE} > 0$ were considered potential ROS events¹ based, in part, on the fact that $5 \text{ mm} \cdot \text{d}^{-1}$ exceeds the early spring evapotranspiration rates determined in modelling studies and the literature for the sub-humid regions of the Canadian Prairie (Armstrong et al., 2015) and therefore $5 \text{ mm} \cdot \text{d}^{-1}$ has the potential during spring, subject to frozen soil infiltrability,

¹The $5 \text{ mm} \cdot \text{d}^{-1}$ threshold was used by Dumanski et al. (2015, in review) in determining sources of streamflow contributions in Smith Creek, a Canadian prairie stream in an agricultural catchment.

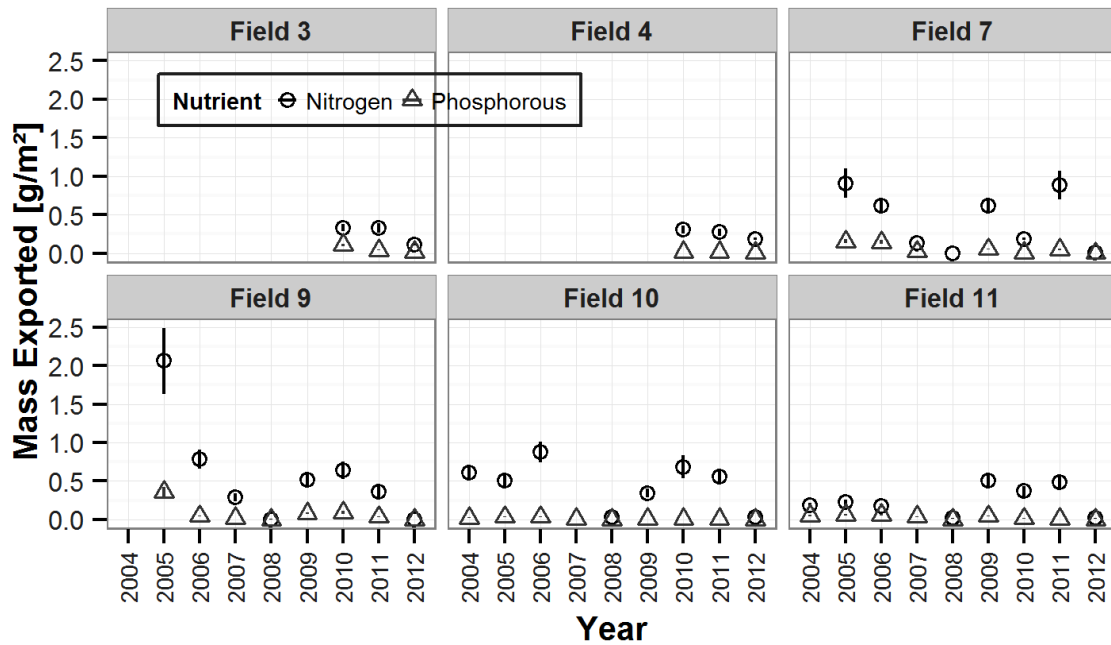


Figure 3.10: Total Phosphorous and Total Nitrogen Annual Mass Flux. Figure shows the provided mass flux data with the calculated error for the calculated mass fluxes.

to induce or increase EOF runoff. There were two potential ROS events identified: 1) April 12-13, 2005 where rainfall amounted to 20 *mm* at the Twin watershed gauge in a 48*h* period without generating EOF runoff on the Twin fields whereas runoff was generated and chemical samples were drawn on the Sub-basin2 fields, and 2) April 8, 2011 where rainfall amounted to 11 *mm* at the Twin watershed in a 24*h* period and recorded EOF runoff on the Sub-basin2 fields continued to recede during the day (refer to Figure B.7). A total of 13 samples were collected during these potential ROS events.

3.2.3 Soil Sampling

Soil chemistry surveys

After harvest, fall soil samples were taken on each of F3, F4, F10 and F11. Samples were drawn from the 0 – 5 *cm* depth, 0 – 15 *cm* depth, and 15 – 60 *cm* depth on 3 transects at each of upper, mid, and lower slope positions, each with 4 GPS referenced sample locations (Elliott, 2014). This amounted to 12 samples at each depth for P and 12 samples at the

0 – 15 *cm* and 15 – 60 *cm* depths for NO₃–N (the 0 – 5 *cm* depth was not sampled for NO₃–N after 2007). The soil samples were processed at the AgVise labs in Northwood, ND using the sodium bicarbonate OlsenP method which is standard for calcareous soils (Frank et al., 2012) and a potassium chloride extraction method for NO₃–N (Gelderman and Beegle, 2012). In the ensuing discussions, Soil P and Soil N values refer to the field means of the 12 samples.

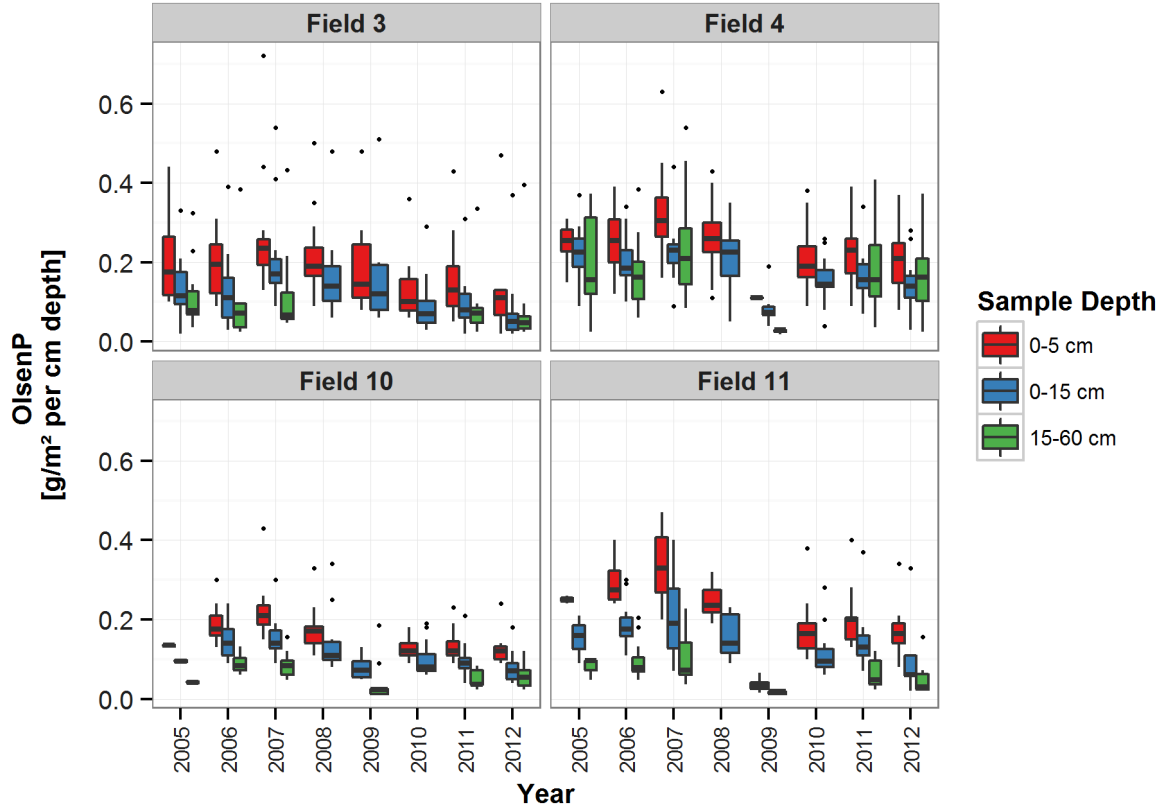


Figure 3.11: Normalized Soil P Sample Results. OlsenP results for years 2005-2012 on fields 3, 4, 10, and 11. The values presented are normalized by the sample depth. The black dots are the outliers to the boxplot whiskers which extend to $1.5 \times$ inter-quartile range; the mid-hinge, the median; and the lower and upper hinge the first and third quartiles, respectively.

OlsenP values were initially reported in $mg \cdot kg^{-1}$, while data for NO₃–N was reported in $g \cdot m^{-2}$ based on core depths and soil densities. OlsenP values were converted to $g \cdot m^{-2}$ using a standard bulk density for the soil of $1.2 g \cdot cm^{-3}$ for the 15 – 60 *cm* samples and $1.0 g \cdot cm^{-3}$ for the 0 – 15 *cm* samples due to the high organic content in the surface horizon

of these Chernozemic soils (Equation 3.2):

$$\text{OlsenP} [g \cdot m^{-2}] = \text{OlsenP} [mg \cdot kg^{-1}] \cdot 1.2 \cdot d \cdot 0.01 \quad (3.2)$$

where sample depth, d , is in cm .

To facilitate the comparison of the P and N nutrient contents at the various sampled depths, the results were normalized by sample depth (Figures 3.12 and 3.11). In both Figure 3.11 and Figure 3.12, the stratification of nutrient mass in the soil horizons is evident. Soil P and N levels are higher in the surface horizons than in the deeper layers. As discussed in Section 2.3.4, it is the surface layers that interact with and influence runoff concentrations.

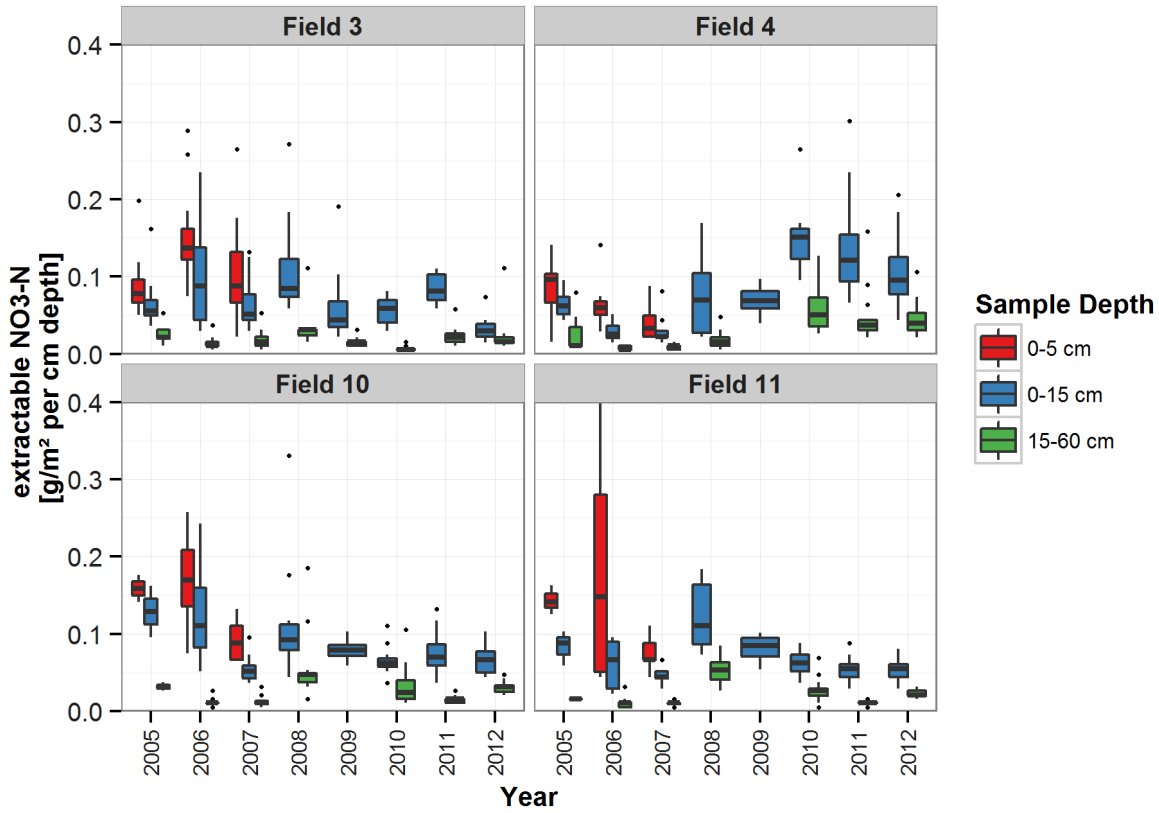


Figure 3.12: Normalized Soil N Sample Results. Extractable $\text{NO}_3\text{-N}$ results for years 2005-2012 on fields 3, 4, 10, and 11. The values presented are normalized by the sample depth. The black dots are the outliers to the boxplot whiskers which extend to $1.5 \times$ inter-quartile range; the mid-hinge, the median; and the lower and upper hinge the first and third quartiles, respectively.

Soil moisture surveys

Post harvest soil moisture sampling was conducted on the Twin fields (F10 and F11). Punch soil probes were used to take two composite samples per field at 7-23 *cm* depth. Samples were used to determine gravimetric soil moisture contents (Equation 3.3) and converted to volumetric moisture contents using a bulk density of $1.1 \text{ g} \cdot \text{cm}^{-3}$ and calculated in Equation 3.4 yielding similar gravimetric, Θ_m , and volumetric, Θ soil water contents:

$$\Theta_m = \left[\frac{W_{wet} - W_{dry}}{W_{dry}} \right] \cdot 100 \quad (3.3)$$

$$\Theta = \Theta_m \times \frac{\rho_s}{\rho_w} \quad (3.4)$$

where ρ_s represents the bulk density of the soil, ρ_w the density of water ($1.0 \text{ g} \cdot \text{cm}^{-3}$), and W_{dry} and W_{wet} the weight of dry and wet soil in *g*. Soil samples were oven dried at 105°C for 48 *h* to determine dried sample weight (Elliott, 2013; Russel, 1988). Annual field averages with standard error are shown in Figure 3.13.

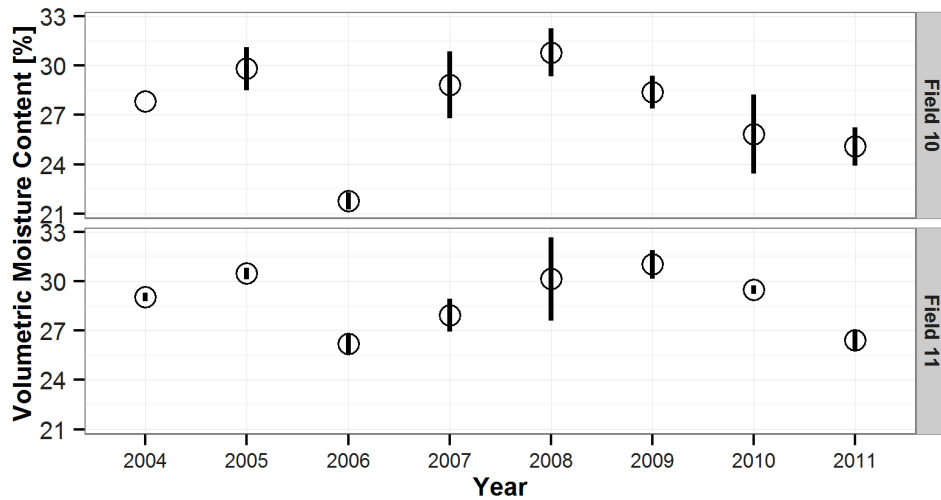


Figure 3.13: Fields 10 and 11 Fall Soil Moisture Contents. Fall soil volumetric moisture contents taken on the Twin fields (F10 and F11). The circle represents the average of the samples and the bar represents the standard deviation.

3.2.4 Snow Sampling

Snow depth and density surveys

March snow surveys for both depth and density were performed on fields 3, 4, 10 and 11. The intent of the survey was to capture the peak snow water equivalent (SWE) accumulated on the field immediately prior to spring melt. The snow surveys were performed in three transects of four GPS marked locations at upper, mid, and lower slope locations and the calculations shown in Equations 3.5 - 3.7 used to calculate SWE:

$$\rho_s = \frac{M_s}{A_{x.s.} \cdot d_s} \quad (3.5)$$

$$\gamma_s [-] = \frac{\rho_s}{\rho_{water}} \quad (3.6)$$

$$SWE = d_s \cdot \gamma_s [-] \quad (3.7)$$

Snow depths (d_s) in *cm* and snow masses (M_s) in *g* were measured at each location and used to calculate density (ρ_s in Equation 3.5) in $g \cdot cm^{-3}$ and SWE (Equation 3.7) in *mm* for a total of 12 samples per field. A snow sampler with a cross sectional area, $A_{x.s.}$, of 45.34 cm^2 was used for these samples. Field SWE values presented subsequently are calculated based on the average SWE (μ_{SWE}) of the these 12 samples.

In these shallow prairie snowcovers, density did not vary with depth (Figure 3.14) as is typical (Pomeroy and Gray, 1995). Rather, there is evidence in a few samples (relative density, $\gamma_s > 0.4$ in Figure 3.14) that a melt occurred prior to the survey and therefore density actually increased with decreasing depth. This has been observed in nature as is the result of non uniform densification of the snowcover due to a variety of factors, one being the uneven distribution of melt energy into snowcovers (Faria, 1998) which on the Prairie may result from the advection of sensible heat near tufts of residue or vegetation poking through the snow.

Snow chemistry surveys

Phosphorous and nitrogen chemistry samples were taken on the same transects as the snow surveys. Snow chemistry samples were processed according to the methods described in

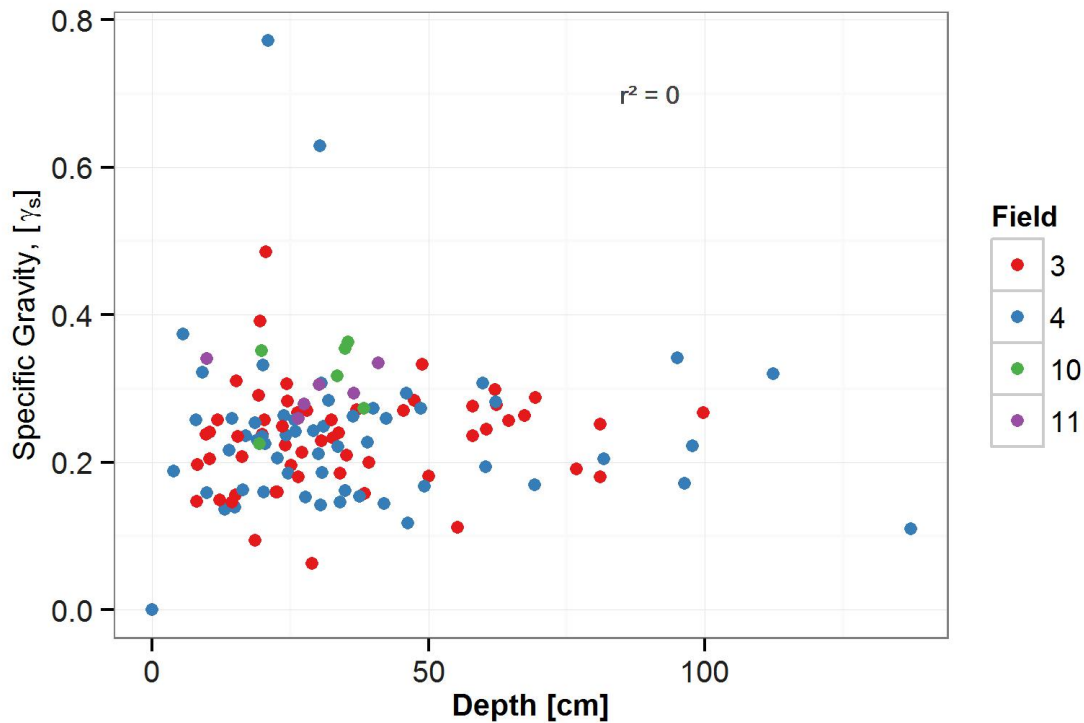


Figure 3.14: Snow depth vs density plot. Snow depth is plotted against specific gravity to illustrate that there is no variation of density with depth. The coefficient of variation (CV) for depth measurements was found to be 0.57 ± 0.24 and for density 0.27 ± 0.16 .

[Tiessen et al. \(2011\)](#). Samples were processed at the Fisheries and Oceans Canada's Freshwater Institute Laboratory in Winnipeg, MB (FWI) [Freshwater Institute \(2003a,b,c,d,e\)](#):

- Nitrogen and Phosphorous** Total ammonia, NH_3 , analyses used sulphuric acid to stabilize the aliquot before reacting with hypochlorite and an alkaline phenol using nitroprusside as a reaction catalyst. The analyses for nitrate-nitrite, NO_3 , reduced nitrate to nitrite by cadmium-copper couple before reacting the aliquot with hydrochloric acid to form nitrous acid which with sulphanilamide produces a pink azo dye. The method for TDN and TDP analyses applied acidic oxidizing conditions and UV decomposition to the aliquot to convert inorganic and organic N to NH_3 before measuring as NH_3 and organic P to orthophosphate before measuring as soluble reactive phosphorous, SRP. The sample aliquot for SRP analyses was reacted with acid, molybdate and antimony (a colour enhancer) to form a blue complex specific to orthophosphate.

Field concentrations presented are the mean of the determined concentration for each of the 12 samples. The mass of solute, in $g \cdot m^{-2}$, in the snowcover is calculated based on the mean concentration, μ_{conc_S} , in mg/l , mean SWE, μ_{SWE} , in mm , and field area, A_f , in km^2 as shown in Equation 3.8.

$$\begin{aligned} \text{mass} &= \frac{\mu_{conc_S} \cdot \mu_{SWE} \cdot A_f}{A_f} \\ &= \mu_{conc_S} \cdot \mu_{SWE} \cdot \frac{1}{1000} \end{aligned} \tag{3.8}$$

The annual snow concentrations and depths for each field are shown in Figures B.8 and B.9, respectively. Overall annual average snow concentrations for NH_3 ranged 0.27-0.62 $mg \cdot l^{-1}$; for NO_3 0.24-0.46 $mg \cdot l^{-1}$; and for TDP 0.03-0.11 $mg \cdot l^{-1}$. Overall annual March snow water equivalent (SWE) observations varied annually from a low in 2012 of 33 ± 21 mm and a high in 2006 of 109 ± 57 mm .

CHAPTER 4

DATA ANALYSES AND KEY MESSAGES

This chapter highlights how the assumptions of the conceptual model, to be presented in Chapter 5, were generated based on the processes inferred from the data and supported by the literature. The investigation of the field hydrochemistry, soils, and snow observational data along with the agricultural record is categorized into four key themes: the annual field scale nutrient budget; EOF concentration and flow relationship; rainfall and snowmelt runoff composition; and field nutrient sources during meltwater runoff.

4.1 The agricultural field scale nutrient budget

The hydrochemistry, snow survey and agricultural record data, coupled with literature and industry standards were used to determine the annual field scale inputs and outputs of phosphorous and nitrogen to the Sub-basin2 and Twin fields. The farming year (Section 3.2.1) has been used here.

The formulation for the inputs and outputs are shown in Figures 2.1a and 2.1b and are summarized below and in Figures 4.1 and 4.2:

- Phosphorous fertilizers, when applied, were applied in the spring with the nitrogen pass (as diammonium phosphate) otherwise nitrogen was applied as urea. Annual rates of fertilization for years when fertilizer was applied ranged $1.1\text{--}3.9\text{ g}\cdot\text{m}^{-2}$ with an average $2.0\text{ g}\cdot\text{m}^{-2}$ for P and ranged $5.4\text{--}15.7\text{ g}\cdot\text{m}^{-2}$ with an average $9.0\text{ g}\cdot\text{m}^{-2}$ for N.
- Atmospheric deposition rates were not measured on site and not available from Environment Canada’s CAPMoN network (Environment Canada, 2015b), as such wet deposition measurements were taken from the United States National Atmospheric Deposition Program site NADP-08 located at $48^{\circ}78'N$, $97^{\circ}76'W$ approximately 50 km away from these fields. The wet deposition data along with modelled wet and dry

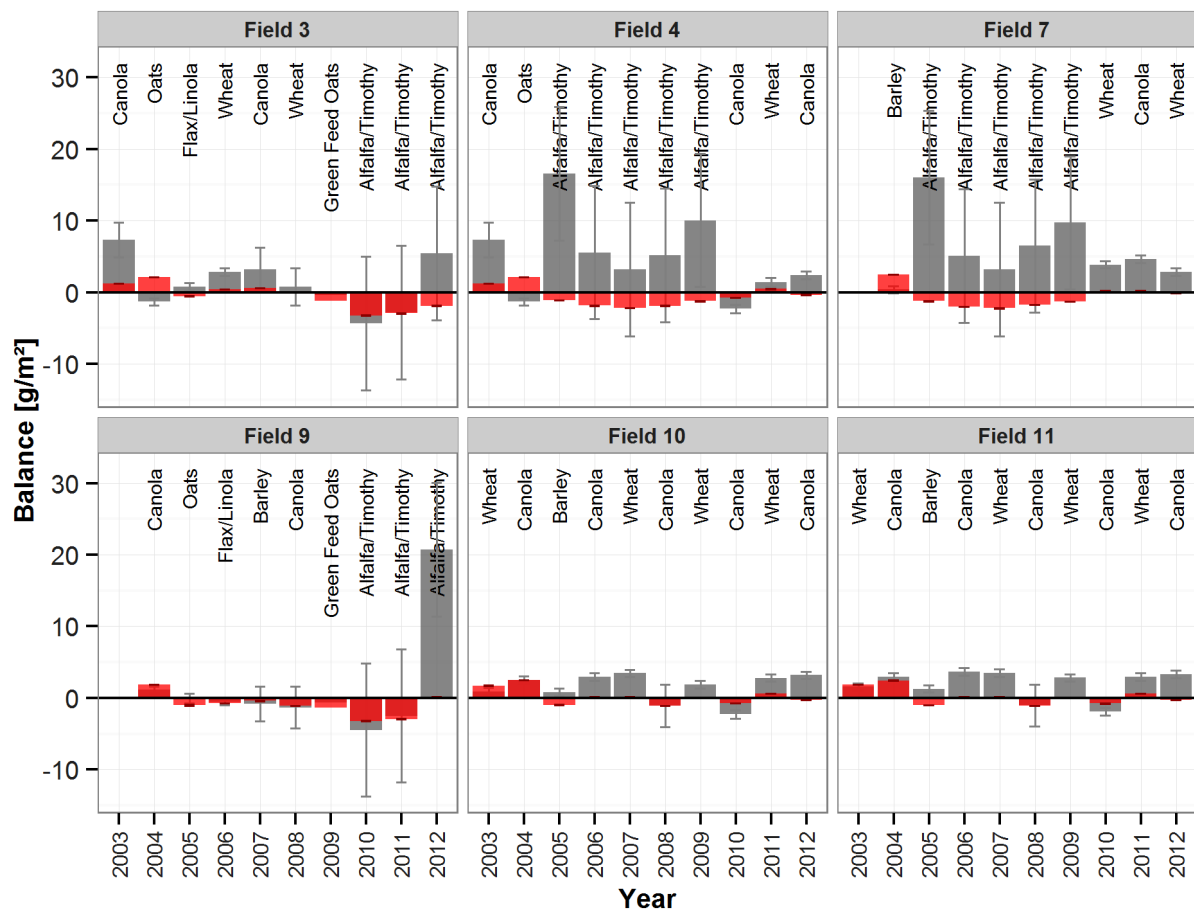


Figure 4.1: Phosphorous and Nitrogen Field Scale Net Mass Balance. The annual field scale nutrient balance for phosphorous (red) and nitrogen (grey) are shown by the bars. The lines illustrate the quantifiable error in the net balances calculated for phosphorous (black lines) and nitrogen (grey lines).

deposition numbers were used to generate the bulk N deposition numbers for these fields¹. P deposition numbers were calculated from the N deposition numbers based on the ratio of N:P provided in the literature. Rates of annual P deposition ranged $0.05\text{--}0.17\text{ g} \cdot \text{m}^{-2}$ and N deposition ranged $0.83\text{--}1.29\text{ g} \cdot \text{m}^{-2}$. The N range fell within that reported in the literature whereas the maximum P values ranged slightly above

¹Four years of modelled data were used to generate these bulk deposition estimates: Environment Canada's GEM model (1998), US Environmental Protection Agency's CMAQ (2000), and Environment Canada's AURAMS, A Unified Regional Air-quality Modelling System, (2002,2006). These four models provided comparable annual dry, wet and total deposition rates. These rates were averaged and a ratio of wet:dry deposition developed and applied to the NADP-08 wet deposition data to generate annual bulk deposition rates.

(Cadle, 1991; Chambers et al., 2001; Köchy and Wilson, 2001).

- The blowing snow losses of field P and N in snow relocated to riparian areas and ditches were determined. An estimated quantity of P and N deposited with the snow was determined based on a percentage of the annual bulk deposition rates based on the number of snow covered days per year. 20% of the snow was estimated to be transported off of the field and with the blowing snow 20% of the P and N deposited was assumed to be lost from the field. As expected these losses are negligible for these fields (Figure 4.2), but if the current practice of forage cropping and minimal tillage were stopped and fields were left fallow and without residue (Pomeroy and Gray, 1995) or precipitation trends resulted in deeper snowcovers (Mahmood et al., 2015), these losses would increase substantially.
- Biological Nitrogen Fixation rates were taken from the literature (Burity et al., 1989; Sask Forage Council, 2008). The fixation rates are highly variable (largely depending on soil N levels and successive years established in addition to moisture, temperature and pH). The range for the Alfalfa/Timothy 60-40 mix was $11 - 30 \text{ g} \cdot \text{m}^{-2}$. Other crops are known to fix N, but at very minimal rates under such managed conditions and were not quantified.
- The P and N removed with the harvest were determined based on the crop type and yield provided in the agricultural record and Canadian Fertilizer Institute (2001) and International Plant Nutrition Institute (2012) rates for uptake and removal. There is much variability in these rates and the mean of the ranges provided were used and multiplied by the recorded yields for each field and year. The error represented reflects the full range of nutrient removal presented in this literature.
- Gaseous losses of N were estimated, specifically volatilized ammonia during fertilizer application (Rochette et al., 2013) and annual denitrification losses based on nitrous oxide losses (Ellert and Janzen, 2008) as a percent of total $\text{N}_2 + \text{N}_2\text{O}$ losses (Burford and Bremner, 1975). 20% from a range of (8-68%) volatilization during urea application was estimated for ammonia based on field pH. Nitrous oxide emissions can be quite

elevated in the spring (Risk et al., 2013) but average $0\text{--}0.4 \text{ g} \cdot \text{m}^{-2}$ annually (Ellert and Janzen, 2008). Dinitrogen losses (completed denitrification) were estimated by Burford and Bremner (1975) to comprise 60% of the combined $\text{N}_2 + \text{N}_2\text{O}$ losses. As such gaseous N loss was estimated at $0.5 \text{ g} \cdot \text{m}^{-2} \pm 0.45 \text{ g} \cdot \text{m}^{-2}$.

- Leaching of N below the rooting zone through the unsaturated soil zone was estimated for these fields. The leaching rates are likely overestimated as fields with optimized fertilization and continuous cropping have proven to leach little to no N (Campbell et al., 1993, 2006). Leaching was not measured on site but it was assumed to occur, therefore it was estimated based on the research of Campbell et al. (1975) who found that an average 0.65% of TN leaches down through cultivated brown Chernozemic prairie soils each year. The data collected for the Sub-basin 2 and Twin fields included observations of fall soil $\text{NO}_3\text{--N}$. Inorganic N comprises a 1-2% of the TN in natural soils of which the majority is NO_3 (Brady and Weil, 2002). In fertilized soils this percentage is larger and 5% was used here (Elliott, 2015; Russel, 1988).
- The mass of P and N transported with runoff at the EOF was tabulated as discussed in Section 3.2.2. There are several years included in the mass balance bar plots where data were not collected² and therefore, no runoff for P and N is shown in Figure 4.2.

Error was estimated for each of the discussed inputs and outputs where data were available. Cumulative error in the net balance was determined by calculating the square root of the summed and squared individual errors in the inputs and outputs. The net balance for P was consistently negative in some fields for a period of consecutive years (Figure 4.1); however no statistically significant decrease (MannKendall, $0.27 < p < 0.71$) was observed in soil P levels³. The P legacy (Kleinman et al., 2011b) or build up of P in the soils to buffer short term (or decadal, McCollum (1991)) changes in P fertilization regimes, as discussed in Section 2.3.2, is likely evident on these fields; although, it is difficult to be conclusive with

²Chemical fluxes were not collected for fields 3 and 4 in 2003-2009 (inclusive); fields 7, 9, 10 and 11 in 2003.

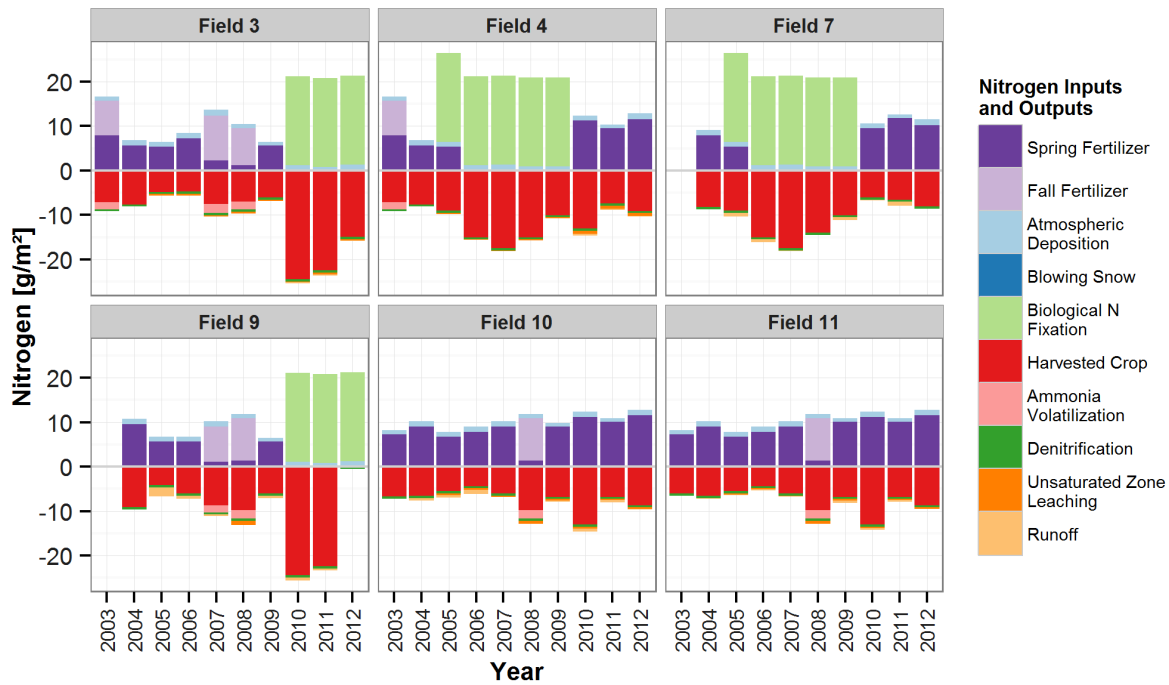
³The MannKendall test for monotonic trends (Hipel and McLeod, 2005; Mann, 1945) R package (McLeod, 2014; R Development Core Team, 2010) was used to look for a trend in Soil P, once it was concluded that these data were not autocorrelated.

a such a short (5-7 year) time series of soil P data. N is much more mobile than P, yet N, in some forms, binds in the soil similarly creating a legacy to buffer short term change in N inputs and outputs. The applicability of this theory to the Sub-basin2 and Twin fields is the subject of the next section.

The breakdown of both of P and N inputs and outputs at the field scale (Figure 4.2) illustrates the large scale of the annual agricultural P and N budgets compared to the P and N that is observed to runoff at the edge-of-field. The uncertainty involved in the prediction of runoff P and N exports is substantial and the error in the calculation is larger (Figure 4.1) than the observed exports of P and N during runoff events. Error would be expected to be even larger on fields that are not as monitored and managed as research fields.



(a) Annual Field Scale Phosphorous Inputs and Outputs to Soil P



(b) Annual Field Scale Nitrogen Inputs and Outputs to Soil N

Figure 4.2: P and N Agricultural field mass balance. These plots illustrate the inputs and outputs contributing to the field scale mass balance calculations for phosphorous and nitrogen shown in Figure 4.1.

4.2 Field scale flows and P and N exports

A simplified approach to predicting field scale exports of P and N is to assume flow dependence. A defined concentration (c) - flow (q) relationship simplifies the chemical process representation required for explaining the variability in edge-of-field (EOF) chemistry. Constant instantaneous concentrations with changing instantaneous flows implies that annual discharge would be linearly related to annually exported loads and could potentially govern the predictive relationship, as discussed in Section 2.3.2. In the broadest definition of invariant chemical supply, [Godsey et al. \(2009\)](#) use a log-log plot of the c vs q data to verify the absence of a $c - q$ relationship (i.e. the slope of log-log plot would be horizontal or slope ≈ 0) through a wide range of flows and comparatively small range of concentrations. In addition to the absence of a $c - q$ relationship, Figure 4.3 shows that the observed ranges of flow and chemistry variability are of similar orders of magnitude (concentration varies over 3 orders of magnitude and flow over 3 orders of magnitude) and, therefore, in spite of slope ≈ 0 it is difficult to claim that EOF chemistry concentrations are invariant when they, in fact, vary nearly as much as the flows do. Streamflow and concentration observations at the sub-catchment, catchment, and watershed level look very different and invariant chemical supply may become more apparent ([Mahmood et al., 2014](#)) and applicable in predictive modelling. At the field scale on these snowmelt runoff dominated fields, c and q are not associated but neither is c invariant; likely due to a combination of reasons such as sub-field variability in soil nutrient concentrations and snowcover chemistry; micro-depressions; and variable contact with vegetation and residue tufts during runoff to the EOF.

Snowmelt, rainfall, and potential rain-on-snow (ROS) events were observed at the EOF and lumped together in Figure 4.3 and B.10. Rain-on-snow events were identified as discussed in Section 3.2.2. Snowmelt, rainfall, and ROS events were separated and plotted on a linear scale in Figure 4.4 with no $c - q$ relationship evident when separated. The 13 data points of the ROS events are absent of an association between $c - q$. It is therefore assumed, based on these plots and the chemical composition of the ROS runoff presented in the following section (Figures 4.6b and 4.6a), that ROS runoff events behave similarly to snowmelt runoff events.

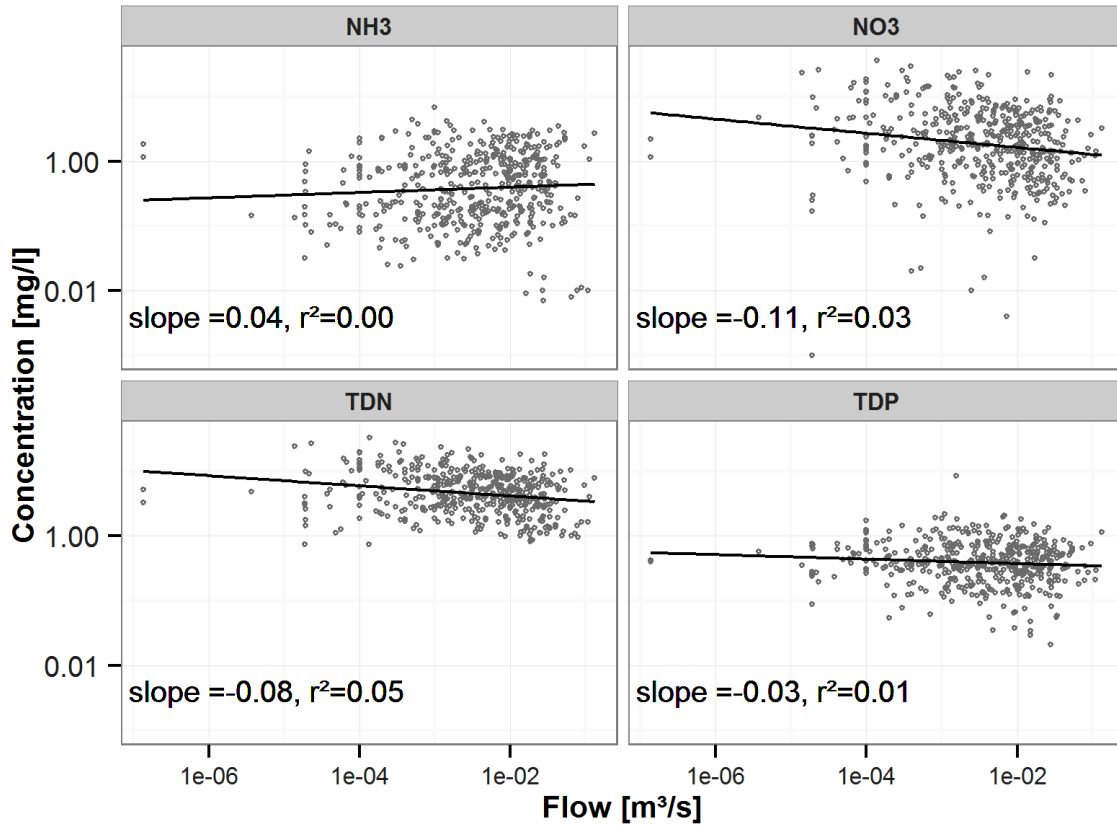


Figure 4.3: Concentration vs EOF discharge plots. The edge-of-field scale runoff data for fields 3, 4, 7, 9, 10 and 11 are plotted here on a \log_{10} - \log_{10} scale. The log-log regression statistics with slope ≈ 0 (which is the power law exponent in Cartesian coordinates) and $r^2 \approx 0$ confirm that there is no concentration - flow relationship. For linear plots of these data refer to Figure B.10 in Appendix C.

4.3 Snowmelt and rainfall runoff nutrient exports

As discussed in Section 2.1.4, the snowmelt contribution to annual runoff volumes is known to comprise $> 80\%$ of the annual runoff volumes on the Prairie with recent history exhibiting an increase in the rain-on-snow (ROS) and rainfall runoff proportion of streamflow. The snowmelt contribution to annual runoff volumes at the edge-of-field (EOF) for the Sub-basin2 and Twin fields was observed to be $88 \pm 21\%$ of the annual EOF runoff volume for the years 2004 – 2012 with a corresponding 84 – 90% contribution to annual nutrient exports (Figure 4.5).

Generally, rainfall runoff modelling of P exports deals with erosive transport to cap-

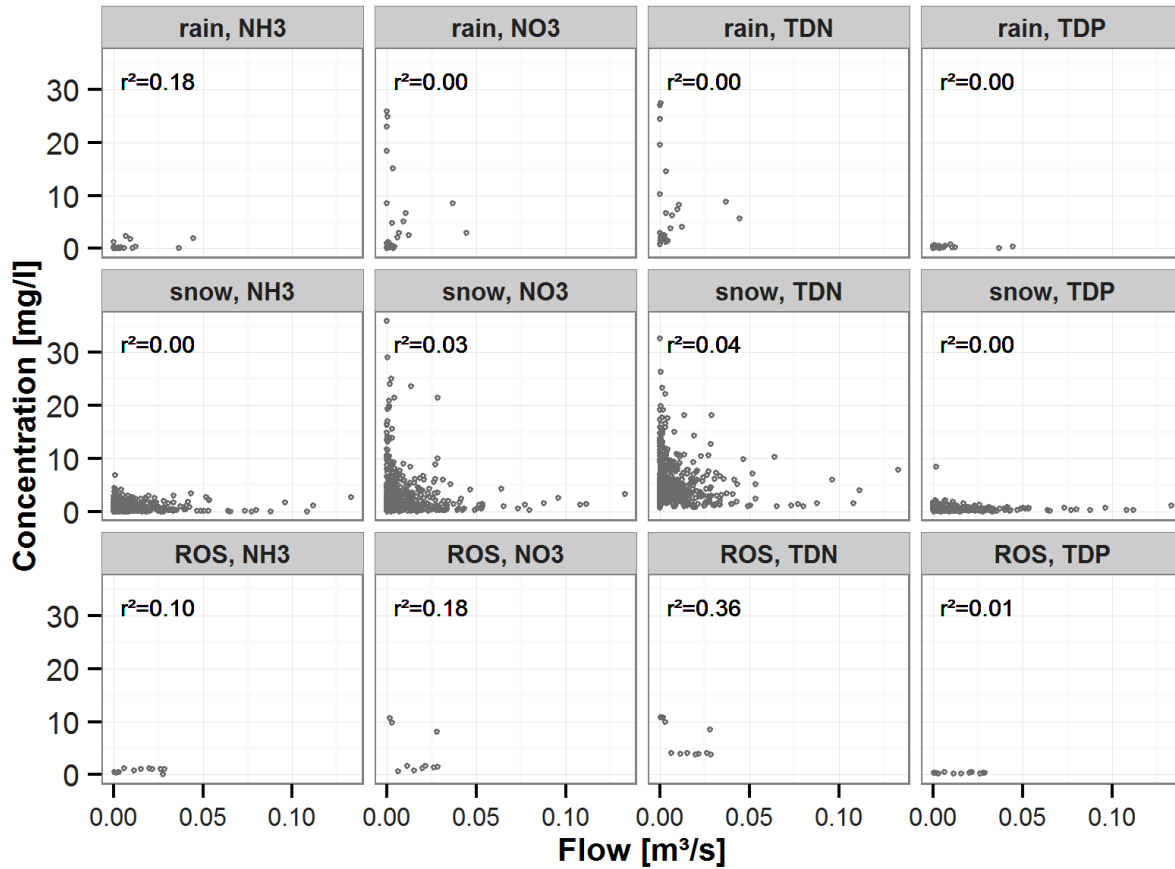


Figure 4.4: Concentration vs EOF discharge plots for rainfall, snowmelt and ROS events. The edge-of-field scale runoff data for fields 3, 4, 7, 9, 10 and 11 are plotted here on a linear scale and separated by rainfall, snowmelt, and ROS runoff events. The regression statistics confirm, again, that there is no concentration - flow relationship.

ture particulate P. The reduced scale (field scale), relatively flat terrain, runoff mechanism (snowmelt), and presence of frozen soils likely contribute to nearly all P being transported to the EOF in the dissolved form (Figure 4.6a). This suggests that erosive particulate transport of P need not be considered, at this scale, for snowmelt runoff events. Particulate transport of N is generally less of a concern than with P and based on the TN–TDN relationship for these fields (Figure 4.6b) particulate N transport can be omitted, at this time, for this model.

A linear least - squares regression (R Development Core Team, 2010) was performed on the TDP–TP and TDN–TN relationship. The P and N regressions contained two very influential data points sampled on March 31, 2005 at 1630 *h* and 2245 *h* (Figure B.11). These samples had an atypical particulate component and were high with TP at 5 and 11

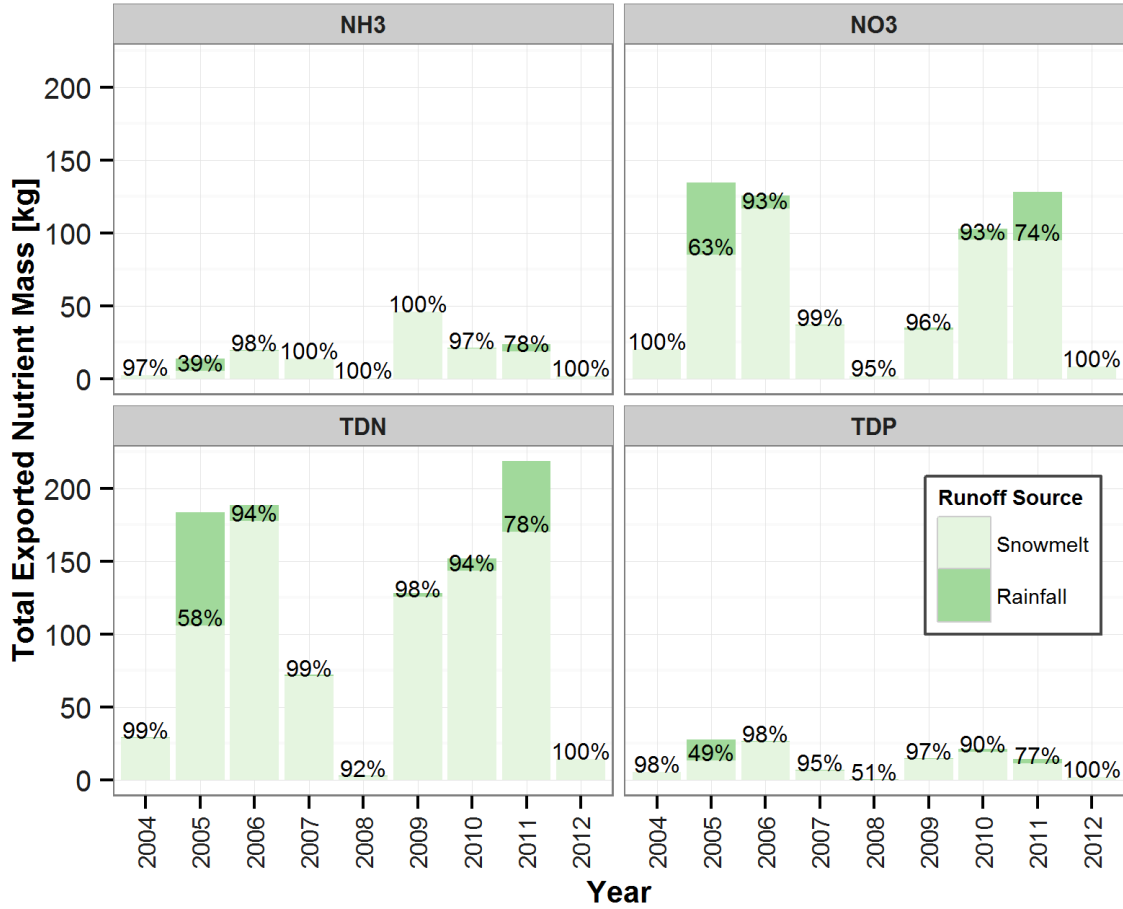


Figure 4.5: Snowmelt Contribution to Nutrient Exports. The annual percent contributions of snowmelt runoff to the annual total of nutrient mass exported during runoff are calculated for the Sub-basin2 and Twin fields and shown in text on the barplot. The average annual snowmelt runoff contributions for NH_3 , NO_3 , TDN, and TDP range 84 – 90% of the total annual nutrient export for these fields.

$\text{mg} \cdot \text{l}^{-1}$ and TN at 32 and 58 $\text{mg} \cdot \text{l}^{-1}$. The regressions for TDP–TP and TDN–TN were slope = 0.48, $r^2 = 0.48$ and slope = 0.75, $r^2 = 0.78$, respectively, when these two data points were included and slope = 0.94, $r^2 = 0.94$ and slope = 0.97, $r^2 = 0.98$, respectively, when excluded. The second regression shows a much tighter association. The first sample was taken an hour prior to the meltwater runoff peak and the second, 5 hours after. The 2005 runoff on Field 9 was a high flow ($\approx 0.150 \text{ m}^3 \cdot \text{s}^{-1}$), early season, one day event that resulted in gully erosion with little time for dissolution during transport. On March 14, 2010 under similar flows ($\approx 0.150 \text{ m}^3 \cdot \text{s}^{-1}$) on the same field, samples were taken with no

notable particulate content ($TDP/TP \approx 1$). Considering the disproportionate influence of two consecutive same-day samples in a 563 sample data set, the regressions as shown in Figure 4.6 are considered valid and representative of the sampled EOF chemistry.

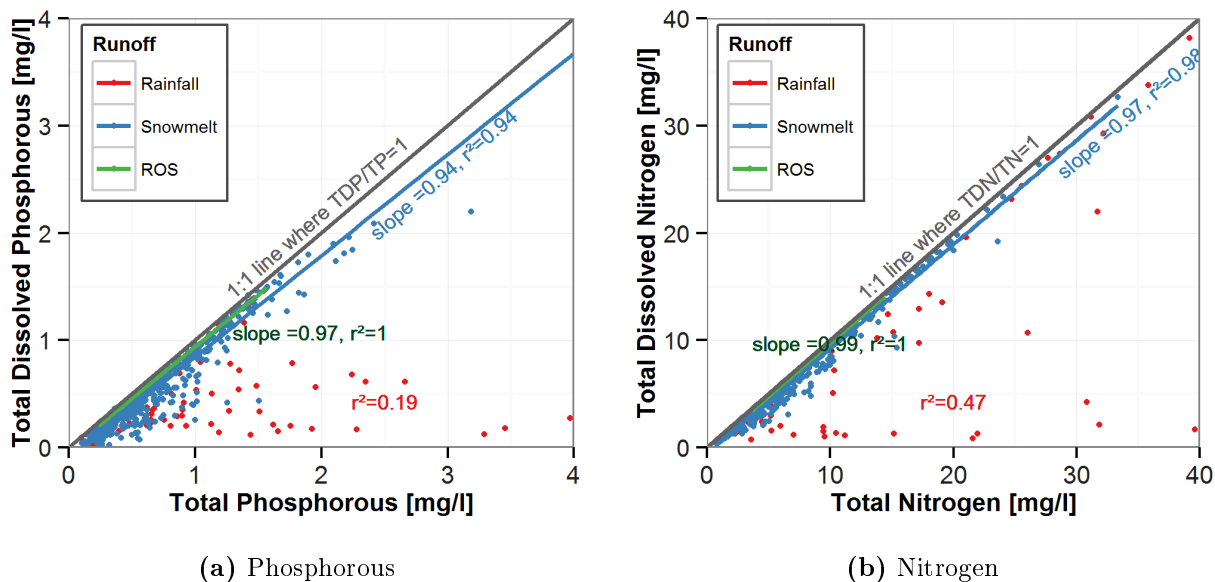


Figure 4.6: Phosphorous and Nitrogen Exports, dissolved vs total fractions. These plots illustrate the rainfall and snowmelt runoff composition for phosphorous (4.6a) and nitrogen (4.6b) at the field scale. These plots extents are zoomed in for clarity but show > 90% of the data. The full extent of the data and outliers are shown in Figure B.11. The least - squares linear regression is performed on the entire limits of the data. There were two data outlier samples for P and N taken on March 31, 2005 that were removed (see text).

The resulting regressions identify a TDP–TP and TDN–TN relationship for ROS and snowmelt runoff events and the lack of a TDP–TP and TDN–TN relationship during rainfall runoff events. The regressions are plotted for all three runoff event types to highlight the fact that snowmelt and ROS runoff events behave differently from rainfall runoff events. A prairie nutrient model should reflect this difference.

4.4 Nutrient sources during snowmelt runoff

At the field scale, snowmelt runoff yields P and N chemistry with a chemical composition different from that of rainfall runoff (Section 4.3). Using the field scale metrics (indicated with a subscript f): concentration factor (CF_f , Equation 4.1) and load factor (LF_f , Equation 4.2), the source of this P and N and the role of the snowcover can be teased out. The concept for

CF_f was taken from [Stein et al. \(1986\)](#) where CF_{Stein} , Equation 5.7 in Chapter 5, is defined as the change in meltwater concentration with time relative to the bulk snowcover concentration. The field scale metric, CF_f (LF_f), is defined as the meltwater solute concentration (mass) at the edge-of-field relative to the bulk snowcover solute concentration (mass):

$$CF_f = \frac{\text{meltwater solute concentration mean}}{\text{bulk snowcover solute concentration mean}} \quad (4.1)$$

$$LF_f = \frac{\text{meltwater solute mass}}{\text{snowcover solute mass}} \quad (4.2)$$

A $CF_f < 1$ and/or $LF_f < 1$ indicate that concentrations/loads were depleted during transport. Typically EOF runoff volumes are only a fraction of the snowcover SWE due to infiltration, therefore a $CF_f = a$ may coincide with an $LF_f < a$ as the mass exported is a product of both concentration and volume. A $CF_f = 1$ and $LF_f = 1$ would indicate that meltwater chemistry was the same as snowcover chemistry and that there was no loss of SWE during transport to the EOF. This use of the CF_f and LF_f to compare snowcover and EOF solute content aids in determining whether snowcover solute concentrations are enriched or depleted during meltwater transport to EOF. Coupling this with the agricultural management practices employed on the field enables the speculation of the source of the solute enriching the EOF meltwater. Figure 4.7 illustrates that TDP and NO_3 were enriched during transport (both the average concentration and load of TDP and NO_3 solute were higher at the EOF than in the snowcover). The annually tilled (AT) fields show an elevated EOF CF_f for NO_3 likely explained by the relationship between tillage and mineralization. The AT fields are subject to fall tillage which encourages mineralization ([Campbell et al., 2008](#); [Tiessen et al., 2011](#)) and the spring release of this new nitrate resident in the surface soil. For NH_3 , the snowcover appears to hold most of the observed NH_3 with some enrichment due to the elution of vegetation NH_3 (fields with vegetation residuals, both forage and minimum tilled (MT) fields, show evidence of increased NH_3 mass exports).

From this analysis the following assumptions, illustrated in Figure 5.1 regarding snowmelt runoff are made:

- The TDP observed at the EOF is sourced from soil and vegetation sources, in addition

to snowcover TDP.

- The EOF NH_3 observed at the EOF is largely sourced from the snowcover and field vegetation NH_3 .
- The EOF NO_3 is likely sourced largely from soil ions in addition to the snowcover and vegetation NO_3 sources.

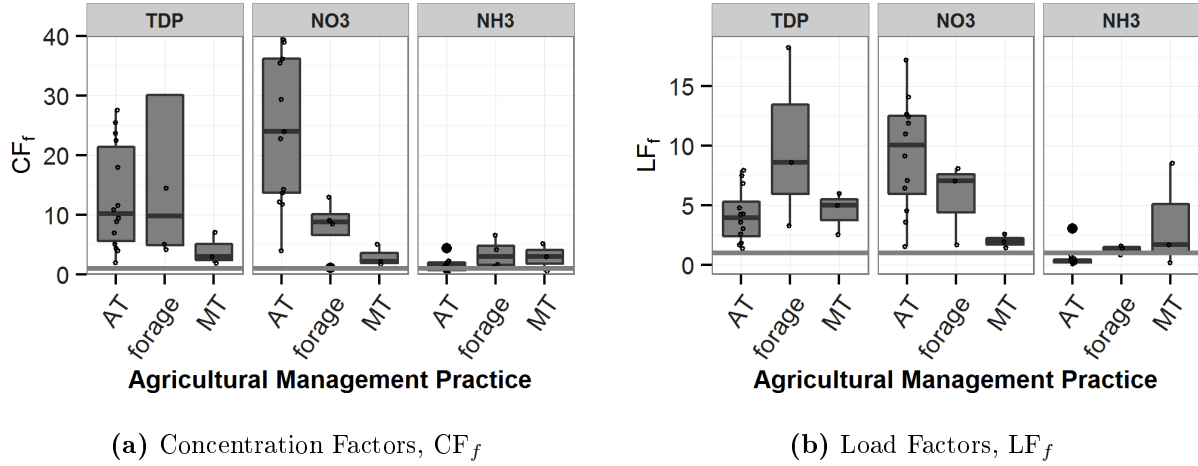


Figure 4.7: Edge-of-field CF_f and LF_f . These plots illustrate the variability in the CF_f (4.7a) and LF_f (4.7b) for the three different crop treatments (AT, forages, and MT) and the three different solutes to be modelled (TDP, NO_3 , and NH_3). The solid grey line marks where the CF_f and LF_f are equal to 1. The grey circles are the sample set from which the boxplots are derived. The black dots are the outliers to the boxplot whiskers which extend to $1.5 \times$ inter-quartile range; the mid-hinge, the median; and the lower and upper hinge the first and third quartiles, respectively.

Generally, $\text{CF}_f \neq 1$ and $\text{LF}_f \neq 1$ indicating that a transformation from the observed snowcover P and N to the observed EOF P and N occurred. The distributions were plotted on a \log_{10} scale using a gaussian kernel smoothing algorithm (R Development Core Team, 2010) to help visualize the change in solute concentrations that occurred (Figures 4.8 and B.12-B.14). TDP and NH_3 concentrations are more variable at the EOF than in the snowcover; NO_3 variability from snowcover to EOF is similar. The annual change in concentrations from snowcover to EOF, CF_f , are shown in Table B.1. Here, it is quickly observed that in 2009 the CF_f for TDP and NO_3 was the lowest observed whereas for 2009, the CF_f for NH_3 was the highest. This lower CF_f might indicate less contact with the soil perhaps due

to an ice layer. The rainfall data (Figure B.1 in Appendix B) and edge-of-field chemistry observations indicate that a basal ice layer may have formed in the fall of 2008 following a light November rain event that occurred on already wet soils. In the presence of a basal ice layer, anoxic conditions may occur resulting in the mineralization process being truncated after ammonification due to the absence of oxygen (Russel, 1988, Chapter 19). This could result in a pool of ionized NH_3 in the soil rather than NO_3 at the onset of melting. This fact combined with reduced meltwater and soil interaction would reduce NO_3 concentrations in the runoff. The observed increase in the CF_f for NH_3 could be related to the reduced nitrification of ionized NH_3 , the fact that vegetative leachate would not be moderated by soil contact during restricted infiltration, or other unknown cause(s).

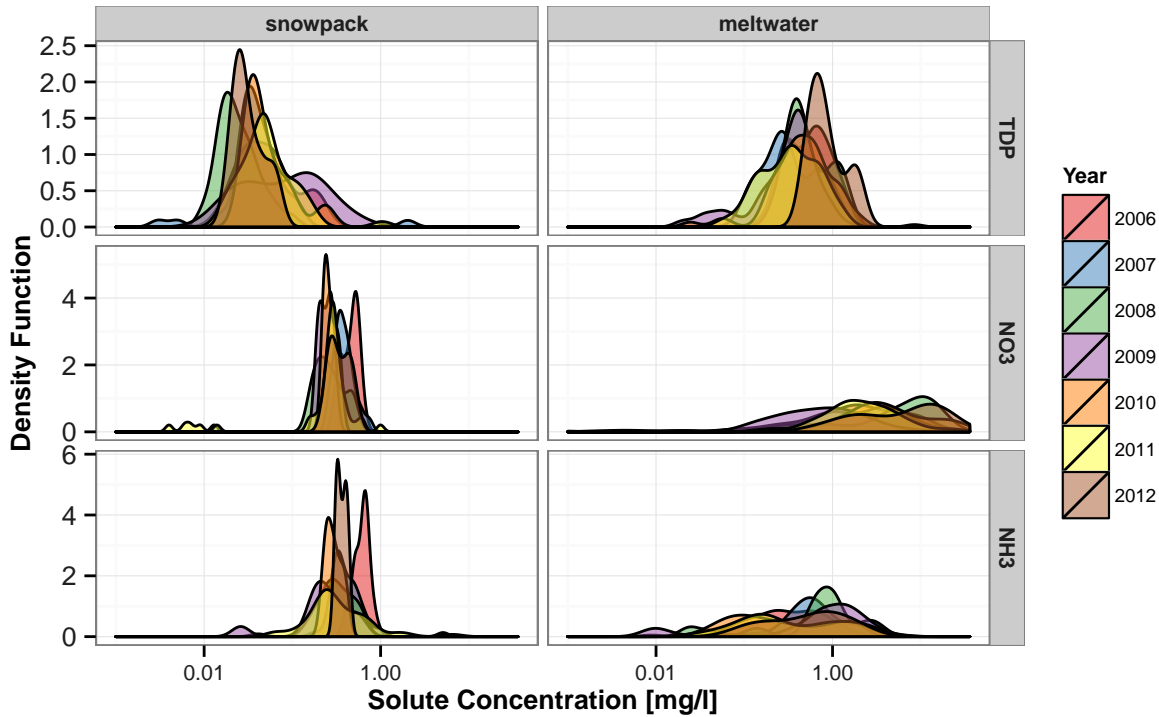


Figure 4.8: Snowcover and EOF Meltwater Solute Probability Density Functions. These are smoothed density function plots (using a gaussian kernel, (R Development Core Team, 2010)) on a \log_{10} scale. These plots illustrate the distribution of sampled concentrations in the snowcover (left) and measured at the EOF (right) for each of several years. For an annual breakdown of the plots for each solute see Figures B.12-B.14 in Appendix B.

As discussed in Section 2.1.4, concrete frost or basal ice formation can restrict runoff contact with the soil. The Sub-basin2 and Twin fields have well drained, organic and granular

Dark Grey Chernozemic soils. The fall volumetric w.c. on the Twin fields ranged between 22 - 31% with an average 28% (Figure 3.13), below the 33% field capacity typical of the Chernozemic soils (FAO Natural Resources Management and Environment Department, 2001). Concrete frost, therefore did not likely form on these fields. An after frost (before snowfall) rainfall event, mid-winter thaw, and the trickle down flow of meltwater and refreezing near the soil surface during spring melt can create a basal ice layer having the same effect (Lilbaek, 2007). Considering the above it is assumed that

- wet soils at freeze-up lead to the subsequent formation of a basal ice layer (In this data set, this pertains specifically to the fall of 2008 affecting the spring runoff of 2009).

This assumption enables the testing of the research hypothesis that restricted infiltration reduces the meltwater interaction with soil and ultimately the transfer of soil ions to the edge-of-field during meltwater runoff (edge-of-field runoff $CF_f \rightarrow 1$ and $LF_f \rightarrow 1$ for both NO_3 and TDP during restricted infiltration runoff events).

4.4.1 Tillage Induced Mineralization

In Section 2.3.3, literature evidence was presented regarding tillage induced mineralization in soils. Observations on the Sub-basin2 research fields, also provide evidence of NO_3 mobilized in the spring following the fall tillage of perennial forage cropping. Figure 4.9 shows high concentrations of nitrate during meltwater runoff from Sub-basin2 fields 4 and 7 which were cultivated in the fall of 2009 following 5 years of perennial forage crops. Based on the literature and field observations, it is assumed that the tillage induced mineralization over the winter period creating a NO_3 pool stored in the surface soil layer, immediately beneath the snowcover. At the onset of melting this NO_3 is transported by the runoff and the NO_3 pool depletes quickly with the snowcover depletion.

Observations also provided evidence that annual tillage practices elevate soil NO_3 and runoff NO_3 concentrations. Fall soil N levels in the 0 – 15 cm horizon differ significantly between annually tilled (AT) and minimum tilled (MT) fields ($p = 0.02$ for two-sample Wilcoxon ranked sum test (R Development Core Team, 2010)) with the soil N being mildly elevated $1.35 g \cdot m^{-2}$ on the AT fields versus $1.12 g \cdot m^{-2}$ on the MT fields. This is consistent

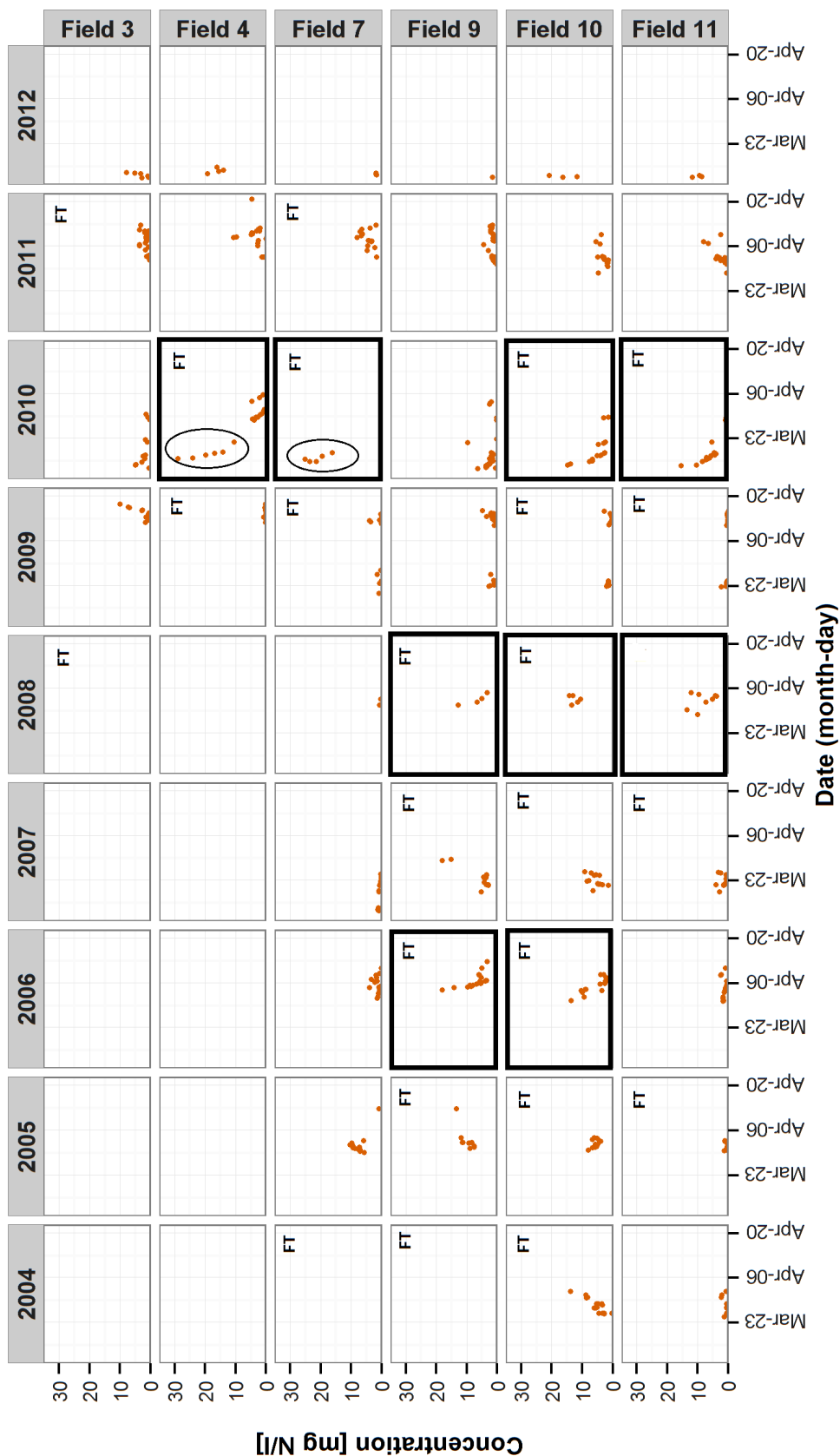
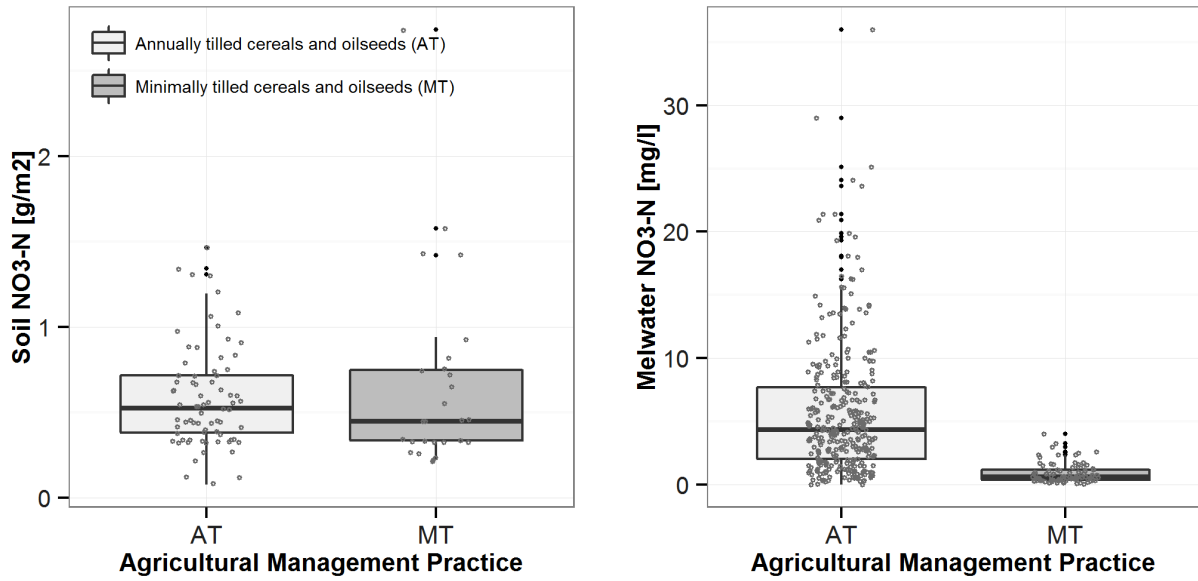


Figure 4.9: NO_3 EOF Time Series. The plots show the time series of samples for NO_3 taken at the EOF during meltwater runoff. The circled years highlight the high concentrations sampled in the runoff at the early stages of the melt event. These high concentrations were attributed to the fall tillage in 2009 that broke up perennial forages in preparation for annual crop seeding in the spring of 2010. FT indicates that fall tillage occurred on that field during the fall of that calendar year. The heavy black boxes indicate fields and years where the NO_3 runoff curve would be considered as decreasing.



(a) Fall Soil Mass of NO₃-N at 0-5 cm depth

(b) EOF Meltwater NO₃-N

Figure 4.10: Tillage Disturbance effects on Soil and Meltwater NO₃. The above plots illustrate the impact of tillage disturbance on the observed fall soil (Figure 4.10a) and EOF meltwater NO₃ concentrations (Figure 4.10b). The grey circles are the sample set from which the boxplots are derived. The black dots are the outliers to the boxplot whiskers which extend to $1.5 \times$ inter-quartile range; the mid-hinge, the median; and the lower and upper hinge the first and third quartiles, respectively.

with [Tiessen et al. \(2010\)](#). Figure 4.10 illustrates the observation that the soil NO₃ levels in the 0–5 cm soil horizons do not differ significantly ($p = 0.43$, two-sample Wilcoxon) between the AT and MT for these same fields and years. The meltwater concentrations, too, observed at the EOF for NO₃ differed significantly ($p < 2.2e - 16$, two-sample Wilcoxon) between the two practices. Tilled fields are subject to higher rates of mineralization, the likely cause of the higher measured NO₃ levels in the 0–15 cm soil horizon ([Campbell et al., 2008](#); [Tiessen et al., 2010](#)), but not in the 0–5 cm horizon where the NO₃ is quickly flushed. It is therefore assumed that the source of the elevated runoff NO₃ concentrations on these fields was fall tillage and the associated over-winter mineralization leaving a mobile pool of NO₃ beneath the snowcover.

The time series concentration trends for NO₃ shown in Figure 4.9 can also be classified as *constant* or *decreasing*. The decreasing melt concentrations follow fall tillage events likely evidence of the flushing of mobile N pools formed over-winter, although not all fall tillage

events create the observed decreasing trend. Fall tillage events are, as established, related to higher runoff concentrations and this can be observed in the Figure 4.9 plots, the boxplots in Figure 4.10, and the CFs calculated for each agricultural practice (Figure 4.7a).

4.4.2 Forage Vegetation as a Leachate Source

Winter wheat, forage, and reduced tillage practices have increased the amount of stubble and growing vegetation resident on fields during fall, winter, and spring melt. As discussed in Section 2.3.3, this vegetation serves as a source, in addition to the soil, of mobile P and N. Freeze-thaw cycling, fresh forages, and actively growing vegetation (forages and winter wheat) have been shown to further enhance the amount of P and N that leaches from this vegetation (Bechmann et al., 2005; Elliott and Henry, 2009; Elliott, 2013; Joseph and Henry, 2008; Liu et al., 2013a; Miller et al., 1994; White, 1973).

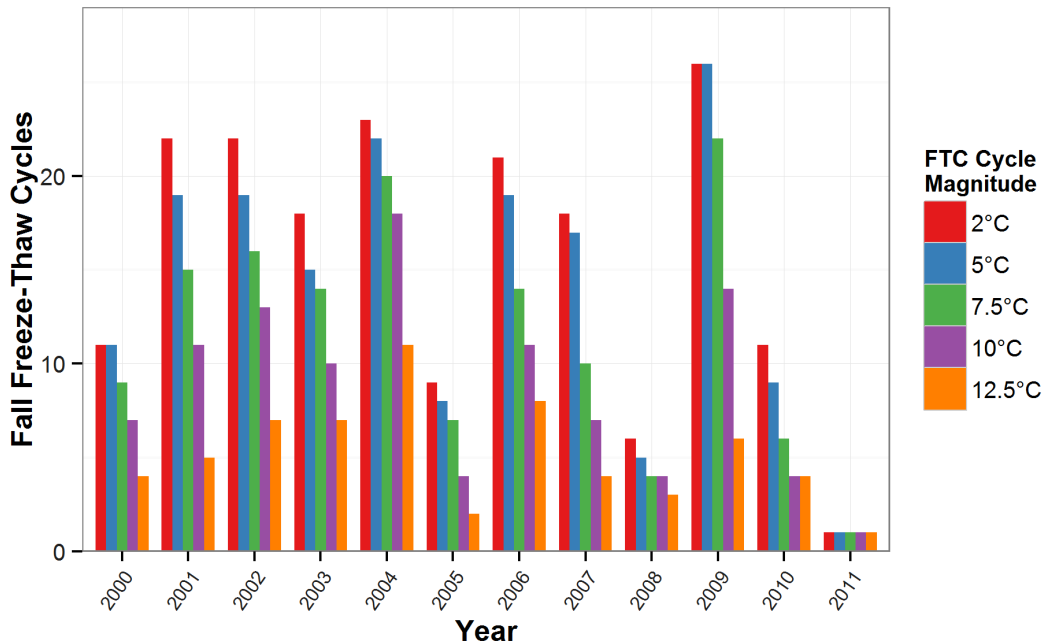


Figure 4.11: Annual Freeze-Thaw Cycle Count. This plot illustrates the count of freeze-thaw cycles that occurred in the fall season on bare ground as interpreted by computer simulation of SWE. FTCs of varying amplitudes were quantified for each year, all cycles had air temperatures at or below -2°C and greater than 0°C .

On the Sub-basin2 and Twin fields freeze-thaw cycles (FTCs) were quantified annually for 11 years extending from the fall of 2001 to post harvest 2011, to verify whether FTCs

could be related to the spring melt runoff events with elevated TDP and TDN measured at the edge-of-field (EOF). Mild ($\leq 10^{\circ}\text{C}$) and extreme ($> 10^{\circ}\text{C}$) FTCs, with a minimum air temperature below -2°C (based on the definition of a killing frost in Saskatchewan ([Government of Saskatchewan, 2008](#))) occurring on bare ground in months later than August and before December (snow of sufficient depth will insulate the ground from the air temperature fluctuations) were investigated. These criteria resulted in an FTC count for each year as illustrated in Figure 4.11.

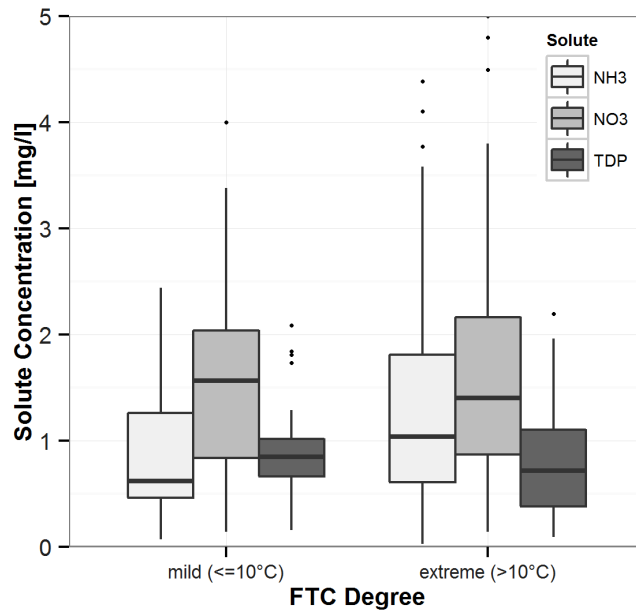


Figure 4.12: EOF Concentrations vs FTCs. This plot categorizes EOF runoff concentrations from fields with mild FTCs ($\leq 10^{\circ}\text{C}$) with fewer than 10 cycles for all temperatures and those with extreme FTCs ($> 10^{\circ}\text{C}$). Ten cycles was a visibly recognizable threshold based on the Figure 4.11 where, if there was a difference in solute concentrations, it might be exposed. According to the counts in Figure 4.11 and the aforementioned criteria, the fall of 2005, 2008 and 2011 which affect the spring runoff events of 2006, 2009, and 2012 respectively were classified as mild. 2009 was removed due to the fact that the basal ice layer would bias the interpretation of FTC impacts on EOF runoff.

Annual average nutrient concentrations on forage fields were compared with FTCs (Figures C.1 and 4.12) to see if there is obvious field evidence to support increased leaching from vegetation related to increased fall FTCs. In Figures C.1 and 4.12 and further analyses of the data, there was no clear relationship with EOF concentrations and the FTC count or degree. This was somewhat expected. First of all, there was no EOF meltwater runoff

data where FTCs had not occurred during the fall to use for comparison. Additionally, crop type, soil moisture, soil P and N, and plant moisture contents are just a few of the factors affecting the response of field vegetation to frost and EOF runoff concentrations. During runoff, phenomenon such as enhanced infiltration of ions ([Lilbaek and Pomeroy, 2010](#)) in the early meltwater runoff where concentrations would be expected to be the highest could also obfuscate any relationship between FTCs and EOF concentrations. The relationship with FTCs and vegetation has been well established in the literature and controlled laboratory experiments. Perhaps the most important point here is that freeze-thaw cycling does occur frequently on these typical Canadian Prairie fields (Figure [4.11](#)).

CHAPTER 5

MODEL DEVELOPMENT

This chapter describes the nutrient and hydrological model setup. The chapter begins with a conceptual description of the Prairie Nutrient Snowmelt Model which describes how the model is designed to (ultimately) nest within an existing model structure that can provide hydrological inputs, perform nutrient mass balance, and predict rainfall runoff nutrient exports. Following the introduction of the conceptual nutrient model, the Cold Regions Hydrological Model (CRHM) set up is described. This provides a description of the hydrological model outputs that serve to drive the nutrient model. The chapter concludes with a detailed discussion of the developed Prairie Nutrient Snow Model structure, assumptions, and equations.

5.1 Prairie Nutrient Snowmelt Conceptual Model

Field scale data and findings in the literature support the differentiation between snowmelt runoff chemistry and rainfall runoff chemistry. The data analyses in Chapter 4 suggests that: 1) the composition of edge-of-field (EOF) meltwater phosphorous and nitrogen is largely dissolved (particulate size $< 45\mu m$) and sourced from vegetation, soil, and atmospheric contributions to the snowcover; 2) the agricultural practices of minimum tillage and forage cropping provide the field vegetation source that interacts with the snowcover and meltwater via leaching; 3) EOF P and N solute concentrations and flows vary independently over several orders of magnitude; and 4) restricted infiltration under basal ice conditions may alter EOF runoff composition.

The field scale data resolution is not sufficient to quantify sub-field variability in EOF hydrochemistry related to 1) flowpaths defined by micro-depressions (i.e. tractor tracks) and 2) fractional snow covered area during snowmelt. Flowpaths have a direct influence on both the

travel time (and therefore solvent-solute contact time) and the sources of solute the solvent interacts with (i.e. a nutrient rich area of the soil or a vegetation clump). Flowpaths can be dynamic and may change in length and location as the melt progresses due to changes in flow volumes and snowcover ablation patterns. Snowmelt does not proceed at a uniform rate over the field (Figure 2.2) and the presence or absence of dirt, vegetation, micro-depressions, and shading, as well as snowcover depth and density all affect the melt rate within the field. Therefore water that runs off at the EOF is sourced from variable locations in the field as the melt progresses. This can be expressed as follows:

$$\frac{\partial c}{\partial x} \neq 0 \quad (5.1)$$

$$\frac{\partial c}{\partial t} \neq 0 \quad (5.2)$$

where c is the solute concentration and $c = c(x, t)$, x the flowpath length across the field, and t time. The field scale data are representative of $\frac{\partial c}{\partial t}$ as it relates to the melt progression but not as it relates to changes in flowpath. Therefore, the developed model accounts for $\frac{\partial c}{\partial t}$ but not $\frac{\partial c}{\partial x}$. Time will be implicitly described with the hydrological processes and CRHM output used as inputs in the nutrient model but not explicitly in the model equations. The sub-field flowpaths will be referred to as the ∂x flowpaths to distinguish them from the runoff flowpaths determined by the infiltration regime (Figure 1.1).

Figure 5.1 illustrates the three major sources of TDP, NO_3 , and NH_3 solute assumed to be eluted, dissolved, and/or diffused into a volume of meltwater and transported by that volume of meltwater to the EOF. On nutrient rich agricultural fields, the meltwater is generally enriched (Figure 4.7a) during transport as such the relationship is described as additive. $\frac{\partial c}{\partial x}$ cannot be described by the field scale data and therefore each unit volume of runoff water is assumed to be enriched or depleted by the same sources of solute as described

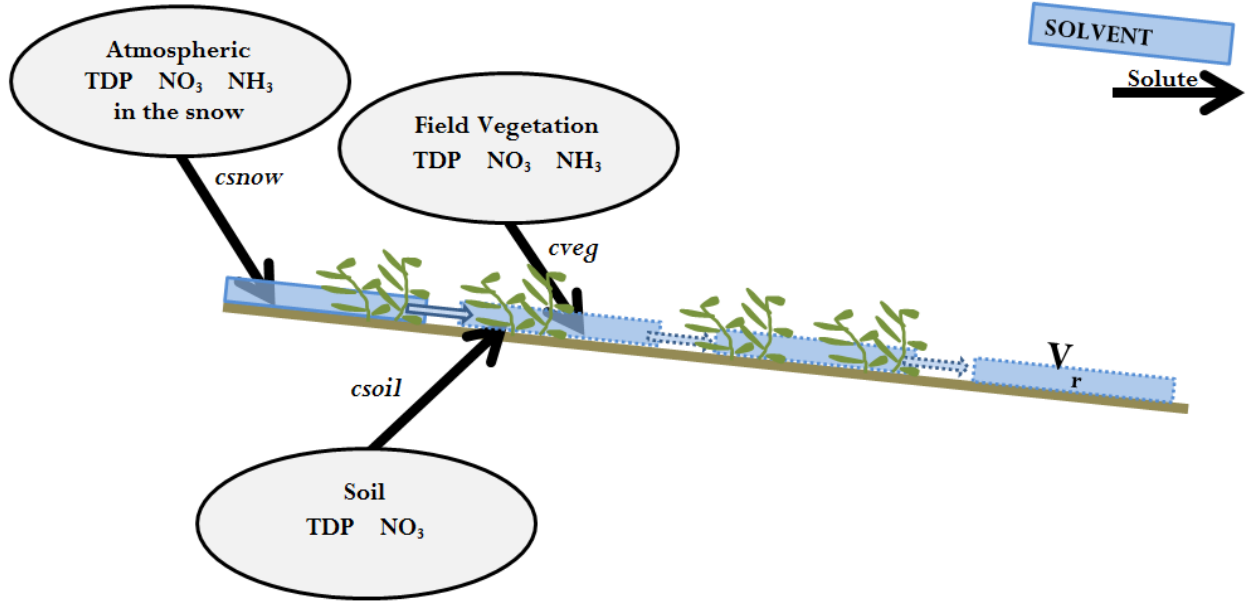


Figure 5.1: Conceptual Model: Sources of P and N in Field Scale Snowmelt Runoff. Abbreviations: V_r , volume of runoff.

in Equations 5.3-5.4.

$$c_{EOF} = \frac{V_{snow} \cdot csnow + \alpha \cdot V_{soil} \cdot csoil + V_{veg} \cdot cveg}{V_r + V_s} \quad (5.3)$$

where $V_{snow} = V_{soil} = V_{veg} = V_r$

$$V_r \approx V_r + V_s$$

therefore,

$$c_{EOF} = csnow + \alpha \cdot csoil + cveg \quad (5.4)$$

where V_{snow} , V_{soil} , V_{veg} , V_r , and V_s respectively represent the volume of snowmelt runoff, runoff in contact with the soil, runoff in contact with vegetation, volume of runoff, and volume of solids (P and N dissolved, eluted, and/or diffused into the volume of runoff during transport). c_{EOF} , $csnow$, $csoil$, $cveg$ respectively represent the concentration, c of either of TDP, NO_3 , or NH_3 at the EOF, in the snowmelt, in the soil, or leached from vegetation sources. α is a binary variable: for NH_3 , $\alpha = 0$ and for TDP and NO_3 , $\alpha = 1$.

Existing nutrient models that account for snow and cold regions processes do not differentiate between snowmelt runoff P and N and rainfall runoff P and N. Some models do differentiate between saturation and infiltration excess runoff P and N and in so doing utilize

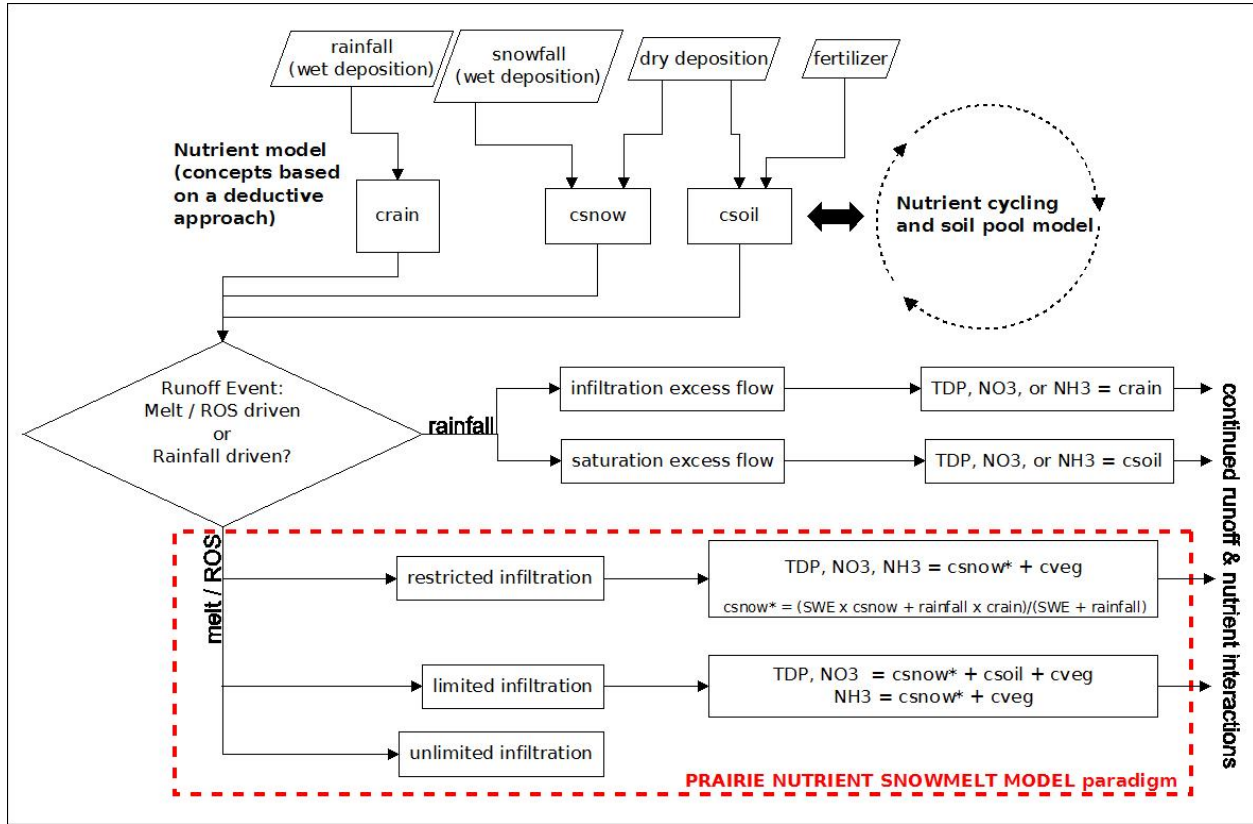


Figure 5.2: Prairie Nutrient Snowmelt Model Paradigm. This figure illustrates the scope of the Prairie Nutrient Snowmelt Model framework that is developed in this thesis (delineated by dotted red line). It also suggests how this model might nest within the framework of an existing nutrient model structure such as HYPE (Lindström et al., 2010). As in Equation 5.4, *csnow*, *csoil*, and *cveg* are related to sources of P and N in the snow, soil, and vegetation. *crain* is related to the P and N in the rain and *csnow** the weighted average of *crain* and *csnow* runoff contributions during a ROS event (Equation 5.5).

the principles of the conservation of mass to predict nutrient exports (Section 2.4). The investigations in Section 4.2 rule out EOF runoff discharge as a means to predict EOF P and N concentrations and illustrate the uncertainty in the field scale mass balance (Section 4.1). Changes in agricultural practices that affect soil P and N require that soil accounting be done and mass conserved in order to aid in the prediction of how these changes might affect runoff losses of P and N. As discussed, there is a decadal buffer in the soils to short term changes in mobile soil nutrient inputs and outputs and therefore changes in soil P and N may not elicit a proportionate (expected) change in runoff P and N concentrations (Sections 2.3.2 and 4.1). If agricultural depletion of mobile P and N pools can be buffered by the soils themselves, this can only be represented by models of soil nutrient processes.

It is assumed that, true to field observations and findings in the literature, all else being equal, meltwater runoff events generate P and N with different dissolved and particulate fractions than rainfall runoff events, in addition to sourcing P and N from the snow, soil, and vegetation (Equation 5.4). A new Prairie Nutrient Snowmelt Model paradigm is proposed to nest within a developed nutrient model structure as shown in the red dotted area of Figure 5.2. The following should be noted:

The Prairie Nutrient Snowmelt Model paradigm presented subsequently is a field scale model. The composition of runoff P and N has been studied and modelled within that context. As runoff water moves from the field to the stream and interacts with riparian zones, stream banks, and stream bed sediments the composition of the P and N fractions changes (Mahmood et al., 2014) and erosion and in-stream processes must be addressed.

The Prairie Nutrient Snowmelt Model distinguishes between restricted, limited, and unlimited infiltration events as defined by Granger et al. (1984). It was hypothesized in Section 4.4 that restricted infiltration events reduce meltwater - soil interaction and thus remove soil as a source of solute for TDP and NO₃. The model, therefore, differentiates between restricted and limited infiltration events. Unlimited infiltration events do not generate runoff as the soils have the capacity to infiltrate all of the meltwater. Rain-on-snow events are treated as snowmelt runoff events with the composition of P and N in the snow calculated as weighted average of snow concentrations and rain concentrations based on the SWE on the field at the time of rainfall and the total rainfall. This is shown in Equation 5.5:

$$c_{snow*} = \frac{SWE \cdot c_{snow} + \text{rainfall} \cdot c_{rain}}{SWE + \text{rainfall}} \quad (5.5)$$

where c_{snow} and c_{rain} represent the concentrations in the snowcover and rainfall respectively, and c_{snow*} the weighted concentration of the snowcover and rainfall contributions to runoff.

5.2 Hydrological Model Platform

CRHM is a modular platform that allows the user to select the most appropriate physics to represent the important physical processes for the site. The modules were selected to configure a model capable of realistic representation of the important hydrological processes

in a cold prairie region based on previous Canadian Prairie simulations ([Fang et al., 2010](#); [Pomeroy et al., 2007b](#)). The hydrological model was configured for the field scale to allow: 1) edge-of-field (EOF) runoff observations to be compared with simulated EOF runoff, and 2) different agricultural management practices to be assessed. The forage and annually tilled cereals and oilseeds fields (AT) in Sub-basin2 were chosen as the subject fields for modelling. Sub-basin 2 fields 7 and 9 were chosen as the development fields for this model, as they are the largest in area and field 9 has the most clearly defined effective drainage area of the Sub-basin2 fields. Field 7 is partner to 9 and subject to opposite agricultural treatments (i.e. Field 7 was under AT practices when Field 9 was under forage practices).

The modules included to simulate the hydrological response from the Sub-basin2 fields 7 and 9 are described below and shown schematically in Figure 5.3. Refer to the CRHM module manual ([Centre for Hydrology, 2014](#)) for more information.

- The observation module reads the meteorological data from file. These data drive the operations of the model and are supplied at hourly intervals, dictating the time step for the model.
- The global radiation module uses the parameter values attached to geographical location such as latitude, elevation, and time. These are used to calculate the theoretical shortwave direct and diffuse solar radiation following the procedures introduced in ([Garnier and Ohmura, 1968](#)) and subsequently modified by ([Gray et al., 1986a](#)) which requires the surface geometry and declination of the sun.
- The observation data did not include solar radiation data, therefore the Annandale module to calculate incoming solar radiation from measured daily maximum and minimum air temperatures was used. Annandale uses the calculations provided in [Annandale et al. \(2002\)](#) as modified by [Shook and Pomeroy \(2011a\)](#) to supply sub daily radiation values to CRHM.
- The long-wave radiation module is based on the work of [Sicart et al. \(2006\)](#). This module relies on the output from the Annandale short-wave module and the HRU variables of temperature, vapour pressure, and relative humidity to calculate longwave

radiation to melting snow. [Sicart et al. \(2006\)](#) proved this method of calculation to be robust in late winter and spring conditions on a Canadian Prairie site, the critical period for runoff and nutrient transport.

- The all-wave radiation module is used to estimate net radiation from incoming short-wave radiation and the Brunt equation for use in the calculation of evaporation during the snow free period. The module was developed with a data set collected from a Canadian Prairie site in southwestern Saskatchewan ([Granger and Gray, 1990](#)).
- The canopy module ([Ellis et al., 2010](#)) calculates snowfall and rainfall interception and, therefore, sub-canopy snowfall and rainfall. Sub-canopy shortwave and longwave radiation are calculated when there is snowcover.
- The prairie blowing snow module calculates blowing snow redistribution and the in-transit sublimation according to [Pomeroy and Li \(2000\)](#).
- The crop growth module is a macro used to linearly simulate annual crop growth patterns based on crop seeding and maturity dates (assumed 2 weeks before the recorded harvest date). Both the crop height [cm/d] and leaf area index (LAI) [$-/d$] were grown to achieve maturity by the input dates according to the agricultural record. At harvest LAI and crop height are reset. Crop height is reset to the stubble height.
- The albedo module is used to determine the change in snow albedo throughout the snow covered and snowmelt period. This module also estimates the start of the melt period. Calculations are based on the work of [Gray and Landine \(1987\)](#) on shallow prairie snow covers and require input variables of daily net radiation, temperature, snowfall, and snowcover SWE.
- Snobal, the energy balance module in CRHM, is used to determine snowmelt as detailed by [Marks et al. \(1999\)](#). This module was designed to resolve the energy balance and quantify the energy available for snowmelt based on the specified time step, in this case hourly.

- The infiltration module was designed specifically to handle frozen prairie soils and the occurrence of unlimited, limited, and restricted infiltration events as described by [Granger et al. \(1984\)](#) and [Gray et al. \(1986b\)](#). For estimating rainfall infiltration into unfrozen soils [Ayers \(1959\)](#) is used.
- The evaporation module employs Penman-Monteith method of quantifying evaporation ([Monteith, 1965](#)) and the influence of surface resistance ([Jarvis, 1976](#); [Verseghy et al., 1993](#)). The Penman-Monteith resistance parameter is adjusted according to the growth stage of the crop. The set of calculations employed in this module is taken from [Armstrong et al. \(2008\)](#).
- The soil module ([Dornes et al., 2008](#); [Fang et al., 2010, 2013](#); [Leavesley et al., 1983](#)) performs the soil moisture balance and drainage calculations. This soil moisture balance includes sub-HRU scale depressional storage, HRU scale pond storage, groundwater storage, and soil column storage. Discharge from groundwater and depressional storage, and runoff from the soil column are also calculated. The soil column is described with two layers: a thin surface recharge layer from which both evaporation and transpiration can occur and a subsurface layer from which transpiration can occur if rooting depth allows. Excess water from the soil column feeds groundwater flow (depressional and pond storage can also feed the groundwater if macropore pore flow is ascribed) and then surface flows. Surface runoff occurs and feeds depressional and pond storage, if the drainage from saturated soils is exceeded or the melt or rainfall rate exceeds the infiltration capacity of the soil column. Both depressional and pond storage can fill up and spill over if surface flows exceed their holding capacity ([Spence and Hosler, 2007](#)). This module is developed to provide process representation based on the Canadian Prairie ([Pomeroy et al., 2007a](#)).
- The routing module relies on [Clark \(1945\)](#) lag and route runoff timing estimation procedure to move runoff from HRU to HRU.

The CRHM platform uses a semi-distributed spatial resolution with Hydrological Response Units (HRUs) which are landscape units with similar soils, vegetation, and topography

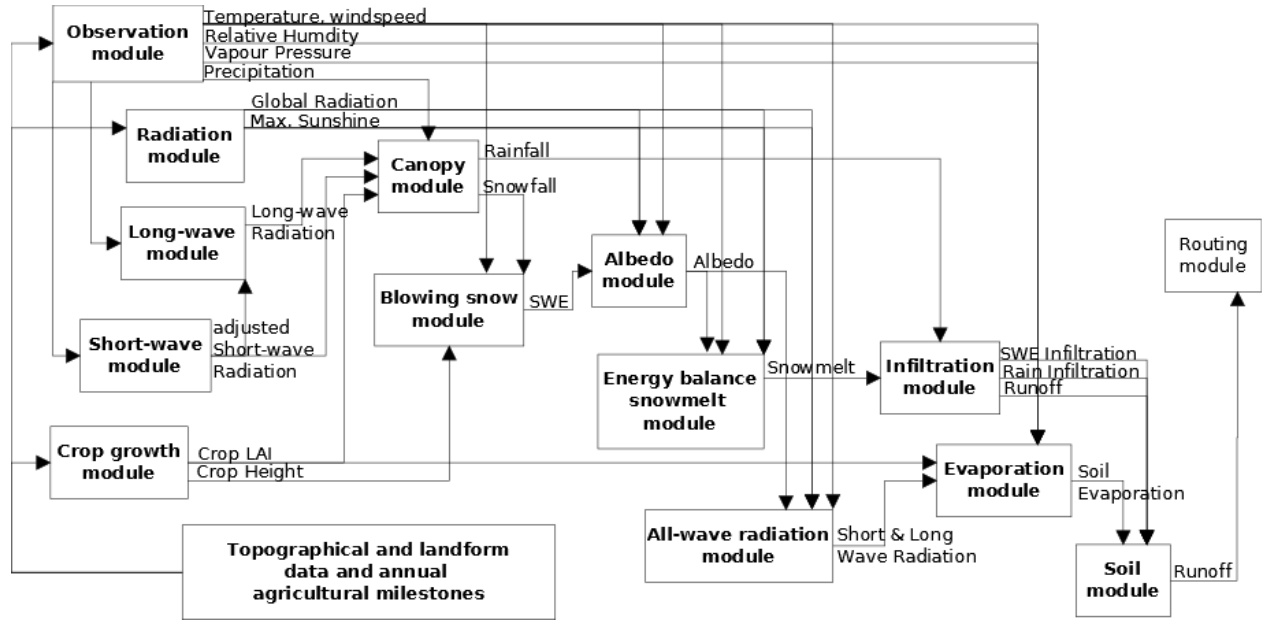


Figure 5.3: Hydrological Model Flowchart. This flowchart illustrates the modules selected from CRHM to simulate the runoff off of fields 7 and 9 in Sub-basin2.

that are likely to yield the same hydrological response when provided the same meteorology for landscape definition. The temporal resolution of the driving meteorological data defines the time step of the model and the resolution at which mass and energy changes are calculated and transferred from one HRU to another. One HRU was suitable to represent the subject Sub-basin2 fields 7 or 9 with its consistent slope, aspect, soil, and vegetation type. Two additional HRUs (Figure 5.4) were used for each model for the purposes of blowing snow transport and providing hydrological context to the subject field of the simulation. The research fields in Sub-basin2 are on the surface hydrologically disconnected - the effective drainage area is defined and consists only of the subject field. In the case of subsurface flow, groundwater flow, and wind transport of snow the subject field is not disconnected. On these fields, overland flow is the primary method of water transport and groundwater and subsurface flow occur rarely at the field scale; but, blowing snow transport is commonplace and to accommodate this (and subsurface and groundwater flow), two additional HRUs were defined based on the data provided for adjacent upstream fields in Sub-basin2. During the simulation of blowing snow transport, snow is relocated to the HRUs with the taller vegetation (i.e. conventionally tilled field to forage field, any field to riparian area).

The CHRM platform has the following main components: 1) observations, 2) parameters,

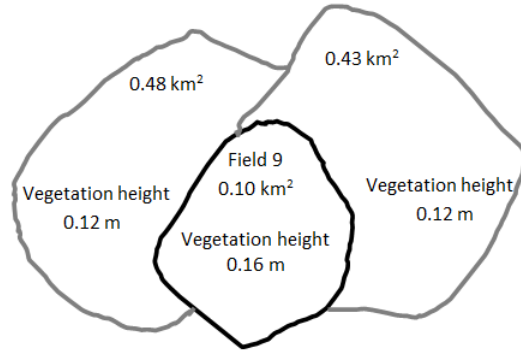


Figure 5.4: Conceptualized Basin setup for CRHM. This schematic illustrates the three HRUs used to generate the field scale simulation. The unnamed fields provide hydrological context (a source of blowing snow) for the Sub-basin field 9 simulation. The same set up is used for Sub-basin field 7.

3) variables 4) state variables, and 5) modules, all described in more detail in [Pomeroy et al. \(2007b\)](#). The observations are time series meteorological data that drive the model operation and dictate the model time step. The observations for this model include air temperature, relative humidity, wind speed, and precipitation observations taken from the Twin watershed site (rainfall data) and an Environment Canada weather station northeast of the watershed ([Mahmood et al., 2015](#)). Parameters are the spatial descriptive data that characterize the HRUs of the site and determine the relationships embedded within the model that control model function. These include latitude, slope and aspect, soil properties, vegetation cover and properties related to evaporation and interception, and prescribed landscape albedo. Parameters were set for these HRUs based on field observations and previous research. Data derived from field observations include seeding and harvest dates, crop type, stubble heights, and soil type. At the field scale, runoff timing and volume were sensitive to stubble height ([Mahmood et al., 2015](#); [Mahmood, 2014](#), pers. comm.) and the prescribed height was based on simulation results to match runoff timing and volume and, therefore heights varied by field and crop type within a range of 5 - 28 *cm*. In reality, stubble height is variable (operator, crop, and equipment dependent) and for these fields typically ranged between 12 and 45 *cm* ([Mahmood et al., 2015](#)). Variables and state variables are declared in the chosen modules. Variables are meteorological driving data such as precipitation, wind speed, and temperature and state variables are dynamic and updated to track changes in the HRU properties such

as soil moisture, snow water equivalent, and albedo during the model operation.

5.3 Prairie Nutrient Snowmelt Model

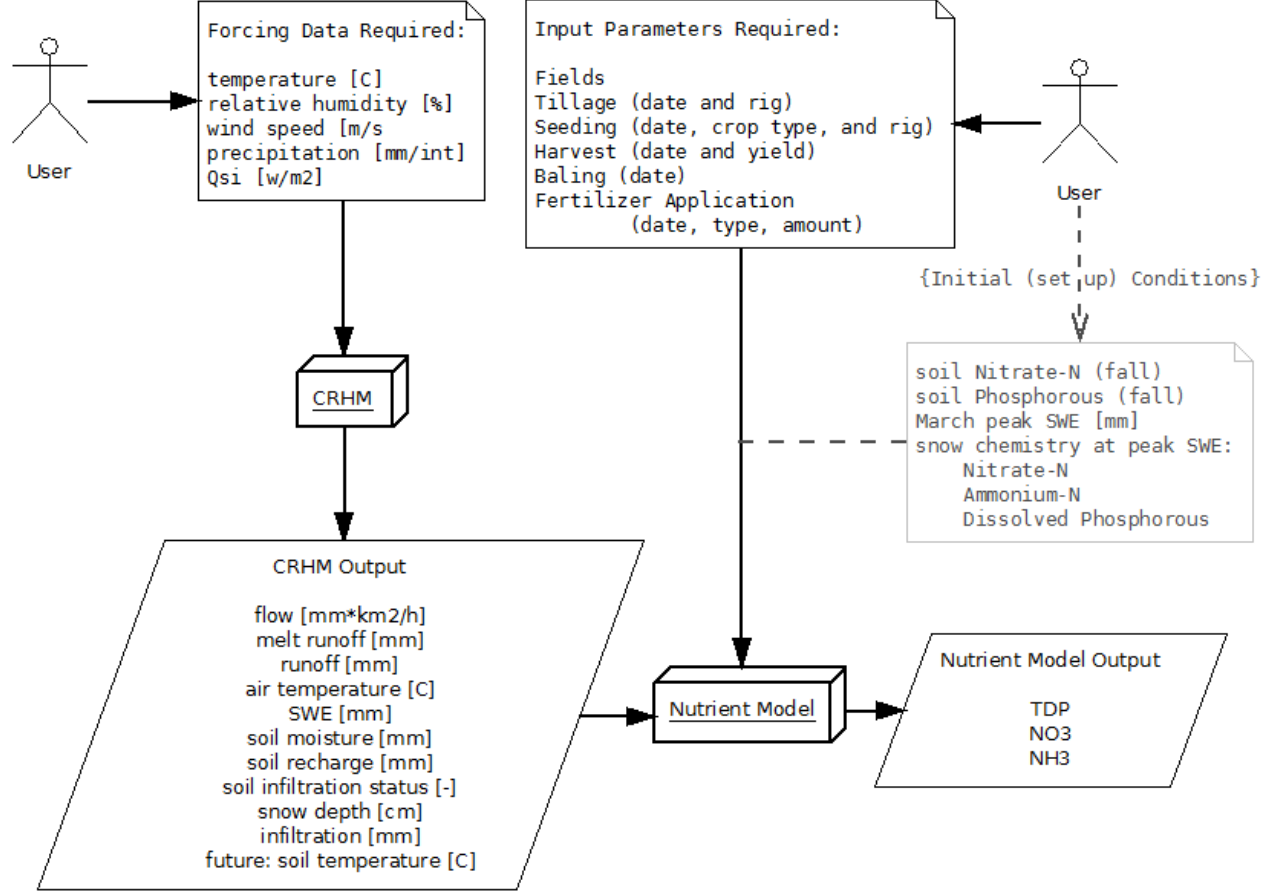


Figure 5.5: Prairie Nutrient Model Structure.

The developed equations for c_{EOF} (Equation 5.4) in the Prairie Nutrient Snowmelt Model rely on field data in addition to inputs from the hydrological model. The data required from both these sources are highlighted in Figure 5.5.

During this model development period, there were several initial conditions required to be input by the User highlighted in the light grey dotted area of Figure 5.5. SWE was included as an initial condition to provide a value for σ_o , the pre-melt standard deviation in the snowcover SWE (Equation 5.10); otherwise, CRHM generated SWE was used to drive the nutrient model.

The observed snowcover and soil P and N concentrations used in the model are the calcu-

lated means of the observed field surveys. This is the base case model scenario. Sensitivity to these observations is investigated in Section 6.3.

The model code as discussed subsequently can be found in Appendix C.

5.3.1 Model Assumptions

The development of the Prairie Nutrient Snowmelt Model involved many assumptions. The four key assumptions structuring the model presented in Section 4.4 are described first, followed by general model assumptions, and concluding with the assumptions related to the physics of the model equations (Section 5.3.2).

The following are the four key assumptions and related process assumptions that structure the model:

- Assumption 1: The TDP observed at the EOF is sourced from soil and vegetation sources, in addition to snowcover TDP.
 - Snowcover TDP ions migrate to the EOF and the initial concentration of TDP eluted from the snowcover is elevated above the bulk snowcover concentrations.
 - On nutrient rich agricultural prairie soils, snow meltwater is enriched with TDP once it contacts the soil, and increased contact time will increase the release of P to the meltwater.
 - TDP observed in the EOF runoff water is linearly related to OlsenP in the surface soils with the relationship $y = mx - b$.
 - Freeze-thaw cycles (FTCs) cause cellular tissues in vegetation to rupture and release TDP that is readily mobilized with meltwater.
- Assumption 2: The NH_3 observed at the EOF is largely sourced from the snowcover and field vegetation NH_3 .
 - Snowcover NH_3 ions migrate to the EOF and the initial concentration of NH_3 eluted from the snowcover is elevated above the bulk snowcover concentrations.

- Under restricted infiltration and therefore, reduced soil contact, NH_3 at the EOF is enriched as a result of reduced nitrification (leaving more mineral readily mobilized NH_3 in the soil and in the protruding residue material).
- FTCs cause cellular tissues in vegetation to rupture and release NH_3 that is readily mobilized with meltwater.
- Assumption 3: The EOF NO_3 is sourced largely from soil ions in addition to the snowcover and vegetation NO_3 sources.
 - Snowcover NO_3 ions migrate to the EOF and the initial concentration of NO_3 eluted from the snowcover is elevated above the bulk snowcover concentrations.
 - NO_3 resides in the soil water of the soil matrix at similar concentrations during frozen and unfrozen soil conditions.
 - The act of tillage mobilizes existing pools of nitrate in the soil and fosters the mineralization of organic N material. A pool of accessible NO_3 therefore, forms beneath the snowcover readily moved with the meltwater in the spring.
 - FTCs cause cellular tissues in vegetation to rupture and release NO_3 that is readily mobilized with meltwater.
- Assumption 4: Wet soils at freeze-up lead to the subsequent formation of a basal ice layer. This occurred in the fall of 2008.

The following are the general assumptions governing model design:

- Soil nutrient cycling was not performed during this stage of the model development. Fertilization and harvest P and N additions and subtractions were assumed to be represented by the fall soil nutrient observations.
- Runoff exports were based on observations of fall soil nutrient levels. These were assumed to remain relatively unchanged over the winter season, except for the occurrence of mineralization after fall tillage events which was accounted for separately.
 - Redistribution of solutes in the soils over the winter season was assumed not to affect the accessibility of the fall measured nutrients in the soils.

- At each hourly time step and throughout the runoff events, soil nutrient supplies were assumed to be sustainable and not significantly reduced by the mass of solute exported in the annual runoff (refer to Figure 4.2).
 - Evapotranspiration from soils was assumed not to affect the concentration of nutrients in the soils.
- The few rainfall runoff events that occur during the model period are accounted for with the intent to nest this model structure within an existing nutrient model structure. Rainfall runoff was calculated in the same fashion as meltwater runoff, except *csnow* was replaced with a constant rainfall chemistry, *crain*. This is an interim solution subject to little scientific critique.
- The Sub-basin2 fields 7 and 9 on which the model was set up, did not have soil and snow observations. Sub-basin2 fields 3 and 4 were assumed to be representative of field 9 and 7, respectively, due to their spatial proximity and identical agricultural treatment.
- Unsaturated zone leaching was not accounted for in this model. It was assumed to have a negligible impact on rooting zone nutrients.
 - The flushing of NO_3 from the upper soil layer (recharge layer) during meltwater infiltration was estimated as it relates to the runoff chemistry only (Equation 5.12).

The following assumptions relate to the equations used in the model:

- The calculation of soil temperature was based on a HYPE (Lindström et al., 2010) empirical algorithm as CRHM does not explicitly calculate soil temperature during the calculation of depth of thaw based on physically-based principles.
- The calculation of snowcover ablation using Essery and Pomeroy (2004) is based on the assumption of homogeneous melt conditions and an observed pre-melt standard deviation in snowcover cover SWE.
- The release of P from soils is estimated based on the empirically derived relationship by Amarawansa (2013) based on laboratory research on Manitoba soils (Equation 5.9).

This relationship does not take into account the water temperature or the contact time of the water and the soil. It was assumed that these changes would have negligible impact on model performance.

- The calculation of meltwater concentration factors, CF_{Stein} in Equation 5.7, is based on the assumption that one melt event occurs in a season and that the mean in the observed March snowcover chemistry is representative of the pre-melt snow chemistry. CF_{Stein} was calculated the same for each solute in spite of observed differences in CFs based on the solute species (Lilbaek, 2007).
- Conventional tillage of perennial crops established a minimum of two years is assumed to result in enhanced mineralization over the winter season (Equation 5.17).
 - The calculation in Equation 5.15 of the over-winter mineralization that occurs is based on the assumption that microbial activity continues at a constant rate until temperatures reach -5°C , the temperature at which microbial activity ceases (Campbell et al., 2005, Table 1). The nitrification rate is based on the daily rate as calculated by Groffman et al. (2001) in field research. The required C and ambient conditions for mineralization to occur were assumed adequate and only altered by temperature (Equation 5.14).
 - Annual fall tillage is assumed to elevate snowmelt runoff NO_3 concentrations over snowmelt runoff NO_3 with no previous fall tillage. This is accounted for with a multiplier related to the degree of fall tillage (1- *tillage*).
- Freeze-thaw cycles (FTC) that occur in the fall, after harvest, prior to snowcover are assumed to cause cellular damage that make readily available TDP, NO_3 , and NH_3 at a rate dependent on the N:P ratios in the crop tissues, the number of FTCs, the empirical relationship found by Bechmann et al. (2005), and the degree of fall tillage (Equations 5.18-5.20).
 - Tillage will reduce the amount of vegetation susceptible to FTC. In this model, conventional tillage is assumed to eliminate any FTC leachate and reduced tillage to reduce, but not eliminate, the amount of leachate.

5.3.2 Model Equations

Field data and established findings in the literature were used to expand on the conceptual equations presented in Figure 5.2 to develop the Prairie Nutrient Snowmelt Model. The summarizing conceptual equation, based on the derivation presented in Equation 5.3, representing the solute concentration at the edge-of-field(EOF) is:

$$c_{EOF} = c_{snow} + \alpha \cdot c_{soil} + c_{veg} \quad (5.6)$$

where c_{EOF} , c_{snow} , c_{soil} , c_{veg} respectively represent the concentration, c , of either of TDP, NO_3 , or NH_3 at the EOF, in the snow meltwater (*snow*), in the soil (*soil*), or leached from vegetation sources (*veg*). α is a binary variable: for NH_3 , $\alpha = 0$ and for TDP and NO_3 , $\alpha = 1$. As in Figure 5.2, during a rain-on-snow (ROS) event c_{snow} may need to be substituted with c_{snow*} (Equation 5.5).

csnow

Runoff over frozen soils on the Canadian prairie is predominantly overland flow as discussed in Section 2.1.4 and under certain conditions (i.e. $\text{CF}_f \rightarrow 1$) the role of the snowcover solute in the meltwater can be important. Further downstream in a catchment, the role of the snowcover solute is diminished by the increased contributions from riparian areas, streambank sediments (Koiter et al., 2013), and pre-event water (Laudon et al., 2004).

Johannessen and Henriksen (1978) and Stein et al. (1986) introduced a concentration factor, CF, for the calculation of meltwater concentrations eluted at the base of the snowcover during melt based on the bulk snowcover concentrations of each solute as discussed in Section 2.1.1. The variability in the eluted concentrations as predicted by a CF may not be observed at the EOF due to additional contributions to EOF solute from soil and vegetation, which in some cases dwarf the contributions from the snowcover solutes; but, the initial higher concentrations under limited infiltration events result in enhanced infiltration of ions into soil (Lilbaek and Pomeroy, 2010) and under restricted infiltration contribute to acute high concentration runoff events into streams, both events of consequence that should be accounted for. The Stein et al. (1986) formula for calculating melt concentration factors,

referred to as CF_{Stein} , is used in the Prairie Nutrient Snowmelt Model, Equation 5.7, to determine the concentrations of ions eluted from the snowcover prior to transit to the EOF:

$$CF_{Stein} = \frac{SWE_t \cdot e^{-k \cdot (SWE_o - SWE_t)} - SWE_{t+1} \cdot e^{-k \cdot (SWE_o - SWE_{t+1})}}{SWE_t - SWE_{t+1}} \quad (5.7)$$

where SWE_o is the snowcover SWE in *mm* just before the onset of melt, SWE_t and SWE_{t+1} the simulated SWE in *mm* at time steps t and $t + 1$, and k a leaching coefficient given a constant value of 0.002 based on an initial fit to the data. The leaching coefficient is a sensitive parameter and as discussed in Lilbaek (2007) “depends on a wide variety of factors such as snowpack flowpaths, distribution of solute in snow, melt-freeze cycles, rain-on-snow, and the possibility of biological activity (e.g. Tranter (1991))”. In the Prairie Nutrient Snowmelt Model, an hourly time step is used. During a melt event, based on CF_{Stein} and the initial bulk concentration in the snowcover, c_o , the eluted concentration of solute in the meltwater is calculated for each time step.

The solute contributions from the snowcover, $csnow$, for each of TDP, NO_3 , and NH_3 termed $csnow_{TDP}$, $csnow_{NO_3}$, and $csnow_{NH_3}$ respectively, are calculated in Equation 5.8:

$$csnow = CF_{Stein} \cdot c_o \quad (5.8)$$

where c_o is the mean concentration in $mg \cdot l^{-1}$ of either TDP, NO_3 or NH_3 in the snowcover at the onset of melt.

csoil

This model assumes that both soil TDP and NO_3 contribute to EOF runoff concentrations, whereas the soil bound NH_3 does not (Section 2.3.3).

The conceptual model Equation 5.6 term $csoil$ will be solved for both TDP and NO_3 and referred to as $csoil_{TDP}$ and $csoil_{NO_3}$ respectively.

$$csoil_{TDP}$$

Section 2.3.4 provides background to the relationship between near surface soil P content and runoff P. The linear relationship established in the laboratory on Manitoba soils as

described in Equation 5.9 and discussed in Section 2.3.4 is used here:

$$\Delta\text{TDP} = 0.035 * \text{OlsenP} - 0.14 \quad (5.9)$$

where ΔTDP represents the absolute change in concentration in $mg \cdot l^{-1}$ of TDP (Amarawansha (2013) used DRP) in the water after ponding and OlsenP the measured soil test value in $mg \cdot kg^{-1}$. There are no data to correct the relationship for temperature or form of P.

In Amarawansha (2013), DRP was assessed weekly after each of 8 weeks of continuous flooding. DRP release generally increased (in non clayey soils) with increased flooding duration having little to no impact on the soil test P, but the magnitude of DRP released after flooding was largely dependent on initial soil test phosphorous. For this research, the Amarawansha (2013) linear relationship for DRP release based on soil P content is used in conjunction with the Essery and Pomeroy (2004) snowcover depletion curve to capture a flushing of mobile nutrient pools in the soil and vegetation, that based on EOF time series plots (Figures 4.9, B.4- B.6), coincided with the depletion of the snowcover¹. The Essery and Pomeroy (2004) snowcover depletion *tanh* relationship was established for snowcovers on reasonably homogeneous surfaces, with consistent slope, aspect, and vegetation, and is therefore suited to simulate the progressive decrease in areal snowcover and the resulting flushing of *csoil* and *cveg* nutrient pools on prairie agricultural fields:

$$f = \tanh \left(1.26 \frac{\overline{\text{SWE}}}{\sigma_o} \right) \quad (5.10)$$

where $\overline{\text{SWE}}$ is the average SWE, in *mm*, at each time step (for this model, hourly) and σ_o represents the pre-melt standard deviation, in *mm*, in snowcover SWE. For years with snow surveys, σ_o can be assessed and valued empirically (Figure 5.6) for years without data, σ_o can be estimated based the coefficients of variation for SWE determined in a prairie environment in Pomeroy et al. (1998b, Table I). TDP contributions to EOF runoff solute are estimated

¹As discussed in Section 2.3.3 over-winter mineralization can occur resulting in the development of pools of mobile N (and P) forming under the snowcover. It is assumed that P and N leached from vegetation is also pooled in the snowcover, soil surface or vegetation. As the snowcover is depleted so are these pools of mineralized and leached P and N. In the absence of data to quantify this flushing, the snowcover depletion curve (Equation 5.10) is used.

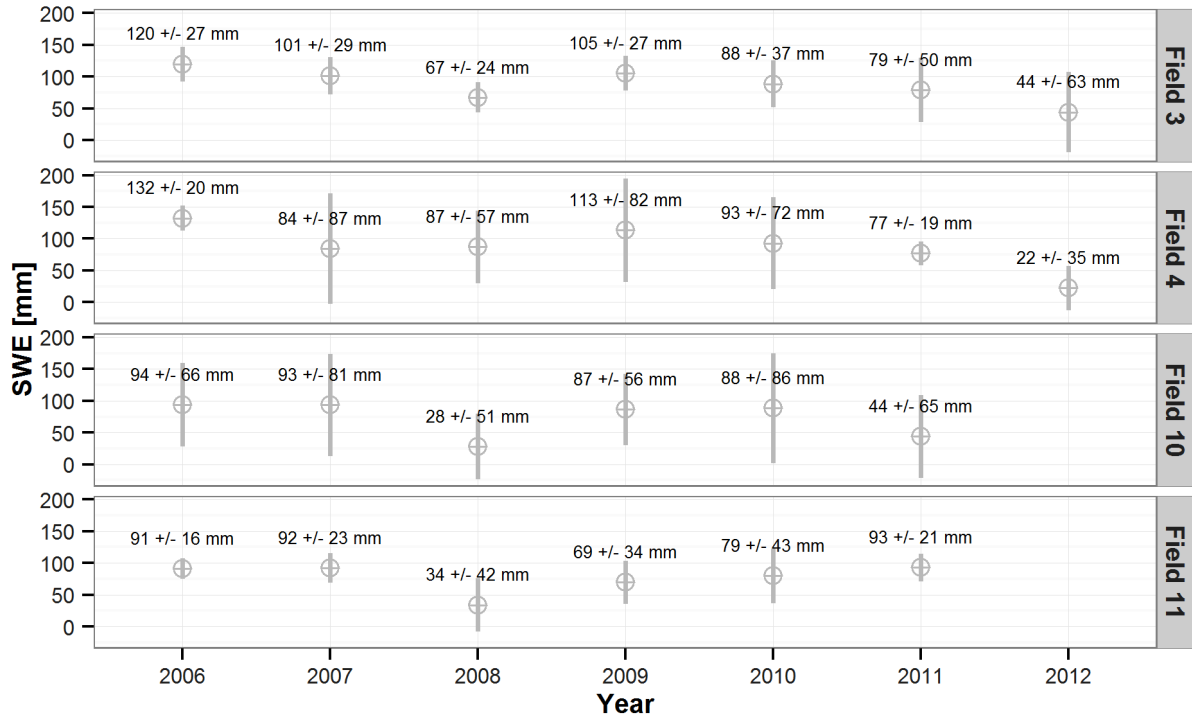


Figure 5.6: Field Snow Surveys. This plot quantifies the standard deviation in the field snow survey depths observed in March. These values are used to parametrize and calculate f in Equation 5.10.

in Equation 5.11:

$$csoil_{TDP} = f \cdot \Delta TDP \quad (5.11)$$

where f is the fractional snow covered area as described in Equation 5.10 and ΔTDP the increase in TDP concentration, in $mg \cdot l^{-1}$, in the runoff as described in Equation 5.9.

$$csoil_{NO_3}$$

There are two primary contributing sources to $csoil_{NO_3}$ that the Prairie Nutrient Snowmelt Model accounts for: 1) the contributions from the measured fall soil N; and 2) the contributions of N related to over-winter mineralization that occurs due to fall tillage.

1) Contributions from fall soil NO_3 : Infiltration under limited conditions (Granger et al., 1984) may occur prior to runoff and leach the upper soil NO_3 by transporting NO_3 down and away from the upper soil horizon. This mechanism has been discussed in Section 2.3.4

and is further described in CREAMS (Knisel, 1980a,b,c,d), a process based field scale model for **C**hemicals, **R**unoff and **E**rosion from **A**gricultural **M**anagement **S**ystems developed in the late 1970s by the United States Department of Agriculture - Agricultural Research Service is shown in Equation 5.12:

$$csoil_{5cm} = k_2 \cdot (csoilwater_{NO_3} - csnow_{NO_3})e^{-k_1 \cdot INF} + csnow \quad (5.12)$$

where $csoilwater_{NO_3}$ is the initial concentration in the top soil layer, $csnow_{NO_3}$ the concentration in the snowcover (Equation 5.8), INF the total infiltration for the melt event, and k_1 and k_2 ² partitioning coefficients given a value here of 0.001 and 0.2, respectively based on visual calibration of the results during modelling.

It is assumed that the bulk of the NO_3 measured in the soil would be found in the soil water solution (Russel, 1988, pp. 666) under unfrozen conditions and in the ice lattice and soil water under frozen soil conditions. This is quantified based on the measured soil mass of NO_3 and the CRHM simulated state variable for soil moisture content in the surface soil layer as shown in Equation 5.13:

$$csoilwater_{NO_3} [mg/l] = \frac{soilN [kg/km^2]}{\Theta_{5cm} [mm]} \quad (5.13)$$

where $csoilwater_{NO_3}$ is the concentration of NO_3 in $[mg/l]$ in the soil moisture, soilN the fall measured mass of soil NO_3 in kg/km^2 . The Θ_{5cm} is the moisture water content in the upper 5 cm of the soil as simulated by CRHM with its state variable for moisture content in the upper (recharge) layer of the soil column.

As with P, and due to available data, the upper 5 cm of the soil is assumed to interact with the meltwater. Evidently, there is a stratification in the soil for NO_3 and due to lack of data (Figure 3.12) the model relies on the 0 – 15 cm observations of the soil NO_3 concentrations and a multiplier (0.55) relating the 0 – 5 cm and 0 – 15 cm soil NO_3 content established during the years when both the 0 – 5 cm and 0 – 15 cm layers were sampled.

2) Contributions related to tillage induced N mineralization: Two conditions related to tillage mobilized nitrate in runoff have been identified in Sections 2.3.3 and 4.4.1: 1)

² k_2 has been added to the original CREAMS equation to account for the transfer of NO_3 into runoff. This is similar to the runoff extract coefficient in CREAMS which is calculated from a rate constant, soil porosity, and soil depth (10 mm typically, 50 mm here). The typical constraint of the leaching extraction coefficient being larger than the runoff extraction coefficient did not apply during snowmelt runoff.

increased nitrate concentrations following fall tillage practices, and 2) a nitrate concentration spike following the fall tillage of perennial forage crops and grassland. There is no difference evident between the soil NO_3 levels in the 0 – 5 *cm* surface soil layer of the MT and AT fields (Section 4.4.1); therefore, the elevated concentrations of AT over MT fields are proposed to be captured with the tillage multiplier $(1 - \textit{tillage})$ where *tillage* is as discussed in Section 3.2.1. To determine the magnitude of the concentration spike following the tillage of perennial forage, mineralization rates are calculated proportional to the number of days between fall tillage and spring melt where the soil temperatures were at or above -5°C (Campbell et al., 2005; Groffman et al., 2001) and therefore favourable for microbial mineralization activities to occur.

- The following describe a $\textit{tillage}_{\text{NO}_3}$ event (Equation 5.15 and 5.16)
 1. A perennial crop must have been cultivated after more than 2 years of consecutive growth
 2. The maximum production of nitrate after fall tillage is determined relative to Groffman et al. (2001) who found a 121 day winter production rate of $0.5 \pm 0.3 \text{ g} \cdot \text{m}^{-2}$ based on a 10 *cm* mineral soil depth.
 3. Days with an average soil temperature above -5°C are assumed favourable for nitrification (nitrification days). The production rate is based on the Groffman et al. (2001) findings adjusted by the nitrification days, a 10*cm* plow depth (Elliott, 2014, pers. comm.), and soil temperature as calculated with Equation 5.14.

Soil temperature is calculated using the HYPE model (Lindström et al., 2010) empirical equation developed for cold regions:

$$T_{\text{soil}} = T_{\text{soil}}(t-1) \cdot \left(1 - \frac{1}{\Delta_{\text{step}}} - k_{\text{wdeep}}\right) + T_{\text{air}} \cdot \frac{1}{\Delta_{\text{step}}} + k_{\text{tdeep}} \cdot k_{\text{wdeep}} \quad (5.14)$$

$$\Delta_{\text{step}} = (k_{\text{soilmem}} + k_{\text{spfrost}} \cdot d_{\text{snow}}) \cdot \text{timesteps}$$

where T_{soil} and T_{air} represent the soil and air temperatures in $^\circ\text{C}$; timesteps, the number of time steps per day; k_{soilmem} the soil temperature memory in days; k_{spfrost} the soil temperature snow dependence in $\text{days} \cdot \text{cm}^{-1}$; d_{snow} snow depth in *cm*; k_{wdeep} deep soil temperature weight,

a unitless value; k_{tdeep} deep soil temperature in °C; and $T_{soil}(t - 1)$ the soil temperature in the previous time step in °C initially set to 5°C based on a calculated average annual air temperature for the site.

Equations 5.15 and 5.16 are used to calculate the NO₃ flux, $ctillage_{NO_3}$ in $mg \cdot l^{-1}$, related to over-winter mineralization:

$$tillage_{NO_3} = \frac{\text{nitrification days}}{121} * 0.8 * 1000 \quad (5.15)$$

$$ctillage_{NO_3} = \frac{tillage_{NO_3}}{\Theta_{10cm}} \quad (5.16)$$

where $tillage_{NO_3}$ is the over-winter nitrification rate in $kg \cdot km^{-2}$ pro-rated as discussed above based on Groffman et al. (2001) 121 day rate upper bound of $0.8 g \cdot m^{-2}$ ($0.5 + 0.3 g \cdot m^{-2}$) and Θ_{10cm} the water content, in mm , in the estimated 10 cm disturbed layer of the soil. This $ctillage_{NO_3}$ function estimates the impacts of tilling perennial forages and is further multiplied by the fractional snow covered area, f (Equation 5.10) to affect the quick depletion of the mineralized nitrate pool with the snowcover depletion (Equation 5.17). This is evident in the observed steep decreasing trend in concentrations (Figure 4.9) on Sub-basin2 fields 4 and 7 in 2010. Soil NO₃ contributions to EOF meltwater chemistry are estimated in Equation 5.17 as:

$$csoil_{NO_3} = (csoil_{5cm} + ctillage_{NO_3}) \cdot f \quad (5.17)$$

cveg

To quantify freeze-thaw cycle (FTC) induced vegetation leaching (Section 4.4.2) in the model, the Bechmann et al. (2005) curve (Table 5.1) and Elliott (2013, Table 4) were used. The total measured water extractable phosphorous (WEP) values in the Bechmann et al. (2005) experiment were high and considered extreme values as the FTCs were performed on non-cold hardy plants, in optimal growing conditions, and on soils with P contents about 5 fold greater than the Sub-basin2 and Twin fields. The Miller et al. (1994) experiments on ryegrass were 15% of the TDP after one FTC where Bechmann et al. (2005) was 40%. In the Bechmann et al. (2005) column leaching experiment, measured DRP concentrations after eight FTCs from 21d rye grass were $9.7 \pm 1.6 mg \cdot l^{-1}$. To predict leaching rates for cold hardy plants, under field conditions, and on soils with much lower P content, these laboratory leaching rates were

adjusted downward initially by an estimated 90% and represented as $k_{maxFTCP} = 0.97mg \cdot l^{-1}$ in Equations 5.18 to 5.20. Based on simulation outcomes this estimated 90% discount appears reasonable.

Freeze-thaw cycles were counted based on CRHM output air temperatures having a diurnal fluctuation with an amplitude $> 10^{\circ}C$ and minimum air temperature below $-2^{\circ}C$ occurring on bare ground in months later than August and before December. These FTC counts were then used to interpolate the percentage of the plant tissue P that would be water extractable based on the [Bechmann et al. \(2005\)](#) curve. As [Bechmann et al. \(2005\)](#) dealt only with P, [Elliott \(2013\)](#) was used to establish a ratio of TDP leached to NH_3 and NO_3 leached.

Table 5.1: Bechmann Curve. The table shows the percent of total TDP released with successive freeze-thaw cycles with an amplitude greater than $10^{\circ}C$ as observed in [Bechmann et al. \(2005\)](#).

number of FTCs	0	1	2	4	6	8
percentage of plant tissue P	0	41.6	60.0	83.2	97.6	100

Limited infiltration implies soil water contact occurs and thus NH_3 and TDP leached concentrations would be depleted as observed in [Elliott \(2013\)](#). In this same experiment, NO_3 leachate was enriched when soil contact was made: the $csoil_{NO_3}$ (Equation 5.17) calculation is assumed to account for this and thus the NO_3 leaching value is not adjusted for soil contact. Under the [Granger et al. \(1984\)](#) restricted infiltration regime the Prairie Nutrient Snowmelt Model assumes no soil contact and therefore leached TDP and NO_3 , and NH_3 are not adjusted (k_{TDP} , k_{NH_3} , and k_{NO_3} in Table 5.2).

The [Miller et al. \(1994\)](#) and [Bechmann et al. \(2005\)](#) experiments were on rye grass and assumed comparable to grasses as listed in the [Canadian Fertilizer Institute \(2001\)](#) report. TDP and NH_3 leached were scaled relative to the P and N contents of the crop on the field verses a grass crop (Table 5.3). The values calculated in Equations 5.18 - 5.20 were reduced by the fall tillage disturbance values, (*tillage*, Section 3.2.1) for reduced tilled fields, unadjusted for forage crops, and given a value of 0 for conventionally tilled fields. The final $cveg_{TDP}$, $cveg_{NH_3}$, and $cveg_{NO_3}$ values were multiplied by the snowcover depletion value, f (Equation 5.10), as the leached values are thought to quickly deplete as contact between the snowcover and vegetation is reduced. The final equations representing FTC leaching of TDP,

Table 5.2: Elliott (2013) Table 4. The table below is an extract from Elliott (2013, Table 4) a laboratory study quantifying leachate from winter wheat and soil during spring melt. The use of this table is tied to the Bechmann et al. (2005) P study, therefore ratios of residue+ active layer were established to relate all of TDP, NH₃, and NO₃ leached to the TDP leached from the residue with no subsequent soil contact and with subsequent soil contact as dictated by the Granger et al. (1984) infiltration regime.

	<i>TDP</i> [mg/l]	<i>NH₃</i> [mg/l]	<i>NO₃</i> [mg/l]
residue	1.58	0.58	0.34
residue + active soil layer	0.53	0.42	4.03
coefficients based on soil contact	$k_{TDP} = 0.33$	$k_{NH_3} = 0.27$	$k_{NO_3} = 0.22$
coefficients based on no soil	$k_{TDP} = 1.0$	$k_{NH_3} = 0.37$	$k_{NO_3} = 0.22$

NH₃, and NO₃ from vegetation are:

$$cveg_{TDP} = (\text{Bechmann} \cdot k_{maxFTCP} \cdot k_{TDP} \cdot k_{Pstoich} + k_{Pjuicy} \cdot \alpha_{newcrop}) \cdot f \quad (5.18)$$

$$cveg_{NH_3} = (\text{Bechmann} \cdot k_{maxFTCP} \cdot k_{NH_3} \cdot k_{Nstoich} + k_{Njuicy} \cdot \alpha_{newcrop}) \cdot f \quad (5.19)$$

$$cveg_{NO_3} = (\text{Bechmann} \cdot k_{maxFTCP} \cdot k_{NO_3}) \cdot f \quad (5.20)$$

where Bechmann is the interpolated percentage of the total plant P that was observed to be water extractable in laboratory experiments after a succession of high amplitude FTCs; $k_{maxFTCP}$, the cold hardy plant adjusted maximum leached TDP concentration in $mg \cdot l^{-1}$; k_{TDP} , k_{NH_3} , and k_{NO_3} the coefficients for leaching based on soil contact; $k_{Pstoich}$ and $k_{Nstoich}$ the stoichiometric P:N ratio adjustments based on crop type (Table 5.3); $\alpha_{newcrop}$ a binary variable set to 1 for new crops and 0 for established crops; k_{Pjuicy} and k_{Njuicy} empirically derived coefficients to supplement typically leached P and N values in $mg \cdot l^{-1}$ on fresh crops (Elliott, 2014); and f the fractional snow covered area.

5.3.3 Model Inputs and Operation

The allocation of the input variables shown in Figure 5.5 as they relate to the model equations is summarized in Table 5.4.

Table 5.3: This table shows the ratio of P and N in various other crops relative to rye grass as shown in the removal data from [Canadian Fertilizer Institute \(2001\)](#).

crop	Relative N content	Relative P content
Rye Grass	1.0	1.0
Winter Wheat	0.51	0.85
Spring Wheat	0.59	0.78
Forage	1.6	1.4
Alfalfa	2.8	2.3
Barley	0.76	1.1
Canola	0.66	1.2
Flax/Linola	0.50	0.52
Green Feed Oats	0.60	0.85
Oats	0.60	0.85

Table 5.4: Model Equations and Inputs.

Equations		Inputs
$csnow_{TDP}$ $csnow_{NH_3}$ $csnow_{NO_3}$ (Equation 5.8)	CF_{Stein} (Equation 5.7)	SWE pre-melt snowmelt chemistry (c_o)
$csoil_{NO_3}$ (Equation 5.17)	$csoil_{5cm}$ (Equation 5.12) $ctillage_{NO_3}$ (Equation 5.16) f (Equation 5.10)	soil moisture infiltration soil NO_3 snow depth air temperature fall tillage crop type seeding date SWE std. dev. in pre-melt snow depth (σ_o)
$csoil_{TDP}$ (Equation 5.11)	ΔTDP (Equation 5.9) f (Equation 5.10)	soil Olsen P SWE σ_o
$cveg_{TDP}$ $cveg_{NH_3}$ $cveg_{NO_3}$ (Equations 5.18 - 5.20)	f (Equation 5.10)	SWE σ_o air temperature fall tillage crop type seeding date

CHAPTER 6

MODEL PERFORMANCE

In this chapter the developed model and relevant hydrological and agricultural context are presented. Following this, the model simulations are compared with the observations and performance statistics applied. In the final section, the sensitivity of the model to important inputs is investigated.

6.1 Agricultural and Hydrological Context

The Prairie Nutrient Snowmelt Model was developed on Sub-basin2 fields 7 and 9 for the farming years of 2009 through 2011.

The fall of 2008 was wet with a total 430 *mm* rainfall including a November rain event that left soils wet at freeze up. As discussed in Section 4.4, this likely resulted in an ice layer forming over the soil at the base of the snowcover. The CRHM model simulations were run to force restricted infiltration in the spring of 2009, as would occur in the presence of a basal ice layer. The fall of 2010 was wet across the southern Saskatchewan and Manitoba. Late rains (and saturated soils) and deep wet snowcovers led to historic flooding in the southern Prairies in spring 2011 responsible for billions of dollars in damage and reparations ([Environment Canada, 2011b](#); [Water Management and Hydrology Section, 2012](#)). The observed snowcover depths in March of 2009, 2010, and 2011 (observed in snow surveys on fields 3 and 4, refer to Section 3.2.4) were 35 ± 21 *cm*, 40 ± 24 *cm*, and 33 ± 27 *cm* respectively. The rainfall, as measured on the Twin fields, amounted to 293 *mm*, 529 *mm*, and 400 *mm* in 2009, 2010, and 2011, respectively.

Figures B.4 - B.6 show that rainfall runoff events were observed on Field 9 in all of 2009, 2010 and 2011 whereas on Field 7 rainfall runoff was observed in 2011 only. Figure 6.1 quantifies the mass exported during these rainfall runoff events. The 2011 rainfall runoff

event on field 7 in 2011 showed substantial mass exported whereas the mass exported during rainfall runoff events on field 9 were 0 – 10% of the annual mass exported.

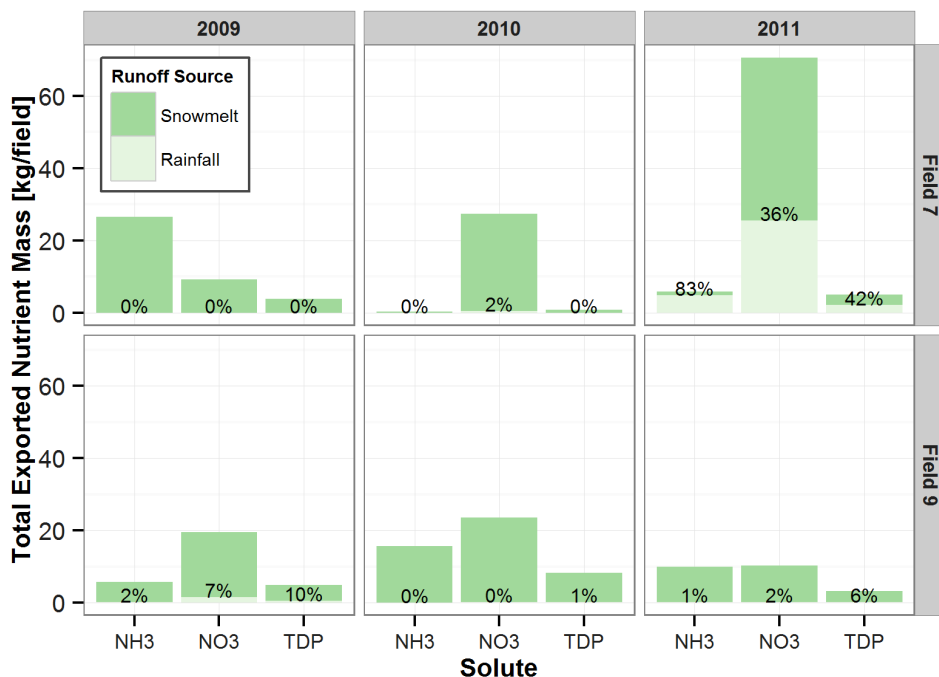


Figure 6.1: Sub-basin2 Fields 7 and 9 Observed Nutrient Exports. The percentages on the bar plot indicate the percent of total annual nutrient mass exported with rainfall runoff events at the field scale for each solute.

Rainfall runoff events will be simulated as discussed in Section 5.3.1.

Field 7 The crops grown on field 7 in 2009, 2010, and 2011 were alfalfa/timothy forage crop, wheat, and canola, respectively. The condition of these fields at the spring of these years, which dictate their categorization was: alfalfa/timothy (forage), tilled forage (AT), and tilled wheat (AT) respectively. The forage crop was neither tilled nor fertilized preceding the spring of 2009 or during the farming year of 2009. In the fall of 2009, field 7 was cultivated to break up a perennial forage crop, and tilled again in fall 2010 and 2011 with conventional or reduced methods (all years *tillage* ≤ 0.6). The 2010 wheat and 2011 canola crops were both fertilized in the spring with a diammonium phosphate and urea application.

Field 9 The crops grown on field 9 in 2009, 2010, and 2011 were forages — green feed oats followed by two years of alfalfa/timothy forage. The condition of these fields at spring of

these years was: tilled canola (AT), alfalfa/timothy crop (forage), and alfalfa/timothy crop (forage), respectively. There was one tillage pass on field 9 during these years, this was in the fall of 2008 when field 9 was conventionally tilled (*tillage* < 0.6) to break up the canola stubble. There was one fertilizer application, a urea pass in the spring of 2009. The green feed oats were planted in spring of 2009 and the alfalfa/timothy later in that season.

6.2 Model Results

The model results presented here are based on the modelling outcomes for fields 7 and 9, the fields used to set up the model. Model performance is based on time series plots and basic statistical data regarding model fit. The Prairie Nutrient Snowmelt Model was set up based on hydrological inputs from CRHM.

6.2.1 Hydrology

Simulated and observed runoff volumes (Figures 6.2a and 6.2b) were compared during the time period in which runoff observations were made. The simulated runoff for field 7 (Figure 6.2a) overestimates observed runoff by 24% (20 mm) in 2009, by 443% (43 mm) in 2010 and 123% (146 mm) in 2011. This should result in simulated nutrient loads in excess of those observed at the field scale. The simulated runoff for field 9 (Figure 6.2b) overestimates observed runoff by 21% (29 mm) and 37% (28 mm) in 2009 and 2011, respectively and underestimates observed runoff by 6% (9 mm) in 2010.

The simulated runoff did not match the variability in flows exhibited by the observations (Figures 6.2c and 6.2d). This is, in part, related to the limitation of the model to calculate snowmelt runoff on the hourly time step. Hourly melt rates are calculated with snobal (the snow energy balance model); but the Prairie Infiltration model uses daily values to quantify snowmelt runoff losing the desired hourly resolution in the process. The overestimation of flows on field 7 is related to the hydrological model generating flows when none were observed, in addition to generating flow rates much higher than those observed (Figure 6.3a). The hydrological model generated subsurface flows during many of these events, (Figure 6.3b), something easily discernible with a process and physics based model. It has been established that overland flow is the dominant runoff mechanism during snowmelt runoff on these fields

and on the Prairie, in general (Section 2.1.4). The subsurface flow generated during these simulations was primarily during rainfall runoff, but even so, the Prairies generally lack subsurface flow (Shook and Pomeroy, 2011b). Therefore, the hydrological model could be revised to eliminate the subsurface flow and hopefully better represent the observations. Simulations would have to be run to verify that changing parameter values for field 7 to eliminate subsurface flow does generate runoff volumes that better represent the observed EOF flows, while at the same time reflecting the real field conditions.

The calculated Nash-Sutcliffe efficiency (NSE), root mean squared error (RMSE) and RMSE-observations standard deviation ration (RSR), percent bias (PBIAS), and coefficient of determination (r^2) for these plots are shown in Table 6.1 with the nutrient statistics for ease of comparison. NSE, RMSE, RSR and PBIAS were calculated in R with the hydroGOF package (Zambrano-Bigiarini, 2014) and r^2 with the core R stats package (R Development Core Team, 2010). Refer to Section D.1 for the statistical measures formulae.

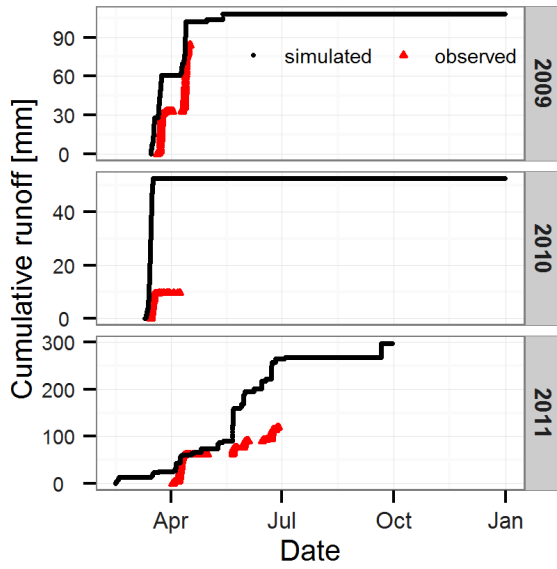
The NSE was -2.21 (field 7), 0.10 (field 9), and 0.44 (field 7 in 2009), RSR ranged 0.75-1.79, and PBIAS ranged $\pm 1 - 20\%$ (Table 6.1). In terms of performance, an NSE close to or less than 0 indicates that the model is offering little in terms of predictive insight and using observed means would be just as effective. An $RSR > 1$ indicates there is more error in the simulation than the observations. In terms of relative performance to other field scale nutrient runoff discharge models in cold regions employing an hourly time step, the published literature provides none (to this author’s knowledge). There are a few field scale runoff modelling studies for sites in warmer climates documented, all using a daily (or monthly) time step (Moriasi et al., 2007; Wang et al., 2012). Moriasi et al. (2007) provide a statistical reference frequently used as the standard in watershed modelling with 994 citations in the ISI Web of Science since its publication. Moriasi et al. (2007) provide a threshold performance target for an $NSE > 0.5$, $RSR < 0.7$, and $PBIAS \leq 25\%$ for monthly time step streamflow validated models. Shorter time steps and runoff validated modelling both tend to be more difficult to simulate and therefore these thresholds should be relaxed accordingly (Moriasi et al., 2007). In the move from monthly to daily time steps the NSE dropped by 40% in the three examples provided (Moriasi et al., 2012) and by 85% in a modelling effort on a 0.78 km^2 Agriculture Canada experimental farm in Quebec (Borah

and Bera, 2004; Laroche et al., 1996). In Table 6.1, hourly time step simulation results are aggregated daily for comparison with some, but not enough, improvement in the statistical performance.

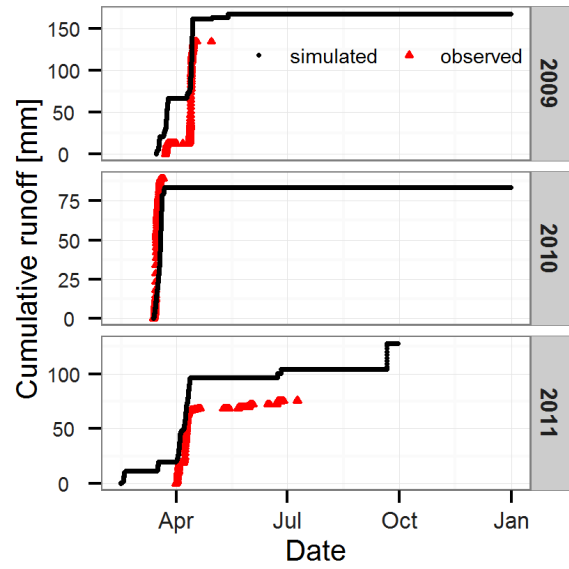
A modelling study on a 0.35 km^2 agricultural field in the Goodwater Creek Experimental Watershed, Missouri provided runoff validated performance based on a daily time step with an $\text{NSE} = 0.72$, $\text{PBIAS} = 23\%$ and an $r^2 = 0.80$ (Wang et al., 2012). It is expected that field runoff during snowmelt would be more challenging to capture and this performance would not be achievable. The work of Rousseau et al. (2013) in Beaurivage Watershed, Quebec illustrates this well with streamflow validation that performed respectively overall ($\text{NSE} = 0.75$) but failed to capture the impact of snowmelt on the streamflow. Relaxing performance expectations to accommodate: 1) the fact that CRHM has a semi-distributed spatial resolution and fields 7 and 9 each comprised one HRU with no sub-field disaggregation provided (no $\frac{\partial c}{\partial x}$), 2) the hourly time step, 3) the predominance of snowmelt runoff, 4) that this simulation is runoff not streamflow based, and 5) calibration has not been discussed (as it was not performed), the hydrological performance on fields 7 and 9 is poor. This poor performance obfuscates assessment of the nutrient model performance while it points to the challenges of small scale hydrological modelling and the large data requirements to simulate hydrology at this scale meaningfully.

6.2.2 Nutrient Model

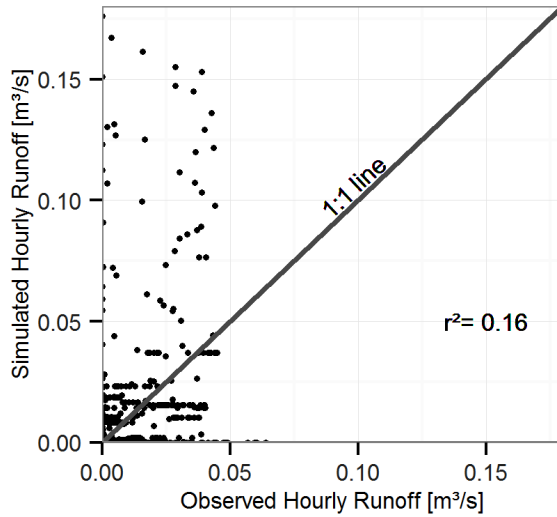
The corresponding nutrient loads simulated for fields 7 and 9 are shown in Figures 6.4a and 6.4b. It was expected that the simulated exported solute mass from field 7 in 2010 and 2011 would be overestimated based on the hydrological simulations for field 7. Mass exported in 2011 was overestimated for NO_3 in 2011 by 425%, for NH_3 in 2010 by 230% and for TDP in 2009 and 2011 by 106% and 398%, respectively (Figure 6.4a). In 2010, both NO_3 and TDP were underestimated and in 2011, the same were overestimated. The exported mass of solute off of field 9 was underestimated by 9 - 56% except for NO_3 in 2011, and TDP in 2009 and 2011 where values were overestimated by 70%, 23%, and 6%, respectively (Figure 6.4b). As discussed in Section 5.1 and shown in Equations 5.3 and 5.4, concentrations at the EOF are calculated independent of discharge. Nutrient mass



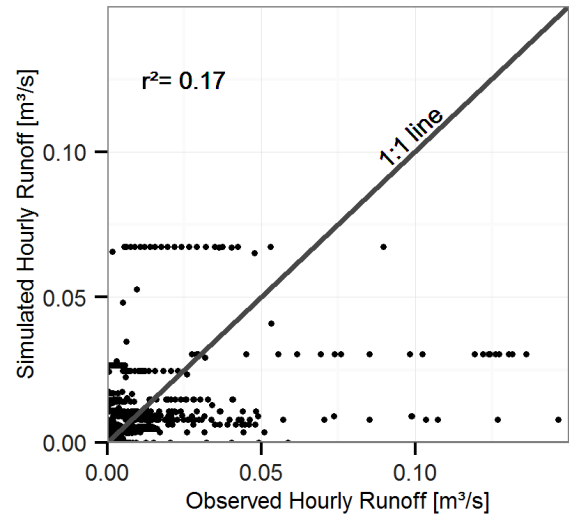
(a) Field 7 Cumulative Runoff



(b) Field 9 Cumulative Runoff



(c) Field 7 Simulated vs Observed (hourly)



(d) Field 9 Simulated vs Observed (hourly)

Figure 6.2: Simulated and Observed Runoff.

exports were therefore calculated based on observed EOF flows, rather than simulated EOF flows, to further evaluated model performance. Figures 6.4c and 6.4d plot simulated nutrient mass export, using observed flows, with observed mass export. On field 7 model performance deteriorated in all simulations except for TDP and NO_3 in 2011 and NH_3 in 2010, whereas on field 9 model performance improved in all simulations except for TDP and NO_3 in 2010 (refer

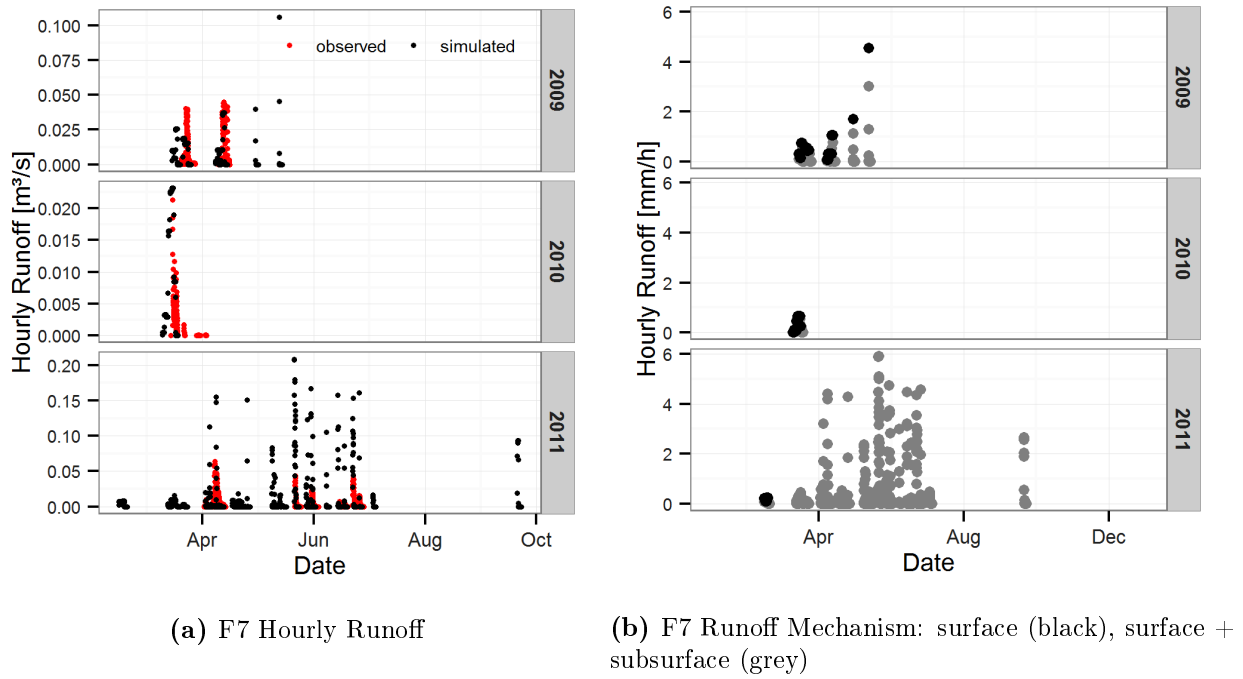
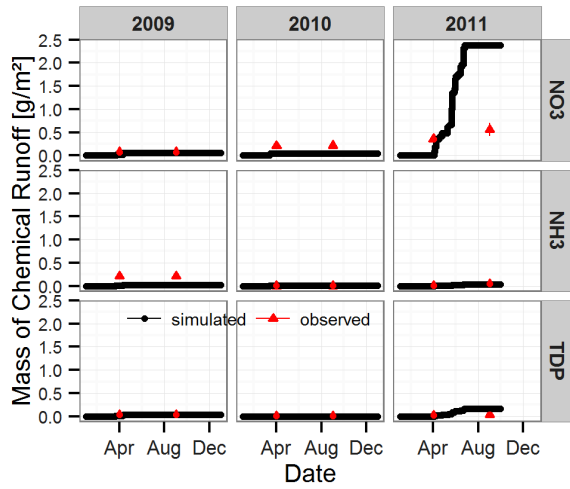


Figure 6.3: F7 Hourly Simulated and Observed Runoff.

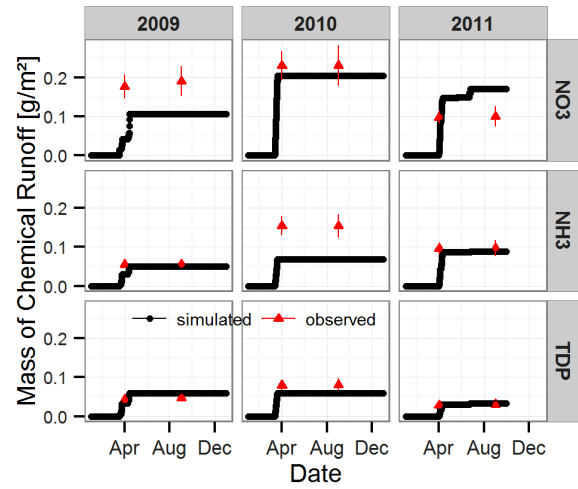
to Table D.1 for tabulated performance comparing the methods). The lack of a consistent significant improvement in model performance indicates that model constructs for both the hydrological and nutrient simulation could be improved.

Fields 7 and 9 were cropped differently. It is therefore feasible that the model constructs for forage cropping (the crop type during 3 of 4 best performing years) and its associated agricultural practices (field 7 2009, field 9 2010, 2011) are more representative than the model constructs for AT practices (field 7 2010, 2011; field 9 2009). As mentioned in Section 5.3.1, field 3 and 4 soil chemistry was assumed representative of fields 7 and 9. The model performance is sensitive to soil TDP and NO_3 (Section 6.3) and, therefore, non-representative soil chemistry on fields 3 and 4 could easily adversely impact model performance.

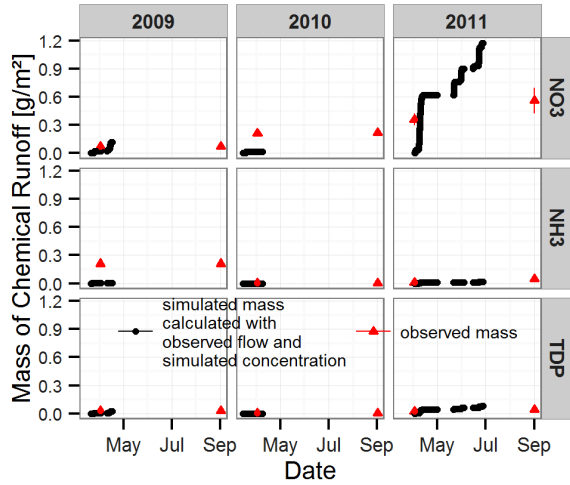
The simulated hourly EOF solute concentrations and the observed concentrations are plotted in Figure 6.5. The inability of the Prairie Nutrient Snowmelt model to capture the variability observed in concentrations is likely related to the inability of the model to capture $\frac{\partial c}{\partial x}$ as discussed in Section 5.1, which is related to the spatial resolution of the hydrological model. Figure 6.6 illustrates how well simulated concentrations match the observed concentrations. The target 1:1 line, where simulated concentrations are equal to observed



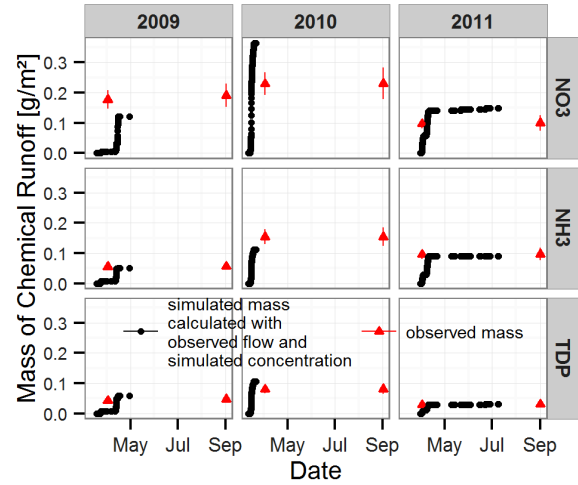
(a) Field 7



(b) Field 9



(c) Field 7



(d) Field 9

Figure 6.4: Simulated and Observed EOF Nutrient Mass Exports. The red triangles with red error bars represent the calculated observed nutrient mass export and associated error. The pair of red triangles in each frame, in sequence, represent the nutrient mass exports associated with melt runoff, and annual total runoff. Figures 6.4a and 6.4b compare simulated mass (using simulated flows and concentrations) with observed mass whereas Figures 6.4c and 6.4d compare simulated mass, calculated using observed flows and simulated concentrations, with observed mass export. The tabulated results of the simulated mass exported using both methods are provided in Table D.1.

concentrations, is shown. The calculated NSE, RSR, RMSE, PBIAS and r^2 for these plots and the aggregated daily plots (Figure D.2) are shown in Table 6.1. Statistical performance for aggregate mean daily concentrations is improved for some measures but the improvement

is neither consistent nor significant.

The performance statistics representing the nutrient model are most relevant for years where the hydrological simulation represented the observed EOF runoff. This includes all the forage years (field 7 2009; field 9 2010-2011) plus one AT year (field 9 2009). The PBIAS for fields 7 and 9 were 17% and 145% for TDP, 78% and 237% for NO_3 , and -30% and 86% for NH_3 . Comparing this with the monthly streamflow validated threshold provided by [Moriasi et al. \(2007\)](#) of $\pm 70\%$ for P and N, these PBIAS results are respectable. All of the RSR values are > 0.9 and the NSE values < 0.19 , whereas r^2 ranged 0.13 - 0.44. Again, the hourly time step, runoff validated, snowmelt dominated, and field scale (one HRU to represent the field) spatial resolution of the model need to be considered.

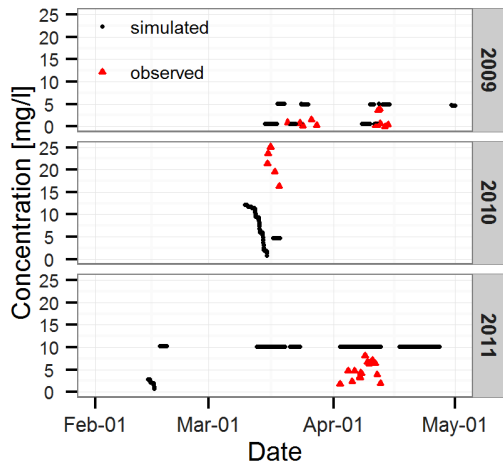
The simulated annual field concentration factors (CF_f) and load factors (LF_f) are plotted in Figures 6.7a and 6.7b, respectively. Again, snow surveys were not performed on fields 7 and 9 and, as with soil, fields 4 and 3 data were used instead (fields 4 and 3 are very near 7 and 9 and treated agriculturally congruent to fields 7 and 9, respectively). The spring of 2009 was assumed to have a basal ice layer that resulted in restricted infiltration and eliminated meltwater contact with the soils, and $\text{LF}_f \rightarrow 1$ and $\text{CF}_f \rightarrow 1$ for TDP and NO_3 whereas $\text{NH}_3 \gg 1$ under the same conditions. As illustrated by the boxplots in Figure 6.7 the CF_f for TDP is very high. The field categorization in spring 2009 was forage and AT for field 7 and 9 respectively. In the case of a forage crop and restricted infiltration, vegetative leaching rates would not be moderated by the soil and would be elevated as a result, one possible explanation for the high simulated CF_f and LF_f for TDP; but further investigation is required for a full explanation. The NO_3 CF_f and LF_f are lower in 2009 than 2010 and 2011, which is in line with the posed hypothesis. For NH_3 , a slightly elevated LF_f and CF_f were expected and simulated, in line with the model assumptions.

The overall model performance based on statistics is poor and does not instil confidence in the posed hypothesis. The assumptions comprising the nutrient model equation, $c_{EOF} = c_{snow} + \alpha \cdot c_{soil} + c_{veg}$ (Section 5.1), were designed to test the research hypothesis that restricted infiltration during snowmelt runoff eliminates contact with the soil and the transfer of soil ions to the EOF runoff. The structural assumptions are based on observations and the literature and are reasonably sound, in spite of the poor model performance. Further

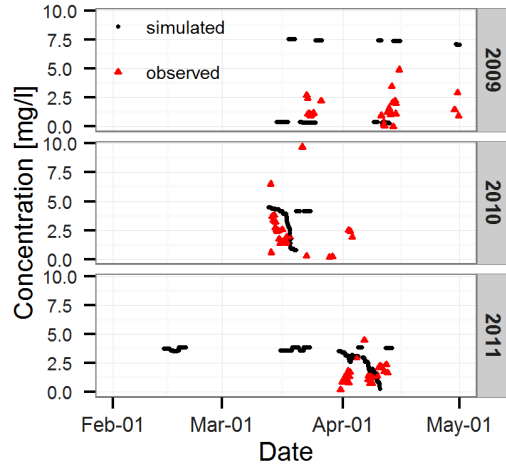
experimentation, field monitoring, model testing and validation are, therefore, required to test the hypothesis and refine these assumptions. As such, the research question regarding the field scale nutrient response during frozen soil runoff remains open to further scientific inquiry.

Table 6.1: Model Performance Statistics. The hourly statistics are presented for each field followed by aggregated daily statistics. Concentrations are averaged for the daily statistics. The plots related to the daily aggregated statistics can be found in Appendix D Figures D.1 and D.2.

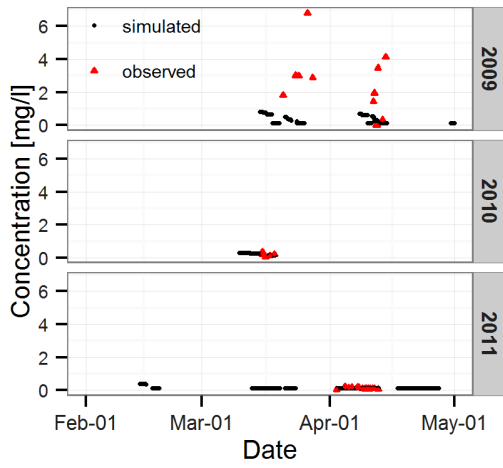
Hydrology					Nutrients					
NSE	PBIAS	RMSE	RSR	r ²	Solute	NSE	PBIAS	RMSE	RSR	r ²
Sub-basin 2 field 7, 2009-2011										
Hourly										
-2.21	25%	0.02 $m^3 \cdot s^{-1}$	1.79	0.16	TDP	-2.49	61%	0.34 $mg \cdot l^{-1}$	1.84	0.00
					NO ₃	-0.91	72%	6.4 $mg \cdot l^{-1}$	1.36	0.00
					NH ₃	-0.22	-76%	1.10 $mg \cdot l^{-1}$	1.01	0.03
Aggregated Daily										
-1.58	53%	0.01 $m^3 \cdot s^{-1}$	1.60	0.25	TDP	-2.76	34%	0.37 $mg \cdot l^{-1}$	1.88	0.29
					NO ₃	-0.79	73%	7.00 $mg \cdot l^{-1}$	1.30	0.02
					NH ₃	-0.17	-72%	0.91 $mg \cdot l^{-1}$	1.05	0.51
Sub-basin 2 field 9, 2009-2011										
Hourly										
0.27	6%	0.01 $m^3 \cdot s^{-1}$	0.85	0.32	TDP	-0.34	24%	0.22 $mg \cdot l^{-1}$	1.13	0.57
					NO ₃	-4.60	74%	2.48 $mg \cdot l^{-1}$	2.32	0.01
					NH ₃	-1.01	-30%	0.72 $mg \cdot l^{-1}$	1.38	0.11
Aggregated Daily										
-1.58	53%	0.01 $m^3 \cdot s^{-1}$	1.60	0.25	TDP	-2.76	34%	0.37 $mg \cdot l^{-1}$	1.88	0.29
					NO ₃	-0.79	73%	7.00 $mg \cdot l^{-1}$	1.30	0.02
					NH ₃	-0.17	-72%	0.91 $mg \cdot l^{-1}$	1.05	0.51
Sub-basin 2 field 7, 2009										
Hourly										
0.44	-20%	0.01 $m^3 \cdot s^{-1}$	0.75	0.46	TDP	-4.32	145%	0.51 $mg \cdot l^{-1}$	2.11	0.20
					NO ₃	-5.78	237%	3.66 $mg \cdot l^{-1}$	1.54	0.21
					NH ₃	-1.25	-86%	2.16 $mg \cdot l^{-1}$	1.58	0.13
Aggregated Daily										
0.60	-13%	0.01 $m^3 \cdot s^{-1}$	0.62	0.62	limited data for statistical analyses					



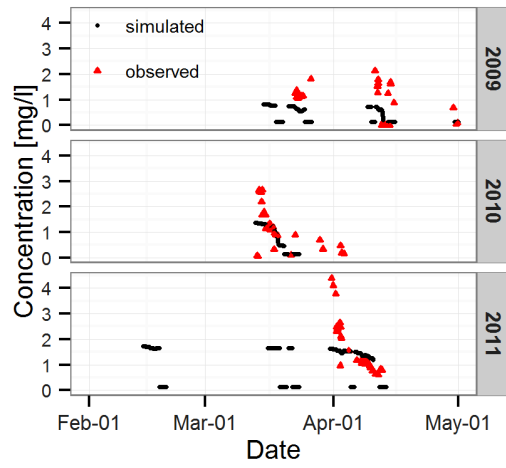
(a) Field 7 NO₃



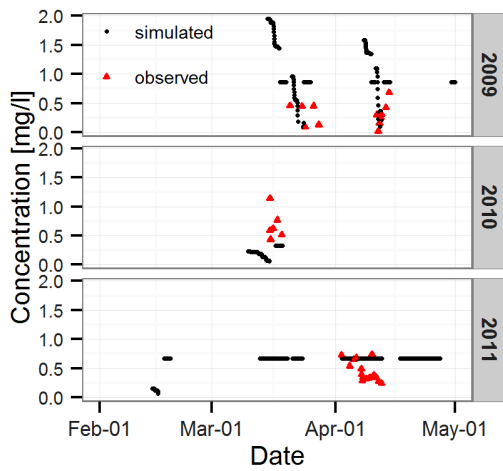
(b) Field 9 NO₃



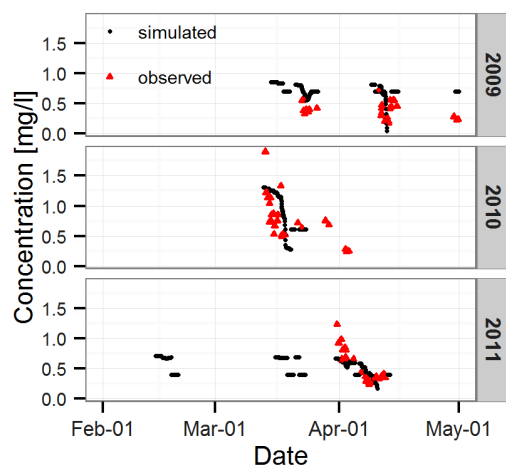
(c) Field 7 NO₃



(d) Field 9 NH₃

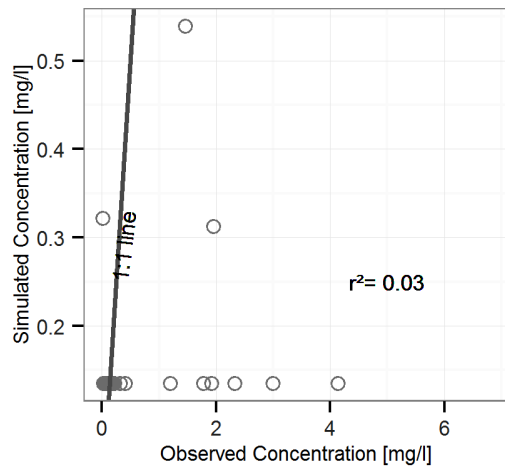


(e) Field 7 TDP

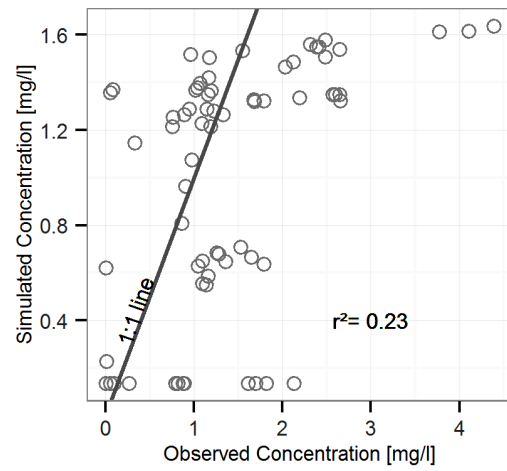


(f) Field 9 TDP

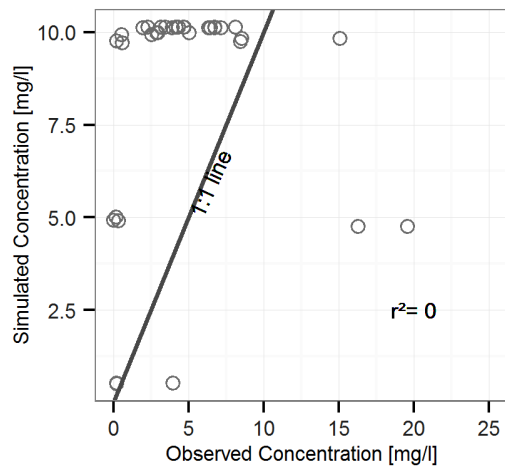
Figure 6.5: Simulated and Observed EOF Concentration Time Series.



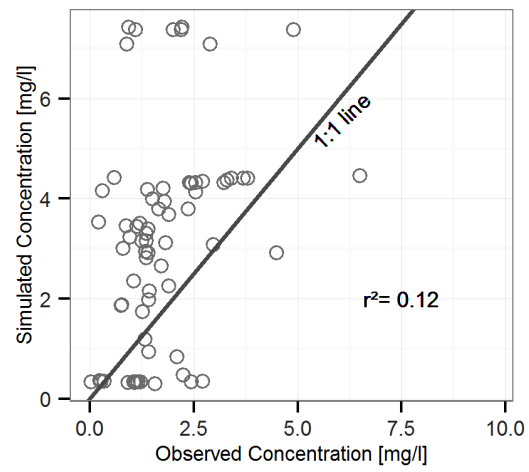
(a) Field 7 NH_3



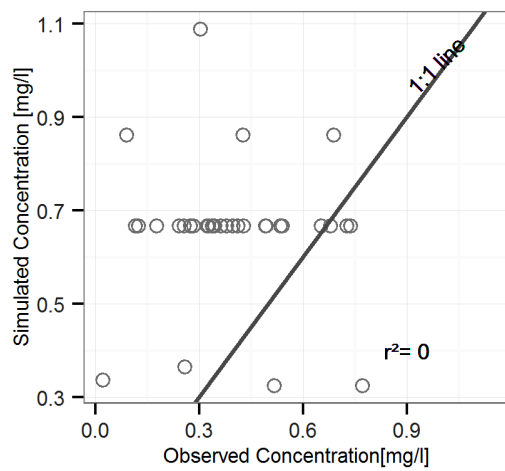
(b) Field 9 NH_3



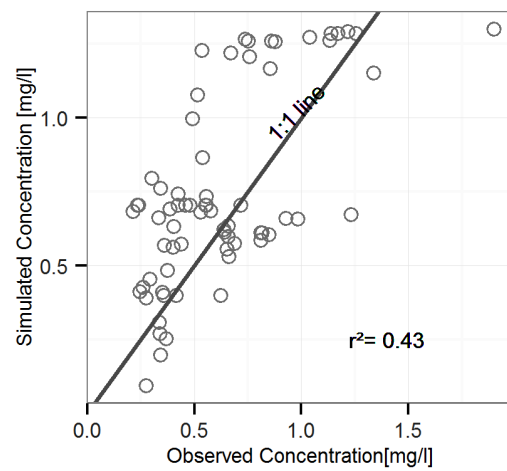
(c) Field 7 NO_3



(d) Field 9 NO_3

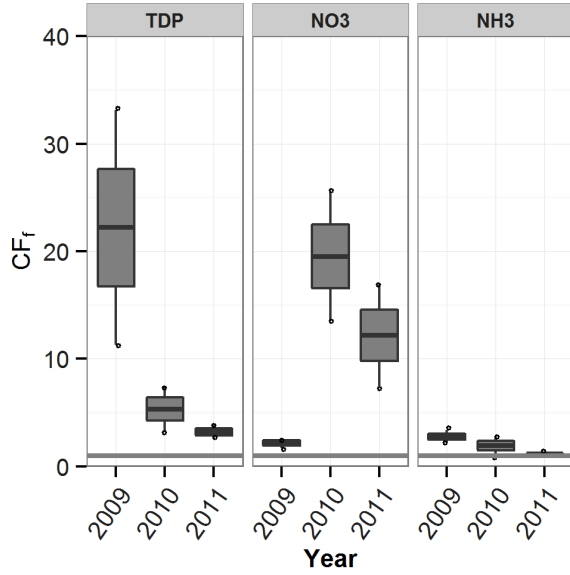


(e) Field 7 TDP

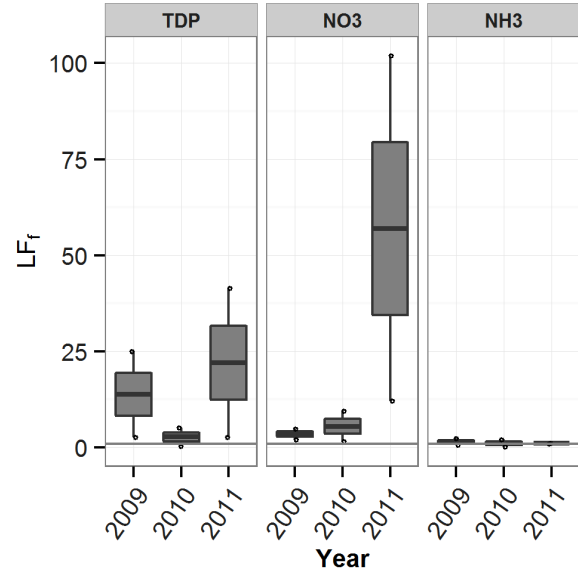


(f) Field 9 TDP

Figure 6.6: Simulated vs Observed EOF Concentration Plots.



(a) Simulated Concentration Factors



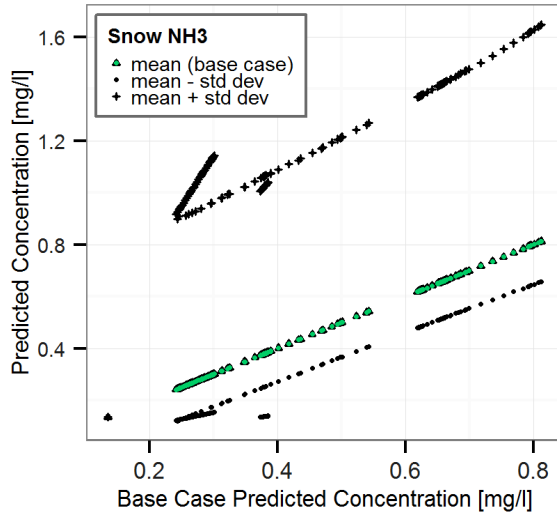
(b) Simulated Load Factors

Figure 6.7: Simulated EOF CF_f and LF_f . These plots illustrate the variability in the CF_f (6.7a) and LF_f (6.7b) for the three different years simulated and the three different solutes to be modelled (TDP, NO_3 , and NH_3). The solid grey line marks where the CF_f and LF_f are equal to 1. The grey circles are the sample set from which the boxplots are derived. The black dots are the outliers to the boxplot whiskers which extend to $1.5 \times$ inter-quartile range; the mid-hinge, the median; and the lower and upper hinge the first and third quartiles, respectively.

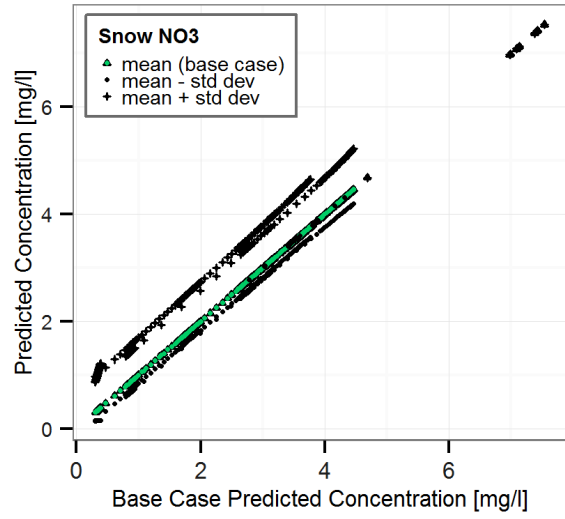
6.3 Model Sensitivity

The construction of the Prairie Nutrient Snowmelt Model, or any model, is a “rough approximation of why something has occurred” (Feynman, 1995) based on the designer’s conceptions of the system. It will be wrong. The only way to use this modelling tool is to test hypotheses and not as a tool to take its deterministic outcomes as absolutes. The model itself is the scientific hypothesis as discussed in this paper; but the tool can also be used to test additional hypotheses. This requires an understanding of the uncertainty and limits of the model structure some of which is revealed with analysis of the model’s sensitivity to changes in its variables and parameters.

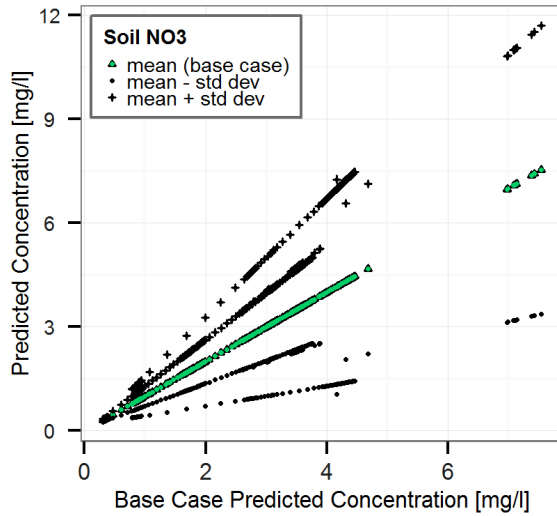
Here, the sensitivity of the model to changes in snowcover and soil chemistry input variables is investigated. Snowcover chemistry and soil chemistry are fundamental to the predictive capability of the Prairie Nutrient Snowmelt Model. As discussed, the soil contributions to EOF solute are substantial. The variability in the observed snow and soil P and N (in the case of model set up) and in the ability of the model to predict snow and soil P and N (in the future) is expected to impact the simulated results quite significantly. The sensitivity of the predicted EOF solute concentration to changes in the soil and snow P and N based on the observed variations in snowcover and soil P and N is assessed (Figures 6.8a, 6.8b, and D.3). The base case predicted EOF concentrations were generated using the mean of the observed snowcover and soil P and N solutes as discussed in Section 5.3. This base case is the subject of the model performance evaluation (Section 6.2). The base case is plotted against itself and the two predicted variations that were generated using 1) the observed mean + standard deviation (std dev) in snowcover and soil P and N, and 2) the observed mean – standard deviation in snowcover and soil P and N. The distance between the base case and the predictive variations is indicative of the sensitivity in model response to changes in these variables. Based on the large contribution of snowcover NH_3 to the simulated EOF NH_3 , it is expected that the model would be sensitive to changes in the NH_3 snowcover chemistry, with the opposite being true of the snowcover NO_3 and the EOF NO_3 relationship. Figures 6.8a with the large spread between the base case and predictive variations, and 6.8b with tightly plotted base case and predictive variations, corroborate this. Shown in Figures 6.8c



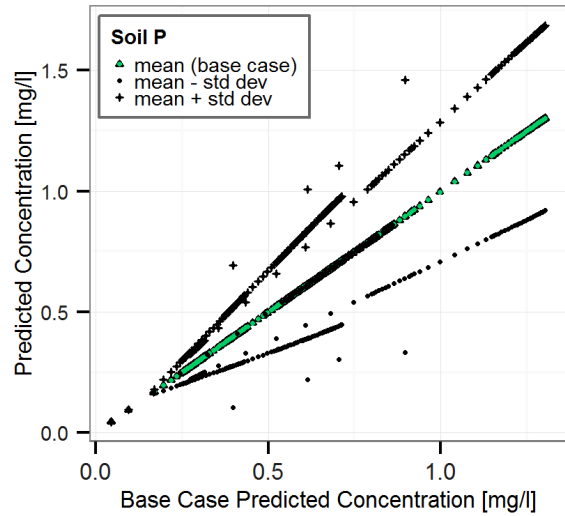
(a) Field 7, Snowpack NH_3 and EOF NH_3



(b) Field 9, Snowpack NO_3 and EOF NO_3



(c) Field 9, Soil NO_3 and EOF NO_3



(d) Field 9, Soil P and EOF TDP

Figure 6.8: Sensitivity Plots. These plots illustrate the increased sensitivity of NH_3 to changes in snowcover chemistry as compared to NO_3 and the respective sensitivity of both EOF NO_3 and EOF TDP to changes in soil NO_3 and soil P.

and 6.8d, changes in soil NO_3 and soil TDP elicit a strong response in predicted EOF NO_3 and TDP, respectively.

The sensitivity of the model to changes in NH_3 in the bulk snowcover concentrations of NH_3 emphasizes the importance of capturing the snowfall accumulation and associated SWE along with the atmospheric deposition and redistribution of the snowcover during winter.

In Canada, the network of atmospheric deposition stations is widely spaced and focused on central and eastern Canada and, therefore, not likely to serve the input needs of models on the Canadian Prairie ([Environment Canada, 2015b](#)). As done in Section 4.1, USA deposition station data and large scale deposition models could be sought to fill in and estimate annual bulk N where observations are not available. This is a source of error that has the potential to bias model outcomes, especially for NH_3 . In any snowcover, additional sources of total ammonia need to be considered. The fields used to develop this model were ungrazed and removed from large NH_3 emitters. Urine and dung from grazing cattle ([Smith et al., 2011](#)) and winter spread manure ([Coelho et al., 2012](#)) can be significant sources of ammonia to a snowcover. The impact of both on a snowcover, where relevant, would need to be accurately accounted for, requiring additional model functionality, to predict EOF NH_3 . Sections 2.3.1 and 4.1 illustrate the small scale of the runoff P and N in the context of an agricultural soil mass balance. It is both complex and critical to quantify soil P and N accurately, especially in light of the sensitivity of predicted EOF NO_3 and TDP to changes in soil NO_3 and soil TDP. The Prairie Nutrient Snowmelt Model assumed that observed fall soil P and N would remain relatively unchanged under snowcover and be adequate to predict runoff P and N at the EOF. As discussed in Section 2.3.1, to effectively predict what impact changes to the agricultural management practices might have, mass balance must be performed within the model within the context of a legacy chemical supply that is thought to manifest, especially for P on these and many other agricultural fields (Section 4.1).

CHAPTER 7

SUMMARY DISCUSSION AND CONCLUSIONS

7.1 Summary Discussion

7.1.1 Inductive Model Development

The process used to develop a nutrient hydrology model suitable for application in cold regions was inductive, based heavily on both the analysis and interpretation of field hydrochemistry data and the current state of the art in the literature. Field data from the South Tobacco Creek Sub-basin² and Twin watersheds, Manitoba were investigated for insights pertaining to the field scale nutrient mass balance, the relationship of runoff discharge rates to concentration, snowmelt and rainfall runoff composition, and nutrient sources on the field during snowmelt runoff as they relate to P and N in the snowcover.

The annual field scale budget of nutrients is large in an agricultural context. The actual runoff loss of nutrients from the field is small by comparison, but the persistence of the runoff loss of nutrients has resulted in a build up of nutrients in receiving waters in quantities that are harmful to the aquatic ecosystem (i.e. Lake Winnipeg). The easily dissolved and mobilized nutrients, TDP, NO_3 , and NH_3 are of the most concern to crop growth and downstream aquatic health. In the context of modelling, the mass balance of the field scale nutrient budget needs to include the soil cycling of P and N to quantify the fractions of P and N that are mobile at the time of a runoff event. In the case of snowmelt runoff events, activities in the soils over-winter that might affect this are fall tillage induced mineralization and the redistribution of soil moisture and salts in frozen soils. In addition to the small magnitude of the runoff loss of P and N, it is noted in the literature that fertilizers are applied in surplus of crop needs, producing an annual net balance of P and N on the fields which has led to the development of a nutrient legacy in soils (Section [2.3.1](#)). This legacy is thought to buffer the response of soils to changes in agricultural management practices. Calculation

of the field scale budget for the subject fields in this research showed that the P budget was frequently, and on some fields consistently, negative for several years without a reduction in soil phosphorous levels. This is an indication that there is a nutrient legacy on the Canadian Prairie fields that will further complicate the prediction of nutrient exports and delay the response of a field to changes in agricultural management practices.

Review of field scale data provided no predictive relationship between field scale discharge and concentrations, although it has been found in field scale runoff on the Canadian Prairie that runoff discharge rate is one of several primary predictors of runoff FWMCs in the Twin watershed of South Tobacco Creek, Manitoba (Liu et al., 2013b). The field scale investigation performed here provides no evidence that the implementation of agricultural management practices to slow or reduce discharge rates (but not cumulative annual discharge) would impact runoff concentrations due to the lack of any $c - q$ relationship (Section 4.2). The melt process is spatially and temporally variable based on minor heterogeneities such as exposed vegetation, slight aspect changes and shading, and exposed soil ridges and therefore meltwater will not necessarily be homogeneous in composition as it will be influenced by the route (∂x flowpath) it travels from snowcover to edge-of-field (EOF). The field data showed that there is spatial variability in both the snowcover solute concentrations and the soil nutrient content (Sections 3.2.3 and 3.2.4) both of which might contribute to lack of discharge and concentration relationship at the field scale.

The snowmelt runoff composition is unique from the composition of rainfall runoff (Section 4.3). On the relatively flat, dry and cold Canadian Prairie snowmelt runoff is predominantly dissolved fractions and as a result, erosion and methods to mitigate erosion can be ignored at the field scale for both P and N. In review of the data, one year of high particulate in the runoff as a result of gully erosion on the field was discovered and removed from the data set as anomalous. It can be expected that field scale snowmelt runoff in cold regions is comprised primarily of dissolved fractions; but ultimately a model capable of determining the occurrence of erosive conditions in the presence of frozen soils and snowmelt is important. Agricultural management practices to abate erosion could then be applied proactively to mitigate the problem.

Field scale metrics, CF_f and LF_f , were used to identify the contributing sources of P

and N in meltwater runoff at the field scale. TDP and NO_3 sources were identified based on the data and consistent with the literature as snow (atmospheric deposition), soil, and vegetation. NH_3 sources were limited to snow and vegetation. The soil bound NH_3 was not a significant contributor to runoff NH_3 during melt. Vegetation as a source of P and N in runoff is related to the tendency of vegetation cells to be damaged by frost and release TDP, NO_3 , and NH_3 to snow and meltwater. In cold regions, therefore agricultural management practices such as minimum tillage and forage cropping have been found culpable as a source of persistent and elevated (when compared with meltwater from annually tilled fields)) TDP and TDN in meltwater runoff.

7.1.2 A Cold Regions Nutrient Hydrology Model

The Cold Regions Hydrological Model (CRHM) platform was used to represent the important hydrological processes and simulate overland runoff off of two fields (7 and 9) in the agricultural Sub-basin2 watershed of South Tobacco Creek, Manitoba. During the 2009-2011 simulation period, the spring field conditions of field 7 (0.13 km^2) and field 9 (0.10 km^2) were categorized as one season of forage crop followed by two years of annually tilled cereals and oil seeds (AT); and one year of AT followed by two years of forage, respectively. The edge-of-field (EOF) overland discharge simulated by CRHM captured the timing of the runoff event; but tended to overestimate the runoff observed at the edge-of-field. On field 7, the hydrological model generated more runoff events and higher discharge rates than were observed. On field 9, there were fewer occasions of the model generating runoff that was not observed and this resulted in much better EOF discharge performance. A possible explanation for the model generating runoff where none was observed could be the observation of convective storms at Twin that did not extend to the neighbouring Sub-basin2 field 7. Determining the spatial extent of the frequent convective storms ([Fang et al., 2010](#)) on the Canadian Prairie requires a dense monitoring network that does not exist on the vast Prairie. The elevated discharge rates simulated for field 7 were generally related to rainfall runoff (as they occurred in later summer) and potentially related to lower modelled evapotranspiration rates creating higher soil moisture conditions and therefore generating runoff. The sources of discharge from field 7 were further investigated, revealing that the 2011 runoff generated by CRHM was largely

subsurface flow, a process thought to rarely exist in the upper reaches of a catchment on the Canadian Prairie. It is not likely that the hydrological model is revealing the occurrence of a process that needs to be considered, but rather that the model setup needs to be revisited and the parameters adjusted to better reflect field conditions. Simulation of runoff without the subsurface flow volumes would underestimate the observations indicating that there are likely multiple factors contributing to the poor representation of the discharge at EOF for field 7.

This Prairie Nutrient Snowmelt Model was designed to capture the snowmelt runoff event each spring based on several assumptions about the behaviour of the runoff and nutrients based on the literature and field hydrochemistry data. The hypothesis of the nutrient model was that meltwater flowpath will vary the interaction with the sources of phosphorous, P, and nitrogen, N on the field and determine the edge-of-field (EOF) runoff nutrient concentrations. The frozen soil flowpaths are described by the [Granger et al. \(1984\)](#) infiltration regimes of restricted, limited, and unlimited. Runoff during restricted infiltration was assumed to eliminate the contact of meltwater with soils and result in lower CF_f s for NO_3 and TDP at the EOF as observed in the data. Soils were assumed to hold total ammonia, NH_3 , tightly to the soil matrix therefore soil was assumed not to be a source of NH_3 in runoff. Restricted infiltration, was observed to elevate the runoff CF_f for NH_3 more so than other years. Data were insufficient to explain this observation; but, it could be related to elevated vegetative leachate concentrations in the absence of soil contact ([Elliott, 2013](#)). Process assumptions defined how the snow, soil, and vegetation sources on the field led to transport of P and N in the meltwater. These assumptions included over-winter mineralization induced by annual fall tillage events and tillage of perennial forage crops in addition to the leaching of P and N from freeze-thaw damaged tissues of field vegetation as sources of P and N mobilized by the meltwater.

Wet fall soils and a late fall rain event in 2008 were thought to create a basal ice layer on the soils beneath the snowcover present at melt in spring 2009 resulting in restricted infiltration. Previous research by [Lilbaek and Pomeroy \(2008\)](#) and [Lilbaek \(2007\)](#) used the composition of solute in the meltwater to discern flowpaths in field and laboratory experiments. In this research, the concentrations of the solutes and the ability of the Prairie

Nutrient Snowmelt Model to capture the observed concentrations in 2009 were used to validate the hypothesis of flowpath being a determinant in EOF concentrations. The challenges to the simulation were that simulated TDP concentrations were high, evident in the elevated CF_f for 2009 (Figure 6.7a). Similar to NH_3 , leached TDP concentrations from vegetation are higher when not moderated by soil contact (Elliott, 2013). This likely indicates that leached TDP concentrations in absence of soil contact are, in reality, not as high as predicted in the laboratory (and incorporated into the model) and that further investigation and model development, testing, and validation are required to resolve this. Anecdotal evidence in the spring snowmelt of 2015 on the south Saskatchewan Canadian Prairie is one indication that the impacts of basal ice on flowpath merit further investigation. The winter of 2015 was subject to several early melt and subsequent snowfall events creating an ice sheet on the surface of soils. The major runoff event occurred in late March and early April. This runoff of meltwater over minimum tilled fields was observed to be quick and produce atypically clear runoff waters. Only later in the melt period, once the ice sheet began to disappear off the field, and meltwater contact with the soil was achieved, did the runoff waters become their usual murky yellow colour (Burns, 2015, pers. comm.). Further research, to capture overland runoff over basal ice and the resulting solute concentrations is required to fully validate the posed hypothesis.

The relationship of tillage to enhanced mineralization rates is established in the literature and observed in these field data. The additional observation that tillage of perennially established forages causes a large increase in mineralization rates and pooling of NO_3 under the snowcover was captured in the literature related to soil unsaturated zone leaching concentrations but not so in the snowmelt runoff concentrations. Comparison of observed and simulated NO_3 concentrations on field 7 in the spring of 2010 (Figure 6.5) shows that the model does capture the initial spike but not the magnitude of the concentrations observed. The observation of the NO_3 spike during runoff in the spring of 2010 (Figure 4.9) coupled with the literature and model performance merits inclusion in the model, although further research into quantifying the spike and validation of model on sites following tillage of perennial forages is required.

The role of freeze-thaw cycling (FTC) induced cell lyses and leaching of P and N to

meltwater is well established in the literature; but, difficult to isolate in the field data due to numerous factors such as soil nutrient levels, differing vegetation types, and lack of comparative data during years without the occurrence of FTCs. The occurrence of FTC induced leaching from vegetation was assumed to be representative of reality and therefore included in the model. Again, there is little to discredit inclusion of this process in the model construct and more field research on the Canadian Prairie where variables are controlled or at least measured is required to fully validate (or invalidate) the inclusion of this process in a Canadian Prairie Snowmelt Nutrient model.

The agricultural management practices of minimum tillage and forages have contributed to the continual presence of vegetation on agricultural fields. Both practices, contribute to the leaching of P and N to runoff meltwater, an initially unforeseen complication of this agricultural management practice. A model such as the Prairie Nutrient Snowmelt Model could better account for this provided sufficient observations on which to build a model; which are as yet lacking in real world observations (there are several laboratory investigations).

The primary contribution of this modelling approach is that the nutrient model was paired with a deductive physics-based representation of the important cold regions Prairie hydrological processes. The basis of the inductive approach was the incorporation of a series of assumptions regarding nutrient sources and interactions controlled by flowpath (Section 5.3.1). These assumptions provided the structural framework for the model with the model Equation 5.4, $c_{EOF} = c_{snow} + \alpha \cdot c_{soil} + c_{veg}$, and the research hypothesis of restricted infiltration removing the soil contribution, c_{soil} , from the equation. These assumptions can only be conditionally accepted at this time based on the fact that nutrient model performance is not conclusive and cannot be adequately evaluated in light of the challenges that the field scale hydrological modelling posed. Further research and monitoring coupled with model development and testing are needed to conclusively validate the assumptions framing the model. This inductive - deductive pairing could potentially determine the impact of meltwater flowpath on runoff composition at the EOF. This is a worthwhile step in an effort to assess the impact of cold regions processes that control field scale export of P and N solute. The inductive - deductive model structure allows the addition of more complexity to the nutrient structure as required to investigate the impact of additional hydrological or

biogeochemical processes.

7.2 Conclusion

Field data and peer reviewed literature indicate that snow (atmospheric deposition to the snowcover), soil, and vegetation are the three primary sources of P and N contributing to snowmelt runoff on cultivated Canadian Prairie fields. The nutrient budget on these fields is large with losses due to the runoff of P and N being small comparatively. Regardless, TDP, NH_3 , and NO_3 have persisted in receiving streams and lakes in quantities deleterious to the health of the aquatic ecosystems. The implementation of agricultural management practices such as minimum tillage and forages has since been identified as a contributor to the persistent losses of TDP, NH_3 , and NO_3 from fields. A nutrient hydrology model was developed to capture the contribution of vegetation to losses of these solutes from fields. Flowpaths were identified during snowmelt runoff based on the infiltration regimes of restricted, limited, and unlimited, and hypothesized to determine the interaction of meltwater with the field sources of phosphorous and nitrogen. Vegetation, when present on prairie fields, consistently contributes to meltwater solute. Only soil contributions are eliminated under restricted infiltration as a result of a basal ice layer forming on the soil surface beneath the snowcover. This flowpath can substantially reduce solute concentrations at the edge-of-field during snowmelt runoff, but will not eliminate the contributions of vegetation leachate or snow solute to snowmelt runoff.

The inductive modelling approach to nutrient transport coupled with a process based model used to develop an inductive - deductive model shows that:

- the model is an important first step in recognizing the importance of cold regions hydrological processes, specifically the prediction of restricted infiltration and its impact on solute transport from cultivated Canadian Prairie fields. Due to poor hydrological model performance and data limitations it is difficult to say conclusively, but rather potentially, that:
 - restricted infiltration reduces the concentration difference between NO_3 and TDP in the snowcover and meltwater at the EOF indicating that access to the soil ions

is eliminated, and

- soil NH_3 is not a significant source of NH_3 in snowmelt runoff at the EOF.
- modelling diffuse agricultural nutrient runoff and cold regions hydrology at the field scale on an hourly time step is a non trivial exercise with high data demands.

This inductive - deductive modelling exercise is a first step in simulating EOF snowmelt runoff of TDP, NO_3 , and NH_3 . At this time, more work is required to formulate a model capable of a full range of nutrient process simulation for cold regions, with the minimum required complexity. Further development, testing, and validation on other fields and sites are required to develop a truly robust representation of the reality, an investment in both research time and monitoring.

REFERENCES

- AAFC (2010), Watershed Evaluation of Beneficial Management Practices (WEBs) South Tobacco Creek / Steppler, *Tech. rep.*, Agriculture and Agri-Food Canada.
- Agriculture and Agri-Food Canada (2010a), Watershed Evaluation of Beneficial Management Practices (WEBs) Technical Summary #3 Hydrological and Integrated Modelling Components Four-year review (2004/5 - 2007/8), *Tech. rep.*, Government of Canada and Ducks Unlimited, Ottawa, ON.
- Agriculture and Agri-Food Canada (2010b), Watershed Evaluation of Beneficial Management Practices (WEBs) Technical Summary #1 Biophysical Component Four-year review (2004/5 - 2007/8), *Tech. rep.*, Government of Canada and Ducks Unlimited, Ottawa, ON.
- Amarawansa, E. A. G. S. (2013), The Effect of Flooding and Reducing Conditions on Phosphorus Dynamics in Manitoba Soils, Masters of science, University of Manitoba.
- Annandale, J. G., N. Z. Jovanovic, N. Benadé, and R. G. Allen (2002), Software for missing data error analysis of Penman-Monteith reference evapotranspiration, *Irrigation Science*, 21(2), 57–67, doi:10.1007/s002710100047.
- Appelo, C. A. J., and D. Postma (2005), Redox Processes, in *Geochemistry, Groundwater and Pollution*, second ed., chap. 9, pp. 415–487, A.A. Balkema Publishers, Amsterdam, doi:10.1201/9781439833544.ch9.
- Appels, W. M., P. W. Bogaart, and S. E. van der Zee (2011), Influence of spatial variations of microtopography and infiltration on surface runoff and field scale hydrological connectivity, *Advances in Water Resources*, 34(2), 303–313, doi:10.1016/j.advwatres.2010.12.003.
- Arheimer, B., and J. Olsson (2003), Integration and Coupling of Hydrological Models with Water Quality Models: Applications in Europe, in *Technical reports in hydrology and water resources*, 75., World Meteorological Organization (WMO) - (WMO/TD, 1174).
- Armstrong, R. N., J. W. Pomeroy, and L. W. Martz (2008), Evaluation of three evaporation estimation methods in a Canadian prairie landscape, *Hydrological Processes*, 22(15), 2801–2815.
- Armstrong, R. N., J. W. Pomeroy, and L. W. Martz (2015), Variability in evaporation across the Canadian Prairie region during drought and non-drought periods, *Journal of Hydrology*, 521, 182–195, doi:10.1016/j.jhydrol.2014.11.070.
- Arnold, J. G., and N. Fohrer (2005), SWAT2000: Current capabilities and research opportunities in applied watershed modeling, *Hydrological Processes*, 19(3), 563–572.

- Arnold, J. G., and J. R. Williams (1987), Validation of the SWRRB-simulator for water resources in rural basins, *Journal of Water Resources Planning and Management*, 8(6), 635–645.
- Arnold, J. G., R. Srinivasan, R. S. Muttiah, and J. R. Williams (1998), Large area hydrologic modelling and assessment: Part I. model development, *Journal of the American Water Resources Association*, 34(1), 73–89.
- Austnes, K., O. Kaste, L. S. Vestgarden, and J. Mulder (2008), Manipulation of Snow in Small Headwater Catchments at Storgama, Norway: Effects on Leaching of Total Organic Carbon and Total Organic Nitrogen, *AMBIO: A Journal of the Human Environment*, 37(1), 38–47, doi:10.1579/0044-7447(2008)37[38:MOSISH]2.0.CO;2.
- Ayers, H. D. (1959), Influence of soil profile and vegetation characteristics on net rainfall supply to runoff, in *Proceedings of Hydrology Symposium No. 1: Spillway Design Floods*, National Research Council Canada, Ottawa, pp. 198–205.
- Baan, C. D., M. C. J. Grevers, and J. J. Schoenau (2009), Effects of a single cycle of tillage on long-term no-till prairie soils, *Canadian Journal of Soil Science*, pp. 521–530.
- Banaszuk, P., M. Krasowska, and A. Kamocki (2011), Modeling Hydrological Flow Paths During Snowmelt Induced High Flow Event in a Small Agricultural Catchment, in *Modelling of Hydrological Processes in the Narew Catchment*, edited by D. Mirosław-Swiątek and T. Okruszko, pp. 63–78, Springer Berlin Heidelberg, Warsaw, Poland, doi: 10.1007/978-3-642-19059-9.
- Basu, N. B., et al. (2010), Nutrient loads exported from managed catchments reveal emergent biogeochemical stationarity, *Geophysical Research Letters*, 37(23), n/a–n/a, doi:10.1029/2010GL045168.
- Basu, N. B., S. E. Thompson, and P. S. C. Rao (2011), Hydrologic and biogeochemical functioning of intensively managed catchments: A synthesis of top-down analyses, *Water Resources Research*, 47, W00J15, doi:10.1029/2011WR010800.
- Bechmann, M. E., P. J. A. Kleinman, A. N. Sharpley, and L. S. Saporito (2005), Freeze-thaw effects on phosphorus loss in runoff from manured and catch-cropped soils., *Journal of Environmental Quality*, 34(6), 2301–9, doi:10.2134/jeq2004.0415.
- Blackwell, M. S. A., P. C. Brookes, N. Fuente-Martinez, P. J. Murray, K. E. Snars, J. K. Williams, and P. M. Haygarth (2009), Effects of soil drying and rate of re-wetting on concentrations and forms of phosphorus in leachate, *Biology and Fertility of Soils*, 45(6), 635–643, doi:10.1007/s00374-009-0375-x.
- Bodhinayake, W., and B. C. Si (2004), Near-saturated surface soil hydraulic properties under different land uses in the St Denis National Wildlife Area, Saskatchewan, Canada, *Hydrological Processes*, 18(15), 2835–2850, doi:10.1002/hyp.1497.
- Borah, D. K., and M. Bera (2004), Watershed-scale hydrologic and nonpoint-source pollution models: review of applications, *Transactions of the ASAE*, 47(3), 789–804.

- Bracken, L., and J. Croke (2007), The concept of hydrological connectivity and its contribution to understanding runoff-dominated geomorphic systems, *Hydrological Processes*, *21*, 1749–1763.
- Brady, N. C., and R. R. Weil (2002), Nitrogen and Sulfur Economy of Soils, in *The Nature and Property of Soils*, edited by S. Helba, D. Yarnell, K. Linsner, and M. Carnis, 13th ed., pp. 543–591, Prentice Hall, Upper Saddle River, New Jersey.
- Brimblecombe, P., S. Clegg, T. D. Davis, D. S. Shooter, and M. Tranter (1987), Laboratory observations of the preferential loss of major ions from melting snow, *Water Resources Research*, *21*, 1279–1286.
- Brunet, N. N., and C. J. Westbrook (2012), Wetland drainage in the Canadian prairies: Nutrient, salt and bacteria characteristics, *Agriculture, Ecosystems & Environment*, *146*(1), 1–12, doi:10.1016/j.agee.2011.09.010.
- Buda, A. R., P. J. A. Kleinman, M. S. Srinivasan, R. B. Bryant, and G. W. Feyereisen (2009), Effects of hydrology and field management on phosphorus transport in surface runoff, *Journal of environmental quality*, *38*(6), 2273–2284, doi:10.2134/jeq2008.0501.
- Burford, J., and J. Bremner (1975), Relationships between the denitrification capacities of soils and total, water-soluble, and readily decomposable soil organic matter, *Soil Biology and Biochemistry*, *7*, 389–394.
- Burity, H. a., T. C. Ta, M. a. Faris, and B. E. Coulman (1989), Estimation of nitrogen fixation and transfer from alfalfa to associated grasses in mixed swards under field conditions, *Plant and Soil*, *114*(2), 249–255, doi:10.1007/BF02220805.
- Burns, J. (2015), in conversation, regarding meltwater runoff on fields near Wynyard, SK.
- Burns, T. (2013), in conversation, regarding domestic well nitrate levels.
- Cade-Menun, B. J., G. Bell, S. Baker-ismail, Y. Fouli, K. Hodder, D. W. McMartin, C. Perez-valdivia, and K. Wu (2013), Nutrient loss from Saskatchewan cropland and pasture in spring snowmelt runoff, *Canadian Journal of Soil Science*, (93), 445–458, doi:10.4141/CJSS2012-042.
- Cadle, S. H. (1991), Dry Deposition to Snowpacks, in *Seasonal Snowpacks: Processes of Compositional Change NATO ASI Series G, Vol. 28*, edited by T. D. Davies, M. Tranter, and H. G. Jones, pp. 21–66, Springer-Verlag, Berlin, Germany.
- Cameron, K., H. Di, and J. Moir (2013), Nitrogen losses from the soil/plant system: a review, *Annals of Applied Biology*, *162*(2), 145–173, doi:10.1111/aab.12014.
- Campbell, C. A., W. Nicholaichuk, and F. G. Warder (1975), Effect of a wheat summerâfallow rotation on subsoil nitrate, *Canadian Journal of Soil Science*, *55*(3), 279–286.
- Campbell, C. A., R. P. Zentner, F. Selles, and O. O. Akinremi (1993), Nitrate leaching as influenced by fertilization in the Brown soil zone, *Canadian Journal of So*, *73*(4), 387–397.

- Campbell, C. A., F. Selles, R. P. Zentner, R. De Jong, R. Lemke, and C. Hamel (2006), Nitrate leaching in the semiarid prairie : Effect of cropping frequency, crop type, and fertilizer after 37 years, *Canadian Journal of Soil Science*, 86(4), 701–710, doi:10.4141/S05-008.
- Campbell, C. A., R. P. Zentner, P. Basnyat, R. Dejong, R. Lemke, R. Desjardins, and M. Reiter (2008), Nitrogen mineralization under summer fallow and continuous wheat in the semiarid Canadian prairie, *Canadian Journal of Soil Science*, 88(5), 681–696.
- Campbell, J. L., M. J. Mitchell, P. M. Groffman, L. M. Christenson, and J. P. Hardy (2005), Winter in northeastern North America : a critical period for ecological processes, *Frontiers in Ecology and the Environment*, 3(6), 314–322.
- Canada Fertilizer Institute (2013), About Fertilizer, <http://cfi.ca/>.
- Canadian Council of Ministers of the Environment (2004), Canadian Water Quality Guidelines for the Protection of Aquatic Life - Phosphorus: Canadian Guidance Framework for the Management of Freshwater Systems, in *Canadian Environmental Quality Guidelines*, p. 6, Winnipeg.
- Canadian Fertilizer Institute (2001), Nutrient Uptake and Removal by Field Crops Western Canada 2001, *Tech. rep.*
- Carpenter, S. R., N. F. Caraco, D. L. Correll, R. W. Howarth, A. N. Sharpley, and V. H. Smith (1998), Nonpoint Pollution of Surface Waters with Phosphorus and Nitrogen, *Ecological Applications*, 8(3), 559–568.
- Centre for Hydrology (2014), Cold Regions Hydrological Model Platform Modules Library.
- Cey, E. E., D. L. Rudolph, and J. Passmore (2009), Influence of macroporosity on preferential solute and colloid transport in unsaturated field soils., *Journal of contaminant hydrology*, 107(1-2), 45–57, doi:10.1016/j.jconhyd.2009.03.004.
- Chambers, P. A., M. Guy, E. S. Roberts, M. N. Charlton, R. Kent, C. Gagnon, G. Grove, and N. Foster (2001), Nutrients and their Impact on the Canadian Environment, *Tech. rep.*, Agriculture and Agri-Food Canada, Fisheries and Oceans Canada, Health Canada and Natural Resources Canada.
- Clark, C. O. (1945), Storage and the unit hydrograph, in *Proceedings of the American Society of Civil Engineering*, pp. 1419–1447.
- Coelho, B. B., R. Murray, D. Lapen, E. Topp, and A. Bruin (2012), Phosphorus and sediment loading to surface waters from liquid swine manure application under different drainage and tillage practices, *Agricultural Water Management*, 104, 51–61, doi:10.1016/j.agwat.2011.10.020.
- Colbeck (1987), Snow metamorphism and classification, in *Seasonal Snowcovers: Physics, Chemistry, Hydrology. NATO ASI Series C, Vol. 211*, edited by H. G. Jones and W. F. Orville-Thomas, p. 1, D. Reidel Publishing Co.

- Colbeck, S. C. (1981), A simulation of enrichment of atmospheric pollutants in snow cover runoff, *Water Resources Research*, *17*, 1383–1388.
- Conley, D. J., H. W. Paerl, R. W. Howarth, D. F. Boesch, S. P. Seitzinger, K. E. Havens, C. Lancelot, and G. E. Likens (2009), Ecology. Controlling eutrophication: nitrogen and phosphorus., *Science*, *323*(5917), 1014–5, doi:10.1126/science.1167755.
- Corriveau, J., P. A. Chambers, A. G. Yates, and J. M. Culp (2011), Snowmelt and its role in the hydrologic and nutrient budgets of prairie streams, *Water Science & Technology*, *64*(8), 1590, doi:10.2166/wst.2011.676.
- Corriveau, J., P. a. Chambers, and J. M. Culp (2013), Seasonal Variation in Nutrient Export Along Streams in the Northern Great Plains, *Water, Air, & Soil Pollution*, *224*(7), 1594, doi:10.1007/s11270-013-1594-1.
- Dasch, J. M., and S. H. Cadle (1986), Dry deposition to snow in an urban area, *Water Air and Soil Pollution*, *84*(29), 297–308.
- Davis, R. E. (1991), Links between snowpack physics and snowpack chemistry, in *Seasonal Snowpacks: Processes of Compositional Change NATO ASI Series G, Vol. 28*, edited by T. D. Davis, M. Tranter, and H. G. Jones, pp. 115–138, Springer-Verlag, Berlin, Germany.
- Deelstra, J., S. H. Kvaerno, K. Granlund, A. S. Sileika, K. Gaigalis, K. Kyllmar, and N. Vagstad (2009), Runoff and nutrient losses during winter periods in cold climates requirements to nutrient simulation models, *Journal of Environmental Monitoring*, *11*(3), 602–609, doi:10.1039/b900769p.
- Dornes, P., J. W. Pomeroy, A. Pietroniro, S. K. Carey, and W. L. Quinton (2008), Influence of landscape aggregation in modelling snow-cover ablation and snowmelt runoff in a sub-arctic mountainous environment, *Hydrological Sciences Journal/Journal des Sciences Hydrologiques*, *53*(4), 725–740.
- Dornes, P. F. (2013), How To Combine Inductive and Deductive Approches To Prediction?, in *Putting Prediction in Ungauged Basins into Practice*, edited by J. W. Pomeroy, C. Spense, and P. H. Whitdfield, chap. 10, pp. 153–174, Canadian Water Resources Association.
- Dumanski, S., J. W. Pomeroy, and C. J. Westbrook (2015), Hydrological regime changes in a Canadian Prairie Basin, *Hydrological Processes (special issue)*.
- Eastman, M., A. Gollamudi, N. Stämpfli, C. Madramootoo, and A. Sarangi (2010), Comparative evaluation of phosphorus losses from subsurface and naturally drained agricultural fields in the Pike River watershed of Quebec, Canada, *Agricultural Water Management*, *97*(5), 596–604, doi:10.1016/j.agwat.2009.11.010.
- Eaton, A. D., L. S. Clesceri, E. Rice, and A. E. Greenberg (2005), *Standard Methods for the examination of water and wastewater*, 21st ed., APHA-AWWA-WEF, Publication Office, American Public Health Association, Washington, DC.

- Ellert, B. H., and H. H. Janzen (2008), Nitrous oxide, carbon dioxide and methane emissions from irrigated cropping systems as influenced by legumes, manure and fertilizer, *Canadian Journal of Soil Science*, 88(2), 207–217, doi:10.4141/CJSS06036.
- Elliott, A. C., and H. A. L. Henry (2009), Freeze-thaw cycle amplitude and freezing rate effects on extractable nitrogen in a temperate old field soil, *Biology and Fertility of Soils*, 45(5), 469–476, doi:10.1007/s00374-009-0356-0.
- Elliott, J. (2013), Evaluating the potential contribution of vegetation as a nutrient source in snowmelt runoff, *Canadian Journal of Soil Science*, 5(May 2012), 1–9, doi:10.4141/CJSS2012-050.
- Elliott, J. A. (2014), in conversation.
- Elliott, J. A. (2015), in conversation.
- Ellis, C., J. W. Pomeroy, T. Brown, and J. MacDonald (2010), Simulation of snow accumulation and melt in needleleaf forest environments, *Hydrology and Earth System Sciences*, 14(6), 925–940.
- Elser, J. J., T. Andersen, J. S. Baron, A.-K. Bergström, M. Jansson, M. Kyle, K. R. Nydick, L. Steger, and D. O. Hessen (2009), Shifts in lake N:P stoichiometry and nutrient limitation driven by atmospheric nitrogen deposition., *Science (New York, N. Y.)*, 326(5954), 835–7, doi:10.1126/science.1176199.
- Environment Canada (1979a), Phosphorous, orthophosphate, in *Analytical methods manual. Part 2.*, Inland Waters Directorate, Water Quality Branch, Environment Canada, Ottawa, ON.
- Environment Canada (1979b), Phosphorous, total, in *Analytical methods manual. Part 1.*, Inland Waters Directorate, Water Quality Branch, Environment Canada, Ottawa, ON.
- Environment Canada (2008), National Inventory Report 1990-2008 Part 1 Greenhouse Gas Sources and Sinks in Canada, *Tech. rep.*
- Environment Canada (2011a), Water quality status and trends of nutrients in major drainage areas of Canada- Technical Summary, *Tech. rep.*, Water Science and Technology Directorate.
- Environment Canada (2011b), Canada’s Top Ten Weather Stories for 2011, 1. Historic Flood Fights in the West.
- Environment Canada (2015a), Climate Normals Data, <http://www.climate.weatheroffice.gc.ca>, Climate ID 5021736 Miami Orchard and 5020720 Deerwood.
- Environment Canada (2015b), The Canadian Air and Precipitation Monitoring Network (CAPMoN) Network Map and List of Sites.

- Essery, R., and J. Pomeroy (2004), Implications of spatial distributions of snow mass and melt rate for snow-cover depletion: theoretical considerations, *Annals of Glaciology*, 38(1), 261–265, doi:10.3189/172756404781815275.
- European Union (2000), Directive 2000/60/EC of the European Parliament and of the Council of 23 October 2000 establishing a framework for Community action in the field of water policy.
- Fang, X., and J. W. Pomeroy (2008), Drought impacts on Canadian prairie wetland snow hydrology, *Hydrological Processes*, 22(15), 2858–2873, doi:10.1002/hyp.7074.
- Fang, X., and J. W. Pomeroy (2009), Modelling blowing snow redistribution to prairie wetlands, *Hydrological Processes*, doi:10.1002/hyp.
- Fang, X., J. W. Pomeroy, C. J. Westbrook, X. Guo, A. G. Minke, and T. Brown (2010), Prediction of snowmelt derived streamflow in a wetland dominated prairie basin, *Hydrology and Earth System Sciences*, 14(6), 991–1006, doi:10.5194/hess-14-991-2010.
- Fang, X., J. W. Pomeroy, C. R. Ellis, M. K. MacDonald, C. M. DeBeer, and T. Brown (2013), Multi-variable evaluation of hydrological model predictions for a headwater basin in the Canadian Rocky Mountains, *Hydrology and Earth System Sciences*, 17(4), 1635–1659, doi:10.5194/hess-17-1635-2013.
- FAO Natural Resources Management and Environment Department (2001), Lecture notes on the major soils of the world: Mineral Soils conditioned by a Steppic Climate.
- Faria, D. (1998), The energetics of boreal forest snowmelt, Msc, University of Saskatchewan.
- Federal-Provincial-Territorial Committee on Drinking Water (2013), Nitrate and Nitrite in Drinking Water Document for Public Comment.
- Feynman, R. P. (1995), *Six Easy Pieces: essentials of physics, explained by its most brilliant teacher*, Addison-Wesley, Reading, Mass.
- Fitzhugh, R. D., C. T. Driscoll, M. Peter, G. L. Tierney, T. J. Fahey, and J. P. Hardy (2001), Effects of soil freezing disturbance on soil solution nitrogen , phosphorus , and carbon chemistry in a northern hardwood ecosystem, pp. 215–238.
- Flaten, D. N. (2014), in conversation.
- Frank, K., D. B. Beegle, and J. Denning (2012), Phosphorous (Revised January 1998), in *North Central Research Publication No. 221 (Revised). Recommended Chemical Soil Test Procedures for the North Central Region*, edited by M. Nathan and R. Gelderman, pp. 6.1–6.9, Agricultural Experiment Stations of Illinois, Indiana, Iowa, Kansas, Michigan, Missouri, Nebraska, North Dakota, Ohio, South Dakota and Wisconsin, and the U.S. Department of Agriculture cooperating.
- Freshwater Institute (2003a), Ammonia Nitrogen, Method No. FWI-NH3 Version 2.03.
- Freshwater Institute (2003b), Nitrite and Nitrate Nitrogen, Method No. FWI-N Version 2.04.

- Freshwater Institute (2003c), Total Dissolved Nitrogen, Method No. FWI-TDN Version 2.03.
- Freshwater Institute (2003d), Total dissolved phosphorus, Method No. FWI-TDP Version 2.03, doi:10.1016/0043-1354(85)90313-6.
- Freshwater Institute (2003e), Soluble Reactive Phosphorus, Method No. FWI-SRP Version 2.0.
- Galloway, J. N., et al. (2004), Nitrogen cycles: past, present, and future, *Biogeochemistry*, 70, 153–226.
- Garnier, B. J., and A. Ohmura (1968), A method of calculating the shortwave radiation income of slopes, *Journal of Applied Meteorology*, 7, 796–800.
- Gelderman, R. H., and D. B. Beegle (2012), Nitrate-Nitrogen (Revised January 1998), in *North Central Research Publication No. 221 (Revised). Recommended Chemical Soil Test Procedures for the North Central Region*, edited by M. Nathan and R. Gelderman, pp. 5.1–5.4, Agricultural Experiment Stations of Illinois, Indiana, Iowa, Kansas, Michigan, Missouri, Nebraska, North Dakota, Ohio, South Dakota and Wisconsin, and the U.S. Department of Agriculture cooperating.
- Gérard-Marchant, P., W. D. Hively, and T. S. Steenhuis (2006), Distributed hydrological modelling of total dissolved phosphorus transport in an agricultural landscape, part I: distributed runoff generation, *Hydrology and Earth System Sciences Discussions*, 10, 245–261, doi:10.5194/hessd-2-1537-2005.
- Glozier, N. E., J. A. Elliott, B. Holliday, J. Yarotski, and B. Harker (2006), Water quality characteristics and trends in a small agricultural watershed: south tobacco creek, manitoba, 1992-2001, *Tech. rep.*, Environment Canada, Saskatoon, SK.
- Godsey, S. E., J. W. Kirchner, and D. W. Clow (2009), Concentration â discharge relationships reflect chemostatic characteristics of US catchments, *Hydrological Processes*, 1864(23), 1844–1864, doi:10.1002/hyp.
- Gottfried, K., G. Girard, G. Bowman, J. Moyer, I. Hanuta, S. Shpiruk, and L. Kletke (2004), Tobacco Creek Model Watershed People, landscape, planning, action, *Tech. Rep. December 2004*.
- Government of Canada (1999), Canadian Environmental Protection Act.
- Government of Canada (2012), Wastewater Systems Effluent Regulations (SOR/2012-139).
- Government of Manitoba (), Winter Wheat-Production and Management.
- Government of Saskatchewan (2008), Early Frost and Nitrates - FAQ.
- Granger, R. J., and D. M. Gray (1990), A Net Radiation Model for Calculating Daily Snowmelt in Open Environments, *Nordic hydrology*, 21(4-5), 217–234, doi:10.2166/nh.1990.017.

- Granger, R. J., D. M. Gray, and G. E. Dyck (1984), Snowmelt infiltration to frozen Prairie soils, *Canadian Journal of Earth Sciences*, *21*(6), 669–677, doi:10.1139/e84-073.
- Granieli, E., and K. Flynn (2006), Chemical and physical factors influencing toxin content, in *Ecology of Harmful Algae*, edited by E. Graneli and J. Turner, ebook ed., pp. 229–241, Springer Berlin Heidelberg.
- Gray, D. M., and R. J. Granger (1986), In situ measurements of moisture and salt movement in freezing soils, *Canadian Journal of Earth Sciences*, *23*(5), 696–704.
- Gray, D. M., and P. G. Landine (1987), Albedo model for shallow prairie snow covers, *Canadian Journal of Earth Sciences*, *24*(9), 1760–1768.
- Gray, D. M., J. W. Pomeroy, and R. J. Granger (1986a), Prairie Snowmelt Runoff, in *Proceedings, Water Research Themes, Conference Commemorating the Official Opening of National Hydrology Research Center*, pp. 49–68, Canadian Water Resources Association, Saskatoon, SK.
- Gray, D. M., R. J. Granger, and P. G. Landine (1986b), Modelling snowmelt infiltration and runoff in a prairie environment, in *Proceedings of the Symposium: Cold Regions Hydrology, American Water Resources Association*, pp. 427–438.
- Gray, M., and P. G. Landine (1988), An energy-budget snowmelt model for the Canadian Prairies, *Canadian Journal of Earth Sciences*, *25*, 1292–1303.
- Groenendijk, P., and J. G. Kroes (1999), Modelling the nitrogen and phosphorous leaching to groundwater and surface water with ANIMO 3.5, *Tech. rep.*, Winand Staring Centre, Wageningen (the Netherlands).
- Groenevelt, P., and B. Kay (1974), On the interaction of Water and Heat Transport in Frozen and Unfrozen Soils: II. The Liquid Phase, *Soil Science Society of America Journal*, *38*(3), 400–404.
- Groffman, P. M., C. T. Driscoll, J. Timothy, J. P. Hardy, R. D. Fitzhugh, and L. Geraldine (2001), Effects of mild winter freezing on soil nitrogen and carbon dynamics in a northern hardwood forest, *Biogeochemistry*, *56*, 191–213.
- Hager, W. H. (1988), Mobile flume for circular channel, *Journal of Irrigation and Drainage Engineering*, *114*(3), 520–534.
- Han, C.-W., S.-G. Xu, J.-W. Liu, and J.-J. Lian (2010), Nonpoint-source nitrogen and phosphorus behavior and modeling in cold climate: a review, *Water Science and Technology*, *62*(10), 2277–2285, doi:10.2166/wst.2010.464.
- Harlan, R. L. (1973), Ground conditioning and the groundwater response to surface freezing, *Tech. rep.*, Department of Environment, Government of Canada, Ottawa, Ontario.

- Haslauer, C. P., D. L. Rudolph, and N. R. Thompson (2004), An Investigative Framework for Assessing the Impact of Changes in Agricultural Land-Use Practices on Municipal Groundwater Quality: The Woodstock Case., in *4th Annual Joint International Association of Hydrogeologists (IAH) and Canadian Geotechnology Society (CGS) and Canadian Geotechnology Society Conference*, Quebec City, Quebec.
- Hayashi, M. (2013), The Cold Vadose Zone: Hydrological and Ecological Significance of Frozen-Soil Processes, *Vadose Zone Journal*, *12*(4), doi:10.2136/vzj2013.03.0064.
- Hayashi, M., G. van der Kamp, and D. L. Rudolph (1998), Water and solute transport between a prairie wetland and adjacent upland, 1. Water balance, *Journal of Hydrology*, *207*, 42–55.
- Hillel, D. (1980), *Fundamentals of Soil Physics*, 413 pp., Academic Press, New York.
- Hipel, K., and A. McLeod (2005), *Time Series Modelling of Water Resources and Environmental Systems*, electronic ed., <http://www.stats.uwo.ca/faculty/aim/1994Book/>.
- Hively, W. D., P. Gérard-Marchant, and T. S. Steenhuis (2006), Distributed hydrological modeling of total dissolved phosphorus transport in an agricultural landscape, part II: dissolved phosphorus transport, *Hydrology and Earth System Sciences Discussions*, *10*, 263–276, doi:10.5194/hessd-2-1581-2005.
- Hodson, A. (2006), Biogeochemistry of snowmelt in an Antarctic glacial ecosystem, *Water Resources Research*, *42*(11), n/a–n/a, doi:10.1029/2005WR004311.
- Holtan, H., and A. Stuanes (1988), Phosphorus in soil, water and sediment: an overview, *Hydrobiologia*, *34*(170), 19–34.
- International Plant Nutrition Institute (2012), IPNI Estimates of Nutrient Uptake and Removal, <http://www.ipni.net/article/IPNI-3296>.
- Ireson, A. M., G. van der Kamp, G. Ferguson, U. Nachshon, and H. S. Wheeler (2013), Hydrogeological processes in seasonally frozen northern latitudes: understanding, gaps and challenges, *Hydrogeology Journal*, *21*(1), 53–66, doi:10.1007/s10040-012-0916-5.
- Jame, Y.-W., and D. Norum (1980), Heat and Mass Transfer in a Freezing Unsaturated Porous Medium, *Water Resources Management*, *16*(4), 811–819.
- Jarvis, P. (1976), The interpretation of the variations in leaf water potential and stomatal conductance found in canopies in the field, *Philosophical transactions of the Royal Society of London. Series B, Biological sciences*, *273*, 593–610, A Discussion on Watet Relations of Plants.
- Johannessen, M., and A. Henriksen (1978), Chemistry of snow meltwater: changes in concentration during melting, *Water Resources Research*, *14*, 615–619.
- Johnsson, H., L. Bergstrom, P.-E. Jansson, and K. Paustian (1987), Simulated nitrogen dynamics and losses in a layered agricultural soil, *Agriculture, Ecosystems & Environment*, *18*(4), 333–356, doi:10.1016/0167-8809(87)90099-5.

- Johnsson, H., M. Larsson, K. Martensson, and M. Hoffmann (2002), SOILNDB: a decision support tool for assessing nitrogen leaching losses from arable land, *Environmental Modelling & Software*, *17*(6), 505–517, doi:10.1016/S1364-8152(02)00013-0.
- Jones, H. G. (1999), The ecology of snow-covered systems: a brief overview of nutrient cycling and life in the cold, *Hydrological Processes*, *13*(14-15), 2135–2147, doi:10.1002/(sici)1099-1085(199910)13:14/15<2135::aid-hyp862>3.3.co;2-p.
- Jones, H. G., and J. W. Pomeroy (2001), Early spring snowmelt in a small boreal forest watershed: influence of concrete frost on the hydrology and chemical composition of streamwaters during rain - on - snow events, in *58th Eastern Snow Conference*, pp. 209–218, Ottawa, ON.
- Joseph, G., and H. A. Henry (2008), Soil nitrogen leaching losses in response to freeze-thaw cycles and pulsed warming in a temperate old field, *Soil Biology and Biochemistry*, *40*(7), 1947–1953, doi:10.1016/j.soilbio.2008.04.007.
- Joshi, B., and C. Maule (2000), Simple analytical models for interpretation of environmental tracer profiles in the vadose zone, *Hydrological Processes*, *14*, 1503–1521.
- Kahan, T. F., S. N. Wren, and D. J. Donaldson (2014), A pinch of salt is all it takes: chemistry at the frozen water surface, *Accounts of chemical research*, *47*(5), 1587–94, doi:10.1021/ar5000715.
- Ketterings, Q. M., and P. Barney (2010), Phosphorus Soil Testing Methods Agronomy Factsheet Series, *Tech. rep.*, Department of Crop and Soil Sciences, Cornell University Cooperative Extension.
- Killham, K. (1994), *Soil Ecology*, 242 pp., Cambridge University Press, Cambridge.
- Kleinman, P., A. Sharpley, A. Buda, R. McDowell, and A. Allen (2011a), Soil controls of phosphorus in runoff: Management barriers and opportunities, *Canadian Journal of Soil Science*, *91*(3), 329–338, doi:10.4141/cjss09106.
- Kleinman, P. J. A., A. N. Sharpley, R. W. McDowell, D. N. Flaten, A. R. Buda, L. Tao, L. Bergstrom, and Q. Zhu (2011b), Managing agricultural phosphorus for water quality protection: principles for progress, *Plant and Soil*, *349*(1-2), 169–182, doi:10.1007/s11104-011-0832-9.
- Klemes, V. (1983), Conceptualization and scale in hydrology, *Journal of Hydrology*, *65*, 1–23.
- Knisel, W. G. (1980a), CREAMS: A Field Scale Model for Chemicals, Runoff and Erosion from Agricultural Systems, in *Conservation Research Report no. 26.*, edited by W. G. Knisel, U.S. Department of Agriculture, Washington, DC.
- Knisel, W. G. (Ed.) (1980b), *Volume I. Model Documentation*, 643 pp., United States Department of Agriculture, Conservation Research Report No. 26.
- Knisel, W. G. (Ed.) (1980c), *Volume II. User Manual*, 643 pp., United States Department of Agriculture, Conservation Research Report No. 26.

- Knisel, W. G. (Ed.) (1980d), *Volume III. Supporting Documentation*, 643 pp., United States Department of Agriculture, Conservation Research Report No. 26.
- Köchy, M., and S. D. Wilson (2001), Nitrogen deposition and forest expansion in the northern Great Plains, *Journal of Ecology*, *89*, 807–817.
- Koiter, A. J., D. A. Lobb, P. N. Owens, E. L. Petticrew, K. H. D. Tiessen, and S. Li (2013), Investigating the role of connectivity and scale in assessing the sources of sediment in an agricultural watershed in the Canadian prairies using sediment source fingerprinting, *Journal of Soils and Sediments*, *13*, 1676–1691, doi:10.1007/s11368-013-0762-7.
- Krogh, S. a., J. W. Pomeroy, and J. McPhee (2015), Physically Based Mountain Hydrological Modeling Using Reanalysis Data in Patagonia, *Journal of Hydrometeorology*, *16*(2007), 172–193, doi:10.1175/JHM-D-13-0178.1.
- Lake Winnipeg Stewardship Board (2009), Manitoba’s Progress Towards Implementing Recommendations of the Lake Winnipeg Stewardship Board, A Report to the Minister of Water Stewardship, *Tech. Rep. December*, Lake Winnipeg Stewardship Board, Gimli, MB.
- Laroche, A., J. Gallichand, R. Lagace, and A. Pesant (1996), Simulating atrazine transport with HSPF in an agricultural watershed, *Journal of Environmental Engineering*, *122*(7), 622–630.
- Laudon, H., J. Seibert, S. Köhler, and K. Bishop (2004), Hydrological flow paths during snowmelt: Congruence between hydrometric measurements and oxygen 18 in meltwater, soil water, and runoff, *Water Resources Research*, *40*(3), WR03,102, doi:10.1029/2003WR002455.
- Leavesley, G. H., R. W. Lichty, B. M. Troutman, and L. G. Saindon (1983), *Precipitation-runoff modelling system: user’s manual*, 4238 pp., US Geological Survey, Reston, Virginia.
- Li, S., J. A. Elliott, K. H. D. Tiessen, J. Yarotski, D. A. Lobb, and D. N. Flaten (2011), The effects of multiple beneficial management practices on hydrology and nutrient losses in a small watershed in the Canadian prairies., *Journal of environmental quality*, *40*(5), 1627–42, doi:10.2134/jeq2011.0054.
- Lilbaek, G. (2007), Compositional change of meltwater infiltrating frozen ground, *American Geophysical Union*, (February), 242.
- Lilbaek, G., and J. W. Pomeroy (2008), Ion enrichment of snowmelt runoff water caused by basal ice formation, *2766*(April), 2758–2766, doi:10.1002/hyp.
- Lilbaek, G., and J. W. Pomeroy (2010), Laboratory evidence for enhanced infiltration of ion load during snowmelt, *Hydrology and Earth System Sciences*, *14*(7), 1365–1374.
- Lindenschmidt, K.-e., and G. Ollesch (2004), Physically-based hydrological modelling for non- point dissolved phosphorus transport in small and medium-sized river basins, *Hydrological Sciences Journal*, *49*(December), 495–510.

- Lindström, G., J. Rosberg, and B. Arheimer (2005), Parameter precision in the HBV-NP model and impacts on nitrogen scenario simulations in the Ronnea River, Southern Sweden, *Ambio*, *34*, 533–537.
- Lindström, G., C. Pers, J. Rosberg, J. Strömqvist, and B. Arheimer (2010), Development and testing of the HYPE (Hydrological Predictions for the Environment) water quality model for different spatial scales, *Hydrology Research*, *41* (3-4), 295, doi:10.2166/nh.2010.007.
- Litke, D. W. (1999), Review of Phosphorus Control Measures in the United States and Their Effects on Water Quality, *Tech. rep.*, United States Geological Survey, Denver, Colorado.
- Liu, J., R. Khalaf, B. Ulén, and G. Bergkvist (2013a), Potential phosphorus release from catch crop shoots and roots after freezing-thawing, *Plant and Soil*, *371* (1-2), 543–557, doi:10.1007/s11104-013-1716-y.
- Liu, K., J. A. Elliott, D. A. Lobb, D. N. Flaten, and J. Yarotski (2013b), Critical Factors Affecting Field-Scale Losses of Nitrogen and Phosphorus in Spring Snowmelt Runoff in the Canadian Prairies, *Journal of Environmental Quality*, *42* (2), 484–496, doi:10.2134/jeq2012.0385.
- Liu, K., J. A. Elliott, D. A. Lobb, D. N. Flaten, and J. Yarotski (2014a), Nutrient and sediment losses in snowmelt runoff from perennial forage and annual cropland in the Canadian Prairie, *Journal of Environmental Quality*, *43*, 1644–1655.
- Liu, K., J. A. Elliott, D. A. Lobb, D. N. Flaten, and J. Yarotski (2014b), Conversion of Conservation Tillage to Rotational Tillage to Reduce Phosphorus Losses during Snowmelt Runoff in the Canadian Prairies, *Journal of Environmental Quality*, *43*, doi:10.2134/jeq2013.09.0365.
- Macrae, M., T. Redding, I. Creed, W. Bell, and K. Devito (2005), Soil, surface water and ground water phosphorus relationships in a partially harvested Boreal Plain aspen catchment, *Forest Ecology and Management*, *206* (1-3), 315–329, doi:10.1016/j.foreco.2004.11.010.
- Mahmood, T. (2014), in conversation.
- Mahmood, T., J. W. Pomeroy, H. S. Wheeler, H. M. Baulch, and J. A. Elliott (2014), Understanding the Influence of Cold Region Processes on Nutrient Exports from a Prairie Agricultural Basin (poster), in *Canadian Geophysical Union Joint Annual Meeting with Canadian Society of Soil Science and Mantle Convection Workshop May 26 - 30, 2014*.
- Mahmood, T., J. W. Pomeroy, H. S. Wheeler, and H. M. Baulch (2015), Hydrological responses to dry and wet conditions in an agricultural cold region, *in review*.
- Mahowald, N., et al. (2008), Global distribution of atmospheric phosphorus sources, concentrations and deposition rates, and anthropogenic impacts, *Global Biogeochemical Cycles*, *22* (4), n/a–n/a, doi:10.1029/2008GB003240.
- Mann, H. B. (1945), Non-parametric tests against trend, *Econometrica*, *13*, 163–171.

- Marks, D., J. Domingo, D. Susong, L. T. and D. Garen (1999), A spatially distributed energy balance snowmelt model for application in mountain basins, *Hydrological Processes*, *13*, 1935–1959.
- Matzner, E., and W. Borken (2008), Do freeze-thaw events enhance C and N losses from soils of different ecosystems? A review, *European Journal of Soil Science*, *59*(2), 274–284, doi:10.1111/j.1365-2389.2007.00992.x.
- Maule, C. P., and J. Stein (1990), Hydrologic Flow Path Definition and Partitioning of Spring Meltwater, *26*(12), 2959–2970.
- McCollum, R. E. (1991), Buildup and Decline in Soil Phosphorus: 30-Year Trends on a Typic Umprabult, *Agronomy Journal*, *83*, 77–85.
- McDowell, R. (2012), Minimising phosphorus losses from the soil matrix., *Current opinion in biotechnology*, *23*(6), 860–865, doi:10.1016/j.copbio.2012.03.006.
- McLeod, A. (2014), Kendall Rank correlation and Mann-Kendall trend test. <http://www.stats.uwo.ca/faculty/aim>.
- Miles, J. J., M. C. Eimers, R. L. North, and P. J. Dillon (2013), Spatial distribution and temporal variability in the forms of phosphorus in the Beaver River subwatershed of Lake Simcoe, Ontario, Canada, *Inland Waters*, *3*, 179–186, doi:10.5268/IW-3.2.531.
- Miller, M., E. Beauchamp, and J. Lauzon (1994), Leaching of Nitrogen and Phosphorus from the Biomass of Three Cover Crop Species, *Journal of Environmental Quality*, *23*(2), 267–272.
- Milly, P. C. D., J. Betancourt, M. Falkenmark, R. M. Hirsch, W. Zbigniew, D. P. Lettenmaier, and R. J. Stouffer (2008), Stationarity Is Dead : Whither Water Management ?, *Science*, *319*(February), 573–574.
- Monteith, J. (1965), Evaporation and Environment, *Symposia of the Society for Experimental Biology*, *19*, 205–234.
- Moriasi, D. N., J. G. Arnold, M. W. Van Liew, R. L. Binger, R. D. Harmel, and T. L. Veith (2007), Model evaluation guidelines for systematic quantification of accuracy in watershed simulations, *Transactions of the American Society of Agricultural and Biological Engineers*, *50*(3), 885–900.
- Moriasi, D. N., B. N. Wilson, J. G. Arnold, and P. H. Gowda (2012), Hydrologic and Water Quality Models: Use, Calibration, and Validation, *Transactions of the American Society of Agricultural and Biological Engineers*, *55*(4), 1241–1247.
- Nachshon, U., A. Ireson, G. van der Kamp, and H. Wheeler (2013), Sulfate salt dynamics in the glaciated plains of North America, *Journal of Hydrology*, *499*, 188–199, doi:10.1016/j.jhydrol.2013.07.001.
- Ospar Commission (1998), Eutrophication Strategy.

- Özgül, M., A. Günes, A. Esringü, and M. Turan (2012), The effects of freeze-and-thaw on phosphorus availability in highland soils in Turkey, *Journal of Plant Nutrition and Soil Science*, 175(6), 827–839, doi:10.1002/jpln.201100407.
- Parsons, D. F., M. Hayashi, and G. van der Kamp (2004), Infiltration and solute transport under a seasonal wetland: Bromide tracer experiments in Saskatoon, Canada, *Hydrological Processes*, 18(11), 2011–2027, doi:10.1002/hyp.1345.
- Pierson, D. C., and C. H. Taylor (1985), Influence of Snowcover Development and Ground Freezing on Cation Loss from a Wetland Watershed during Spring Runoff, *Canadian Journal of Fisheries and Aquatic Sciences*, 42(12), 1979–1985, doi:10.1139/f85-245.
- Pomeroy, J., and H. Jones (2005), Hydrochemical Processes in Snow Covered Basins, *Encyclopedia of Hydrological Sciences*, doi:10.1002/0470848944.hsa169.
- Pomeroy, J., D. de Boer, and L. Martz (2007a), Hydrology and water resources, in *Saskatchewan: Geographic Perspectives*, edited by B. Thraves, M. Lewry, J. Dale, and H. Schlichtmann, pp. 63–80, CRRC, Regina, SK.
- Pomeroy, J., X. Fang, C. Ellis, and M. Guan (2011), Sensitivity of Snowmelt Hydrology on Mountain Slopes to Forest Cover Disturbance, *Tech. Rep. 10*.
- Pomeroy, J. W., and D. M. Gray (1995), Snowcover accumulation, relocation, and management, *Tech. rep.*, Minister of Supply and Services Canada, Ottawa, ON.
- Pomeroy, J. W., and H. G. Jones (1996), Wind-blown Snow: Sublimation, Transport and Changes to Polar Snow, in *Chemical Exchange between the Atmosphere and Polar Snow*, nato asi s ed., pp. 453–490.
- Pomeroy, J. W., and L. Li (2000), Prairie and arctic areal snow cover mass balance using a blowing snow model, *Journal of Geophysical Research*, 105(D21), 26,619–26,634.
- Pomeroy, J. W., T. D. Davies, and M. Tranter (1991), The impact of blowing snow on snow chemistry, in *Seasonal Snowpacks: Processes of Compositional Change NATO ASI Series G, Vol. 28*, edited by T. D. Davies, M. Tranter, and H. G. Jones, pp. 71–114, Springer-Verlag, Berlin.
- Pomeroy, J. W., T. Brown, G. Kite, D. M. Gray, R. J. Granger, and A. Pietroniro (1998a), PBS-SLURP MODEL, *Tech. rep.*, SaskWater and the Upper Assiniboine River Basin Study NHRI Contribution Series No. CS-98003, Pomeroy1998.
- Pomeroy, J. W., D. M. Gray, K. R. Shook, B. Toth, R. L. H. Essery, a. Pietroniro, and N. Hedstrom (1998b), An evaluation of snow accumulation and ablation processes for land surface modelling, *Hydrological Processes*, 12(15), 2339–2367, doi:10.1002/(SICI)1099-1085(199812)12:15<2339::AID-HYP800>3.0.CO;2-L.
- Pomeroy, J. W., T. D. Davies, H. G. Jones, P. Marsh, N. E. Peters, and M. Tranter (1999), Transformations of snow chemistry in the boreal forest : accumulation and volatilization, 2273(June 1998).

- Pomeroy, J. W., D. M. Gray, T. Brown, N. R. Hedstrom, W. L. Quinton, R. J. Granger, and S. K. Carey (2007b), The cold regions hydrological model: a platform for basing process representation and model structure on physical evidence, *Hydrological*, *21* (19), 2650–2667, doi:10.1002/hyp.
- Pomeroy, J. W., X. Fang, K. Shook, and P. H. Whitfield (2013), Predicting in ungauged basins using physical principles obtained using the deductive, inductive, and abductive reasoning approach, in *Putting Prediction in Ungauged Basins into Practice*, edited by J. W. Pomeroy, C. Spense, and P. H. Whitdfield, chap. 4, pp. 41–62, Canadian Water Resources Association.
- Pote, D. H., T. C. Daniel, D. J. Nichols, A. N. Sharpley, P. A. Moore, D. M. Miller, and D. R. Edwards (1999), Relationship between Phosphorus Levels in Three Ultisols and Phosphorus Concentrations in Runoff, *Journal of Environmental Quality*, *28*, 170–175.
- R Development Core Team (2010), R: A language and environment for statistical computing.
- Radcliffe, D. E., J. Freer, and O. Schoumans (2009), Diffuse phosphorus models in the United States and europe: their usages, scales, and uncertainties., *Journal of environmental quality*, *38* (5), 1956–67, doi:10.2134/jeq2008.0060.
- Risk, N., D. Snider, and C. Wagner-Riddle (2013), Mechanisms leading to enhanced soil nitrous oxide fluxes induced by freeze thaw cycles, *93*, 1–14, doi:10.4141/CJSS2012-071.
- Roberts, W. M., M. I. Stutter, and P. M. Haygarth (2012), Phosphorus retention and remobilization in vegetated buffer strips: a review., *Journal of environmental quality*, *41* (2), 389–99, doi:10.2134/jeq2010.0543.
- Rochette, P., D. A. Angers, M. H. Chantigny, M.-o. Gasser, J. D. Macdonald, D. E. Pelster, and N. Bertrand (2013), NH₃ volatilization , soil NH₄⁺ concentration and soil pH following subsurface banding of urea at increasing rates, *Canadian Journal of Soil Science*, *93* (2), 261–28, doi:10.4141/CJSS2012-095.
- Rousseau, A. N., S. Savary, D. W. Hallema, S. J. Gumiere, and E. Foulon (2013), Modeling the effects of agricultural BMPs on sediments, nutrients, and water quality of the Beau-rivage River watershed (Quebec, Canada), *Canadian Water Resources Journal*, *38* (2), 99–120, doi:10.1080/07011784.2013.780792.
- Russel, E. (1988), *Russel's Soil Conditions and Plant Growth*, 11th ed., Longman Scientific and Technical/John Wiley & Sons, New York, New York.
- Sánchez, M., and J. Boll (2005), The effect of flow path and mixing layer on phosphorus release, *Journal of Environment Quality*, *34*, 1600–1609, doi:10.2134/jeq2004.0306.
- Sask Forage Council (2008), Growing Forage Legumes in rotation with annual crops.
- Schindler, D. W. (1977), Evolution of phosphorus limitation in lakes, *Science*, *195* (4275), 260–2, doi:10.1126/science.195.4275.260.

- Schindler, D. W. (2012), The dilemma of controlling cultural eutrophication of lakes., *Proceedings. Biological sciences / The Royal Society*, 279(1746), 4322–33, doi:10.1098/rspb.2012.1032.
- Schindler, D. W., and S. E. Bayley (1993), The biosphere as an increasing sink for atmospheric carbon: estimates from increase nitrogen depositio, *Global Biogeochemical Cycles*, 7(4), 717–733.
- Schindler, D. W., P. J. Dillon, and H. Schreier (2006), A review of anthropogenic sources of nitrogen and their effects on Canadian aquatic ecosystems, *Biogeochemistry*, 79(1-2), 25–44, doi:10.1007/s10533-006-9001-2.
- Schindler, D. W., A. P. Wolfe, R. Vinebrooke, A. Crowe, J. M. Blais, B. Miskimmin, R. Freed, and B. Perren (2008), The cultural eutrophication of Lac la Biche, Alberta, Canada: a paleoecological study, *Canadian Journal of Fisheries and Aquatic Sciences*, 65, 2211–2223, doi:10.1139/F08-117.
- Shanley, J. B., and A. Chalmers (1999), The effect of frozen soil on snowmelt runoff \hat{A} at Sleepers River , Vermont, *Hydrological Processes*, 13, 1843–1857.
- Sharpley, A. (1995), Dependence of Runoff Phosphorus on Extractable Soil Phosphorus, *Journal of Environmental Quality*, 24(5), 920–926.
- Sharpley, A. N. (1985), The selective erosion of plant nutrients in runoff, *Soil Science Society of America Journal*, 49, 1527–1534.
- Shook, K., and J. Pomeroy (2011a), Synthesis of incoming shortwave radiation for hydrological simulation, *Hydrology Research*, 42, 433–446, doi:10.2166/nh.2011.074.
- Shook, K. R., and J. W. Pomeroy (2011b), Memory effects of depressional storage in Northern Prairie hydrology, *Hydrological Processes*, 25(25), 3890–3898, doi:10.1002/hyp.8381.
- Si, B. C., and E. de Jong (2007), Determining long-term (decadal) deep drainage rate using multiple tracers., *Journal of Environmental Quality*, 36(6), 1686–94, doi:10.2134/jeq2007.0029.
- Sicart, J. E., J. W. Pomeroy, R. Essery, and D. Bewley (2006), Incoming longwave radiation to melting snow : observations, sensitivity and estimation in northern environments, *Hydrological Processes*, 20(17), 3697– 3708.
- Skougstad, M. W., M. J. Fishman, L. C. Friedman, D. E. Erdmann, and S. S. Duncan (1979), Nitrogen, ammonia, colorimetric, in *Techniques of water-resources investigations of the United States Geological Survey. Book 5. Laboratory Analysis*, pp. 425–427, US Government Printing Office, Washington, DC.
- SMHI (2015), SMHI HypeWeb, <http://hypeweb.smhi.se/arctichype/about/>. date accessed: 2015-03-28.

- Smith, A., J. Schoenau, H. A. Lardner, and J. Elliott (2011), Nutrient export in run-off from an in-field cattle overwintering site in East-Central Saskatchewan, *Water Science and Technology*, 64(9), 1790–1795, doi:10.2166/wst.2011.747.
- Smith, C. D. (1985), *Hydraulic Structures*, University of Saskatchewan Printing Services, Saskatoon, SK, Canada.
- Soil Classification Working Group (1998), *The Canadian system of soil classification*, NRC Research Press, Ottawa, Ontario.
- Spence, C., and J. Hosler (2007), Representation of stores along drainage networks in heterogeneous landscapes for runoff modelling, *Journal of Hydrology*, 347(3-4), 474–486, doi:10.1016/j.jhydrol.2007.09.035.
- Stein, J., H. Jones, J. Roberge, and W. Sochanska (1986), The prediction of both runoff quality and quantity by the use of an integrated snowmelt model, *IAHS-AISH publication*, (155), 347–358.
- Steppuhn, H., H. Krouse, and D. Erickson (1975), Contributions to runoff from a melting prairie snow patch as traced by Oxygen-18, in *43rd Annual Meeting of the Western Snow Conference, April.*, pp. 1–14.
- Stevenson, F., and M. Cole (Eds.) (1999), *Cycles of Soil Carbon, Nitrogen, Phosphorus, Sulfur, Micronutrients*, second ed., 418 pp., John Wiley and Sons Inc.
- Stumm, W., and J. J. Morgan (1996), *Aquatic Chemistry Chemical Equilibria and Rates in Natural Waters*, third ed., 1003 pp., John Wiley and Sons Inc., New York.
- Stumpp, C., and M. J. Hendry (2012), Spatial and temporal dynamics of water flow and solute transport in a heterogeneous glacial till: The application of high-resolution profiles of $\delta^{18}\text{O}$ and $\delta^2\text{H}$ in pore waters, *Journal of Hydrology*, 438-439, 203–214, doi:10.1016/j.jhydrol.2012.03.024.
- Tattari, S., I. BÄrlund, S. Rekolainen, M. Posch, K. Siimes, H.-R. Tuhkanen, and M. Yli-Halla (2001), Modeling sediment yield and phosphorus transport in Finnish clayey soils, *Transactions of the ASAE*, 44(2), 297–307.
- Thompson, S. E., N. B. Basu, J. Lascurain, A. Aubeneau, and P. S. C. Rao (2011), Relative dominance of hydrologic versus biogeochemical factors on solute export across impact gradients, *Water Resources Research*, 47, W00J05, doi:10.1029/2010WR009605.
- Tiessen, K. H. D., J. A. Elliott, J. Yarotski, D. A. Lobb, D. N. Flaten, and N. E. Glozier (2010), Conventional and conservation tillage: influence on seasonal runoff, sediment, and nutrient losses in the Canadian Prairies., *Journal of environmental quality*, 39(3), 964–80, doi:10.2134/jeq2009.0219.
- Tiessen, K. H. D., J. A. Elliott, M. Stainton, J. Yarotski, D. N. Flaten, and D. A. Lobb (2011), The effectiveness of small-scale headwater storage dams and reservoirs on stream water quality and quantity in the Canadian Prairies, *Journal of Soil and Water Conservation*, 66(3), 158–171, doi:10.2489/jswc.66.3.158.

- Tranter, M. (1991), Controls on the composition of snowmelt, in *Seasonal Snowpacks: Processes of Compositional Change NATO ASI Series G, Vol. 28*, edited by T. D. Davis, M. Tranter, and H. G. Jones, pp. 241–271, Springer-Verlag, Berlin, Germany.
- Tranter, M., P. Brimblecombe, T. D. Davis, C. E. Vincent, and P. W. Abrahams (1986), The chemical composition of snowpack, snowfall and meltwater in the Scottish Highlands - evidence for preferential elution, *Atmospheric Environment*, 20, 517–525.
- USEPA (2000), EPA National Nutrient Strategy.
- van Bochove, E., H. G. Jones, F. Pelletier, and D. Prevost (1996), Emission of N₂O from agricultural soil under snow cover: a significant part of N budget, *Hydrological Processes*, 10(11), 1545–1549, doi:10.1002/(SICI)1099-1085(199611)10:11<1545::AID-HYP492>3.0.CO;2-0.
- van Bochove, E., G. Thériault, P. Rochette, H. G. Jones, and J. W. Pomeroy (2001), Thick ice layers in snow and frozen soil affecting gas emissions from agricultural soils during winter, *Journal of Geophysical Research*, 106(D19), 23,061–23,071.
- van Bochove, E., G. Thériault, J.-T. Denault, F. Dechmi, S. E. Allaire, and A. N. Rousseau (2012), Risk of phosphorus desorption from Canadian agricultural land: 25-year temporal trend., *Journal of environmental quality*, 41(5), 1402–12, doi:10.2134/jeq2011.0307.
- van der Kamp, G., and M. Hayashi (2009), Groundwater-wetland ecosystem interaction in the semiarid glaciated plains of North America, *Hydrogeology Journal*, 17, 203–214, doi:10.1007/s10040-008-0367-1.
- van der Kamp, G., M. Hayashi, and D. Gallen (2003), Comparing the hydrology of grassed and cultivated catchments in the semi-arid Canadian prairies, *Hydrological Processes*, 17(3), 559–575, doi:10.1002/hyp.1157.
- Verseghy, D. L., N. A. McFarlane, and M. Lazare (1993), CLASS - A Canadian land surface scheme for GCMs, II. Vegetation model and coupled runs, *International Journal of Climatology*, 13, 347–370.
- Viney, N. R., and M. Sivapalan (2000), *LASCAM: The Large Scale Catchment Model User Manual Version 2*, 75 pp., Center for Water Research, University of Western Australia.
- Wang, X., J. Williams, and P. Gassman (2012), EPIC and APEX: Model use, calibration, and validation, *Transactions of the American Society of Agricultural and Biological Engineers*, 55(1996), 1447–1462.
- Watanabe, K., and M. Flury (2008), Capillary bundle model of hydraulic conductivity for frozen soil, *Water Resources Research*, 44, W12,402, doi:10.1029/2008WR007012.
- Water Management and Hydrology Section (2012), 2011 Post - Flood Report for the Souris River Basin, *Tech. rep.*, US Army Corps of Engineers.

- Watershed Evaluation Group Department of Geography University of Guelph (2013), Hydrologic and Integrated Modelling for Examining BMP Effects in the South Tobacco Creek Watershed, Manitoba, in *Proceedings for the RRB Water Quality and Watershed Modeling Meeting Session 2*.
- Wellen, C., A.-R. Kamran-Disfani, and G. B. Arhonditsis (2015), Evaluation of the Current State of Distributed Watershed Nutrient Water Quality Modeling, *Environmental Science & Technology*, 49, 3278–3290, doi:10.1021/es5049557.
- Wheater, H., et al. (2013), *Water and Agriculture in Canada: Towards Sustainable Management of Water Resources*, 259 pp., Council of Canadian Academies.
- White, E. (1973), Water-Leachable Nutrients from Frozen or Dried Prairie Vegetation, *Journal of Environmental Quality*, 2(1), 104–107, doi:10.2134/jeq1973.00472425000200010015x.
- Woodbury, J. D., C. a. Shoemaker, Z. M. Easton, and D. M. Cowan (2014), Application of SWAT with and without Variable Source Area Hydrology to a Large Watershed, *Journal of the American Water Resources Association*, 50(1), 42–56, doi:10.1111/jawr.12116.
- Yang, J. Y., R. De Jong, C. F. Drury, E. C. Huffman, V. Kirkwood, and X. M. Yang (2007a), Development of a Canadian Agricultural Nitrogen Budget (CANB v2.0) model and the evaluation of various policy scenarios, *Canadian Journal of Soil Science*, 87(Special Issue), 153–165, doi:10.4141/S06-063.
- Yang, Q., L. F. Leon, W. G. Booty, I. W. Wong, C. McCrimmon, P. Fong, P. Michiels, J. Vanrobaeys, and G. Benoy (2014), Land Use Change Impacts on Water Quality in Three Lake Winnipeg Watersheds, *Journal of Environmental Quality*, 43, 1690–1701, doi:10.2134/jeq2013.06.0234.
- Yang, W., A. N. Rousseau, and P. Boxall (2007b), An integrated economic-hydrologic modeling framework for the watershed evaluation of beneficial management practices, *Journal of Soil and Water Conservation*, 62(6), 423–432.
- Yang, W., X. Wang, S. Gabor, L. Boychuk, and P. Badiou (2008), Water Quantity and Quality Benefits from Wetland Conservation and Restoration in the Broughton âs Creek Watershed, *Tech. Rep. October 2008*, Ducks Unlimited, unnumbered report.
- Young, R. A., C. A. Onstad, D. D. Bosch, and W. P. Anderson (1987), AGNPS: Agricultural Non-Point Source Pollution Model: a watershed analysis tool., *Tech. rep.*, USDA-Agricultural Research Service, Conservation Research Report 35, USDA, Washington, DC.
- Zambrano-Bigiarini, M. (2014), hydroGOF: Goodness-of-fit functions for comparison of simulated and observed hydrological time series. <http://cran.r-project.org/package=hydroGOF>.
- Zhao, L. T., and D. M. Gray (1999), Estimating snowmelt infiltration into frozen soils, *Hydrological Processes*, 13(12-13), 1827–1842, doi:10.1002/(sici)1099-1085(199909)13:12/13<1827::aid-hyp896>3.0.co;2-d.

Zoski, E. (2015), Agriculture and Agri-Food Canada, email correspondence.

APPENDIX A

LITERATURE REVIEW SUPPORTING DATA

A.1 Phosphorous Mass Balance Scratch Sheet

The input and output fluxes for the annual phosphorous mass balance in agricultural soils (Figure 2.1a) were generated from the literature presented in Chapter 2. The calculations are summarized below. The annual period used here extends post harvest to post harvest (October 31 to November 1 generally) and considers the important input and outputs of P for an ungrazed prairie agricultural field growing winter wheat.

Atmospheric deposition for P, discussed in Section 2.1.1, varies $0.001 - 0.074 g \cdot m^{-2} \cdot yr^{-1}$ with a mean of $0.04 g \cdot m^{-2} \cdot yr^{-1}$ for P. P fertilizer application rates average $0.74 g \cdot m^{-2} \cdot y^{-1}$ on the Canadian Prairie (Chambers et al., 2001, Appendix 3). $1.5 g \cdot m^{-2}$, a rate suited to winter wheat fertilization, was used here (Government of Manitoba). The $0.67 - 5.2 g \cdot m^{-2}$ range of P taken off with the harvest is crop and yield dependent (Canadian Fertilizer Institute, 2001): $1.1 g \cdot m^{-2}$ of P would be removed with a winter wheat crop having a $3360 kg \cdot ha^{-1}$ ($50 bu \cdot ac^{-1}$) yield. As discussed in Section 2.1.2 snow is relocated with wind and with that snow P may be lost. The P in the snowcover, from atmospheric deposition, could be relocated to a riparian zone or other area with taller vegetation during wind distribution. With a winter wheat crop and stubble on the field and modest snowcover depths, the wind transport of snow and solute is minimal. This is roughly estimated to amount to 10% of the annual deposition or $0.003 g \cdot m^{-2}$. The annual runoff of P is estimated at $0.003 g \cdot m^{-2}$ based on the research of Li et al. (2011) in the South Tobacco Creek Watershed, Manitoba.

A.2 Nitrogen Mass Balance Scratch Sheet

The input and output fluxes for the annual phosphorous mass balance in agricultural soils (Figure 2.1b) were generated from the literature presented in Chapter 2. The calculations are summarized below. The calculations are summarized below. The annual period used here extends post harvest to post harvest (October 31 to November 1 generally) and considers the important input and outputs of N for an ungrazed prairie agricultural field growing winter wheat.

Atmospheric deposition for N, discussed in Section 2.1.1, varies $0.68 - 2.2 g \cdot m^{-2} \cdot yr^{-1}$. An annual deposition rate at 25% of the maximum of the range ($0.35 g \cdot m^{-2}$ was used here due to the relative smoothness and openness of the terrain and far distance from urban emitters. N fertilizer application rates range $1.5 - 17 g \cdot m^{-2} \cdot y^{-1}$ on the Canadian Prairie (Yang et al., 2007a, Table 1). $8.0 g \cdot m^{-2}$, a rate suited to winter wheat fertilization on the Prairie, was used here (Yang et al., 2007a, Table 1). Nitrogen fixation rates range $0.4 - 20 g \cdot m^{-2} \cdot y^{-1}$ with non leguminous crops at the low end with a rate of $0.4 g \cdot m^{-2} \cdot y^{-1}$ (Chambers et al., 2001; Yang et al., 2007a). The $4.6 - 18.8 g \cdot m^{-2}$ range of N taken off with the harvest is crop and yield dependent (Canadian Fertilizer Institute, 2001): $5.2 g \cdot m^{-2}$ of N would be removed with a winter wheat crop having a $3360 kg \cdot ha^{-1}$ ($50 bu \cdot ac^{-1}$) yield. As discussed in Section 2.1.2 snow is relocated with wind and with that snow N may be lost. The atmospheric N in the snowcover is not conserved during transport. Some N would be lost in transport from a

field to a riparian zone or other area with taller vegetation during wind distribution. With a winter wheat crop and stubble on the field and modest snowcover depths, the wind transport of snow and solute is minimal. This is roughly estimated to amount to 10% of the annual deposition of N or $0.03 \text{ g} \cdot \text{m}^{-2}$. Denitrification rates range $0.04 - 0.4 \text{ g} \cdot \text{m}^{-2} \cdot \text{y}^{-1}$ on the Canadian Prairie (Ellert and Janzen, 2008). A rate of $0.18 \text{ g} \cdot \text{m}^{-2}$ was used for this crop. Volatilization rates have been reported to range 8 – 68% of N applied as urea (Rochette et al., 2013). For this field, 10% of the applied N was assumed to volatilized amounting to $0.8 \text{ g} \cdot \text{m}^{-2}$. Unsaturated zone leaching rates were estimated at $0.18 \text{ g} \cdot \text{m}^{-2}$, the mean of the reported range by Campbell et al. (2006) in research at Swift Current in southwest Saskatchewan. The annual runoff of N is estimated at $0.20 \text{ g} \cdot \text{m}^{-2}$ based on the research of Li et al. (2011, Table 2) in the South Tobacco Creek Watershed, Manitoba.

A.3 CREAMS Formulae

Knisel (1980a,b) and others (Arnold and Williams, 1987; Young et al., 1987) assume the surface layer that interacts with runoff water to be 10 mm and that any infiltration that occurs prior to the generation of surface runoff will also flush this surface layer via convective transport of the solute with the infiltrate:

$$\frac{dc}{dt} = k_1 f(t)(c_r - c) \quad (\text{A.1})$$

where c and t represent concentration and time, k_1 is a rate constant for downward movement, c_r the concentration of NO_3 in the rainfall, and $f(t)$ is the infiltration rate. To determine the concentration in the soil, c_1 after infiltration this expression can be integrated and evaluated with total infiltration, $F = \int f(t)dt$. This yields:

$$\begin{aligned} \int_{c_o}^{c_1} \frac{dc}{(c_r - c)} &= \int_0^t k_1 f(t)dt \\ -\ln(c_r - c)|_{c_o}^{c_1} &= k f(t)|_0^t \\ \ln(c_r - c)|_{c_o}^{c_1} &= -k f(t)|_0^t \\ \ln(c_r - c_1) - \ln(c_r - c_o) &= -k f(t)t \\ e^{\ln(c_r - c_1) - \ln(c_r - c_o)} &= e^{-kF} \\ \frac{e^{\ln(c_r - c_1)}}{e^{\ln(c_r - c_o)}} &= e^{-kF} \\ \frac{c_r - c_1}{c_r - c_o} &= e^{-kF} \\ c_r - c_1 &= (c_r - c_o)e^{-kF} \\ -c_1 &= (c_r - c_o)e^{-kF} - c_r \\ c_1 &= (c_o - c_r)e^{-k_1 F} + c_r \end{aligned} \quad (\text{A.2})$$

where c_o is the concentration of NO_3 in the soil. To determine what concentration of NO_3 is transferred to surface runoff, a partitioning coefficient is calculated, a common practice in the simplification and conceptual rendering of complex physical processes.

APPENDIX B

FIELD SCALE DATA ANALYSES PLOTS

Table B.1: Mean snowcover and EOF solute concentrations. The concentrations in this table are the annual observed averages for the March snow survey concentrations and the edge-of-field runoff concentrations. CF_f is defined in Equation 4.1 as the mean snowcover solute concentration divided by the mean EOF solute concentration. 2009, highlighted in grey, is the year that a restricted infiltration event was assumed to occur impacting the EOF CF_f for each solute (refer to Section 4.4).

Year	Snowpack Concentration [mg/l]	EOF Concentration [mg/l]	CF_f
Phosphorous(TDP)			
2006	0.0686	0.6145	8.9
2007	0.0859	0.4217	4.9
2008	0.0282	0.6222	22.0
2009	0.1191	0.3825	3.2
2010	0.0636	0.6441	10.1
2011	0.0795	0.4244	5.3
2012	0.0341	0.9600	28.1
Nitrate (NO3)			
2006	0.4648	3.7014	8.0
2007	0.3903	3.0912	7.9
2008	0.2849	7.3115	25.7
2009	0.2416	1.1833	4.9
2010	0.2716	6.6963	24.6
2011	0.2882	3.2561	11.3
2012	0.3531	8.6234	24.4
Ammonia (NH3)			
2006	0.6236	0.4368	0.7
2007	0.5241	1.0198	1.9
2008	0.3380	0.7800	2.3
2009	0.2761	1.1760	4.3
2010	0.2967	0.5901	2.0
2011	0.5220	0.7482	1.4
2012	0.3645	0.7655	2.1

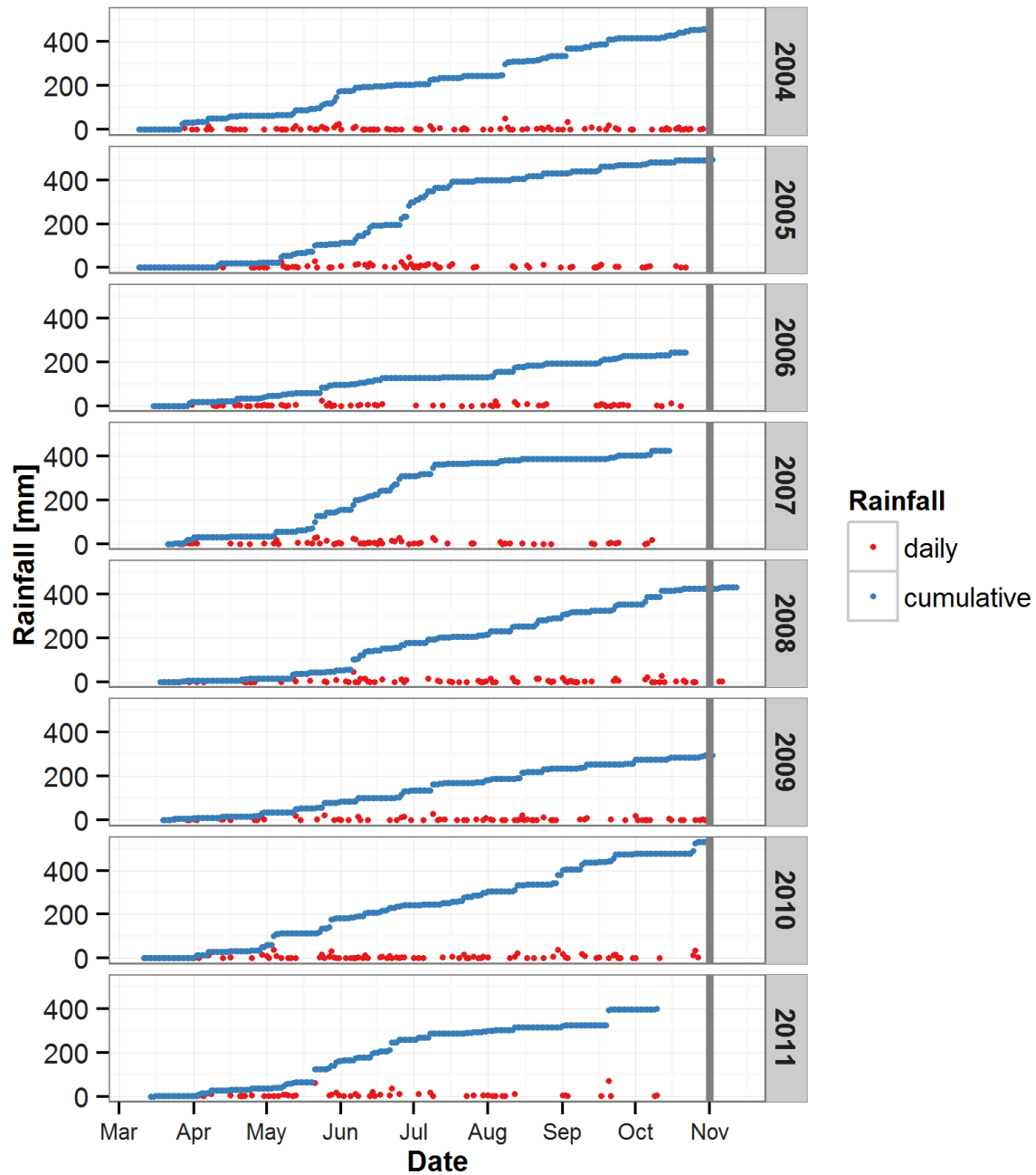


Figure B.1: Annual Observed Rainfall. This series of plots illustrates the cumulative and daily rainfall observed on fields 3, 4, 7, 9, 10 and 11. Primarily, results were measured at the gauge on fields 10/11 except for 2008 where the late rain event was captured on the field 4 gauge (the field 10/11 gauge malfunctioned early in the season and recordings ceased November 5, 2008).

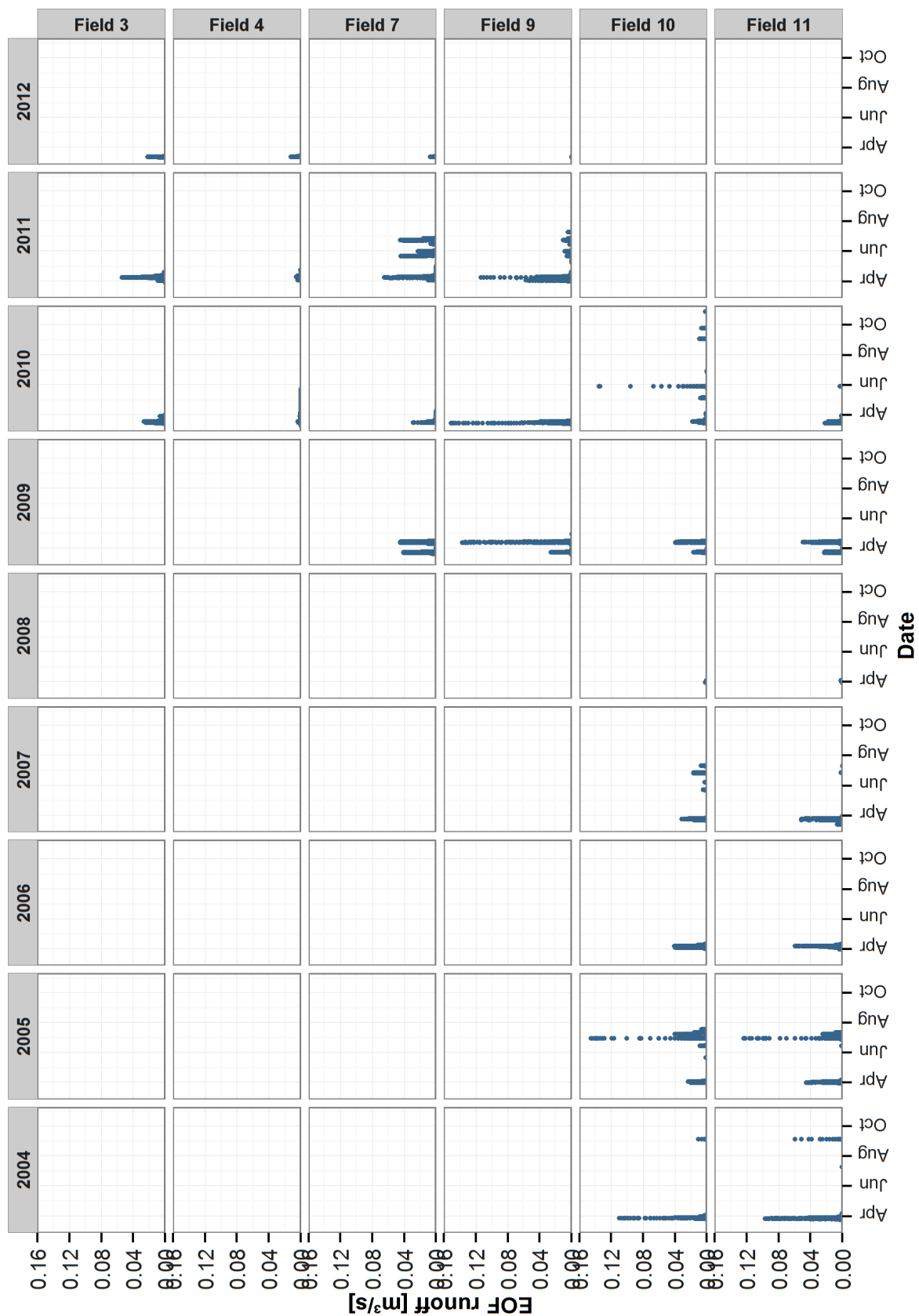


Figure B.2: Observed 15 minute Edge-of-Field Runoff.

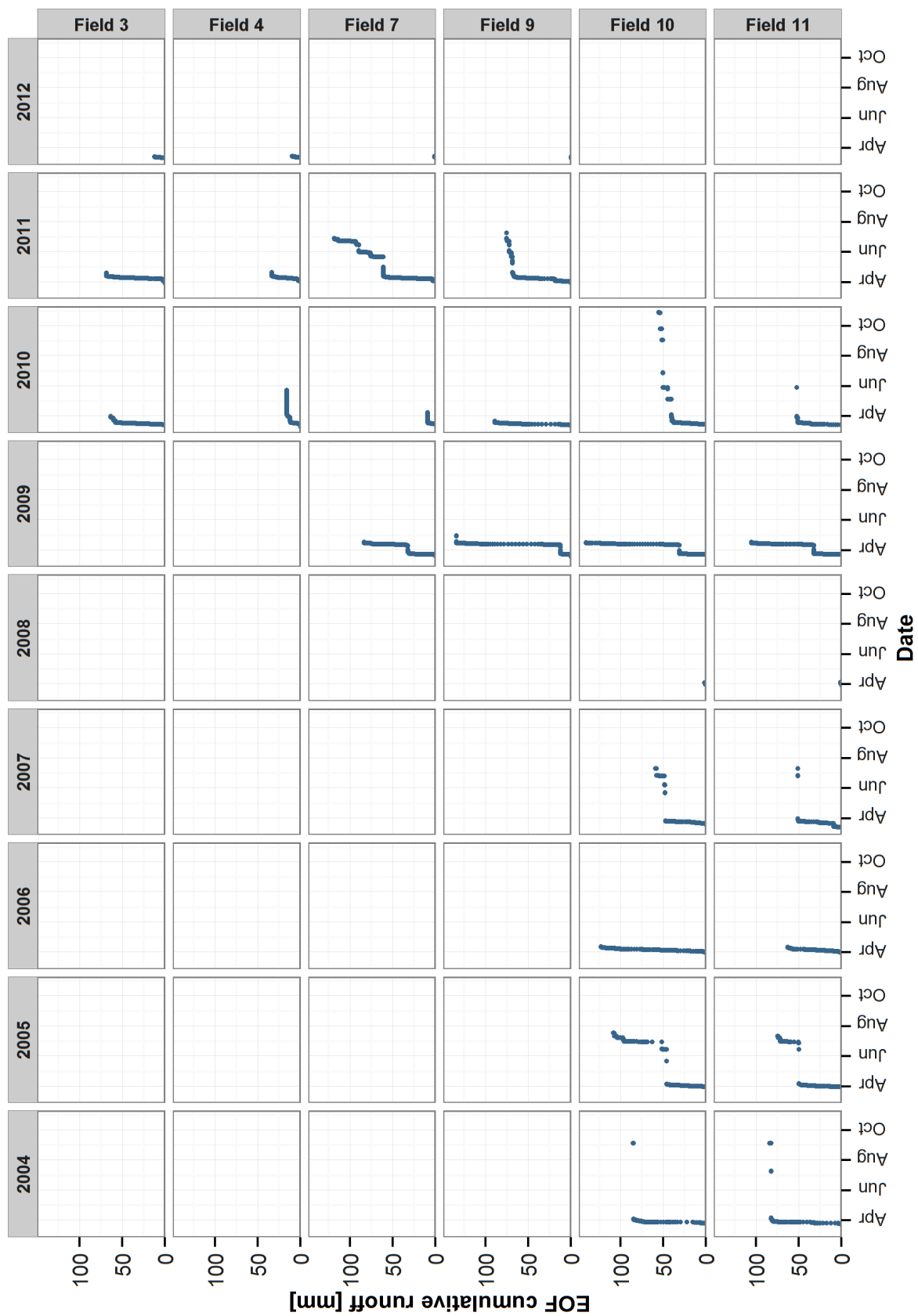


Figure B.3: Observed Cumulative Edge-of-Field Runoff.

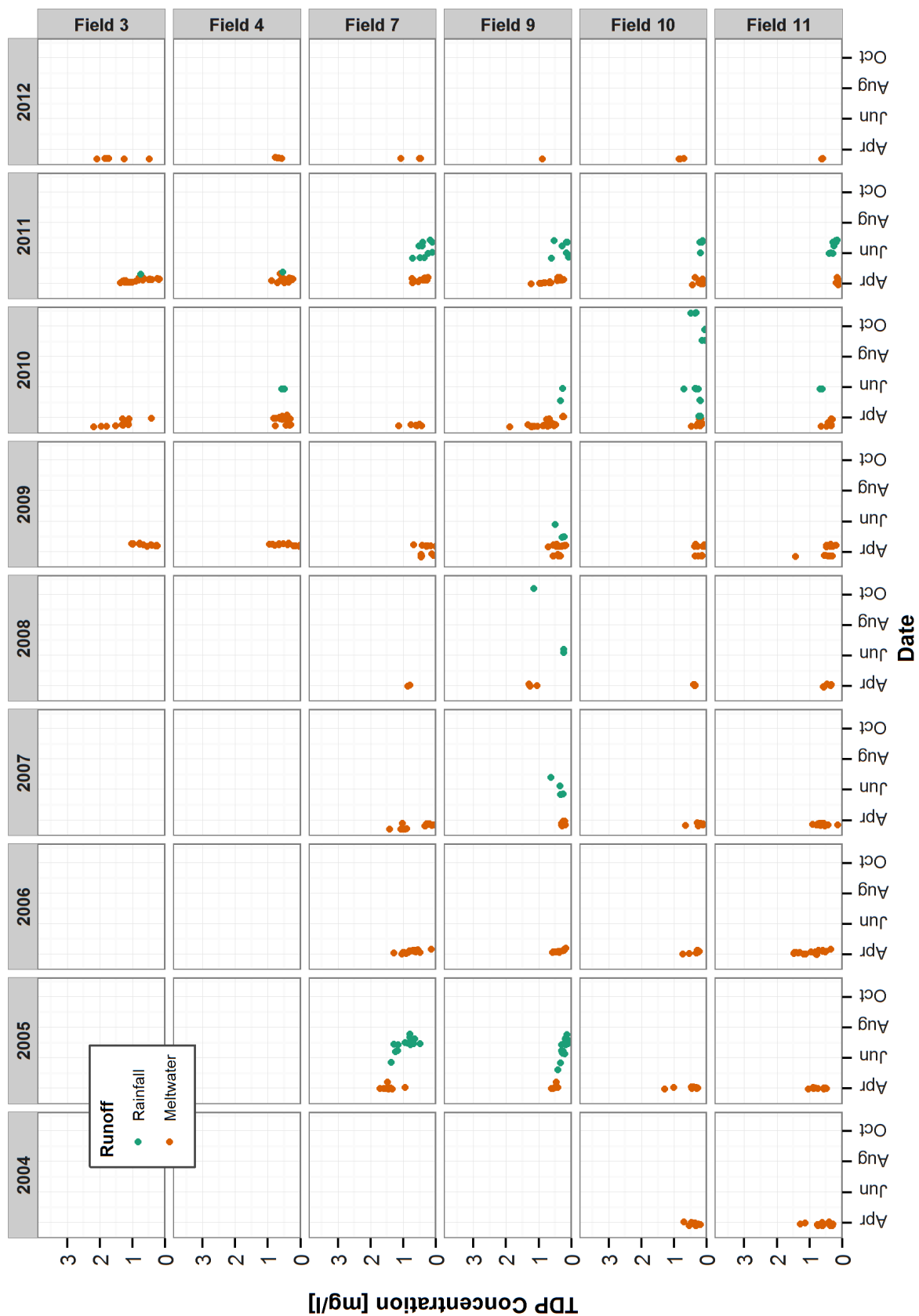


Figure B.4: Observed Dissolved Phosphorous Concentration at the Edge-of-Field.

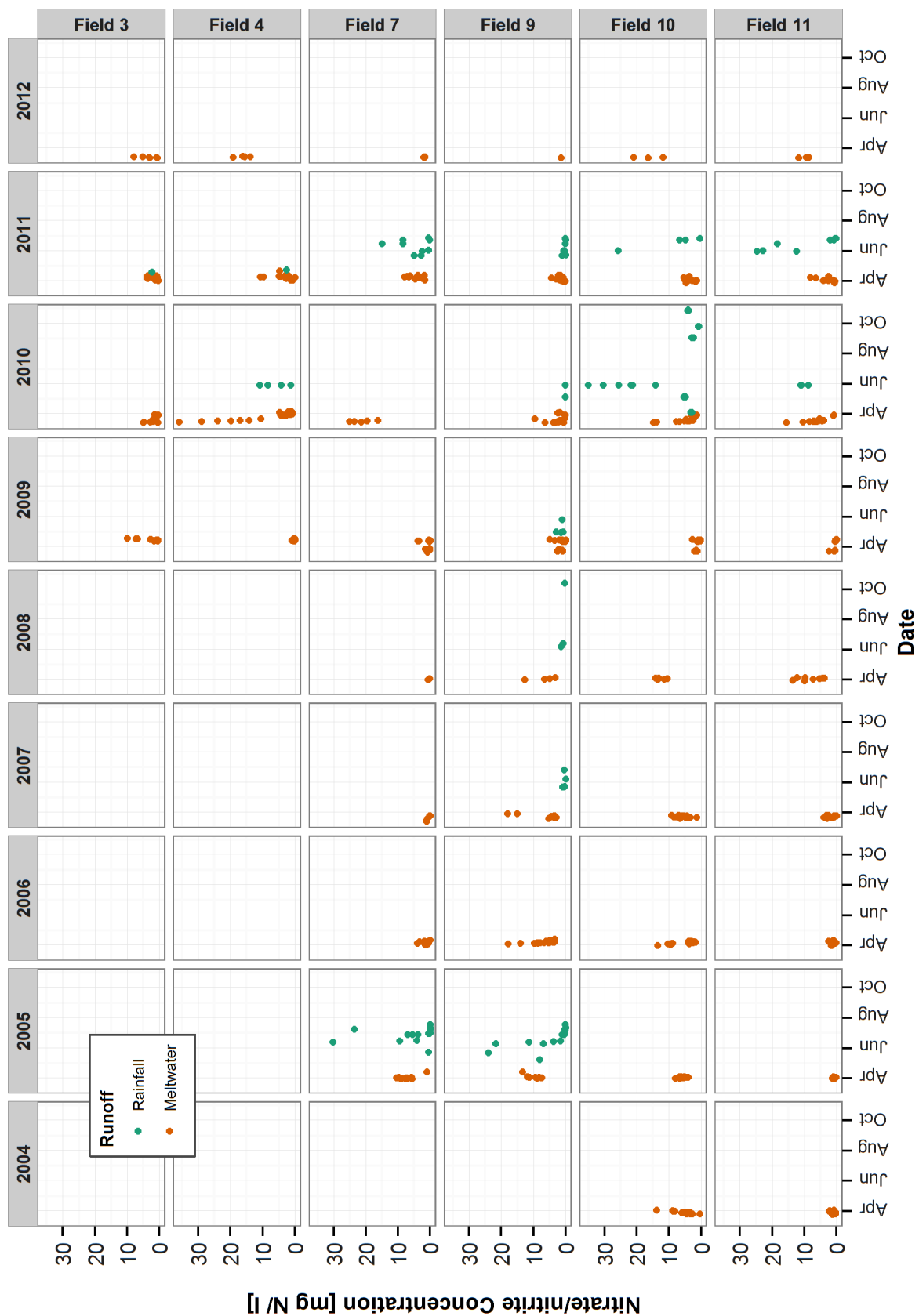


Figure B.5: Observed Nitrate Concentration at the Edge-of-Field.

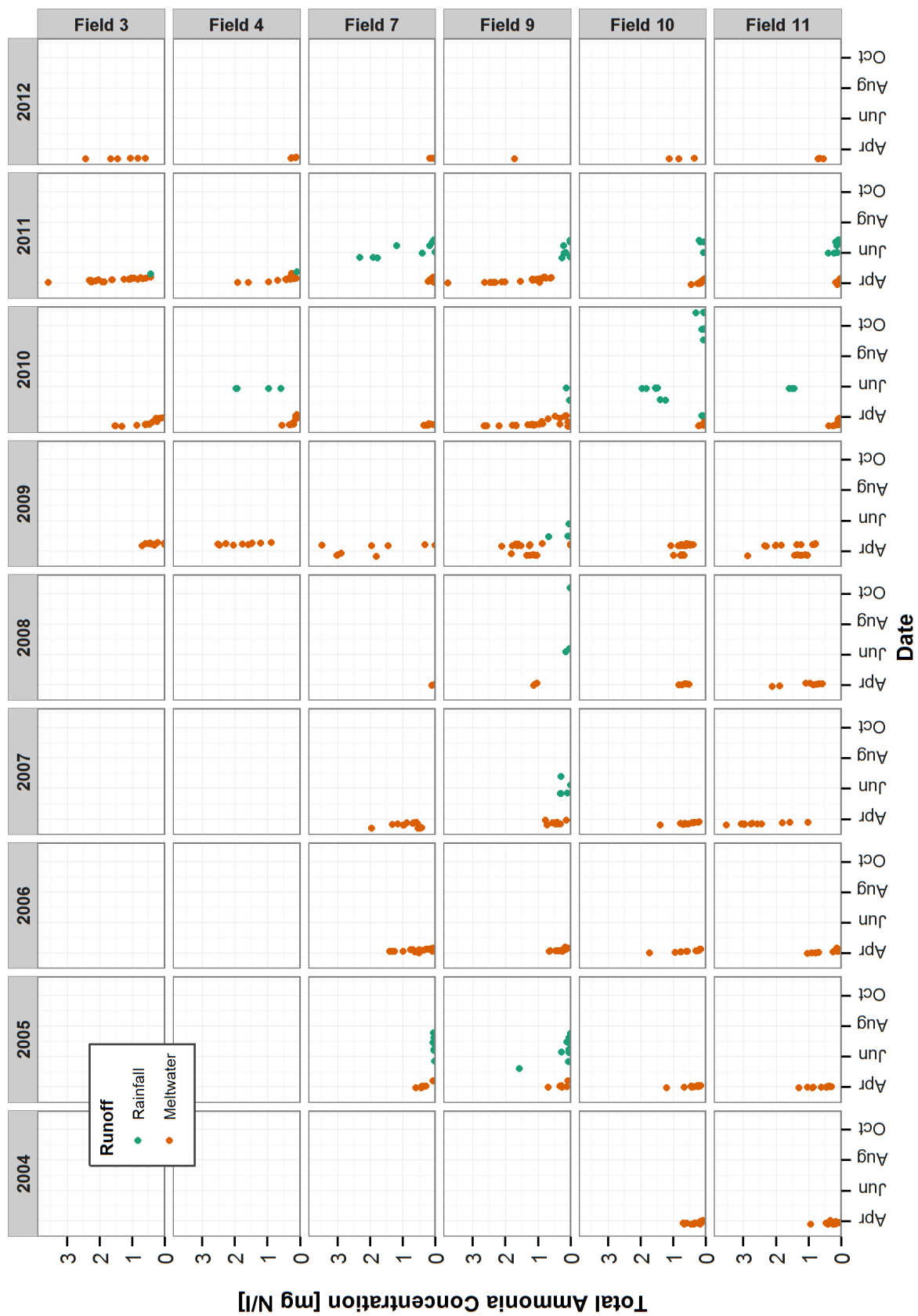


Figure B.6: Observed Ammonia Concentration at the Edge-of-Field.

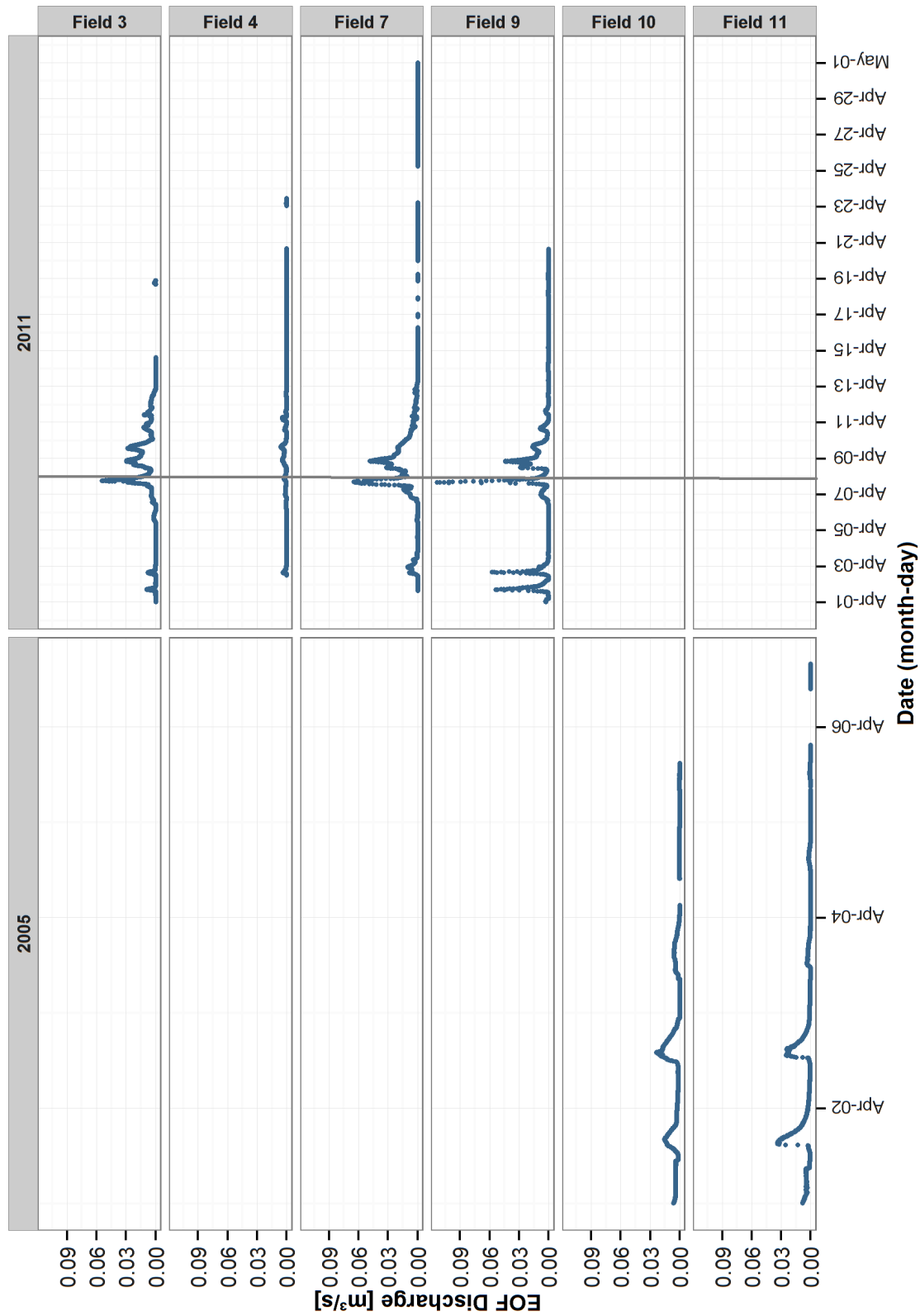


Figure B.7: Observed 15 minute Edge-of-Field Runoff During potential ROS Events. The vertical line is on April 8, 2011 the date of the second potential ROS event. The first potential event in 2005 shows no recorded runoff on Fields 10 and 11. Flows were not recorded on Fields 3-9 during these years (Figure B.2).

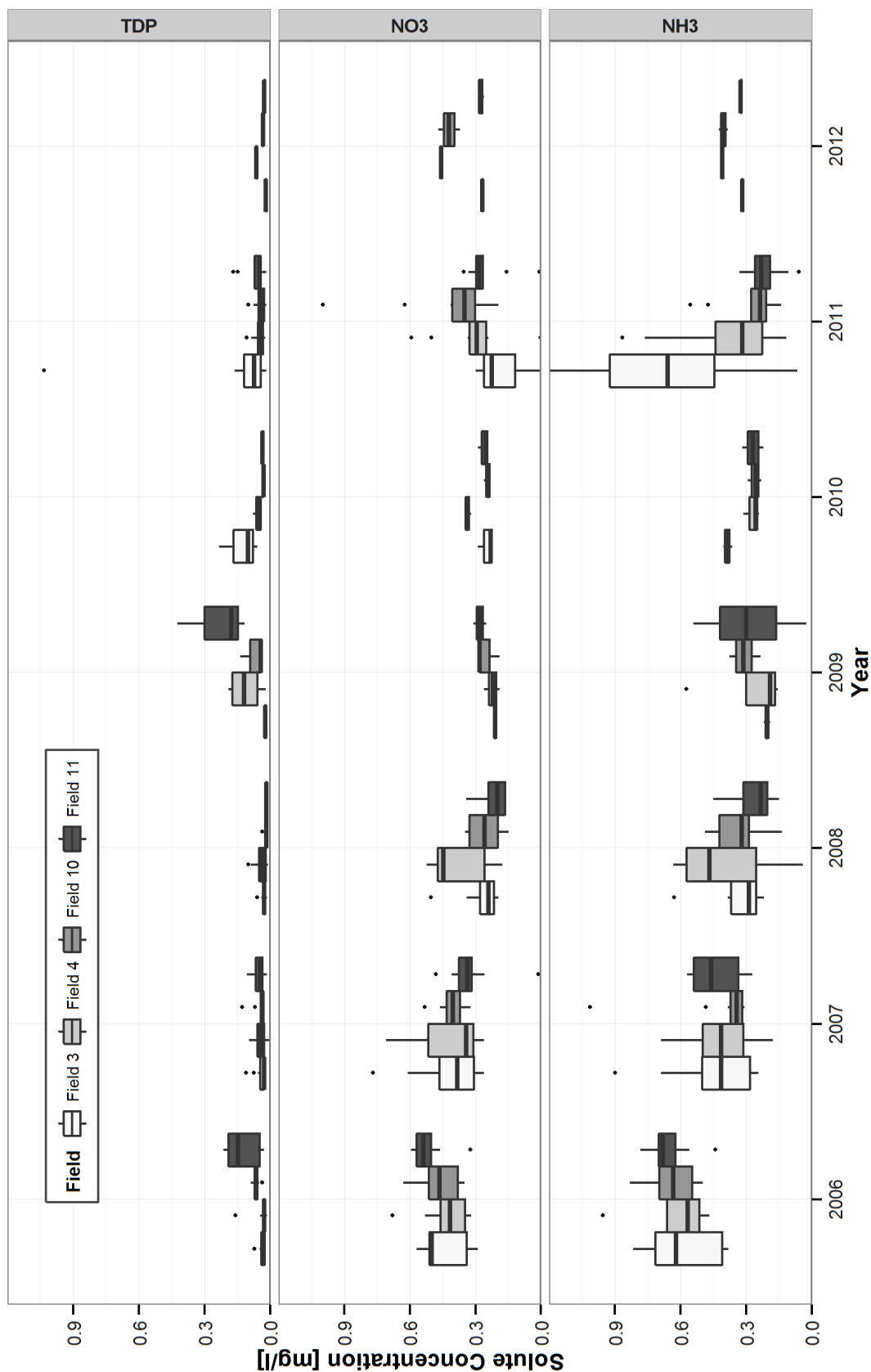


Figure B.8: Annual Observed Snowcover Nutrient Concentrations. March snow surveys for 2006-2012 as performed on fields 3, 4, 10, and 11. The boxplots are done in R ([R Development Core Team, 2010](#)) with the upper and lower hinges representing the first and third quartiles; the mid-hinge the median; and the whisker extents, 1.5 times the inter-quartile range.

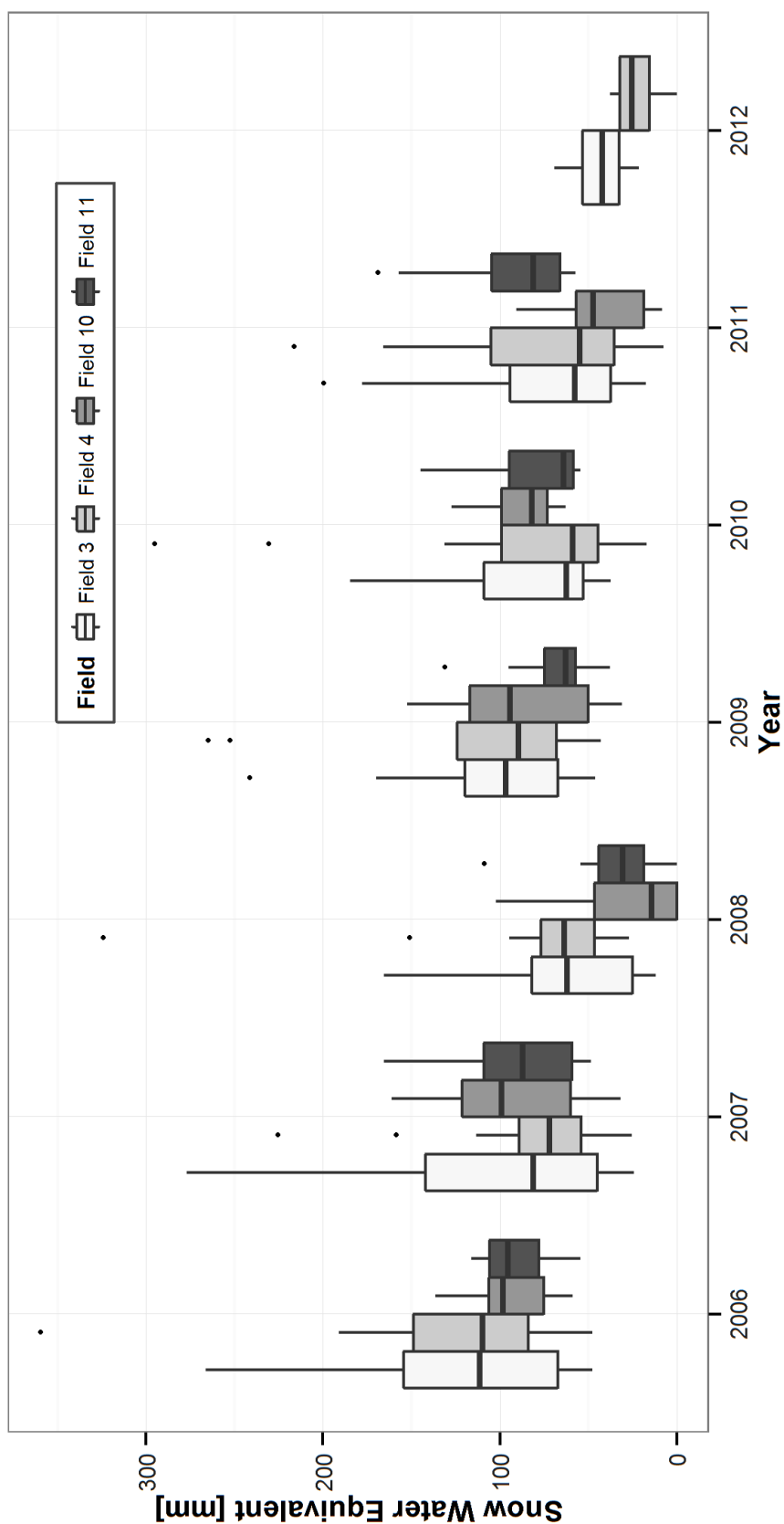


Figure B.9: Annual Observed March Snowcover SWE. March snow surveys for 2006-2012 as performed on F3, F4, F10, and F11. The boxplots are done in R ([R Development Core Team, 2010](#)) with the upper and lower hinges representing the first and third quartiles; the mid-hinge the median; and the whisker extents, 1.5 times the inter-quartile range.

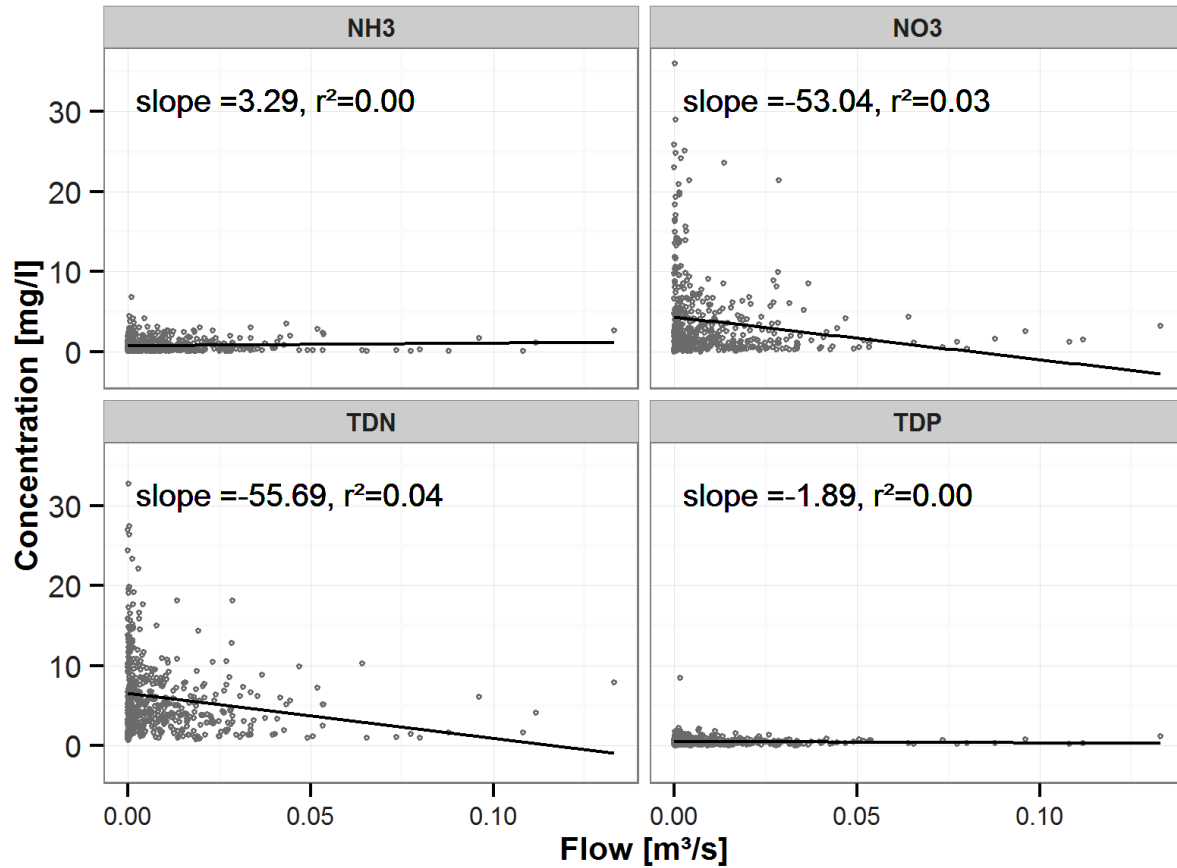
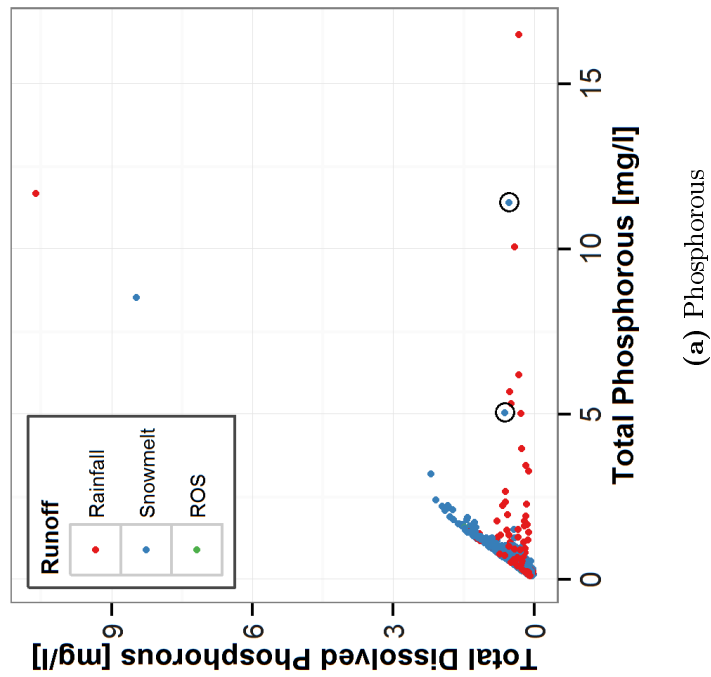
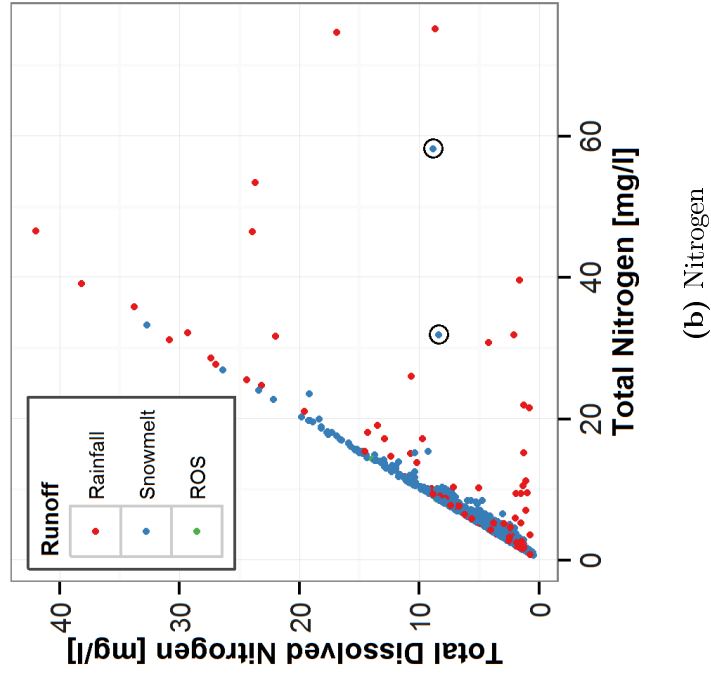


Figure B.10: EOF Concentration vs Discharge. The edge-of-field scale runoff data for fields 3,4,7,9,10 and 11 are plotted here on a linear scale. A linear regression is attempted and fails. There is no linear relationship between EOF flows and concentrations.



(a) Phosphorous



(b) Nitrogen

Figure B.11: Phosphorous and Nitrogen Exports, dissolved vs total fractions (all data). These plots show the full extents of the data including the two outliers (circled) removed from the regressions in Figure 4.6.

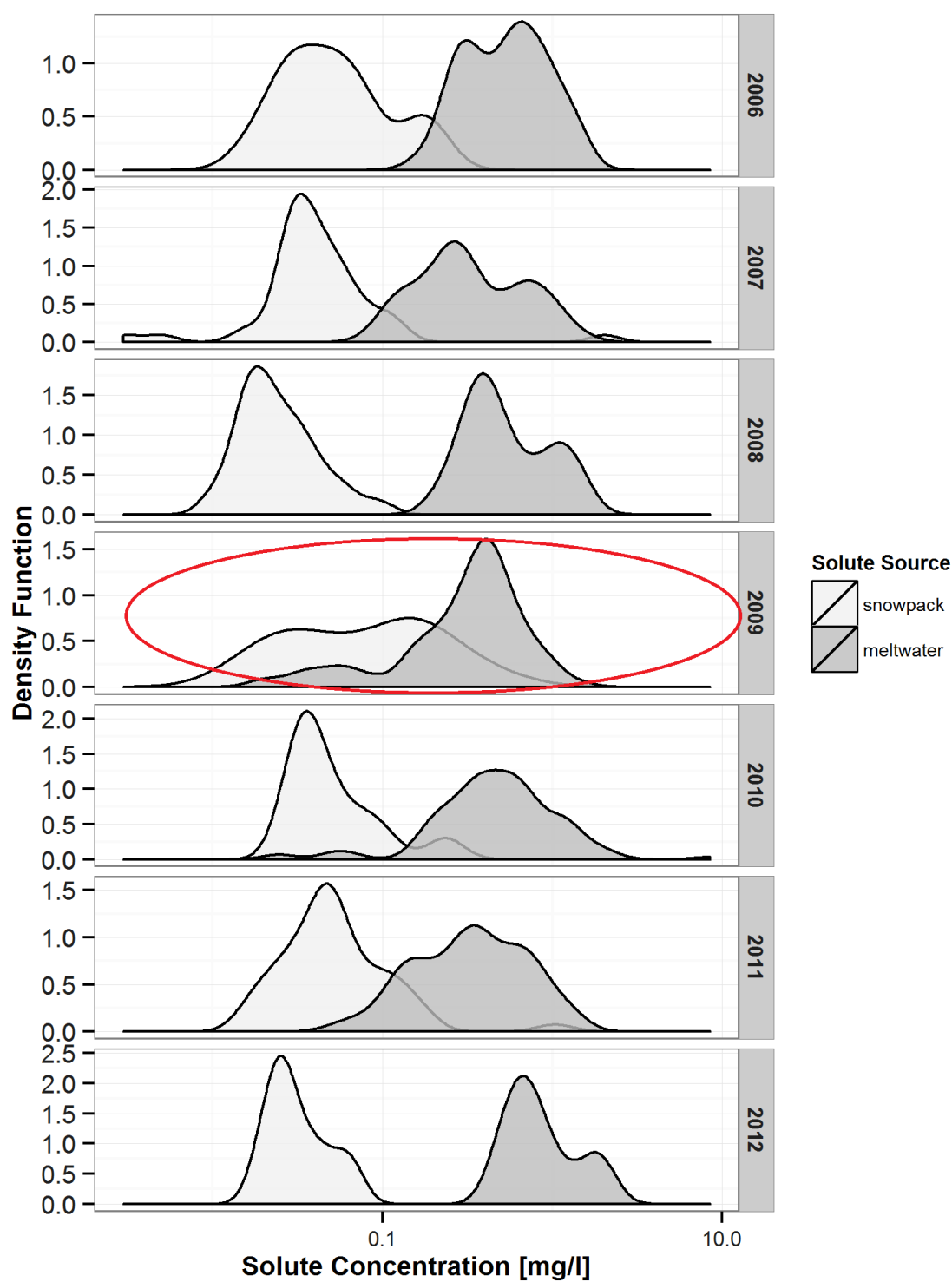


Figure B.12: Annual TDP Density Distribution Plots. Distribution density plots for TDP to compare the concentration change from snowcover to edge of field. Mean concentrations for each of the snowcover and edge-of-field are tabulated in Table B.1

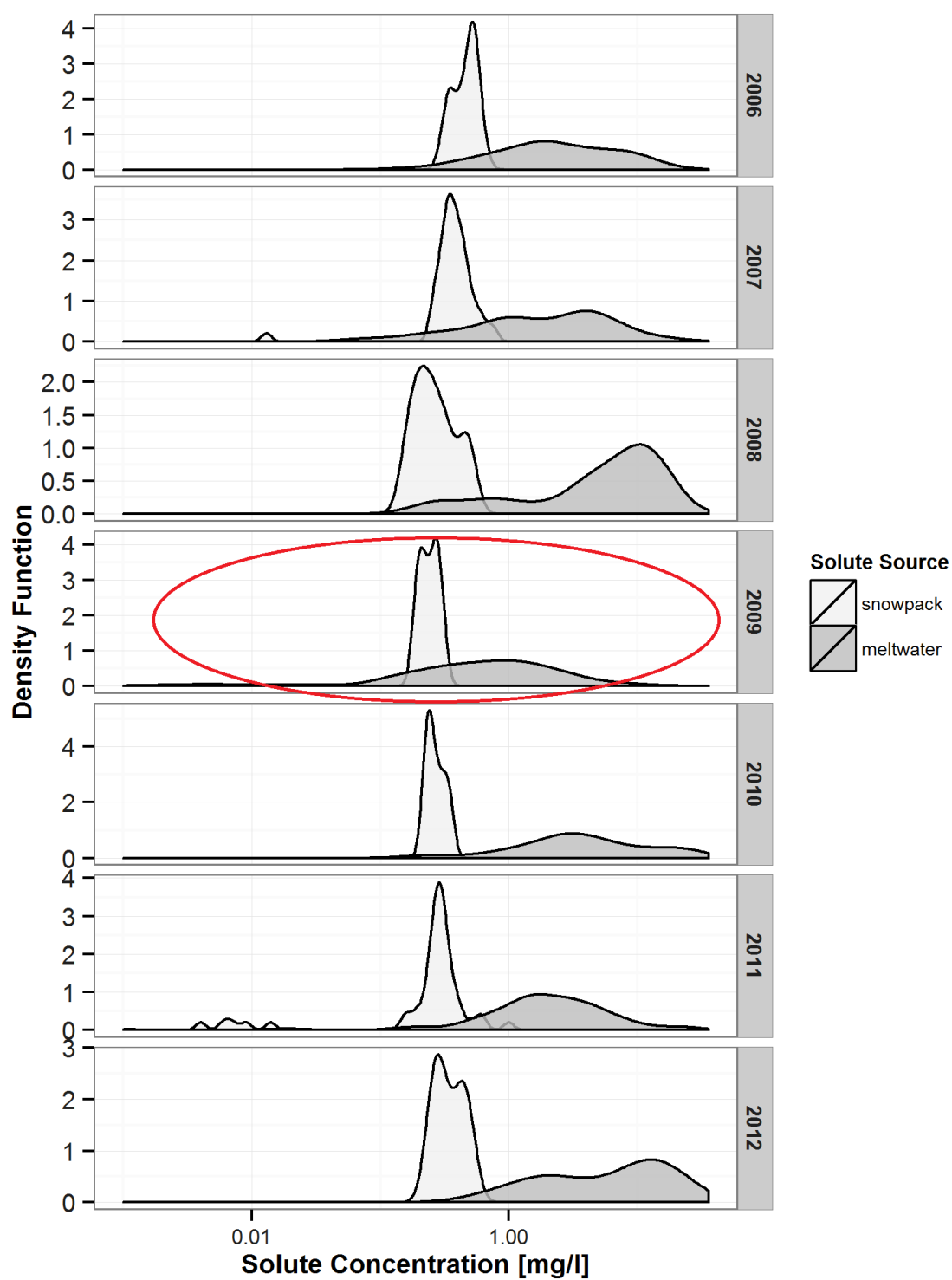


Figure B.13: Annual NO₃ Density Distribution Plots. Distribution density plots for NO₃ to compare the concentration change from snowcover to edge-of-field. Mean concentrations for each of the snowcover and edge-of-field are tabulated in Table B.1

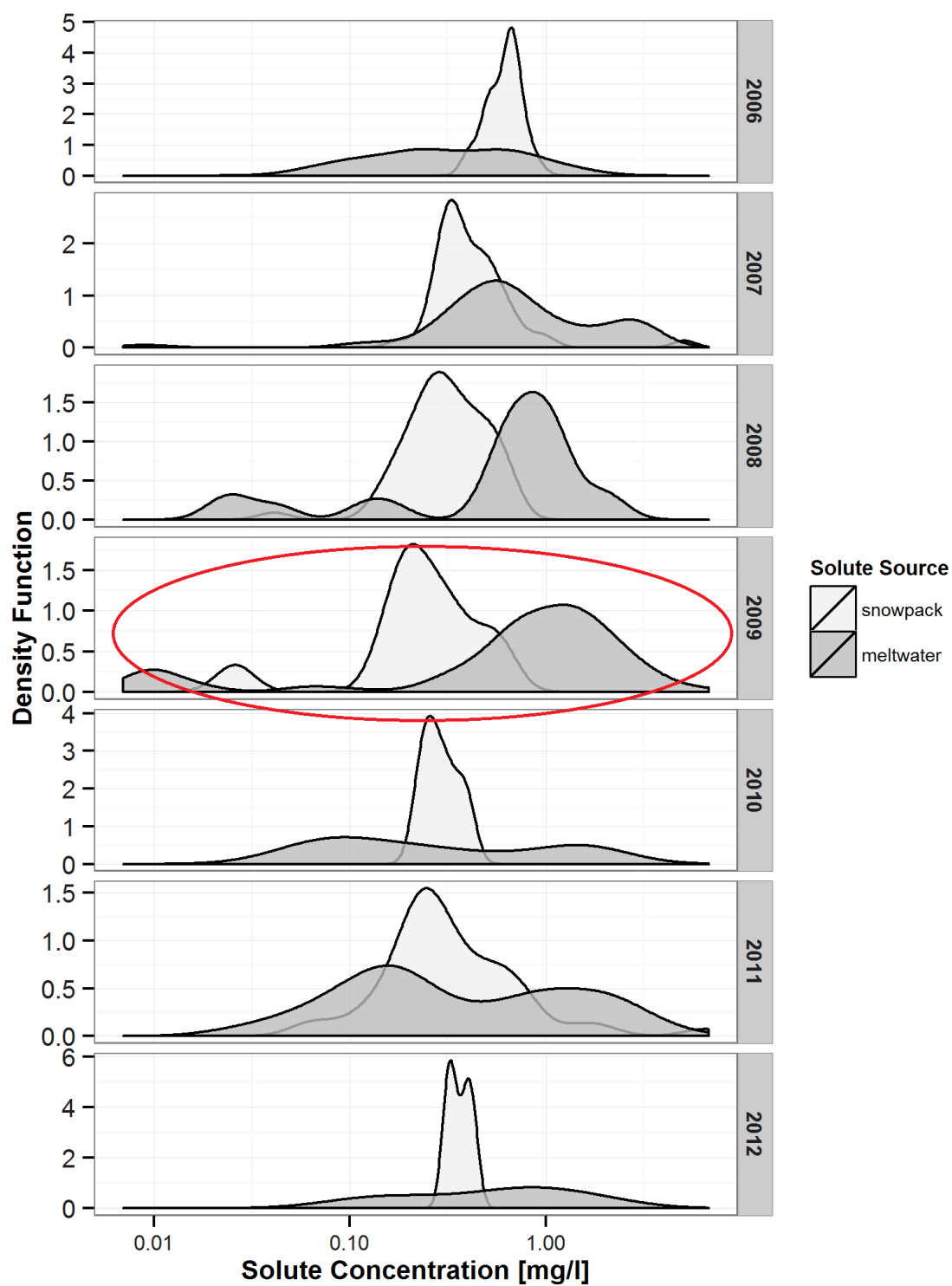


Figure B.14: Annual NH_3 Density Distribution Plots. Distribution density plots for NH_3 to compare the concentration change from snowcover to edge of field. Mean concentrations for each of the snowcover and edge-of-field are tabulated in Table B.1

APPENDIX C

MODEL DEVELOPMENT PLOTS AND MODEL CODE

C.1 Model Plots

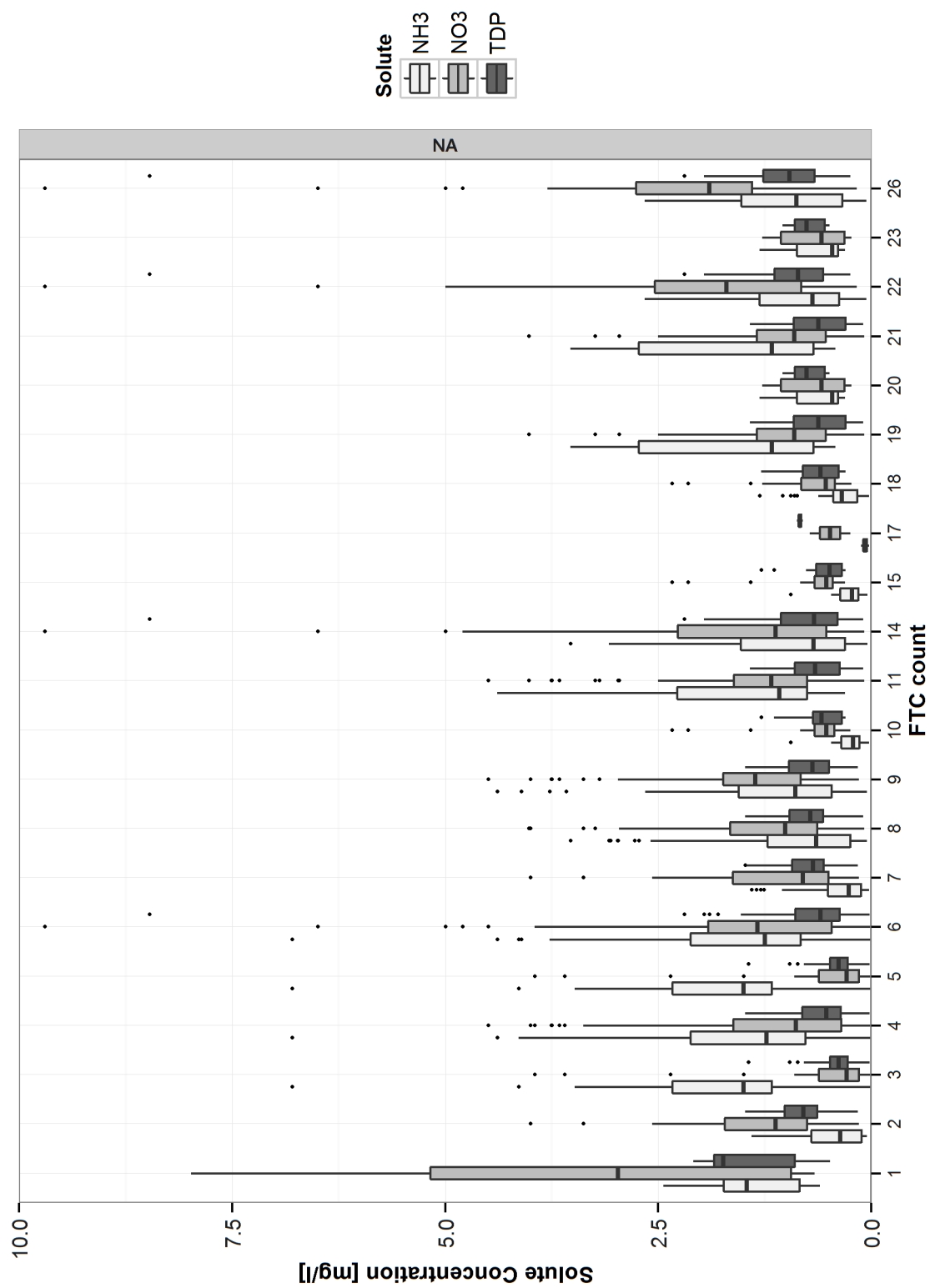


Figure C.1: EOF Solute Concentrations and Freeze Thaw Cycle Counts. The plot is binned into minimum FTC magnitudes and grouped by solute.

C.2 Model Code

C.2.1 main.R

```
# the main program
Version <- "Version6"

setwd("c:\\Users\\User\\Documents\\MScThesis\\code\\MY_MODEL\\Version6")

library(ggplot2)
library(reshape2)
#library(ggsubplot)
library(scales)
library(plyr)
library(dplyr)
library(tseries)
library(stats)
#library(Metrics)
library(hydroGOF)
library(grid)

source("c:\\Users\\User\\Documents\\MScThesis\\code\\MY_MODEL
\\Version6\\CVd.R")
source("c:\\Users\\User\\Documents\\MScThesis\\code\\MY_MODEL
\\Version6\\musigma.R")
source("c:\\Users\\User\\Documents\\MScThesis\\code\\MY_MODEL
\\Version6\\EsseryPomeroy2004.R")
source("c:\\Users\\User\\Documents\\MScThesis\\code\\MY_MODEL
\\Version6\\strptime.R")
source("c:\\Users\\User\\Documents\\MScThesis\\code\\MY_MODEL
\\Version6\\runoff_PN.R")
source("c:\\Users\\User\\Documents\\MScThesis\\code\\MY_MODEL
\\Version6\\Amarawansha2013.R")
source("c:\\Users\\User\\Documents\\MScThesis\\code\\MY_MODEL
\\Version6\\new_concentration.R")
source("c:\\Users\\User\\Documents\\MScThesis\\code\\MY_MODEL
\\Version6\\grassland_disturbance.R")
source("c:\\Users\\User\\Documents\\MScThesis\\code\\MY_MODEL
\\Version6\\freeze_thaw_cycles.R")
source("c:\\Users\\User\\Documents\\MScThesis\\code\\MY_MODEL
\\Version6\\Bechmann2005_TDPcurve.R")
source("c:\\Users\\User\\Documents\\MScThesis\\code\\MY_MODEL
\\Version6\\NP_stoichiometry.R")
source("c:\\Users\\User\\Documents\\MScThesis\\code\\MY_MODEL
\\Version6\\calculate_csoilN03.R")
#source("c:\\Users\\User\\Documents\\MScThesis\\code\\MY_MODEL
#\\Version6\\soil_freezing_characteristic.R")
source("c:\\Users\\User\\Documents\\MScThesis\\code\\MY_MODEL
\\Version6\\soil_temperature.R")
source("c:\\Users\\User\\Documents\\MScThesis\\code\\MY_MODEL
\\Version6\\calculate_max_subnivean_nitrification_days.R")
source("c:\\Users\\User\\Documents\\MScThesis\\code\\MY_MODEL
\\Version6\\Stein_etal_1986.R")
source("c:\\Users\\User\\Documents\\MScThesis\\code\\MY_MODEL
```

```

    \\Version6\\rainfall_chem.R")
source("c:\\Users\\User\\Documents\\MScThesis\\code\\MY_MODEL
    \\Version6\\load_chemograph.R")
source("c:\\Users\\User\\Documents\\MScThesis\\code\\MY_MODEL
    \\Version6\\simvsobs_hydrograph.R")
source("c:\\Users\\User\\Documents\\MScThesis\\code\\MY_MODEL
    \\Version6\\plots.R")
source("c:\\Users\\User\\Documents\\MScThesis\\code\\MY_MODEL
    \\Version6\\sensitivity_plots.R")
source("c:\\Users\\User\\Documents\\MScThesis\\code\\MY_MODEL
    \\Version6\\EOFchem_contributing_fractions.R")

#set global plotting themes

paper_plot_format <-
  theme(plot.title=element_text(face="bold",size="12",color="grey12"),
        axis.title=element_text(face="bold",size="12"),
        #axis.text.x=element_text(angle=0),
        strip.text=element_text(face="bold",colour="grey12",
                                size="12"),
        legend.title=element_text(face="bold",size="12"),
        legend.text=element_text(size="12"))+
  theme(axis.text=element_text(size=12,colour="grey12"))+
  theme(axis.text.x=element_text(size=6,colour="grey12",angle=-90))+
  theme_bw()

#set global plotting themes
theme_set(theme_bw())

Field <- c(3,4,7,9,10,11)
Area <- c(8.33,2.45,12.7,10.2,4.05,6.04) #[ha]
areas <- data.frame(Field,Area)
areas$Area <- areas$Area*0.01 #[km2]

#
# CRHM INPUTS
# outflow [mm*km^2/int] = [l/int] (for m3 would have to divide by flow/1000)
# Fieldno. <- 9
# crhm.output <- read.table("c:\\Users\\User\\Documents\\WIP
#                          \\F9CRHM_output_nov25.csv",header=T,sep=" ",skip=0)
#
Fieldno. <- 7
crhm.output <- read.table("c:\\Users\\User\\Documents\\WIP
                          \\F7CRHM_output_nov25.csv",header=T,sep=" ",skip=0)
#
#force crackstat to 10 (restricted infiltration for the spring melt of 2009)
#for SWE>0 and month <5, make crackstat =10
#
crhm.output$crackstat <-
  ifelse(crhm.output$SWE>0&crhm.output$Year==2009&crhm.output$MM<5,
        10,
        crhm.output$crackstat)

```

```

# # #create date time string
crhm.output$date <- strptime(crhm.output[,1],crhm.output[,2],
                             crhm.output[,3],crhm.output[,4],0)
#change the flow units to mm/h from mm*km2/h
# #divide by the area in kilometers
this_field <- subset(areas,areas$Field==Fieldno.)
crhm.output$flow <- crhm.output$outflow/this_field$Area##[mm/h]
crhm.output$runoff.outflow <- crhm.output$runoutflow/this_field$Area ##[mm/h]

##extract relevant columns from the table
SWEts.sim <- crhm.output[,c("dd","mm","Year","date","SWE","flow",
                           "soilmoisture","runoff","outflow","runoutflow",
                           "runoff.outflow","meltrunoff","airtemp","soilrechr",
                           "actInfiltrate",
                           "Tsnow_1","zsnow","crackstat")]

#read in the snowchem, seasonal average
snowchem <- read.table("c:\\Users\\User\\Documents
                      \\WIP\\snowchem_averages_2014july16.csv",
                      header=T,sep=" ",skip=0)
#convert to mg/l from ug/l
snowchem[,3:10] <- snowchem[,3:10]/1000
#extract relevant columns from the table
snowchem.obs <- snowchem[,c("Year","Field","TDN","TDP","NO3NO2","NH4")]
snowchem.obs <- rename(snowchem.obs,c("TDN"="snow.TDN","TDP"="snow.TDP",
                                       "NO3NO2"="snow.NO3","NH4"="snow.NH4"))

#read in the fieldchem observations
fieldchem <- read.table("c:\\Users\\User\\Documents\\
                      WIP\\fieldchem_obs_2014july17.csv",header=T,sep=" ",skip=0)

#extract fieldchem for the relevant field

fieldchem.obs <-
  subset(fieldchem[,c("date","Field","TDN","TDP","NO3.NO2","NH4")],
         fieldchem$Field==Fieldno.)

#fieldchem.obs <- fieldchem[,c("date","Field","TDN","TDP","NO3.NO2","NH4")]
fieldchem.obs.melt <- melt(fieldchem.obs,
                          measure=c("TDN","TDP","NO3.NO2","NH4"),
                          variable.name="name",value.name="number",na.rm=F)

#load in the observed March SWE average depths and standard deviations
# the F7 and F9 fields were not surveyed and use the corresponding
# years from F4 and F3 respectively
swe.observed <-
  read.table("c:\\Users\\User\\Documents\\WIP\\SWEstddevs.txt",
            header=T,sep="\t",skip=0)
Peaksws.obs <- swe.observed[,c("Year","Field","SWE.mm.","SWE.mm.sd")]

#read in the soil file, this file was created with err columns in

```



```

# the MAIN soilsurveys.R analyses code
soil <- read.table("c:\\Users\\User\\Documents\\MScThesis\\data\\
                  soilsurvey_processed.csv",header=T,sep=",",skip=0)
#select depth that want soil measurements from
# for Olsen P: 0-5cm units are [mg/kg]
# for extrN: 0-15 cm units are kg/ha
soil5 <- subset(soil[,c("Field","Year","OlsenP","OlsenP.err")],soil$Depth=="0-2")
soil15 <- subset(soil[,c("Field","Year","extrN.kgha","extrN.kgha.err")],
                 soil$Depth=="0-6")
temp <- merge(soil5,soil15,by=c("Field","Year"))
#duplicate field 3 to make field 9 data
#duplicate field 4 to make field 7 data
#close field proximities and same treatment make this substitution viable
temp1 <- subset(temp,temp$Field==3)
temp1$Field <- 9
temp2 <- subset(temp,temp$Field==4)
temp2$Field <- 7

temp <- rbind(temp,temp1,temp2)
temp <- rename(temp,c("extrN.kgha"="extrN","extrN.kgha.err"="extrN.err"))

#change units of extrN [kg/ha] to [kg/km2]
#0.01ha/km2
#soil$extrN <- soil$extrN*100

#extract relevant columns from the data set
soil.obs <- temp[,c("OlsenP","extrN","Field","Year","extrN.err","OlsenP.err")]
rm("temp","temp1","temp2")

#read in the mass balance file
mb <- read.table("c:\\Users\\User\\Documents\\WIP
                 \\Ag_milestones_mass_balance(foragealfalfafix).csv",
                 header=T,sep=",",skip=0)
mb.user <- mb[,c("Field","Year","FtilpasTotal","CropName","Seedyer","Ag")]

#####
# run the main nutrient calculation file
runoffPN <-
  runoff_PN(SWEts.sim,Peaksw.e.obs,Fieldno.,snowchem.obs,fieldchem,
            fieldchem.obs.melt,soil.obs,mb.user,Version)

#main plots
plots(runoffPN,fieldchem,fieldchem.obs.melt,Fieldno.)

# calculate resulting loads
runoffPN <- load_chemograph(Fieldno.,runoffPN,Version,areas)

#plot the simulated and observed hydrographs
runoffPN <- simvsobs_hydrograph(areas,paper_plot_format,runoffPN,Fieldno.,Version)

#contributing fractions:csnow,csoil,cveg
#barplot
EOFchem_contributing_fractions(runoffPN,Fieldno.)
#####

```

```

#sensitivity to soil and snow changes
#####

#to perform a sensitivity analysis alternate what the input values are
hold <- soil.obs$OlsenP
soil.obs$OlsenP <- soil.obs$OlsenP-soil.obs$OlsenP.err
runoffPN.sensitivity <- runoff_PN(SWEts.sim,Peaksw.e.obs,Fieldno.,
                                snowchem.obs,fieldchem,fieldchem.obs.melt,
                                soil.obs,mb.user,Version)
runoffPN$eof.TDP.min <- runoffPN.sensitivity$eof.TDP

soil.obs$OlsenP <- hold+soil.obs$OlsenP.err
runoffPN.sensitivity <- runoff_PN(SWEts.sim,Peaksw.e.obs,Fieldno.,
                                snowchem.obs,fieldchem,fieldchem.obs.melt,
                                soil.obs,mb.user,Version)
runoffPN$eof.TDP.max <- runoffPN.sensitivity$eof.TDP

#check snow chemistry sensitivity
#need snowchem with std in observed chemistry
snowchem.sens <- read.table("c:\\Users\\User\\Documents
                          \\MScThesis\\data\\snow_oct14.csv",
                          header=T,sep=" ",skip=0)

#subset the wanted variables
snowchem.sens <- snowchem.sens[,c("Field","YEAR","N03N02","NH4","TDP")]
#convert from ug/L to mg/L
snowchem.sens <- data.frame(snowchem.sens[,1:2],snowchem.sens[,3:5]/1000)
snowchem.sens <-
  rename(snowchem.sens,c("YEAR"="Year","N03N02"="snow.N03",
                        "TDP"="snow.TDP","NH4"="snow.NH4"))

#find the mean and std dev
snowchem.sens.musigma <-
  aggregate(snowchem.sens[,c("snow.TDP","snow.N03","snow.NH4")],
            list(snowchem.sens$Year,snowchem.sens$Field),FUN=musigma)

#rename
snowchem.sens.musigma <- rename(snowchem.sens.musigma,
                              c("Group.1"="Year","Group.2"="Field"))
temp5 <- subset(snowchem.sens.musigma,snowchem.sens.musigma$Field<5)
temp5$Field[temp5$Field==4] <- 7
temp5$Field[temp5$Field==3] <- 9
snowchem.sens.musigma <- rbind(snowchem.sens.musigma,temp5)

#substitute snowchem, each of min, max and TDP, NH4, and N03
senssnow <- merge(snowchem.obs,data.frame(snowchem.sens.musigma[,1:2],
                                         snowchem.sens.musigma$snow.TDP[1],
                                         snowchem.sens.musigma$snow.TDP[2],
                                         snowchem.sens.musigma$snow.NH4[1],
                                         snowchem.sens.musigma$snow.NH4[2],
                                         snowchem.sens.musigma$snow.N03[1],
                                         snowchem.sens.musigma$snow.N03[2])
                ,by=c("Field","Year"))

#TDP snow avg-std dev
snowchem.obs$snow.TDP <-
  ifelse(senssnow[,7]-senssnow[,8]>=0,senssnow[,7]-senssnow[,8],0)

```

```

snowchem.obs$snow.NO3 <-
  ifelse(senssnow[,11]-senssnow[,12]>=0,senssnow[,11]-senssnow[,12],0)
snowchem.obs$snow.NH4 <-
  ifelse(senssnow[,9]-senssnow[,10]>=0,senssnow[,9]-senssnow[,10],0)
runoffPN.sensitivity <-
  runoff_PN(SWEts.sim,Peaksw.e.obs,Fieldno.,snowchem.obs,fieldchem,
            fieldchem.obs.melt,soil.obs,mb.user,Version)
runoffPN$eof.TDP.minsnow <- runoffPN.sensitivity$eof.TDP
runoffPN$eof.NO3.minsnow <- runoffPN.sensitivity$eof.NO3
runoffPN$eof.NH3NH4.minsnow <- runoffPN.sensitivity$eof.NH3NH4

#TDP snow avg+std dev
snowchem.obs$snow.TDP <- senssnow[,7]+senssnow[,8]
snowchem.obs$snow.NO3 <- senssnow[,11]+senssnow[,12]
snowchem.obs$snow.NH4 <- senssnow[,9]+senssnow[,10]
runoffPN.sensitivity <-
  runoff_PN(SWEts.sim,Peaksw.e.obs,Fieldno.,snowchem.obs,
            fieldchem,fieldchem.obs.melt,soil.obs,mb.user,Version)
runoffPN$eof.TDP.maxsnow <- runoffPN.sensitivity$eof.TDP
runoffPN$eof.NO3.maxsnow <- runoffPN.sensitivity$eof.NO3
runoffPN$eof.NH3NH4.maxsnow <- runoffPN.sensitivity$eof.NH3NH4
#NO3

# sensitivity plots
fieldchem <- subset(fieldchem,fieldchem$Field==Fieldno.)
sensitivity_plots(runoffPN,fieldchem,Fieldno.)

```

C.2.2 CVd.R

```

CVd <- function(x){
  # calculates coeff. of variation
  mu <- mean(x,na.rm=T)
  sigma <- sd(x,na.rm=T)

  results <- sigma/mu

  return(results)
}

```

C.2.3 musigma.R

```

musigma <- function(x){
  # calculates coeff. of variation
  mu <- mean(x,na.rm=T)
  sigma <- sd(x,na.rm=T)

  results <- c(mu,sigma)

  return(results)
}

```

C.2.4 EsseryPomeroy2004.R

```
EsseryPomeroy2004 <- function(SWE.bar,sigma.knot){
  # calculates the snow cover depletion curve for
  # homogenous melt conditions (i.e. the prairie)
  # taken from Essery and Pomeroy 2004
  # returns f, the fractional area retaining snow cover
  # inputs required are SWE.bar (the average SWE remaining) and
  # sigma.knot the pre-melt standard deviation in the snowpack SWE

  f <- tanh(1.26*(SWE.bar/sigma.knot))
  #SCD <- cbind(date,f)

  return(f)
}
```

C.2.5 strptime.date.R

```
strptime.date <- function(Year,month=3,day=15,hour=0,minute=0){
# this function takes 5 vectors of numbers and converts them to a date
# first a date string is created then a date with striptime format

datestring <- as.character(paste(Year,"-",month,"-",day," ",hour,":",
                                minute,sep=""))

#sstrptime creates a list format vector that can not be melted
date <- strptime(datestring,format="%Y-%m-%d %H:%M")

return(date)
}
```

C.2.6 runoff_PN.R

```
runoff_PN <- function(SWEts.sim,Peakswe.obs,Fieldno.,snowchem.obs,
                      fieldchem,fieldchem.obs.melt,soil.obs,mb.user,Version)
{
  # this functions operates all of the nutrient calculations and
  # communications with other functions
  #

# merge the data sets so that have an observed

# to get the melt runoff correct, we need to change the soil years + 1 year
# therefore extract the years 2007 to 2010 and change them to 2008 to 2011

soil.obs$Year <- soil.obs$Year+1

temp1 <- merge(merge(Peakswe.obs,soil.obs,by=c("Field","Year")),
              snowchem.obs,by=c("Field","Year"))
SWEts.sim$Field <- Fieldno.
runoffPN <- merge(SWEts.sim,temp1,by=c("Field","Year"))
```

```

#calculate the soil temperature in the upper soil horizon
  runoffPN$Tsoil <- soil_temperature(runoffPN$airtemp,runoffPN$zsnow)

# run the runoffPN function with the vectors created by merging the data

  runoffPN$f <- EsseryPomeroy2004(runoffPN$SWE,runoffPN$SWE.mm.sd)

# run the deltaTDP function using soil test phosphorous, Olsen P to get
# the absolute change
  runoffPN$deltaTDP.ponded.conc <- Amarawansha2013(runoffPN$OlsenP)

# add a spring nitrate flux component for disturbed grasslands and
# general fall tillage
  temp4 <- mb.user$Year-mb.user$Seedyyear
  mb.user$consecutive.years <-
    c(0,temp4[1:9],0,temp4[11:19],0,temp4[21:28],0,temp4[30:37],0,temp4[39:47],0,
      temp4[49:57])

# return soil temperature
  #runoffPN$Tsoil <- soil_temperature(runoffPN$airtemp,runoffPN$zsnow)

# calculate snow covered days with soiltemperature above -5C
  max_subnivean_nitrifying_days <-
    calculate_max_subnivean_nitrification_days(runoffPN$dd,runoffPN$mm,
                                              runoffPN$Year,runoffPN$SWE,
                                              runoffPN$Tsoil)

# calculate the flux related to the mineralization - nitrification activity
# in the soils when the temperature is above -5C
# grassland.disturbance [kg.km2]
  #mb.user$grassland.disturbance <-
# grassland_disturbance(mb.user$Field,mb.user$Year,mb.user$FtilpasTotal,
# mb.user$consecutive.years,max_subnivean_nitrifying_days)
#
#function returns two columns:
# col[1] related to nitrification
# col[2] mineralization
  grassland.disturbance <-
  grassland_disturbance(mb.user$Field,mb.user$Year,mb.user$FtilpasTotal,
                        mb.user$consecutive.years,max_subnivean_nitrifying_days)
  mb.user$grassland.disturbance.nitrification <- grassland.disturbance[,1]
  mb.user$grassland.disturbance.mineralization <- grassland.disturbance[,2]

# calculate the concentration of the meltwater runoff,
# based on Stein et al (1986)
  Stein.CFs <-
    Stein_etal_1986(runoffPN$Year,runoffPN$mm,runoffPN$dd,runoffPN$date,
                    runoffPN$snow.NO3,runoffPN$snow.NH4,runoffPN$snow.TDP,
                    runoffPN$SWE,runoffPN$SWE.mm.,runoffPN$f,runoffPN$meltrunoff)
  runoffPN$snowNO3.cf <- Stein.CFs$NO3.cfs
  runoffPN$snowNH4.cf <- Stein.CFs$NH4.cfs
  runoffPN$snowTDP.cf <- Stein.CFs$TDP.cfs

#return an array with 3 columns, [1]nitrate, [2]ammonium, [3]phosphate

```

```

# do I need this?
# mb.user$tillage_accessibility_factor <- ifelse(FtilpasTotal<0.6,3,0)

#rainfall chemistry
#returned in a vector TDP,N03,NH4
rain <- rainfall_chem()

#add two columns, one for N stoichiometric adjustment relative to ryegrass and
#one for P stoichiometric adjustment relative to ryegrass

#calculate NH4 concentrations using f and the following major contributors
#contributors to eof.NH4:
# 1)snow NH4 (deposition component)
# 2)snow NH4 - from vegetation leachate
#use zero till as the base (stubble), and
#add surcharge for forage and winter wheat crops for future calculations
#taken from field survey measurements at this time (both dep and leachate in
#one number)
#need to know the error associated with this measurement
# 3)during snowmelt, additional NH3 contributed from vegetation leachate
#calculated this number based on Elliott(2012)
#need to verify that there was freeze thaw cycling and the extent of it(CRHM)
#using CRHM hru_t, based calculated on bare ground fall FTCs
#this number will be used to scale the constants taken from Elliott(2012) which
#was based on 3 diurnal FTCs prior to melt to Bechmann2005 curve
# 4)the soil is a sink for NH3 leachate, so once meltwater interacts
# with the soil, the NH3 contributions from vegetation are moderated slightly
# the numbers used for this are based on Jane Elliott's (2012) work
# 5-N/A)juicy greens, new crop plantings are subject to elevated leachate
# contributions where is the evidence for this? NOT DONE CURRENTLY
# 6-N/A)based on lo moisture (20%) on F10 in 2006 and high NH4 in runoff,
# is there a relationship between low soil moisture and NH3 release? NO
# 7-N/A)what about fall NH4 application, does it correspond? [NOT APPARENT]

#the leaching values in the Bechmann curve were performed on rye grasses
#therefore this values need to be adjusted by the NP stoichiometry in the
#crops on these fields
#Pcontent this crop / P content ryegrass
#N content this crop / N content ryegrass

crop <- subset(mb.user$CropName, mb.user$Field==Fieldno.&(
  mb.user$Year>=min(SWEts.sim$Year-1)&
  mb.user$Year<max(SWEts.sim$Year)))
Year <- c(min(SWEts.sim$Year):max(SWEts.sim$Year))

crops.grown <- data.frame(Year,crop)

#fall.FTCs returns BechmannFTCs,vegleachedP,vegleachedNH,soilleachedN03

```

```

#therefore, freeze thaw cycling adding to N03 flux is taken care of here
#freeze_thaw_cycles returns values based on forage / catch cropping
#these values need to be adjusted accordingly (merge with mb.user first)

fall.FTCs <- freeze_thaw_cycles(SWEts.sim,crops.grown)
fall.FTCs$Field <- Fieldno.

#this merge drops all fields and years will not be represented in fall.FTCs when
#the command all.x is changed to FALSE (make a decision on preference here)

#run a .temp merge to adjust Bechmann values as discussed above

mb.user.temp <- merge(mb.user,fall.FTCs,by=c("Field","Year"),all.x=F)

#adjustment to Bechman based on Fall tillage
mb.user.temp$adjustment.to.Bechmann <- ifelse(mb.user.temp$Ag=="forage",
1,
ifelse(mb.user.temp$FtilpasTotal>0.48 &
mb.user.temp$Ag=="annual crop",
mb.user.temp$FtilpasTotal,
ifelse(mb.user.temp$FtilpasTotal<=0.48,
0,
1)))

fall.FTCs[,c("vegleachedP","vegleachedP.soilcontact","vegleachedNH",
"vegleachedNH.soilcontact","vegleachedN03")] <-
fall.FTCs[,c("vegleachedP","vegleachedP.soilcontact","vegleachedNH",
"vegleachedNH.soilcontact","vegleachedN03")]*
mb.user.temp$adjustment.to.Bechmann

rm(list=c("mb.user.temp"))

mb.user <- merge(mb.user,fall.FTCs,by=c("Field","Year"),all.x=T)

#N03 will leach from SOIL, NH requires the presence of vegetation!, different
#source, same cause

#add a vegetation leaching factor to EOF flow, try Jane's numbers
#more simply use tillage as an indicator of vegetation, years that there was
#fall tillage
#would indicate stubble or winter crops, year without fall tillage the opposite
#
#
runoffPN <- merge(runoffPN,mb.user,by=c("Field","Year"))

#not USED: leachateP.rate <- 0.40 #mg/l ##perhaps remove this somewhat
#arbitrary value?
juicy.greensP <- 0.25 #mg/l

```

```

juicy.greensN <- 0.75#mg/l

runoffPN$new.or.established <- ifelse(runoffPN$Year-1==runoffPN$Seedyar,1,0)

runoffPN$veg.leachateP <- ifelse(runoffPN$FtilpasTotal>0.48,
                                runoffPN$vegleachedP.soilcontact +
                                juicy.greensP*runoffPN$new.or.established
                                ,0)

runoffPN$veg.leachateP.nosoil <- ifelse(runoffPN$FtilpasTotal>0.48,
                                         runoffPN$vegleachedP +
                                         juicy.greensP*runoffPN$new.or.established
                                         ,0)

#calculate EOF TDP concentration using the f and deltaTDP.ponded.conc
#
runoffPN$eof.TDP <-
  ifelse(runoffPN$meltrunoff>0,
    ifelse(runoffPN$crackstat>=10,
      runoffPN$snowTDP.cf+runoffPN$veg.leachateP.nosoil*runoffPN$f,
      ifelse(runoffPN$f>0&runoffPN$crackstat<10,
        ((runoffPN$snowTDP.cf*runoffPN$flow +
          runoffPN$f*
          (runoffPN$deltaTDP.ponded.conc+runoffPN$veg.leachateP)*
          runoffPN$flow)/runoffPN$flow),
          runoffPN$snowTDP.cf)),
    ifelse(runoffPN$outflow>0,
      (runoffPN$deltaTDP.ponded.conc*runoffPN$flow+rain[1]*
        runoffPN$flow)/runoffPN$flow,
      NA))

#version 3
# note that research has found the concentrations of nitrate rimming the
# ice to be similar to that of the bulk, even though some exclusion does
# occur it appears not to increase the concentration of the remaining unfrozen
# soil water moisture in the recharge layer, a 100mm surface layer in the soil
# with a 50% void ratio and capacity of 50mm of water (mm3/mm2)

#only want top 1 cm of the soil which is easily depleted or flushed
#we don't have data for the top 2" / 5 cm of soil
#but we do for years 2005-2007
#the summary for fields F3,4,10,11 0-2"S0ilN/0-6" S0il N
# Min. 1st Qu.  Median    Mean 3rd Qu.  Max.
# 0.4058 0.4506 0.5367 0.5523 0.5969 0.8033
#Summary for fields F3 and F4 0-2"S0ilN/0-6" S0il N
# Min. 1st Qu.  Median    Mean 3rd Qu.  Max.
# 0.4058 0.4294 0.4931 0.5645 0.7107 0.8033
#can mimic 0-2" horizon by multiplying the 0-6" values by 0.55

```



```

#if this is run, the numbers are way too high, again, add 0.2 multiplier
runoffPN$csoilN03 <- 0.2*((0.55*runoffPN$extrN*100)/
                    ifelse(runoffPN$soilrechr>25,25,runoffPN$soilrechr))
#nitrate exlusion
#runoffPN$csoilN03 <- 0.2*(runoffPN$extrN*100*0.55)/(5*10/10)
# [kg/km2]/[mm] = [mg/l]
runoffPN$csoilN03.max <- 0.2*((0.55*(runoffPN$extrN+runoffPN$extrN.err)*100)/
                    ifelse(runoffPN$soilrechr>25,
                            25,
                            runoffPN$soilrechr))
runoffPN$csoilN03.min <- 0.2*((0.55*(runoffPN$extrN-runoffPN$extrN.err)*100)/
                    ifelse(runoffPN$soilrechr>25,
                            25,
                            runoffPN$soilrechr))

#CREAMS calculation for concentrations of N03 in the runoff
runoffPN$actInfiltrate[is.na(runoffPN$actInfiltrate)] <- 0
temp.infil <- ddply(runoffPN[,c("Year","actInfiltrate")],.(Year),
                    transform,cumInfil=cumsum(actInfiltrate))
runoffPN$cumInfil <- temp.infil$cumInfil

k1 <- 1
k <- .001

temp <- runoffPN[,c("csoilN03","csoilN03.min","csoilN03.max")]

runoffPN$CREAMSI160 <- temp*0

runoffPN$CREAMSI160 <- rename(runoffPN$CREAMSI160,
                             c("csoilN03"="avg","csoilN03.min"="min",
                               "csoilN03.max"="max"))

for (i in 1:3){

runoffPN$CREAMSI160[i] <-
  ifelse(runoffPN$meltrunoff>0,
        (temp[,i]-runoffPN$snowN03.cf)*exp(-k*runoffPN$cumInfil)+
        runoffPN$snowN03.cf,
        ifelse(runoffPN$flow>0,
              (temp[,i]-rain[2])*exp(-k*runoffPN$cumInfil)+rain[2],
              temp[,i]))
i <- i+1
}

# In conversation with Jane Elliot (Nov 18) we discussed the depth of plowing
# to break up perennial crops, 6 inch depth was deemed appropriate for this

```

```

# activity
# a 4" depth more appropriate for regular fall and pre-seeding tillage
# activities
# 6" = 150mm depth
# output [mg/l]
runoffPN$grassland.disturbance.nitrification <-
(runoffPN$grassland.disturbance.nitrification/
  (runoffPN$soilrechr+ifelse(runoffPN$soilmoisture>25,25,runoffPN$soilmoisture)))
  #[kg/km2]/[mm]=[mg/l]

#alternatively, 10% of the usual nitrification didn't complete,
# leaving available NH3 easily transported
# when there is a basal ice layer.
runoffPN$grassland.disturbance.mineralization <-
runoffPN$grassland.disturbance.nitrification*0.10

#there is a problem here with the ice lens, I suspect that it exists prior
# to the start of the melt, but CRHM does not model its existence until a
# chunk of the melt has progresses (too late in my mind)

runoffPN$eof.NO3 <- runoffPN$CREAMSI160*0

for (i in 1:3){

runoffPN$eof.NO3[,i] <-
  ifelse(runoffPN$meltrunoff>0,
    ifelse(runoffPN$crackstat>=10,
      runoffPN$snowNO3.cf+runoffPN$vegleachedNO3,
      ifelse(runoffPN$f>0&runoffPN$crackstat<10,
        runoffPN$snowNO3.cf+
          (runoffPN$CREAMSI160[,i]+
            runoffPN$vegleachedNO3+
            runoffPN$grassland.disturbance.nitrification)*
            runoffPN$f,
            runoffPN$snowNO3.cf+runoffPN$CREAMSI160[,i])),
    ifelse(runoffPN$outflow>0,
      (rain[2]+runoffPN$CREAMSI160[,i]),
      NA))

  i <- i+1
}

##DIAGNOSTIC PLOTS
#####REMOVED#####

```

```

runoffPN$dateM <-
  strptime(as.character(runoffPN$date,format="%m-%d %H:%M"),
           format="%m-%d %H:%M")

#by putting back the 0.33, we are in a way asserting there is less
#soil interaction with ammonium than P, or at least the soil is
#not moderating the NH3 runoff like it does with P
#according to Jane Elliott (2012) it should be 0.72

runoffPN$eof.NH3NH4 <-
  ifelse(runoffPN$meltrunoff>0,
        ifelse(runoffPN$crackstat>=10,
              runoffPN$snowNH4.cf+
              (runoffPN$vegleachedNH+
               runoffPN$grassland.disturbance.mineralization)*runoffPN$f,
            ifelse(runoffPN$f>0&runoffPN$crackstat<10,
                  (runoffPN$snowNH4.cf*runoffPN$flow+(runoffPN$f*
                  (runoffPN$vegleachedNH.soilcontact+
                   juicy.greensN*runoffPN$new.or.established)*
                   runoffPN$flow))/runoffPN$flow,
                  runoffPN$snowNH4.cf)),
        ifelse(runoffPN$outflow>0,
              rain[3],
              NA))

#####

runoffPN$mm <- as.numeric(as.character(runoffPN$date,format="%m"))
runoffPN$dd<- as.numeric(as.character(runoffPN$date,format="%d"))
runoffPN$HH <- as.numeric(as.character(runoffPN$date,format="%H"))
#

temp <- data.frame(runoffPN[,1:58],runoffPN[,61:69],
                  runoffPN$eof.NO3[1],runoffPN$eof.NO3[2],runoffPN$eof.NO3[3],
                  runoffPN$CREAMSI160[1],runoffPN$CREAMSI160[2],
                  runoffPN$CREAMSI160[3])
temp <- rename(temp,c("avg"="eof.NO3","min"="eof.NO3.min","max"="eof.NO3.max",
                    "avg.1"="CREAMSI160","min.1"="CREAMSI160.min",
                    "max.1"="CREAMSI160.max"))

return(temp)
}

```

C.2.7 Amarawansha2013.R

```

Amarawansha2013 <- function(OlsenP){
  # calculates the absolute change in surface water
  # DRP based on Olsen P (not a good predictor)
  # taken from Amarawansha(2013) MSc work with Don Flaten

```

```

# there are stronger predictors (DPS and WEP for example)
# this was done at summer water temperatures, not spring temperatures
# spring rates of DRP release would likely be lessened.
# returns the absolute change

delta.abs <- 0.14*-1 + 0.035*OlsenP

return(delta.abs)
}

```

C.2.8 new_concentration.R

```

new_concentration <- function(pool,vol){
  #this is the HYPE code notation
  #pool| soil pool [kg/km2]
  #vol | volume [mm]
  #conc| concentration [mg/l]
  #
  #it is used in at this point to
  #take extraN03N in kg/km2 and soil moisture[mm] and calculate
  #the concentration of N03[mg/l] in the soil water, we can only guess at NH4 at this point
  #but won't do that here
  #in hype this is equivalent to csoilij(i,j,i_on)

  conc <- ifelse(vol>0,pool/vol,0)

  #csoilN03 <- extraN03N/soilmoisture
  return(conc)
}

```

C.2.9 grassland_disturbance.R

```

grassland_disturbance <-
function(Field,Year,FtilpasTotal,consecutive.years,N03days)
{

#mineralization --> nitrification flux with fall breakup of perennial forages
# / grassland
#Campbell et al (2005) paper "Winter in northeastern North America:
# a critical persion for ecological processes"
# found that 0.6 N/m2 was the Dec-Mar nitrification rate (Groffman et al. 2001)
# need Nov through March so used 0.5 +/- 0.3 g/m2 for mineral soil at a
# depth to 10 cm for 4 months.
# assuming a 5 month snow covered season in Manitoba
# 0.5*5/4=0.625 g/m2 <- 625 +/- 300 kg/km2

#adjust the mineralization rate of 0.9 g N/m2 similarly
#0.75 +/- g/m2 for mineral soil, 5 month winter 0.75*5/4=0.94 +/- kg/km2

# this rate should be sensitive to environmental changes,
# i.e. warmer winter temperatures would increase

```

```

# the nitrification rate
# colder soil temperatures (i.e. < 5C might cause this activity to cease)
# according to references in Table 1 in
# Campbell et al (2005)

#121 is the number of days in Dec through March,
# the days used to calculate 0.5 g/m2
N03days$max_nitrification_rate <- (N03days$days/121*0.8)*1000 #kg/km2
N03days$max_mineralization_rate <- (N03days$days/121*0.9)*1000 #kg/km2

#binary, if tillage of perennial crops applies, then 1, else 0
#grassland.disturbance <- ifelse(FtilpasTotal<0.6&consecutive.years>2,1,0)

#instead of binary: if tillage of perennial crops applies, then 1,
#else if just AT tillage
#multiply by the 1-FtilpasTotal

grassland.disturbance <- ifelse(FtilpasTotal<0.6&consecutive.years>2,
                                1,
                                ifelse(FtilpasTotal<1.0&consecutive.years<=2,
                                        1-FtilpasTotal,
                                        0))

N03days <- rename(N03days,c("farming.Year"="Year"))
temp <- merge(data.frame(grassland.disturbance,Field,Year),
              N03days,by=c("Year"),all.x=T)

index <- order(temp$Field,temp$Year)

temp <- temp[index,]

nitrification <- ifelse(is.na(temp$max_nitrification_rate),
                        temp$grassland.disturbance,
                        temp$grassland.disturbance*
                        temp$max_nitrification_rate)

mineralization <- ifelse(is.na(temp$max_mineralization_rate),
                          temp$grassland.disturbance,
                          temp$grassland.disturbance*
                          temp$max_mineralization_rate)

results <- data.frame(nitrification,mineralization)

rm("temp")

return(results)
}

```

C.2.10 freeze_thaw_cycles.R

```

freeze_thaw_cycles <- function(temp.df,crops.grown){

```

```

#source("c:\\Users\\User\\Documents\\WIP\\
#MY_MODEL\\Version2\\Bechmann2005_TDPcurve.R")

#this function calculates the number of freeze thaw cycles that
#occur in the fall of a given year
#the fall freeze thaw cycle (FTC) counts contribute to spring release of
#leached P & N

#there are two sources of P and N during FTCs: from vegetation release and soil
#(microbes and roots cellular lysis)
#nitrate released from vegetation is small compared to that released from soils
#(Elliott2012;Joseph2008)
#nitrate release from vegetation is on the same scale as that of P (Miller1994)
#ammonium release is about 25% of the magnitude of P and N (Miller1994) but
#is buffered by the soil (Elliott2012)
#
#large FTC amplitudes (>10C) are associated with enhanced nutrient release
#with repeated FTCs up to the point of all the biomass P & N
#in the vegetation (Bechmann2005)
#small amplitude FTCs seem to consistently release P & N (Joseph2008)

temp.df <- temp.df[,c("dd","mm","Year","airtemp","SWE")]

#extract a vector of the unique years simulated in the data frame
#years <- unique(temp.df$Year)[not needed use, count command instead]

#FTCs have the most effect on soil & veg P+N leaching
#when the soil is bare (Joseph&Henry2008) and the vegetation is growing
#therefore, count FTCs when there is no snow and in the fall
#before veg has gone dormant for the winter
#a freeze thaw cycle is considered to have an impact on cellular
#structure of the vegetation when the cycle spans, 10C with a low
#of at least -2C (at a minimum)
#large FTC cycle amplitudes (>10C) for enhanced nutrient release with
#repeated FTCs

temp.df <- subset(temp.df,temp.df$SWE==0&(temp.df$mm>8&temp.df$mm<12))
temp1 <- aggregate(temp.df$airtemp,by=list(temp.df$dd,temp.df$mm,temp.df$Year),
FUN=max)
temp1 <- rename(temp1,c("x" = "max"))
temp2 <- aggregate(temp.df$airtemp,by=list(temp.df$dd,temp.df$mm,temp.df$Year),
FUN=min)
temp2 <- rename(temp2,c("x" = "min"))
temp3 <- cbind(temp2,temp1$max)
temp3 <-
  rename(temp3,c("Group.1"="dd", "Group.2"="mm", "Group.3"="Year",
    "temp1$max" = "max"))

temp3$diff <- temp3$max-temp3$min

#using a daily temp fluctuation from -2 min and greater than 10C amplitude
temp4 <- subset(temp3,temp3$min<(-2)&temp3$diff>10)

```

```

fall.FTCs <- count(temp4,vars="Year")
fall.FTCs <- rename(fall.FTCs,c("Year"="fall","freq"="FTCs"))

#based on the theory of Bechmann 2005, needs to be revised if theory changes
#fall.FTCs$BechmannFTCs <- ifelse(fall.FTCs$FTCs>8,8,fall.FTCs$FTCs)

#the spring affected is the year after the fall, year + 1
fall.FTCs$Year <- fall.FTCs$fall+1

#just looking at plots of the N data and P data from 2010 and other years
#specifically F3 and F9, the P release is 1.0 to 1.5 ppm (use an average 1.25 ppm)
#larger than the previous year
#from vegetation for N, it'd be equivalent to P
#loss from soils for NO3 due to FTC would be different
#the 2010 year is the 100% year because the FTC exceeded 8
#everything is scaled off the 1.29 ppm P release from forage crops

# to convert mg/g to a concentration (observed 9.7 +/- 1.6 mg/l)
# Ulen1997 found only 0.5g/kg (mg/g) of total P in the vegetation,
# a fraction of that obs in lab by Bechmann
# Bechman Watson and Berk soil P levels ~100 mg/kg while the
# STC fields are about 20mg/kg or less
P.FTCs.release.max <- 0.97 #reported = 1 just didn't want to change
                        #all the plots #mg/l

#used Bechmann2005_TDPcurve to get the percentage surcharge for the FTCs

Bechmann.percentage <- (Bechmann2005_TDPcurve(fall.FTCs$FTCs))/100

#according to elliot2012, the soil moderated values
#need to be increased to reflect just residue leaching
#Table 4. 0.53/1.58 soil/residue for TDP = 0.33
#Table 4. 0.42/0.58 soil/residue for NH3 = 0.72
#Table 4. 4.03/0.34 soil/residue for NO3 = 11.8 (1/11.8=0.084)

fall.FTCs$vegleachedP <- Bechmann.percentage*P.FTCs.release.max*1.58
fall.FTCs$vegleachedP.soilcontact <- Bechmann.percentage*P.FTCs.release.max*0.33
#.27 multiplier taken from Elliott(2012) Table 4. NH3/TDP in residue
# but because assumed soil contact used Table 4. NH3/TDP in soil
fall.FTCs$vegleachedNH <- Bechmann.percentage*P.FTCs.release.max*.37
fall.FTCs$vegleachedNH.soilcontact <- Bechmann.percentage*P.FTCs.release.max*.27

#leached Nitrate is small compared to that from soil, therefore use Elliott(2012)
#to set NO3 values used Table 4 residue, active, combined samples to scale
#0.34/4.03=0.084 for NO3
#these numbers are higher than Jane's b/c of the use of forages and Miller(1994)
#where NO3 and P releases were found to be on the same order of magnitude
#initial runs showed that these values are just too high, perhaps
#not the full soil contact, experiments were not the same as field runoff
fall.FTCs$vegleachedNO3 <- (Bechmann.percentage*(P.FTCs.release.max*0.22))
                        #changed from (P.FTCs.release.max/0.084

```

```

fall.FTCs$vegleachedN03.soilcontact <-
  (Bechmann.percentage*(P.FTCs.release.max*2.55))

#add a vegleachedN03 as well (same as the P leached)
#fall.FTCs$vegleachedN03 <- (Bechmann.percentage*P.FTCs.release.max)

#according to Elliott(2012) the ammonia vegetation leached # is
#moderated by the soil, but this # is quite volatile and difficult
#to quantify, in addition to the fact,
#the NH4 loss from the soil pool during runoff is quite
#inconsequential (conversation with Don Flaten Sep 2014)

rm(list=c("temp.df","temp1","temp2","temp3"))

#current leaching estimates were made for rye grass
#rates adjusted for other crop types relative to the stoichiometry of rye grass
NP.stoichiometry <- NP_stoichiometry()

crops.merged <- merge(crops.grown,NP.stoichiometry,by=c("crop"))
order_index <- order(crops.merged$Year)
crops.merged <- crops.merged[order_index,]

#multiply the vegleachate values by the adjusted stoichiometric
#/ P&N crop content values

fall.FTCs$vegleachedP <- fall.FTCs$vegleachedP*crops.merged$P
fall.FTCs$vegleachedNH <- fall.FTCs$vegleachedNH*crops.merged$N
fall.FTCs$vegleachedP.soilcontact <-
  fall.FTCs$vegleachedP.soilcontact*crops.merged$P
fall.FTCs$vegleachedNH.soilcontact <-
  fall.FTCs$vegleachedNH.soilcontact*crops.merged$N
fall.FTCs$vegleachedN03 <- fall.FTCs$vegleachedN03*crops.merged$P
fall.FTCs$vegleachedN03.soilcontact <-
  fall.FTCs$vegleachedN03.soilcontact*crops.merged$N

#didn't do the nitrate value at this point

return(fall.FTCs) #this is a 7 column df of years,fall FTCs for
                  #each year and leached P,NH,N03 and soilN03
}

```

C.2.11 Bechmann2005_TDPcurve.R

```

Bechmann2005_TDPcurve <- function(FTCs.input){

  WEP <- c(0,2.6,3.75,5.2,6.1,6.25)

  #according to unpublised Lilbaek thesis, there is always contact with the
  #soil even under basal ice conditions

```



```

#this available WEP is adjusted, why, what was the theory here?
#WEP <- WEP*0.33

FTCs <- c(0,1,2,4,6,8)
#the Miller(1994) work found that N03 losses were on the same scale and
#trends as P, whereas NH4 was a small percent of that (estimated here as ~25%)
#the Bechmann study was based on forages, these have higher N:P ratios than
#cereal and oilseed crops, and the WEP numbers need to be adjusted for that
#the Bechmann numbers are to be understand as maximums because cold hardy plants
#would not be a susceptible to FTCs frost damage (Miller1994)

percentWEP <- (WEP/max(WEP))*100

Bechmann.curve <- data.frame(WEP,FTCs,percentWEP)

#Redfield ratio puts N:P ratios at 16:1
#studies of plant matter(Sadras2006) show 6:1 for cereals and oilseeds
#and 9:1 for forage/legume
#especially for forages, this can be found as high as 16:1 (Fystro)

FTCs.input.percentage <-
  approx(x=Bechmann.curve$FTCs,y=Bechmann.curve$percentWEP,
        xout=FTCs.input,rule=1:2,ties=mean)

return(FTCs.input.percentage$y)
}

```

C.2.12 NP_stoichiometry.R

```

NP_stoichiometry <- function(){

#####
#N:P stoichiometry of various crops
#the stoichiometry will be used to set leaching rates
#current leaching is based on rye grass
#multipliers will be set from rye grass
#####
#N(CFI2001

#crop      N:P  source      P205  rem #s)
#rye grass  (7.4) 7.9  Figure 1 (Wilman1994), grassCFI2001  27    92
#winter wheat  5.3  CFI2001      23    47
#spring wheat  6.0  CFI2001      21    54
#forage       8.5  grass / clover from CFI2001      38.5  143
#alfalfa      9.2  PPI2002 (8.65) / CFI2001 9.78) average  62    261
#Barley       5.4  CFI2001      30    70
#Canola       4.8  PPI2002      33    61
#flax/linola  7.6  CFI2001      14    46
#Green Feed Oats 5.6  CFI2001 (oats)      23    55
#Oats        5.6  CFI2001      23    55
#Alfalfa/timothy 9.4  CFI2001 60-40 alfalfa/grass      48    193.4

```

```

crop <- c("Rye Grass","Winter Wheat","Wheat","Forage","Alfalfa",
         "Barley","Canola","Flax/Linola","Green Feed Oats","Oats",
         "Alfalfa/Timothy")

NtoP <- c(7.4,5.3,6.0,8.5,9.2,5.4,4.8,7.6,5.6,5.6,9.4)

#at this time, FTCs are related back to ryegrass
P <- c(27,23,21,38.5,62,30,33,14,23,23,48)
P <- P/P[1]

N <- c(92,47,54,143,261,70,61,46,55,55,193)
N <- N/N[1]

NPstoich <- data.frame(crop,NtoP,N,P)
return(NPstoich)
}

```

C.2.13 calculate_csoilNO3.R

```

calculate_csoilNO3 <-
  function(soilrechr,extrN,mobile.water,theta.e = 0.5,SSA=140,Tsoil=270)
  {
    #This function is taken from SWAT. The soil water NO3 content is
    #calculated and then load removed from the soil NO3 is calculated
    #by multiplying surface runoff volume x csoilNO3
    #the units used in SWAT are not quite these ones (see SWAT,page269)

    #csoilNO3 = concentration of NO3 in soilwater [mg/l] [kg/mm]
    #extrN = soilNO3-N [kg/km2] , [kg/ha]
    #mobile.water = surface runoff + infiltrate [mm]
    #SATwater = saturated water content of the soil [mm] subject
    #to change during frozen and unfrozen conditions
    #theta.e = fraction of porosity from which anions are excluded

    SATwater <- soil_freezing_characteristic(SSA,Tsoil)*soilrechr

    csoilNO3 <- (extrN*(1-exp(-mobile.water/((1-theta.e)*SATwater))))
      /mobile.water #[kg/mm]

    #change to mg/mm
    csoilNO3 <- csoilNO3 * 1e6 #[mg/mm]

    return(csoilNO3)
  }

```

C.2.14 soil_temperature.R

```

soil_temperature <- function(Tair,dSNOW){
  #this is taken from the HYPE model for Tsoil(t)
  # ref: soil_proc.f90 calculate_soiltemp & subroutine:
  # calculate_weighted_temperature

```

```

# constants with given values for Swedish conditions
# CRHM produces a variable z_s the total snowcover depth in [m]
# CRHM produces T_s_l which is the temperature [celsius] of the
# lower layer in the snowpack

cSOILMEM <- 30 #[d] soil temperature memory
cSPFROST <- 10 #[d/cm] soil temperature snow dependence
cTDEEP <- 5 #[celsius] deep soil temperature
cWDEEP <- .001 #[-] deep soil temperature weight
timesteps_per_day <- 24 #HYPE is daily time step model, CRHM produces hourly data
#Tair #[celsius] air temperature

Tsoil_prev <- 5 #[C] just set an initial soil temperature based on the
#          air temperature

# Tsoil is the soil temperature in celsius
# dSNOW #[cm] snow depth
Tsoil <- rep(0,length(Tair))

for (i in 1:length(Tair)){
  Tsoil[i] <-
    Tsoil_prev*(1-1/((cSOILMEM+cSPFROST*dSNOW[i])*timesteps_per_day)-cWDEEP)+
    Tair[i]*(1/((cSOILMEM+cSPFROST*dSNOW[i])*timesteps_per_day))+cTDEEP*cWDEEP
  Tsoil_prev <- Tsoil[i]
  i <- i+1
}

return(Tsoil)
}

```

C.2.15 calculate_max_subnivean_nitrification_days.R

```

calculate_max_subnivean_nitrification_days<- function(dd,mm,Year,SWE,Tsoil){
  # the input data.frame (df) needed to have
  # dd,mm,Year,SWE,Tsoil
  #this function calculates the number of snow covered days where
  #the soil temperature was at or above -5°C
  #provides this count for each winter season
  #number used in spring runoff calculation

  #df <- runoffPN[,c("dd","mm","Year","SWE","Tsoil")]
  df <- data.frame(dd,mm,Year,SWE,Tsoil)

  df <- aggregate(df[,c("Tsoil","SWE")],by=list(df$dd,df$mm,df$Year),FUN=mean)
  df <- rename(df,c("Group.1"="dd","Group.2"="mm","Group.3"="Year"))

  df$farming.Year <- rep(0,dim(df)[1])
  for (i in 1:dim(df)[1]){
    df$farming.Year[i] <- ifelse(df$mm[i]>8&df$mm[i]<=12,
                                df$Year[i]+1,
                                df$Year[i])

    i <- i+1
  }
}

```

```

#subset with the days after September and before the disappearance of snow
#where the soil temperature was above -5C
temp <- subset(df,((df$SWE>0&df$mm<=5)|(df$mm>9))&df$Tsoil>=-5)

temp <- subset(df,df$SWE>0&df$Tsoil>=-5) #superceded

max_days_active <- count(temp,vars="farming.Year")
max_days_active <- rename(max_days_active,c("freq"="days"))

return(max_days_active)
}

```

C.2.16 Stein_etal_1986.R

```

Stein_etal_1986 <- function(Year,mm,dd,date,snow.NO3,snow.NH4,snow.TDP,
SWE,SWE.mm.,f,meltrunoff)
{

#Lilbaek 2008 Compositional change of meltwater rejigged the
#terminology of the Stein et al (1986) paper
#(p 69 Equation 5.7 in her thesis)
# RESOLVED TO use Stein et als original calculations
#   Year Field   SWE.mm. SWE.mm.sd
#   17 2008      7  86.80583  81.74180
#   18 2009      7 113.11667  72.02026
#   19 2010      7  92.82417  86.15372
#   20 2011      7  76.97667  64.75321
#   21 2012      7  22.18000  16.35476

#SWE
#2008  86.80583
#2009 113.11667
#2010  92.82417
#2011  76.97667
#2012  22.18000

df <- data.frame(Year,mm,dd,date,snow.NO3,snow.NH4,snow.TDP,SWE,SWE.mm.,
f,meltrunoff)

first.year <- min(df$Year)
last.year <- max(df$Year)

Year <- c(first.year:last.year)
melt.duration.hrs <- c(NA,192,179,48)
melt.duration.secs <- melt.duration.hrs*3600
SWE.melt <- c(NA,68.3079,58.6001,11.95)

M.bar <- SWE.melt / melt.duration.hrs
#average event melt rate [mm] / [s] = [mm/s]

df <- merge(df,data.frame(Year,M.bar,SWE.melt),by=c("Year"),all.x=T)

```

```

k <- .002 #??a leaching coefficient to which the calculation is very sensitive
      #to, what is the value?
      #likely K falls between .001 and .002

# because charges are neutral or +/- 1, eq/ha = mol/ha
# units of the snow chem data are in mg/l
# mmol/L = mg/L / (gram formula weight)
# meq/L/(charge of ion) = mmol/L

# calculate molar mass (gram formula weight) of NH3, NO3, and HNO3

N <- 14.00674
H <- 1.00794
O <- 15.9994
P <- 30.97376

NO3 <- N+O*3 #[g/mol]
NO3charge <- -1

NH4 <- N+H*4 #[g/mol]
NH4charge <- 1

PO43 <- P+4*O #[g/mol]
PO43charge <- -3

cmeltNO3_o <- df$snow.NO3/NO3*abs(NO3charge)*1e3
  # [ueq/L] bulk, average snowpack concentration of ion just prior to the melt
cmeltNH4_o <- df$snow.NH4/NH4*abs(NH4charge)*1e3
  # [ueq/L] bulk,
cmeltPO43_o <- df$snow.TDP/PO43*abs(PO43charge)*1e3 # [ueq/L] bulk,

cmeltNO3_i <- c(rep(dim(df)[1]-1),0)
cmeltNH4_i <- c(rep(dim(df)[1]-1),0)
cmeltPO43_i <- c(rep(dim(df)[1]-1),0)#

for (i in 1:dim(df)[1]-1){
#cmelt_i[i] <- meq/L
cmeltNO3_i[i] <-
  (cmeltNO3_o[i]/(df$SWE[i]-df$SWE[i+1]))*
  (df$SWE[i]*exp(-k*(df$SWE.melt[i]-df$SWE[i]))-
    df$SWE[i+1]*exp(-k*(df$SWE.melt[i]-df$SWE[i+1])))
cmeltNH4_i[i] <-
  (cmeltNH4_o[i]/(df$SWE[i]-df$SWE[i+1]))*
  (df$SWE[i]*exp(-k*(df$SWE.melt[i]-df$SWE[i]))-
    df$SWE[i+1]*exp(-k*(df$SWE.melt[i]-df$SWE[i+1])))
cmeltPO43_i[i] <-
  (cmeltPO43_o[i]/(df$SWE[i]-df$SWE[i+1]))*
  (df$SWE[i]*exp(-k*(df$SWE.melt[i]-df$SWE[i]))-
    df$SWE[i+1]*exp(-k*(df$SWE.melt[i]-df$SWE[i+1])))

```

```

i=i+1
}
#vector needs to be the same length as the original, add one more number
cmeltN03_i[dim(df)[1]] <- cmeltN03_i[i]
cmeltNH4_i[dim(df)[1]] <- cmeltNH4_i[i]
cmeltP043_i[dim(df)[1]] <- cmeltP043_i[i]

N03.cfs <- cmeltN03_i /abs(N03charge) * N03*1e-3
NH4.cfs <- cmeltNH4_i /abs(NH4charge) * NH4*1e-3
TDP.cfs <- cmeltP043_i /abs(P043charge) * P043*1e-3

results <- data.frame(N03.cfs,NH4.cfs,TDP.cfs) #mg/l

return <- (results)
}

```

C.2.17 rainfall_chem.R

```

rainfall_chem <- function(){
  #rainfall chemistry is based on the freshly fallen snow chemistry in Saskatoon
  #this is the data from an email with Jane Elliott
  #this is inconsequential but should be corrected to
  #actual rainfall chemistry makeup

  TDP <- 0.08 #mg/l
  #TDN=0.35 ppm
  N03 <- 0.15 #mg/l
  NH4 <- 0.135 #mg/l

  results <- c(TDP,N03,NH4)

  return(results)
}

```

APPENDIX D

MODEL PERFORMANCE

D.1 Model Statistics

The formulae for the statistical measures used to evaluate model performance are provided below.

Nash-Sutcliffe Efficiency, NSE

$$\text{NSE} = 1 - \left[\frac{\sum_{i=1}^n (Y_i^{obs} - Y_i^{sim})^2}{\sum_{i=1}^n (Y_i^{obs} - Y^{mean})^2} \right] \quad (\text{D.1})$$

Percent Bias, PBIAS

$$\text{PBIAS} = \frac{\sum_{i=1}^n (Y_i^{obs} - Y_i^{sim}) * (100)}{\sum_{i=1}^n (Y_i^{obs})} \quad (\text{D.2})$$

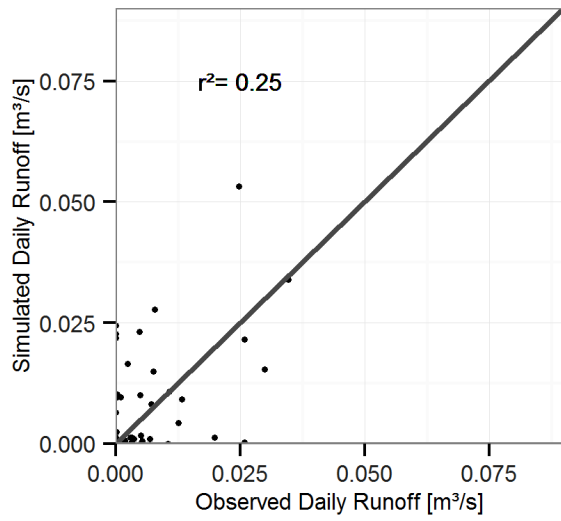
Root Mean Square Error, RMSE

$$\text{RMSE} = \sqrt{\sum_{i=1}^n (Y_i^{obs} - Y_i^{sim})^2} \quad (\text{D.3})$$

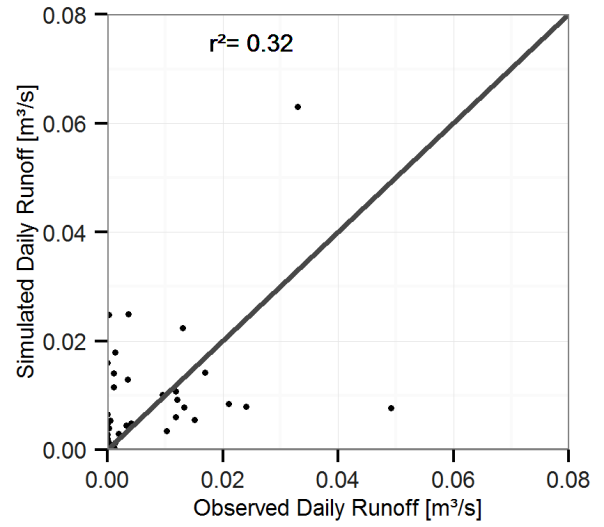
Ratio of RMSE to the standard deviation of the observations, RSR

$$\text{RSR} = \frac{\text{RMSE}}{\text{STD DEV}_{obs}} = \frac{\sqrt{\sum_{i=1}^n (Y_i^{obs} - Y_i^{sim})^2}}{\sqrt{\sum_{i=1}^n (Y_i^{obs} - Y^{mean})^2}} \quad (\text{D.4})$$

D.2 Performance Plots



(a) Field 7 Simulated vs Observed (hourly)

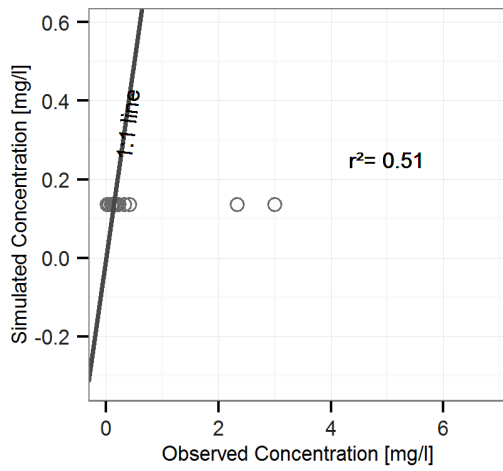


(b) Field 9 Simulated vs Observed (hourly)

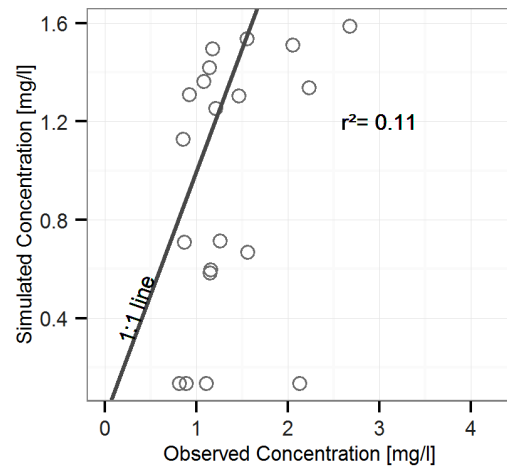
Figure D.1: Simulated and Observed Daily Runoff.

Table D.1: Simulated and Observed EOF Nutrient Mass Exports. The simulated mass exports calculated as a percentage of the observed mass exports are shown here. The simulated mass export is calculated in two ways, the first using simulated flows and concentrations (Figures 6.4a and 6.4b) and the second, using observed flows and concentrations (Figures 6.4c and 6.4d). The shaded cells indicate the better performing method of calculating mass export.

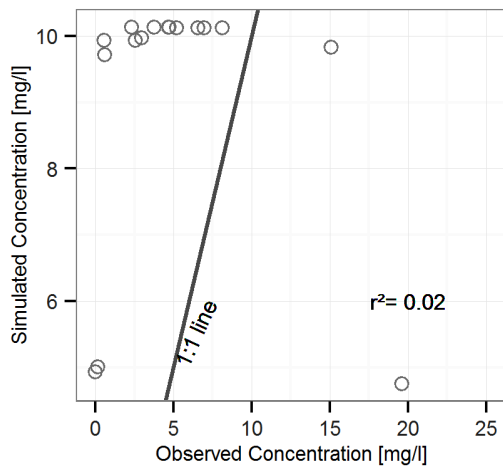
Year	Field 7		Field 9	
	Simulated mass (Figure 6.4a) observed mass	Simulated mass (Figure 6.4c) observed mass	Simulated mass (Figure 6.4b) observed mass	Simulated mass (Figure 6.4d) observed mass
Phosphorous(TDP)				
2009	106%	72%	123%	121%
2010	29%	15%	74%	131%
2011	389%	191%	106%	99%
Nitrate/Nitrite (NO3)				
2009	70%	158%	56%	64%
2010	23%	6.2%	87%	158%
2011	425%	210%	170%	150%
Total Ammonia (NH3)				
2009	8%	3%	89%	89%
2010	230%	19%	44%	73%
2011	70%	34%	91%	93%



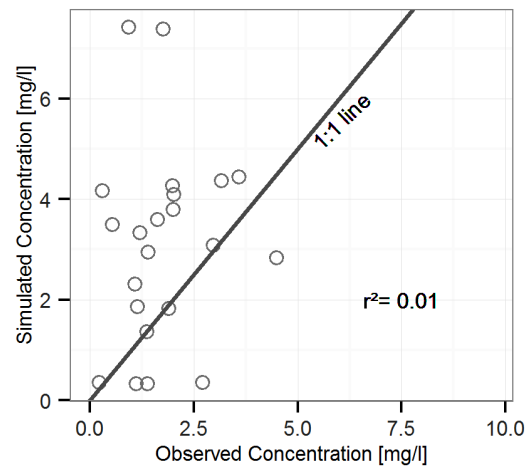
(a) Field 7 NH_3



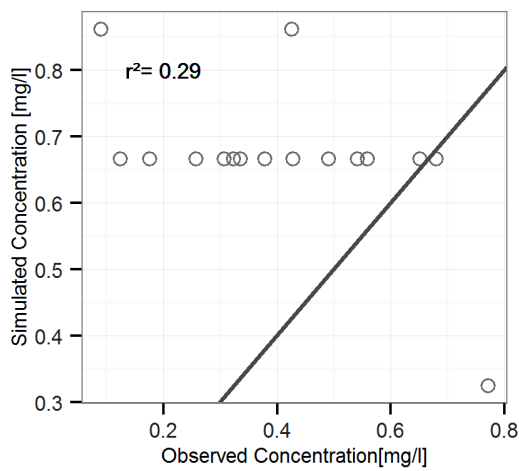
(b) Field 9 NH_3



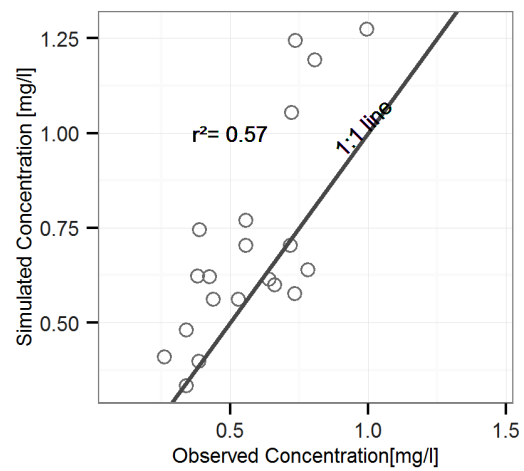
(c) Field 7 NO_3



(d) Field 9 NO_3



(e) Field 7 TDP



(f) Field 9 TDP

Figure D.2: Simulated vs Observed Mean Daily EOF Concentration Plots.

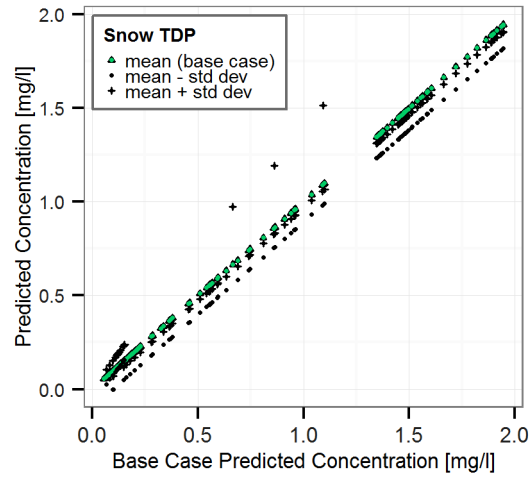


Figure D.3: TDP Snow Sensitivity Plot.